

FTD-HT-66-256

AD 651 073

767-61671

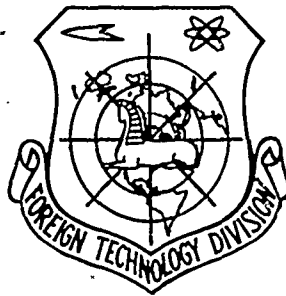
FOREIGN TECHNOLOGY DIVISION



FUNDAMENTALS OF THE THEORY OF DETECTION OF RADAR SIGNALS AND MEASUREMENT OF THEIR PARAMETERS

by

Ya. D. Shirman and V. N. Golikov



Distribution of this
document is unlimited.

ARCHIVE COPY

394

This translation was made to provide the users with the basic essentials of the original document in the shortest possible time. It has not been edited to refine or improve the grammatical accuracy, syntax or technical terminology.

ACCESSION for	
CFSTI	WHITE SECTION <input checked="checked" type="checkbox"/>
DDC	BUFF SECTION <input checked="checked" type="checkbox"/>
UNANNOUNCED	<input type="checkbox"/>
JUSTIFICATION.....	
BY.....	
DISTRIBUTION/AVAILABILITY CODES	
DIST.	AVAIL. and/or SPECIAL
1	

FTD-HT-66-256/1+2

UNEDITED ROUGH DRAFT TRANSLATION

FUNDAMENTALS OF THE THEORY OF DETECTION OF
RADAR SIGNALS AND MEASUREMENT OF THEIR PARAMETERS

By: Ya. D. Shirman and V. N. Golikov

English pages: 284

TM6001135

THIS TRANSLATION IS A RENDITION OF THE ORIGINAL FOREIGN TEXT WITHOUT ANY ANALYTICAL OR EDITORIAL COMMENT. STATEMENTS OR THEORIES ADVOCATED OR IMPLIED ARE THOSE OF THE SOURCE AND DO NOT NECESSARILY REFLECT THE POSITION OR OPINION OF THE FOREIGN TECHNOLOGY DIVISION.

PREPARED BY:

TRANSLATION DIVISION
FOREIGN TECHNOLOGY DIVISION
WP-APB, OHIO.

FTD-HT-66-256/1+2

AFLC-WFAFB-APR 67 141

Date 25 Jan. 19 67

S

Ya. D. Shirman i V. N. Golikov

OSNOVY TEORII
OBNARUZHENIYA
RADIOLOKATSIONNYKH
SIGNALOV I IZMERENIYA
IKH PARAMETROV

Izdatel'stvo "Sovetskoye Radio"
Moskva — 1963

278 pages

FTD-HT-66-256/1+2

CIRC ABSTRACT WORK SHEET								
(01) Acc Nr. TM6001135		(65) SIS Acc Nr.		(40) Country of Info UR			(41) Translation Nr. HT6600256	
(42) Author SHIRMAN, YA. D.; GOLIKOV, V. N.							Priority II Distribution STD	
(43) Source OSNOVY TEORII OBNARUZHENIYA RADIOLOKATSIONNYYKH SIGNALOV I IZMERENIYA IKH PARAMETROV								
(02) City UR	(03) Ref 0000	(04) Yr 63	(05) Vol 000	(06) Iss 000	(07) B. Pg 0001	(45) E. Pg 0278	(73) Date NONE	(47) Subject Code 17
Language RUSS		n/a		MOSKVA		IZDATEL'STVO SOVETSKOYE RADIO		
(39) Topic Tags radar signal analysis, detection probability, white noise, signal correlation, signal to noise ratio, radar signal								
(66) Foreign Title SEE SOURCE								
(09) English Title FUNDAMENTALS OF THE THEORY OF DETECTION OF RADAR SIGNALS AND MEASUREMENT OF THEIR PARAMETERS								
(97) Header Clas 0			(43) Clas 00		(64) Rel 0		(66) Release Expansion	

ABSTRACT: The book deals with the basic aspects of the statistical theory of detecting radar signals and measuring their parameters in the presence of Gaussian interferences, gives the theory and the principles of designing devices with optimum detection and measuring as well as a great number of examples permitting the reader to familiarize himself more quickly with the main problems of the theory and its applications.

The book is intended to serve the students of advanced courses of radio engineering colleges, but may also be useful to aspirants and engineers of similar lines of specialization. English translation; 284 pages

TABLE OF CONTENTS

Foreword.	1
Chapter 1. Basic Concepts of the Theory of Radar Signal De- tection and Measuring Their Parameters	7
§1.1. Qualitative Characteristics of Radar Detection	7
§1.2. Qualitative Characteristics of Radar Measurements	10
§1.3. The Concept of the Mean Risk and a Criterion for the Minimum Mean Risk.	14
§1.4. The Problem of Optimum Detection of Radar Signals and Measuring Their Parameters	20
§1.5. An Example of One-Dimensional Optimum Detection.	22
§1.6. Examples of One-Dimensional Optimum Measurement.	29
Chapter 2. Signals and Interferences in the Theory of De- tection and Measurement.	40
§2.1. Properties of Real Radar Signals	40
§2.2. Basic Models of Radar Signals.	46
§2.3. Fluctuation Interferences and Their Statistical Properties	48
§2.4. White Noise as a Model of Fluctuation Noise.	56
§2.5. Approximation of Signals and Interferences	58
§2.6. Kotel'nikov's Theorem.	59
§2.7. Method of Solving Problems of Detection and Measurement of Radar Signal Parameters on a Fluc- tuation Noise Background	62
Chapter 3. The Probability Ratio For the Fundamental Radar Signal Models in the Presence of Fluctuation Noise in the Form of White Gaussian Noise.	70
§3.1. The Probability Ratio for a Signal With Completely Given Parameters	70
§3.2. The Probability Ratio in the Presence of Unmeas- urable Random Parameters	73
§3.3. Probability Ratio For a Signal With Random Ini- tial Phase	75
§3.4. Probability Ratio For a Signal With Random Am- plitude and Random Initial Phase	77
§3.5. Probability Ratio For a Signal in the Form of a Radiopulse Packet With Random Initial Phases	79
§3.6. Probability Ratio For Signals in the Form of a Packet of Radiopulses With Random Amplitudes and Initial Phases	80
Chapter 4. Theory and Principles of Designing Devices for Optimum Detection and Measurement of Parameters.	84

§4.1. General Considerations Concerning the Construction of Devices for Optimum Detection and Measurement of Parameters.	84
§4.2. Simplest Correlation Circuits of Optimum Receivers	85
§4.3. Use of Optimum Linear Filters in the Construction of Optimum Receivers. Pulse Response of the Optimum Filter	88
§4.4. Signal-To-Noise Ratio At the Output End of an Optimum Filter	95
§4.5. Frequency Characteristic of an Optimum Filter.	97
§4.6. Application of the Method of Envelopes in the Analysis of the Optimum Filtration Process	102
§4.7. Receiver With Optimum Filter in the Case of Random Initial Phase of the Signal.	108
§4.8. Correlation-Filtration Reception	111
§4.9. Receiver With Optimum Filter for a Packet of Radio Pulses with Random Independent Initial Phases	116
§4.10. Optimum Measurement of Delay Time	122
§4.11. The Principle of Broad-Band Radio Pulse Compression.	128
Chapter 5. The Elements of Optimum Detection and Parameter Measuring Devices	133
§5.1. The Elements of Optimum Devices Under Consideration	133
§5.2. Conditions Under Which Multistage Resonance Amplifiers Can Be Applied in Order to Achieve Optimum Filtration	133
§5.3. Use of Delay Lines In the Synthesis of Optimum Filters.	139
§5.4. Optimum Filter For A Coherent Sequence of Radio Pulses	143
§5.5. An Example of Synthesizing an Optimum Filter for the Compression of a Radio Pulse With a Complex Law of Modulation.	147
§5.6. Signal Delay (Memory) Devices.	150
§5.7. Incoherent Storing Devices	152
§5.8. On the Use of the Phenomenon of Dispersion in Delay Lines in the Case of Optimum Filtration of Broad-Band Radio Pulses.	158
§5.9. Correction of the Shape of the Compressed Radio Pulse Envelope	163
Chapter 6. Qualitative Indices of Optimum Parameter Detection and Measurement Devices	167
§6.1. Statement of the Problem	167
§6.2. Characteristics of Optimum Detection of a Signal With Completely Known Parameters	168
§6.3. Characteristics of Optimum Detection of Signals With Random Initial Phase and Random Amplitude and Initial Phase.	173
§6.4. Detection Characteristics of an Incoherent Pulse Packet with Linear-Quadratic and Digital Summation	178
§6.5. Qualitative Indices of Optimum Measurement of the	

Parameters of a Signal With Random Initial Phase (General Considerations)	186
§6.6. Error Scatter of the Optimum Measurement of the Lag time of a Signal With Random Initial Phase at $\tau \gg 1$	193
§6.7. Degenerate Case of Lag Time Measurement at $q \gg 1$	196
§6.8. Threshold Effect in Measurement.	198
§6.9. Error Scatter of the Optimum Measurement of the Doppler Frequency For a Signal with Random Ini- tial Phase	203
Chapter 7. Ambiguity Diagrams of Radar Signals.	206
§7.1. Formula For Optimum Processing of the Radar Sig- nal With Target Motion Control	206
§7.2. Ambiguity Function and Normalization of the Am- biguity Function	209
§7.3. Graphic Representation of the Ambiguity Functions $\rho(\tau, F)$ and $\rho^2(\tau, F)$	211
§7.4. Volume of the Ambiguity Solid $\rho^2(\tau, F)$	213
§7.5. Cross Section of Ambiguity Solids and Character- istics of Optimum Reception Circuits	215
§7.6. Ambiguity Solid of a Rectangular Radio Pulse With Constant Instantaneous Oscillation Frequency	219
§7.8. Ambiguity Solid of Coherent Packets of Radio	225
Pulses	228
§7.9. Ambiguity Solid of a Noiselike Signal.	228
§7.10. On the Conditional Nature of the Ambiguity Dia- grams	234
Chapter 8. Consecutive Repeated Measurements.	239
§8.1. Simplest Models of Target Motion (Models With In- dependent Increments).	239
§8.2. Optimum Successive Processing of the Observation Results for Motions With Independent First In- crements	244
§8.3. Continuous and Interrupted Regimes of Consecutive Processing for Motions With Independent and Sta- tionary First Increments	247
§8.4. Realization of the Optimum Consecutive Processing for a Stable Motion With Stationary First Incre- ment	250
§8.5. Optimum Consecutive Processing of the Observation Results for a Motion With Independent Second In- crements	252
§8.6. Unsteady and Steady Optimum Consecutive Process- ing Regime for a Motion With Independent and Sta- tionary Second Increments.	257
Appendix.	265
Appendix 1. Qualitative Detection Indices With Square Signal Summation	265
Appendix 2. Qualitative Indices of the Optimum Measure- ment of Two Parameters for a Signal With Random Initial Phase	271

Appendix 3. Elements of Resolution Theory	274
References.	279

The book deals with the basic aspects of the statistical theory of detecting radar signals and measuring their parameters in the presence of Gaussian interferences, gives the theory and the principles of designing devices with optimum detection and measuring as well as a great number of examples permitting the reader to familiarize himself more quickly with the main problems of the theory and its applications.

The book is intended to serve the students of advanced courses of radio engineering colleges, but may also be useful to aspirants and engineers of similar lines of specialization.

BLANK PAGE

FOREWORD

An increasing use of statistical methods can be observed in the development of contemporary radio engineering and radar. In particular, problems connected with the random action of weak signals and interferences on the receiver cannot be solved without having recourse to these methods. It is, therefore, comparatively long ago that statistical analysis was introduced into the theory of receivers to which the fundamental works of the Soviet scientists V.I. Siforov and V.I. Bunimovich contributed to a considerable extent.

In the last 10-20 years, however, the range of application of statistical methods has been expanded substantially.

Above all, besides the statistical analysis of concrete variants of the signal receiving and processing circuits, the investigation of the mathematical principles and qualitative characteristics of optimum processing is widespread. In the past, the choice of the concrete processing circuit was connected with a statistical analysis of the individual variants of the circuits or with the choice of optimum values of the individual variants of the circuits or with the choice of optimum values of the individual receiver parameters so that the problem whether the circuit could be designed such as to yield essentially better characteristics always remained unsolved. It was the fundamental work of V.A. Kotel'nikov [1] (1946) which, for the first time made it possible to obtain an idea of the optimum mathematical operations to be applied to the function of time corresponding to oscillations fed to the receiver, in order to obtain the best result in the sense of statistics.

In the past one could only speak of the qualitative characteristics one or another receiver circuit possessed whereas in V.A. Kotel'nikov's work the potential interference suppression was determined, for the first time; it is characterized by the best qualitative radio receiver characteristics which can be obtained for given signal and interference characteristics.

Secondly, together with the introduction of optimum processing as a standard in the statistical analysis of given circuits, statistical synthesis of circuits exactly or approximately corresponding to the mathematical operations of optimum processing begins to be made use of. Previously, before the work of B.A. Kotel'nikov, and even during the following 5-10 years after his publication real circuits of signal processing were designed intuitively on the basis of physical considerations and engineering practice. This situation was also due to the fact that the connections between the mathematical operations of optimum processing and the processes occurring in real circuits had not yet been revealed and realized. At present, we are quite able to approach the problem of a receiver as a specialized computer carrying out exactly or approximately the linear and nonlinear operations of optimum processing.

Furthermore, there is no longer a sharp boundary between the processing of radar signals in circuits of radio receiving and indicating devices, in automation circuits, digital and analog computing technique or, otherwise, between intrareceiver, primary and secondary processing of radar signals. All these aspects of processing are characterized by a combination of mathematical operations which have to be close to the optimum. In radar, such an optimization is particularly important both in the detection of reflected signals and in measuring their parameters. Probably, also operations immediately applied to os-

cillations of the electromagnetic field which act on the receiving antennas of radars will soon be considered to be the initial links of a single processing circuit.

Thirdly, besides the determination of the qualitative characteristics of optimum processing for a given signal, a comparative analysis of the results of optimum (and sometimes also not quite optimum) processing of different signals begins to be made use of in order that the most advantageous among them may be found out. This fact implies that the development of the statistical theory of optimum processing inevitably affects the domain of transmission and coding of emitted signals, and, in particular, of sounding signals in radar.

It was precisely the statistical theory of detection and measurement that helped to find ways of overcoming an essential contradiction which in the past had arisen between two important demands usually made on the designer of a pulsed radar. The first demand is to increase the range of action at the expense of the energy of the station if the peak power of the electrovacuum devices and the waveguide tracts is limited. This is connected with an increase of the energy of the sounding radio pulses at the expense of an increase of their duration. The second demand is to have a high longitudinal resolving power. For simple pulsed signals (without additional frequency or phase modulations or the like) this fact gives rise to a reduction in the duration of the sounding radio pulses, under conditions of processing which are close to the optimum.

The elimination of the contradiction is achieved at the expense of going over to complex sounding radio signals with an additional modulation within the limits of the pulse. Since the product of a frequency band and the duration of such signals is essentially greater than unity, they are called broad-banded. Broad-banded signals are able to

ensure high longitudinal resolving power without destroying the optimality of their processing in receiving. It turns out that a received broad-band radio pulse with given parameters (correct as to amplitude and initial phase) is compressed in time if it passes through the filter which is optimum for it. The longitudinal resolving power of the pulsed radar and its pulse volume are in this case determined by the duration of the compressed radio pulse whose duration is essentially shorter than that of the sounding signal. This fact explains the great attention paid in the last few years to broad-band radio signals and their compression in time, in foreign literature. In the Soviet Union, the principles of compression had been worked out independently and before the corresponding foreign publications had appeared (see, e.g., [14]).

The constructive value of the statistical theory of radar had not been realized at once. One of the pioneers of this theory was the English scientist F.M. Woodward, who had contributed to its development in a high degree. But also he stated in 1953 that the value of this theory mainly lay in the fact that it verified experimental results already well-known.* Developments showed that Woodward's judgment was unnecessarily pessimistic.

The application of the new radiosignals should change not only the aspect of radio receiving, but also that of radio transmitting sets. Once again this attests to the fact that the domains of application of the statistical theory of detection and measurement have outgrown the narrow compass of only one course on radio receiving sets held in higher technical schools.

Consequently, when training specialists in radar it is useful to set forth the statistical theory of detecting and measuring the radar signal parameters as the basis of a separate course on the theoretical

fundamentals of radar (or, at least, of applied information theory).

In the last few years Soviet scientists such as L.A. Vaynshteyn and V.D. Zubakov [5], S.Ye. Fal'kovich [6], L.S. Gutkin [7] and others have published several monographs on problems of the statistical theory of detection and measurement. The first part of a serious collective work [10] edited by G.P. Tartakovskiy was published. The following monographs were published in translation: the short work by F.M. Woodward [4] which has, however, already played a considerable role in the development of radar theory, the voluminous theoretical monograph by D. Middleton [8], the interesting work by K. Helstrom [11] which was published recently.

Nevertheless, means of instruction reflecting both the experience of scientific and pedagogic work in the Higher Technical School are missing. Besides, the technical trend of the theoretical investigations is not sufficiently emphasized in the published works.

The present book is intended to fill this gap.

The book was prepared as a means of instruction and reflects a five-year experience of teaching in Higher Technical Schools where the extent of the material set forth was gradually enlarged.

Having in mind the purpose of the book, the authors endeavored to explain the theoretical results of greatest technological importance, making use, as far as possible, of rather simple mathematical tools.

The book deals with the fundamental aspects of the statistical theory of detecting radar signals and measuring their parameters in the presence of Gaussian interferences; it explains the principles of design and the theory of optimum detection and measuring devices, and gives a great number of examples enabling the reader to familiarize himself with the possible applications of theory. The applications of statistical theory to measuring angular coordinates are not treated in

the present work. Although the book is intended for students of advanced courses in radio engineering institutions, it may be useful for aspirants and engineers of similar lines of specialization.

The authors express their indebtedness to A.Ye. Basharinov, N.I. Kravchenko, G.A. Kostin, I.N. Busygin and Ye.P. Lebedev for several valuable remarks.

Manu-
script
Page
No.

[Footnotes]

5

At the end of the fifth chapter of Woodward's book [1] we read: "The experimenter may feel inclined to think that the theory borders on triviality since it shows what to do, whereas it has been well-known for some time. Such a criticism misses the mark. Investigation shows some theoretical ideal not applying to experience and just the fact that it confirms the experimental conclusions provides the highest satisfaction in it.

Chapter 1

BASIC CONCEPTS OF THE THEORY OF RADAR SIGNAL DETECTION AND MEASURING THEIR PARAMETERS

§1.1. QUALITATIVE CHARACTERISTICS OF RADAR DETECTION

The problem of radar boils down to the obtaining of reliable information on the distribution of targets in space and on their position data. This information is contained in the radio signals reflected by the targets.

Besides useful signals interferences act on the input end of the radar receiver. They give rise to errors in the detection of targets and in the measurement of their coordinates. Other phenomena of random character cause the same result, e.g., fluctuations of secondary radiation, as a result of which the signals are abruptly weakened for isolated instants of time.

Owing to the random character of the signals and interferences the performance of the radar is analyzed by statistical methods and its qualitative characteristics are specified by statistical parameters.

To start with, we shall deal with the qualitative characteristics of radar detection.

The result of the detection process must be the solution to the problem as to whether or not a target is present in the vicinity of an arbitrary point of space within the coverage of the radar. The solution may be adopted under two mutually exclusive conditions:

condition A_1 is "there is a target,"

condition A_0 is "there is no target."

It is implied that these conditions are unknown when the solution is being worked out.

Owing to the interferences and fluctuations of the useful signal two forms of solutions may correspond to each condition:

solution A_1^* is "there is a target,"

solution A_0^* is "there is no target."

After the detection process has been completed, a third solution - "I do not know" - must not exist. Let us pay attention to the fact that the solutions A_1^* and A_0^* are designated in the same way as the conditions, except for the addition of asterisks.

First, we shall consider the case where a target exists (condition A_1). If in this case the solution A_1^* - "there is a target," is forthcoming, one speaks of a correct detection. If under the same condition the solution A_0^* emerges - "there is no target," a target miss takes place. Obviously, a target miss is a most undesirable error in detection.

Qualitative characteristics of detection under the condition of an existing target are the corresponding conditional probabilities of correct detection

$$D = P(A_1^* | A_1) \quad (1)$$

and of target miss

$$\hat{D} = P(A_0^* | A_1). \quad (2)$$

Since the solutions A_1^* and A_0^* are incompatible random events and correspond to the same condition A_1 of an existing target, we have

$$\hat{D} + D = 1. \quad (3)$$

Thus, it is always possible to find the conditional probability of \hat{D} of missing the target if the conditional probability of correct detection D is known. If, e.g., for one scanning cycle $D = 0.75$, the

conditional probability of missing is $\hat{D} = 0.25$. This implies that the radar equipment guarantees, on the average, detection of target in 75% of the cases; in about 25% of the cases the target is not detected.

Let us turn to the case where no target exists (condition A_0). Under this condition, nondetection is correct, i.e., the solution A_0^* - "there is no target." If the solution A_1^* - "there is a target," emerges as the result of the action of interferences, one speaks of a false alarm.

False alarm is a very undesirable error even if, in the following processing, the false information will be screened. False information uselessly burdens the system of radar data processing. It may completely disturb the passage of useful information. In several cases, the fact of the false alarm may of itself also give rise to extremely undesirable consequences.

Qualitative characteristics of detection under the condition of a nonexistent target are the conditional probabilities of false alarm

$$F = P(A_1^* | A_0) \quad (4)$$

and of correct nondetection

$$\hat{F} = P(A_0^* | A_0). \quad (5)$$

Since the incompatible solutions A_1^* and A_0^* correspond to the same condition A_0 , we have

$$F + \hat{F} = 1. \quad (6)$$

If the conditional probability of false alarm F is known, we can always obtain the conditional probability of correct nondetection. If, e.g., considering some element of space, $F = 10^{-4}$, then $\hat{F} = 1 - 10^{-4}$. This implies that the radar equipment gives, on the average, one false alarm in 10^4 observations of the given space element in the case of nonexistent targets, and in 9999 cases it does not give a false alarm.

We note that per time unit a radar usually scans a great number m

of resolvable space elements. If for a space element $F \ll 1/m$, the probability of false alarm \hat{F} for a volume of m elements grows in proportion to m . The probability of correct detection is, in fact, $\hat{F}_m = (\hat{F})^m$, whence

$$F_m = 1 - (1 - F)^m \approx 1 - (1 - mF) = mF.$$

This is also the reason why, in the theory of radar signal detection, one usually works with very low values of admissible probability of false alarm $F_{\text{dop}} = F_m \text{ dop} / m$ for each of the resolvable elements.

On the other hand, one tries to make the probability of correct detection D as high as possible. The latter is particularly difficult to achieve if the target is at a considerable distance and the energy of the reflected signals is extremely low. The boundary of the zone of detection of an individual radar is, therefore, given by the magnitude of the distance at which the probability of correct detection per one scanning cycle is not less than some admissible value D_{dop} . Usually, one chooses $\hat{D}_{\text{dop}} = (0.05-0.5)$, i.e., $D_{\text{dop}} = (0.95-0.5)$. In some cases, the demands made on a radar may be increased abruptly, i.e., sometimes one chooses $\hat{D}_{\text{dop}} = (0.01-0.0001)$, corresponding to $D_{\text{dop}} = (0.99-0.9999)$.

Thus, the conditional probabilities of correct detection D and false alarm F are the basic qualitative characteristics of radar detection. At the limits of the detection zone, the requirements $F \leq F_{\text{dop}}$, $D \geq D_{\text{dop}}$.

§1.2. QUALITATIVE CHARACTERISTICS OF RADAR MEASUREMENTS

The error in the determination of the quantity to be measured is a criterion of the quality of the measurement carried out. The smaller this error, the higher the quality of the measurements.

The errors of measurement are classed as gross blunders, constant and accidental errors. If particular measures are taken to eliminate constant errors and gross blunders, the errors of measurement can be

reduced to the accidental ones.

In measuring the radar signal parameters, the accidental errors are due to the action of interferences on the input end of the receiver, to signal fluctuations, but also to the random behavior of the system of measurements itself.

Fig. 1.1 shows the typical curve of the probability density $p(\varepsilon)$ characterizing the law of distribution of the accidental errors. From this curve, the probability that the magnitude of the error will assume a value within an arbitrary interval from ε to $\varepsilon + \Delta\varepsilon$ may be found. The corresponding probability is equal to $p(\varepsilon)\Delta\varepsilon$ and represented by the crosshatched area in Fig. 1.1. The total area between the

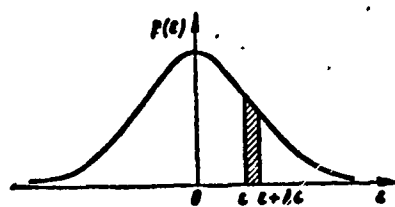


Fig. 1.1. Typical probability density curve $p(\varepsilon)$ of accidental errors.

curve $p(\varepsilon)$ and the axis of abscissas is equal to unity since it is the probability of a certain event which implies that the error may assume any value between $-\infty$ and $+\infty$.

It follows from the curve (Fig. 1.1) that great errors have a low probability, but in individual measurements their possibility is not excluded. The probability that the absolute value of the error ε is lower than ε_0 , is numerically equal to the crosshatched area in Fig. 1.2.

$$P(|\varepsilon| < \varepsilon_0) = \int_{-\varepsilon_0}^{\varepsilon_0} p(\varepsilon) d\varepsilon. \quad (1)$$

Fig. 1.3 shows the diagram of the function dependence $\Phi(\varepsilon_0) = P(|\varepsilon| \leq \varepsilon_0)$. It follows from this diagram that if the value of ε_0 is great enough the inequality $|\varepsilon| < \varepsilon_0$ has a probability close to unity, i.e., is almost certain.

Usually,

- 1) the mean square deviation ε_{skv} ;
- 2) the probable (mean) error ε_{ver}

are considered to be statistical parameters characterizing the accuracy of the measurement. Sometimes other statistical parameters are used as well. In particular, one speaks of the maximum error $\varepsilon_{\text{maks}}$. In several cases, the mean value of the error modulus may be interesting.

For any law of distribution of the accidental errors $p(\varepsilon)$ the mean square deviation of the measurements is determined from the relation

$$\sigma^2 = \int_{-\infty}^{\infty} \varepsilon^2 p(\varepsilon) d\varepsilon. \quad (2)$$

The probable (mean) error ε_{ver} is found from the equation

$$P(|\varepsilon| < \varepsilon_{\text{ver}}) = P(|\varepsilon| \geq \varepsilon_{\text{ver}}) = 0.5, \quad (3)$$

i.e., corresponds to that value of ε_0 for which the crosshatched area in Fig. 1.2 is half of the total area below the curve $p(\varepsilon)$.

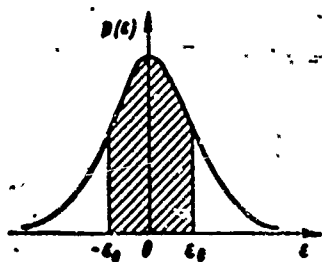


Fig. 1.2. Concerning the calculation of the probability $P(|\varepsilon| < \varepsilon_0)$.

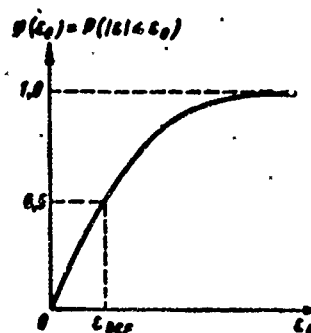


Fig. 1.3. Curve of probability $P(|\varepsilon| < \varepsilon_0) = q(\varepsilon_0)$.

The normal law or Gaussian law is the most usual law of accidental error distribution:

$$p(\varepsilon) = \frac{1}{\sqrt{2\pi}\sigma} e^{-\frac{\varepsilon^2}{2\sigma^2}}, \quad (4)$$

to which the curves shown in Figs. 1.1-1.3 also correspond. In this case,

$$\begin{aligned} P(|\epsilon| < \epsilon_0) &= \int_{-\epsilon_0}^{\epsilon_0} \frac{1}{\sqrt{2\pi}\sigma_{\text{ems}}} e^{-\frac{\epsilon^2}{2\sigma_{\text{ems}}^2}} d\epsilon = \\ &= \frac{2}{\sqrt{2\pi}} \int_0^{\frac{\epsilon_0}{\sigma_{\text{ems}}}} e^{-\frac{x^2}{2}} dx = \Phi\left(\frac{\epsilon_0}{\sigma_{\text{ems}}}\right), \end{aligned} \quad (5)$$

where

$$\Phi(u) = \frac{2}{\sqrt{2\pi}} \int_0^u e^{-\frac{x^2}{2}} dx \quad (6)$$

is the probability integral.

It follows from a comparison of the formulas (3) and (5) that

$$\Phi\left(\frac{\epsilon_{\text{exp}}}{\sigma_{\text{ems}}}\right) = 0.5.$$

Since $\Phi(u) = 0.5$ and $u \approx 0.67 \approx 2/3$, we have for the normal law

$$\epsilon_{\text{exp}} \approx \frac{2}{3} \sigma_{\text{ems}}, \quad (7)$$

so that it is always possible to find the probable (mean) error if the mean square deviation is known.

Often

$$\epsilon_{\text{max}} = 4\epsilon_{\text{exp}}$$

is taken as the maximum error of the measurements.

In this case, we have for the normal law

$$P(|\epsilon| < \epsilon_{\text{max}}) = \Phi\left(\frac{4\epsilon_{\text{exp}}}{\sigma_{\text{ems}}}\right) = \Phi(8/3) \approx 0.993,$$

i.e., the probability that the accidental error exceeds ϵ_{max} is all in all only 0.7%.

Thus, the distribution law of the accidental error gives the most complete idea of its possible values. The mean square deviation, which is connected to the probable (mean) and maximum errors by simple relations, can be considered the basic parameter characterizing the

accuracy of the measurements in the case of a normal law.

§1.3. THE CONCEPT OF THE MEAN RISK AND A CRITERION FOR THE MINIMUM MEAN RISK

The system of radar information processing has to satisfy contradictory demands.

In order to avoid a target miss, it is, e.g., desirable to solve the problem as to whether it is really present even in the case the signal from the target should be strongly distorted by interferences and the existence of the target cannot be maintained with certainty. Obviously, the probability of false alarm increases in this case.

Thus, we have to make a reasonable compromise between the contradictory factors by choosing a method of information processing which is most favorable from the point of view of all possible conditions of radar. Of course, the solution obtained in this case will not necessarily be the best for any special condition of radar (existence of a target, nonexistence of a target). It must be optimum on the average, statistically taking into account the probabilities with which all possible conditions of detection or measurement are distributed.

It is advantageous to make use of the concept of the mean risk when studying such contradictory situations. This concept allows us to study the conditions of optimum detection of radar signals and measuring their parameters in a uniform way and starting from sufficiently general positions. It has a wider significance and can also be applied to planning the exploitation of resources in political economy and to planning military operations. We shall explain the nature of the concept of mean risk with the help of examples taken from the domain of radar.

We shall use the term entirety of possible situations in order to designate the entirety of conditions in radar and of the solutions

adopted in this case.

The following situations are possible . section:

- 1) situation $A_0^* A_0$ (correct nondetection);
- 2) situation $A_1^* A_0$ (false alarm);
- 3) situation $A_0^* A_1$ (target is missed);
- 4) situation $A_1^* A_1$ (correct detection).

Usually, any measurement is characterized by the fact that to the measured quantity α some estimate α^* is assigned which is somewhat different from it (on account of which an error $\varepsilon = \alpha^* - \alpha$ is obtained). In this case, the entirety of possible situations corresponds to the entirety of different values of α and α^* .

Each of the situations mentioned is characterized by its probability or probability density. In the case of detection we may speak of the probabilities of situations P_i ($i = 1, 2, 3, 4$), the sum of which is equal to unity:

$$P_1 + P_2 + P_3 + P_4 = P(A_0^*, A_0) + P(A_1^*, A_0) + P(A_0^*, A_1) + P(A_1^*, A_1) = 1. \quad (1)$$

When the parameters are measured, we speak of the probability density of situations $p(\alpha^*, \alpha)$, or the differential

$$dP(\alpha^*, \alpha) = p(\alpha^*, \alpha) d\alpha^* d\alpha,$$

where

$$\int_{-\infty}^{\infty} \int_{-\infty}^{\infty} p(\alpha^*, \alpha) d\alpha^* d\alpha = \int_{(\alpha^*, \alpha)} dP(\alpha^*, \alpha) = 1. \quad (2)$$

To each possible situation we shall assign a certain error charge according to the importance or value of this error. Let a greater (or, at least, an equal), but not a smaller value of the error correspond to a greater error. We shall agree upon considering this value equal to zero for solutions without errors.

The assignment of values to the errors is an important stage of an-

analysis and must take into account all considerations as to the problem to what extent one or another aspect of error is undesirable. In many important cases, however, the rules of optimum processing prove to be independent of the concrete way of assigning values to the errors.

Having in mind the random character of each situation we may assert that also the error charge is a random quantity. Consequently, we may speak of the mean charge or, equivalently, of the mean risk.

The mean risk is calculated according to the rules of finding the mean value (the mathematical expectation value) of an arbitrary random quantity. For the discrete case (detection) it is found from the formula

$$\bar{r} = \sum_i r_i P_i, \quad (3)$$

where r_i is the charge for the i th situation; P_i is its probability.

For the continuous case (measurement) the mean risk is determined by the equation

$$\bar{r} = \int_{(a^*, a)} r(a^*, a) dP(a^*, a).$$

In the analysis of the detection process it is sufficient to assign only two error values: the error value of false alarm

$$r(A_1^*, A_0) = r_f,$$

and the error value of missing the target

$$r(A_0^*, A_1) = r_D.$$

Owing to the multiplication theorem of probabilities the corresponding absolute probabilities will be

$$\left. \begin{aligned} P(A_1^*, A_0) &= P(A_0) P(A_1^* | A_0) = P(A_0) F, \\ P(A_0^*, A_1) &= P(A_1) P(A_0^* | A_1) = P(A_1) \hat{D}. \end{aligned} \right\} \quad (4)$$

In view of the fact that the charge for solutions without error is put equal to zero, from Eq. (3) we obtain the expression for the

mean risk of detection errors in the form

$$\bar{r} = r_f P(A_0) + r_d \hat{P}(A_1). \quad (5)$$

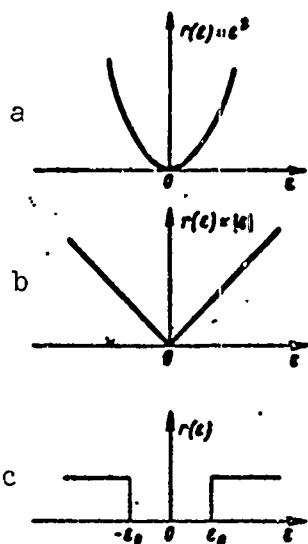


Fig. 1.4. Possible error value functions.

Comparing the different systems of processing radar information we must give the preference to that system for which the mean risk is smallest. Thus, the optimum operating conditions can be found from the criterion of the minimum mean risk. In particular, for the optimum system of detection the quantity calculated from formula (5) must have a minimum.

In the analysis of the measuring process we have to consider the error value to be a function of two variables $r(\alpha^*, \alpha)$. Assuming (e.g., in range finding) that the value of an error of measurement depends only on the difference of the measured quantity and its estimate $\alpha^* - \alpha = \epsilon$, it is sufficient to set up a function $r(\epsilon)$ of only one variable.

Fig. 1.4 shows the possible curves of error values $r(\epsilon)$ as functions of values of the error ϵ . Thus, the curve $r(\epsilon) = \epsilon^2$ (Fig. 1.4a) corresponds to the case in which the value of the error is equal to the square of the error. In this case, obviously,

$$\bar{r} = \bar{\epsilon^2} = \sigma_{\epsilon}^2,$$

i.e., the mean risk is equal to the square of the mean square deviation, and the minimum of the mean risk corresponds to the minimum of the mean square deviation.

The curve $r(\epsilon) = |\epsilon|$ (Fig. 1.4b) corresponds to the case in which the value of the error is equal to the absolute value (modulus of the error). In this case the mean risk is equal to the mean modulus of the error

$$\bar{r} = \bar{|\epsilon|}.$$

and the minimum of the mean risk corresponds to the minimum of the mean error modulus.

The curve (Fig. 1.4c) corresponds to the case where

$$r(\epsilon) = \begin{cases} 0 & \text{for } |\epsilon| < \epsilon_0 \\ 1 & \text{for } |\epsilon| > \epsilon_0 \end{cases}$$

In this case the mean risk is equal to the probability that the error modulus exceeds ϵ_0

$$\bar{r} = \int_{-\infty}^{\infty} r(\epsilon) p(\epsilon) d\epsilon = \int_{-\infty}^{\infty} p(\epsilon) d\epsilon + \int_{-\infty}^{\infty} p(\epsilon) d\epsilon = P(|\epsilon| > \epsilon_0),$$

and the minimum of the mean risk reduces to the minimum of the probability that the error modulus exceeds the given quantity ϵ_0 .

Using the example of measurement analysis we can satisfy ourselves of the fact that the criterion of the mean risk minimum may reduce to any other well-known criterion, in particular, to the criterion of the minimum of mean square deviation if the function of the error value is chosen appropriately.

This fact shows that the criterion of the mean risk minimum is sufficiently general so that we may go over from it to simpler and more special criteria.

The example of detection analysis may convince us of the same fact. In particular, if we put $r_F = r_D = 1$ in Eq. (5), the mean risk will be equal to the total probability of the detection errors

$$\bar{r} = FP(A_0) + DP(A_1).$$

In literature, the condition of this probability being a minimum is called the criterion of the ideal observer. The criterion of mean risk minimum (5) is more general than the criterion of the ideal observer, since it permits us to allow for the different significance of errors of false alarm and missing the target.

If in Eq. (5) the substitution $\hat{D} = 1 - D$ is carried out, we may write

$$\bar{r} = r_D P(A_1) - [D - 1, F] r_D P(A_1), \quad (6)$$

where

$$l_0 = \frac{r_D P(A_1)}{r_F P(A_2)} \quad (7)$$

Since $r_D P(A_1) > 0$, we find that the criterion of the mean risk minimum reduces to the criterion

$$D - l_0 F = \max. \quad (8)$$

Criterion (8) is called weight criterion. It provides for the demand of raising the conditional probability of correct detection D and lowering the conditional probability of false alarm F . In view of all these demands we must try to increase the "weighted" difference $D - l_0 F$. The factor l_0 which is termed a weighted factor depends on the ratio of the error values of each kind and the probabilities of the target being present or absent in the investigated part of space.

Comparing two systems of information processing the first of which is optimum we may write

$$D_{\text{opt}} - l_0 F_{\text{opt}} \geq D' - l_0 F'.$$

Hence

$$D_{\text{opt}} \geq D' + l_0 (F_{\text{opt}} - F'),$$

i.e., for $F' = F_{\text{opt}}$

$$D_{\text{opt}} \geq D'. \quad (9)$$

Relation (9) remains correct also in the case if $F' \leq F_{\text{opt}}$. Otherwise, it may be rewritten in the form

$$\hat{D}_{\text{opt}} \leq \hat{D}'. \quad (10)$$

This fact implies that the optimum system yields the lowest probability of missing among all systems for which the probability of false alarm is not higher than for the optimum system. The given conditions can be chosen to be an independent criterion for the optimality of the system (the Neuman-Pearson criterion). The Neuman-Pearson criterion as well as the criterion of the ideal observer may, thus, be considered

a consequence of the optimality criterion of the system.

Thus, the criterion of the mean risk minimum can be used in analyzing the contradictory conditions of detection and measurement of parameters. The criterion of the mean risk minimum is a comparatively general criterion. In the case of detection, e.g., it reduces to the weight criterion, the Neuman-Pearson criterion and the criterion of the ideal observer. When applied to parameter measuring it reduces, in particular, to the criterion of minimum of mean square deviation.

§1.4. THE PROBLEM OF OPTIMUM DETECTION OF RADAR SIGNALS AND MEASURING THEIR PARAMETERS

The considerations set forth in the preceding sections are sufficiently general and can be applied to analyzing any radar information processing whether immediately entering the input end of the radar or also partly subject to processing.

The analysis of optimum radar information processing is most interesting if information immediately enters the input end of the radar since partial nonoptimum processing may give rise to irreversible losses of information.

In the following we shall, therefore, carry out an analysis of the optimum processing of high-frequency oscillations entering the input end of the radar receiver. Taking into account the specific character of a radar's work these oscillations can be represented in the form

$$y(t) = n(t) + Ax(t, \alpha, \alpha_1, \dots, \beta, \beta_1, \dots). \quad (1)$$

where

$n(t)$ is the oscillation of the interference acting on the input end of the receiver;

A is a discrete random parameter that assumes only two values: $A_0 = 0$ and $A_1 = 1$, corresponding to the conditions of absence or pre-

sence of a useful signal from the target;

$x(t, \alpha_1, \alpha_2, \dots, \beta_1, \beta_2, \dots)$ is a given function of time and the parameters $\alpha_1, \alpha_2, \dots, \beta_1, \beta_2, \dots$. The shape of this function depends, in particular, on the law of modulation of the sounding signal, the method of space scanning, etc.;

$\alpha_1, \alpha_2, \dots$ — are random measurable parameters of the radar signal. The time delay proportional to the distance from the target and the Doppler frequency shift proportional to the radial velocity of the target may be among them;

β_1, β_2, \dots — are random signal parameters whose measurement is not of substantial interest. Among them there are: the amplitude of the signal, the total initial phase of the received signal or the whole of the random initial phases of the pulse oscillations for incoherent emission, etc.

The statistical characteristics of random parameters and processes are considered to be given, i.e., precisely:

- the statistics of interference $n(t)$;
- the pre-experience (a priori) probabilities $P(A_1)$ and $P(A_0) = 1 - P(A_1)$ of the values A_1 and A_0 of the discrete parameter A (in detection);
- the a-priori probability density $p(\alpha_1, \alpha_2, \dots, \beta_1, \beta_2, \dots)$ of the values of measurable and immeasurable parameters; usually, but not always, $p(\alpha_1, \alpha_2, \dots, \beta_1, \beta_2, \dots) = p(\alpha_1, \alpha_2, \dots)p(\beta_1, \beta_2, \dots)$.

In the first place, it is necessary to solve the statistical problem of detection with the help of the adopted function $y(t)$ and the preexperience (a priori) data. This implies that for the quantity A estimates A^* (0 or 1) must be chosen such as to yield the minimum of the mean risk (or, equivalently, the maximum of the weight criterion). In doing so, the law of optimum processing must be established, i.e.,

the entirety of mathematical rules by which the most efficient answer to the problem whether a useful signal is present or not can be given for each choice of the function $y(t)$. Finally, we have to regard the qualitative characteristics of optimum mathematical processing in detection and to consider the methods of its technical realization.

The solution of the statistical problem of measurement will consist in the choice of estimates α_1^* , α_2^* , ... for the measurable parameters α_1 , α_2 , ..., of which we only know the pre-experience (a priori) probability density $p(\alpha_1, \alpha_2, \dots)$. These estimates must be optimum from the point of view of mean risk minimum. For a square value function (which will be given in the following) the latter demand is equivalent to that of the minimum of the mean square deviation. As in the case of detection, we have to regard the qualitative characteristics of optimum processing in the measurements and to consider the methods of realizing it technically.

Before we enter the analysis of the posed problems for comparatively general and practically important cases, we shall consider extremely simple examples of statistical approach to problems of detection and measurement.

§1.5. AN EXAMPLE OF ONE-DIMENSIONAL OPTIMUM DETECTION

Let us consider an indicating instrument whose indication is characterized by the number y (Fig. 1.5). Either the sum of the signal voltage x and of that of the interference n , such that

$$y = x + n, \quad (1)$$

or the voltage of the interference alone

$$y = n. \quad (2)$$

enter the instrument. During the time of observation the quantities x , y and n do not change. The expected value of the signal x is exactly known.

The law of distribution of the random quantity \underline{n} is also assumed to be given: we shall consider it to be a normal one (Gaussian) in the following consideration. According to the measured value of \underline{y} it is necessary to choose the optimum solution which of the two cases (1) or (2) mentioned is taking place.

It is easy to see that the problem formulated is a simpler variant of a more general detection problem (§1.4). Its peculiar feature lies in the fact that instead of the functions of time $y(t)$, $n(t)$ and $x(t)$, α_1 , α_2 , ..., β_1 , β_2 , ... the corresponding one-dimensional quantities are considered: the random quantities \underline{y} and \underline{n} and the nonrandom quantity \underline{x} . In contrast to the general case the quantity \underline{x} does not depend on parameters.

Instead of (1) and (2) we may write one expression

$$\underline{y} = \underline{n} + A\underline{x}, \quad (3)$$

for the sake of uniformity in denotation, in which the discrete parameter A is equal to 0 or 1. Thus, the problem reduces to an estimation of A^* , according to the measured value of \underline{y} , an estimation which must be optimum from the point of view of the criterion of the minimum mean risk or the weight criterion equivalent to it.

Fig. 1.6a shows the probability densities of the random quantity \underline{y} under the conditions of the signal absent $A = A_0 = 0$ or present $A = A_1 = 1$:

$$\begin{aligned} p(y|A_0) &= p_n(y), \\ p(y|A_1) &= p_{sn}(y). \end{aligned} \quad (4)$$

The subscripts "p" and "sp," here, indicate that the mathematical expressions $p_p(y)$ and $p_{sp}(y)$ are different whether there is the interference alone or a signal with interference. The curve $p_{sp}(y)$ is shifted by a constant amount \underline{x} relative to the curve $p_p(y)$. Mathema-

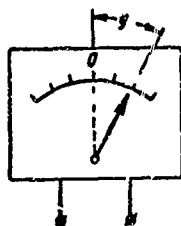


Fig. 1.5. Very simple indicating instrument.

matically, this can be written:

$$p_{en}(y) = p_n(y - x). \quad (5)$$

Any regular solution to the detection problem can be described by a solution function $A^*(y)$ which assumes one of the two values: 0 or 1, according to the value of y .

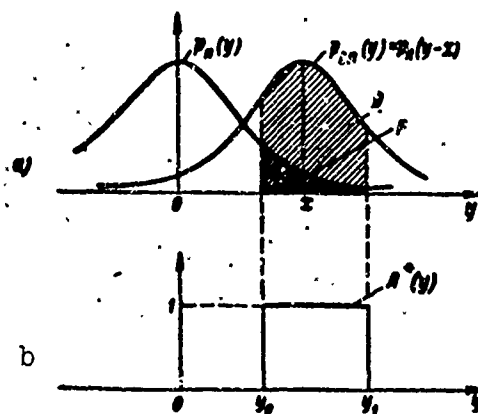


Fig. 1.6. Conditional probability densities $p_p(y)$ and $p_{sp}(y)$ (curves a); diagram of one of the possible solution functions $A^*(y)$ (curve b).

Fig. 1.6b shows the diagram of one of the possible solution functions (not necessarily optimum). It follows from the diagram that in the given case for $y_0 < y < y_1$ a solution with a signal present is taken. The conditional probabilities D and F are, in this case, determined as the probabilities of the random quantity y falling into the interval $y_0 - y_1$ under the conditions "signal - interference" or "interference," respectively. For the special solution function of (Fig. 1.6b) these probabilities are calculated from the formulas

$$\left. \begin{aligned} D &= \int_{y_0}^{y_1} p_{en}(y) dy, \\ F &= \int_{y_0}^{y_1} p_n(y) dy \end{aligned} \right\} \quad (6)$$

and correspond to the crosshatched areas below the curves $p_{sp}(y)$ and

$p_p(y)$ in the diagram (Fig. 1.6a).

If we introduce an arbitrary solution function $A^*(y)$ in the general case, the expressions for D and F may be written as integrals with infinite limits

$$\left. \begin{aligned} D &= \int_{-\infty}^{\infty} A^*(y) p_{cn}(y) dy, \\ F &= \int_{-\infty}^{\infty} A^*(y) p_n(y) dy. \end{aligned} \right\} \quad (7)$$

In fact, the y intercepts for which $A^*(y) = 0$ will all yield zero in the integration. The intercepts for which $A^*(y) = 1$ correspond to areas below the curves $p_{sp}(y)$ and $p_p(y)$ in the same way as was shown in Fig. 1.6a. It is important to realize that the Relations (7) are correct for an arbitrary solution function $A^*(y)$, in contrast to Eqs. (6).

The expression $D - l_0 F$ which corresponds to the weight criterion may then be represented in the form

$$D - l_0 F = \int_{-\infty}^{\infty} p_n(y) A^*(y) [1 - l_0] dy, \quad (8)$$

where

$$l(y) = \frac{p_{cn}(y)}{p_n(y)}. \quad (9)$$

According to the weight criterion, a detection system maximizing the integral (8) is optimum. In order to fulfill this condition, it is sufficient to achieve the greatest value of the expression under the integral sign for each y by choosing the solution function $A^*(y)$ approximately. But this function can only assume two values: 0 or 1, such that, according to the way it is chosen, the expression under the integral sign either vanishes or is multiplied by one. Although the problem of obtaining the maximum is nonstandard it can be solved easily. Obviously, among two numbers — a positive one and zero — the positive number is greater, whereas zero is greater than any negative num-

ber. Consequently, the greatest value of the expression under the integral sign for each y , but also of the integral as a whole, can be obtained in the following way:

1) we put $A^*(y) = 1$, if the expression under the integral sign is positive in this case;

2) we put $A^*(y) = 0$, if for $A^*(y) = 1$ the expression under the integral sign is negative.

Since the probability density $p_p(y)$ is not a negative number, the optimum rule for the solution to the detection problem may be written in the form

$$A^*(y) = \begin{cases} 1, & \text{if } l(y) > l_0, \\ 0, & \text{if } l(y) < l_0. \end{cases} \quad (10)$$

The quantity $l(y) = p_{sp}(y)/p_p(y)$ is termed the probability ratio. The probability ratio is the ratio of the probability densities of the same realization of "y" under two conditions: if the signal and the interference are acting and if the interference is acting alone. Similar to the two probability densities, also the probability ratio cannot be negative.

Thus, the probability ratio criterion, which is a consequence of the general criterion of the mean risk minimum can be used as a criterion of optimum detection. According to the probability ratio criterion, the solution of existing signal is adopted if the probability ratio exceeds some threshold value l_0 . This criterion is the most convenient for practical calculations.

We note that the assumption of a normal (Gaussian) law of interference distribution was not used, as yet. The discussions given are, therefore, valid for any distribution law.

Furthermore, let us assume that the interference is described by a central Gaussian distribution with a dispersion n_0^2 or a standard de-

viation n_0 . Bearing in mind that $y = n$, if there is no signal we have

$$p_n(y) = \frac{1}{\sqrt{2\pi n_0}} e^{-\frac{y^2}{2n_0}} \quad (11)$$

Hence, in view of Eq. (5),

$$p_{en}(y) = \frac{1}{\sqrt{2\pi n_0}} e^{-\frac{(y-x)^2}{2n_0}} \quad (12)$$

In this case, the probability ratio will be

$$l(y) = \frac{e^{-\frac{(y-x)^2}{2n_0}}}{e^{-\frac{y^2}{2n_0}}} = e^{-\frac{x^2}{2n_0}} e^{\frac{xy}{n_0}} \quad (13)$$

Figure 1.7 shows the behavior of $l(y)$ for $x > 0$. The threshold value l_0 is plotted on the axis of ordinates. §1.3 dealt with the possible ways of choosing the values l_0 . Since the curve $l(y)$ is monotone, the condition $l(y) > l_0$ is equivalent to the condition $y > y_0$, and the condition $l(y) < l_0$ is equivalent to the condition $y < y_0$ (Fig. 1.7). Hence, for $x > 0$

$$A_{opt}^*(y) = \begin{cases} 1, & \text{if } y > y_0, \\ 0, & \text{if } y < y_0. \end{cases} \quad (14)$$

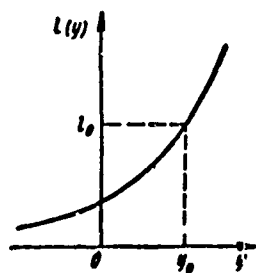


Fig. 1.7. Dependence of probability ratio on the result of observation.

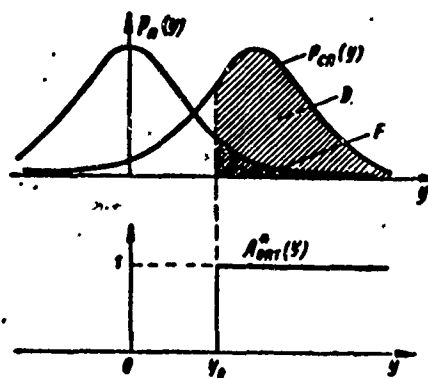


Fig. 1.8. Curves of the conditional probability densities $p_p(y)$, $p_{en}(y)$ and diagram showing the optimum solution function $A_{opt}^*(y)$.

Expression (14) for the optimum solution function shows that the solution function chosen initially (Fig. 1.6b) was not optimum. A diagram analogous to Fig. 1.6, but with the optimum solution function is given in Fig. 1.8.

It follows from Fig. 1.8 that the probability of false alarm F in the case of an optimum solution function corresponds to the area below the curve $p_p(y)$ to the right of the abscissa y_0 . The value y_0 will be called threshold. For a given interference level the probability of false alarm F depends only on the value of y_0 :

$$F = \int_{y_0}^{\infty} p_n(y) dy = \frac{1}{\sqrt{2\pi}} \left[\int_0^{\infty} e^{-\frac{s^2}{2}} ds - \int_0^{\frac{y_0}{n_0}} e^{-\frac{s^2}{2}} ds \right] = \frac{1}{2} \left[1 - \Phi\left(\frac{y_0}{n_0}\right) \right]. \quad (15)$$

where $\Phi(u)$ is the probability integral [(6) §1.2]. This implies that the threshold value can immediately be chosen according to the given level of probability of false alarm, which corresponds to the Neuman-Pearson criterion. A similar approach is most convenient for the real designing of the equipment since it makes it possible to avoid the necessity of taking account of a-priori (pre-experience) data on the or absence of a signal.

The probability of correct detection D corresponds to the area below the curve $p_{sp}(y)$ to the right of the abscissa y_0 :

$$D = \int_{y_0}^{\infty} p_{sn}(y) dy = \frac{1}{\sqrt{2\pi}} \left[\int_0^{\infty} e^{-\frac{s^2}{2}} ds - \int_0^{\frac{y_0 - x}{n_0}} e^{-\frac{s^2}{2}} ds \right] = \frac{1}{2} \left[1 + \Phi\left(\frac{y_0 - x}{n_0}\right) \right].$$

or finally

$$D = \frac{1}{2} \left[1 + \Phi\left(\frac{x - y_0}{n_0}\right) \right]. \quad (16)$$

For a given interference level n_0 is not only a function of the threshold y_0 , but also of the value of the expected signal \underline{x} .

The behavior of $D(x)$ can be plotted qualitatively from an analysis of the area below the curve $p_{sp}(y)$ in Fig. 1.8 and quantitatively in accordance with Eq. (16). For $x = 0$ the value of $D = F$, for $x = y_0$ the value of $D = 0.5$, for $x \gg y_0$ the value of $D \approx 1$. The higher the level of the threshold y_0 , the more the curve $D(x)$ is shifted to the right. This implies that a higher level of the useful signal is required to guarantee the same probability D . The curves drawn in Fig. 1.9 are termed detection curves.

Thus, the very important probability ratio criterion was established by considering the example of analyzing the one-dimensional optimum detection. Subsequently, we shall satisfy ourselves of the fact

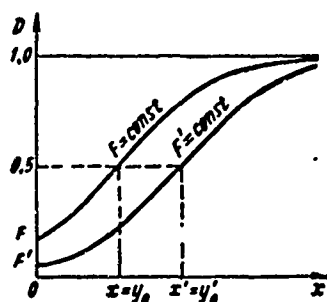


Fig. 1.9. Detection curves of a one-dimensional signal.

that the concept of probability ratio will help us to solve all following problems. From the expression for the probability ratio the optimum solution function $A_{opt}^*(y)$ corresponding to a simple comparison of the magnitude of y with the threshold y_0 was found. The detection curves specifying the qualitative characteristics of optimum detection under different operating conditions of the detec-

tor were plotted. Furthermore, the problems of finding optimum solution functions and plotting detection curves will prove to be important sections of the theory of real signal detection.

§1.6. EXAMPLES OF ONE-DIMENSIONAL OPTIMUM MEASUREMENT

Let us return to the indicating instrument (Fig. 1.5), but put a somewhat different problem. As before, we shall assume that the indication y of the instrument is the sum of the interference \underline{n} and the sig-

nal \underline{x} :

$$y = n + x. \quad (1)$$

In contrast to the preceding case, however, the signal is certainly present, but its value \underline{x} is unknown.

The problem lies in assigning an estimate x^* to the quantity to be measured \underline{x} making use of the measured value of \underline{y} and the a priori known probability density $p_0(x)$ of \underline{x} . In this case, the estimate x^* must satisfy the criterion of mean risk minimum

$$\bar{r} = \int_{-\infty}^{\infty} \int_{-\infty}^{\infty} r(x^*, x) p(x^*, x) dx^* dx = \min, \quad (2)$$

i.e., it must be optimum.

We shall only consider regular solutions where for each measured value \underline{y} a quite definite estimate $x^* = x^*(y)$ is given. Replacing then the probability element

$$p(x^*, x) dx^* dx \text{ by } p(x, y) dx dy,$$

where $p(x, y)$ is the total probability density of the quantities \underline{x} and \underline{y} , we obtain

$$\bar{r} = \int_{-\infty}^{\infty} dy \int_{-\infty}^{\infty} r(x^*, x) p(x, y) dx \text{ at } x^* = x^*(y). \quad (3)$$

Putting, by virtue of the multiplication theorem,

$$p(x, y) = p(y) p(x|y),$$

we may rewrite Expression (3) in the form

$$\bar{r} = \int_{-\infty}^{\infty} dy \int_{-\infty}^{\infty} r(x^*, x) p(y) p(x|y) dx.$$

Or

$$\bar{r} = \int_{-\infty}^{\infty} r(x^*(y)) p(y) dy \text{ for } x^* = x^*(y). \quad (4)$$

where

$$r(x^*(y)) = \int_{-\infty}^{\infty} r(x^*, x) p(x|y) dx. \quad (5)$$

Relation (5) gives the mean risk as calculated for a fixed value of the measured quantity y (the mean value is here taken over x). We say that the conditional mean risk is obtained as the result of this process of taking the mean. The mathematical expectation of the conditional mean risk (4) as calculated by taking account of the probability density of the measured values of y yields the absolute mean risk.

In order to minimize the absolute mean risk (4) it is sufficient to obtain the smallest value of the expression (4) under the integral sign for each y by choosing the estimate function $x^* = x^*(y)$ appropriately. The latter is analogous to the choice of the solution function $A^*(y)$ in the detection problem [(8) §1.5].

The quantity $p(y)$ in Expression (4) is a given function and cannot assume negative values. Consequently, the expression (4) under the integral sign is minimized if for each y the minimum of the conditional mean risk $r(x^*|y)$ is guaranteed.

In this connection, we will return to Relation (5). The post-experience (a posteriori) probability density $p(x|y)$ enters its expression under the integral sign, i.e., the probability density of the quantity x under the condition that the value y has been measured. According to the multiplication theorem

$$p(x, y) = p(x) p(y|x) = p(y) p(x|y)^*, \quad (6)$$

hence

$$p(x|y) = \frac{1}{p(y)} p(x) p(y|x).$$

In order to minimize the conditional mean risk (5) the course of the corresponding curve of the a-posteriori known probability density $p(x|y)$ as a function of x must be known.

Integrating Eq. (6) over the variable x and bearing in mind that

for any y

$$\int_{-\infty}^{\infty} p(x|y) dx = 1$$

being an integral with infinite limits of the probability density, we obtain

$$p(y) = \int_{-\infty}^{\infty} p(x) p(y|x) dx. \quad (7)$$

It follows from the obtained expressions that

$$p(x|y) = \frac{p(x) p(y|x)}{\int_{-\infty}^{\infty} p(x) p(y|x) dx}. \quad (8)$$

Equations (7) and (8) are, respectively, analogous to the formula for the total probability and to Bayes' formula for the probability densities.

Since the denominator of Relation (8) is independent of x , the latter can be represented in the following form for each measured value of y

$$p(x|y) = k_y p(x) p(y|x). \quad (9)$$

The normalizing factor k_y in Eq. (9)

$$k_y = \frac{1}{p(y)} = \frac{1}{\int_{-\infty}^{\infty} p(x) p(y|x) dx} \quad (10)$$

determines the scale of the curve $p(x|y)$ on the x axis such that the area below this curve is equal to unity.

The function $p(x)$ in Eq. (9) describes the a-priori probability density of the values of the signal x , and $p(y|x)$ describes the conditional probability density of the quantity y . By virtue of Eq. [(5) §1.5]

$$p(y|x) = p_n(y - x). \quad (11)$$

Thus, Eq. (9) can be rewritten in the form

$$p(x|y) = k_y p(x) p_n(y - x). \quad (12)$$

We shall illustrate the obtained Relation (12) on the following assumptions:

1) the a-priori probability density of the quantity x is described by the expression

$$p(x) = p_0(x) = \begin{cases} 0 & \text{for } x < x_1 \text{ и } x > x_2, \\ \frac{1}{x_2 - x_1} & \text{for } x_1 < x < x_2; \end{cases}$$

2) the interference distribution obeys a normal law [(11) § 1.5].

Figure 1.10a shows the curve of the a-priori probability density $p_0(x)$. Figure 1.10b shows the curve

$$p(y|x) = p_n(y-x) = \frac{1}{\sqrt{2\pi}n_0} e^{-\frac{(y-x)^2}{2n_0^2}} \quad (13)$$

as a function* of the unknown value of x . This curve is a Gaussian curve, plotted on the x -axis. Its dispersion is equal to n_0^2 , and its mean value is equal to the measured value of y .

Figure 1.10c shows the curve of the a-posteriori probability density $p(x|y)$, obtained by multiplying the curves $p_0(x)$ and $p(y|x)$, taking account of the normalizing factor k_y . The area below this curve is equal to unity. The curve $p(x|y)$ takes into account both the result of measuring y and the a-priori data on the possibility values of the quantity to be measured x and the interference n .

The interference level exerts an essential influence on the a-posteriori distribution. In order to realize this, let us consider two limiting cases:

1) the interference is very weak — small compared to the interval of measurable values ($n_0 \ll x_2 - x_1$):

2) the interference is very strong — great compared to the interval of measurable values ($n_0 \gg x_2 - x_1$).

Figure 1.11a shows the curves $p_0(x)$ and $p(x|y) \approx p(y|x)$ for the

case of a weak interference. In this case, the curve of the a-posteriori distribution is determined by the result of measuring y and the dispersion of the interference n_0^2 .

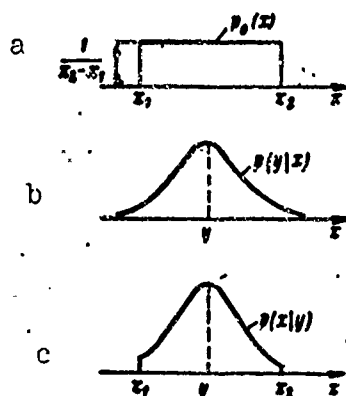


Fig. 1.10. Probability density curves. a) Of a priori $p_0(x)$; b) of the probability density $p(y|x)$ of the measured value of y as a function of the true value of x ; c) of the a-posteriori probability density $p(x|y)$.

Figure 1.11b shows the curves $p(y|x)$ and $p(x|y) \approx p_0(x)$ for the case of strong interference. In this case the curve of the a-posteriori distribution is practically equal to the curve of the a-priori distribution since the results of the measurement are not reliable.

The considered relations and examples of a-posteriori probability density curves $p(x|y)$ permit us to return to the problem of choosing the optimum estimate $x_{\text{opt}}^* = x_{\text{opt}}^*(y)$. We shall require that this estimate should minimize the conditional mean risk (5)

$$r(x^*|y) = \int_{-\infty}^{\infty} r(x^*, x) p(x|y) dx = \min. \\ \text{for } x^* = x_{\text{opt}}^*(y). \quad (14)$$

In the following we shall only use the square error value

$$r(x^*, x) = (x^* - x)^2. \quad (15)$$

This implies that the mean risk and the conditional mean risk reduce to the mean square deviations.

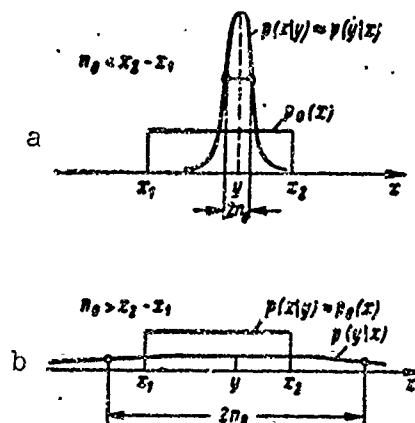


Fig. 1.11. Curves of the a-priori and a-posteriori probability densities: a) For weak interference, $n_0 < x_2 - x_1$; b) for strong interference, $n_0 > x_2 - x_1$.

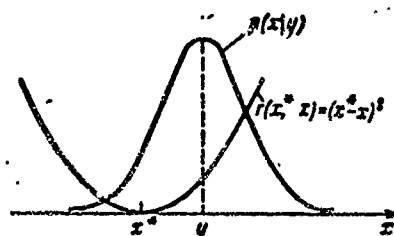


Fig. 1.12. Curves of the a-posteriori probability density curve $p(x|y)$ and the error value $r(x^*, x)$ if the estimate x^* was chosen unfavorably.

Figure 1.12 shows the curve of the a posteriori probability density $p(x|y)$ and the error value curve for an arbitrary estimate x^* . Obviously, the estimate x^* differs considerably from the optimum in the given case, since a considerable error charge corresponds to the most probable values of x , and a value of x with low probability corresponds to the estimate x^* itself.

In order to obtain the optimum estimate, we put the derivative of the conditional mean risk with respect to the estimate x^* equal to

zero, i.e., we put

$$\frac{d}{dx^*} \int_{-\infty}^{\infty} (x - x^*)^2 p(x|y) dx = 0 \text{ for } x^* = x_{\text{opt}}.$$

Hence we obtain that

$$x_{\text{opt}} = \int_{-\infty}^{\infty} x p(x|y) dx = M_1\{x|y\}, \quad (16)$$

i.e., the optimum estimate is found to be the center of gravity (first moment) of the a-posteriori distribution curve. In other words, it is equal to the a-posteriori mathematical expectation of the value x .

Using Eqs. (14)-(16) we find for the magnitude of the conditional mean risk in the case of optimum estimate

$$r(x_{\text{opt}}|y) = \int_{-\infty}^{\infty} [x - M_1\{x|y\}]^2 p(x|y) dx = D\{x|y\}. \quad (17)$$

As can be seen from Eq. (17) the quality of the optimum estimate carried out is determined by the dispersion of the a-posteriori distribution $D\{x|y\}$. The dispersion of the distribution can be expressed in terms of its first and second moments

$$D\{x|y\} = M_2\{x|y\} - M_1^2\{x|y\}, \quad (18)$$

which follows immediately from Expression (17).

Here

$$M_2\{x|y\} = \int_{-\infty}^{\infty} x^2 p(x|y) dx. \quad (19)$$

Taking the mean of the quantity $r(x_{\text{opt}}|y)$ over all possible values of y according to (4), we obtain for the optimum estimates

$$\bar{r} = \int_{-\infty}^{\infty} D\{x|y\} p(y) dy. \quad (20)$$

Equation (20) characterizes the minimum value of the mean square of the error for the entirety of measurement conditions. This minimum is guaranteed by condition (17); if it is fulfilled (for arbitrary y) the estimate has no constant error, i.e.,

$$M_1\{x^* - x\} = M_1\{(x^* - x)|y\} = 0.$$

We shall illustrate the obtained results by the examples of a-posteriori distributions for a onedimensional measurement (Fig. 1.11) in the case of a very strong and a very weak Gaussian interference.

In the case of a very strong interference (Fig. 1.11b) the center of gravity of the a-posteriori distribution curve and the optimum estimate are equal to $\frac{x_1 + x_2}{2}$, independent of the measured value of y . In contrast to this result, the optimum estimate is equal to the measured value of y in the case of a weak Gaussian interference (Fig. 1.11a) since in this case y corresponds to the center of gravity of the a-posteriori distribution curve.

In the case of symmetric convex distribution curves the center of gravity always coincides with the curve maximum. Consequently, the abscissa of the maximum of the a-posteriori distribution curve

$p(x|y)$ is often chosen for the optimum estimate, instead of (16). Such an estimate will be termed most probable estimate. Thus, in the case of $n_0 \ll x_2 - x_1$ considered above the estimate $x^* = y$ is the most probable estimate.

The quality of the optimum estimates x^*_{opt} for the a-posteriori distributions $p(x|y)$ in example (Fig. 1.11) may be established on the basis of Eqs. (17) and (20). For weak Gaussian interferences (Fig. 1.11a) we have

$$r(x^*_{\text{opt}}|y) = D\{x|y\} = n_0^2.$$

Since the mean square of the error is independent of y , it is not changed after taking the mean over y , i.e., we have also $\bar{r} = n_0^2$. For very strong interferences (Fig. 1.11b) the dispersion of the a-posteriori distribution coincides with the dispersion of the a-priori one, and its value is independent of y :

$$\bar{r} = r(x_{\text{opt}}^* | y) = D\{x|y\} = D\{x\},$$

where

$$D\{x\} = \int_{x_1}^{x_2} x^2 \frac{1}{x_2 - x_1} dx - \left[\int_{x_1}^{x_2} x \frac{1}{x_2 - x_1} dx \right]^2 = \frac{(x_2 - x_1)^2}{12}.$$

The optimum root-mean-square deviation of the measurement for the examples (Fig. 1.11) will be: $\sigma_{\text{opt}} = n_0$ for a very weak interference and $\sigma_{\text{opt}} = \frac{x_2 - x_1}{\sqrt{12}}$ for a very strong one. Thus, a variation of the interference from a very strong to a weak one varies the magnitude of this error by $\frac{x_2 - x_1}{n_0 \sqrt{12}}$ times.

With this remark we shall finish the consideration of examples of one-dimensional optimum measurement. It was shown in the course of the consideration that the mean risk can be minimized starting from the a-posteriori distribution curve of the values of the quantity to be measured. In the case of a quadratic error value the optimum estimate corresponds to the center of gravity of this curve and in many cases can be replaced by the most probable estimate. If the a-posteriori distribution is known also the optimum root-mean-square deviation of the measurement can be estimated.

The statistic approach illustrated by the examples of one-dimensional optimum measurement is most widespread in the analysis of the measurement of real radar signal parameters. In doing so, first only single, but then also successive multiple measurements will be considered.

Manu-
script
Page
No.

[Footnotes]

- 31 In the given denotation $p(x)$ and $p(y)$ are different functions, and not the same function with a different argument. This way of labeling which is frequently used in statistics will also be adopted in the following.
- 33 We remind that this curve is represented in Fig. 1.6a or 1.8b as a function of the measured value of y . In this connection, the value of x was considered to be fixed.

Manu-
script
Page
No.

[Transliterated Symbols]

- 10 доп = dop = dopustimyy = admissible
- 12 скв = skv = srednekvadratichnyy = root mean square
- 12 вер = ver = veroyatnyy = probable
- 13 макс = maks = maksimal'nyy = maximum
- 19 опт = opt = optimal'nyy = optimum
- 23 п = p = pomekha = interference
- 23 сп = sp = signal s pomekhoy = signal with interference

Chapter 2

SIGNALS AND INTERFERENCES IN THE THEORY OF DETECTION AND MEASUREMENT

§2.1. PROPERTIES OF REAL RADAR SIGNALS

Let us watch how a radar signal is formed. We consider the target to be point-like and at rest and the conditions of radio-wave propagation to be ideal. Let a radio transmitter produce modulated high-frequency oscillations which are described by the function $s_0(t)$ except for an amplitude factor. Furthermore, since with most of radars the antenna beam for scanning the space is formed according to a law chosen earlier (Fig. 2.1), the transmission factor of the antenna in the direction of the target will be a nonrandom function of time $H_1(t)$.* The sounding radar signal can be described by an expression of the form $s_0(t)H_1(t)$, in this case. The field of the reflected signal arriving from the point-like target with a delay of t_3 will be, except for a factor,

$$s_0(t-t_3)H_1(t-t_3),$$

where $t_3 = \frac{2r}{c}$ (r is the distance from the target).

When the beam of the receiving antenna is formed its transmission factor for oscillations of this field is also a function of time $H_2(t)$. Consequently, the signal entering the input of the receiver is subject to an additional modulation by the function $H_2(t)$ and can be written in the form

$$x(t) = s_0(t-t_3)H_1(t-t_3)H_2(t).$$

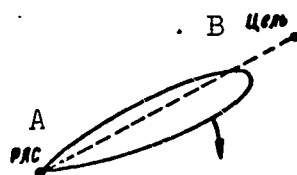


Fig. 2.1. Explanation of the process of radar signal formation in scanning. A) RLS; B) target.

For ordinary single-antenna radars $H_1(t) = H_2(t) = H(t)$. Besides, the displacement of the antenna beam during the time of delay is, as a rule, small compared to the width of the radiation pattern such that

$$H(t - t_s) \approx H(t)$$

and

$$x(t) \approx H^2(t) s_s(t - t_s). \quad (1)$$

Thus, a radar signal that is reflected from a point-like target at rest is a modulated oscillation $x(t)$ whose modulation law is determined both by the way the transmitter modulator works and by the behavior of the antenna beam in transmission and reception. A radar may have several operating conditions, but for each of these conditions the modulation law is considered to be fixed.*

The oscillation $x(t)$ is a high-frequency one, and it can be represented in the form

$$x(t) = X(t) \cos[\omega_0 t + \varphi_x(t)], \quad (2)$$

where ω_0 is the carrier frequency, and $X(t)$ and $\varphi_x(t)$ are functions which usually vary slowly compared to the oscillations of the carrier frequency $\cos \omega_0 t$. These functions describe the laws of the amplitude and phase modulations, respectively.

We shall give some very simple examples of radar signals.

Figure 2.2 shows: a signal in the form of a short radio pulse $x(t)$, its envelope $X(t)$, and also the initial phase $\varphi_x(t)$. In the given case, we note that there is no phase modulation. Consequently, $\varphi_x(t) = \text{const.}$ Such a signal is obtained in the case of a pulse modulation of the transmitter if one pulse is transmitted to the point-like target.

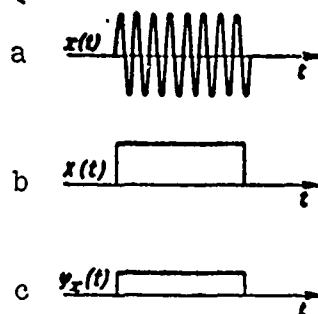


Fig. 2.2. Example of a radio pulse (a); its envelope (b); time-dependence of the initial phase (c).

Figure 2.3a shows a signal in the form of a packet of short radio pulses following one another after a sending time T in the case of uniform antenna beam formation relative to the direction toward the target. Fig. 2.3b shows the envelope of the packet whose shape depends on the modulation law governing the formation of the beam. Fig. 2.3c shows the initial pulse phases on the assumption that the target is at rest, the transmitter pulses have the same in-

initial phase and that the formation of the antenna beam does not give rise to a phase modulation.

Packets whose phase varies from pulse to pulse according to a definite law are termed coherent packets.

Figure 2.4. shows a coherent packet characterized by its phase structure. The variation of the phase from pulse to pulse due to the motion of the target (toward the radar) with a constant radial velocity of $v_r = \text{const}$ is taken into account. For this reason, the path of the electromagnetic oscillations to the target and back is reduced by $r_r = 2v_r T$ during each sending period T . Thus, the phase delay is reduced and the initial phase of the signal is increased by

$$\varphi_r = \frac{2\pi}{\lambda} r_r \quad \text{from pulse to pulse, where } \lambda \text{ is the wavelength.}$$

The difference in the phase structure of the coherent packets in Fig. 2.3. and 2.4 due to the motion of the target is additionally illustrated by Fig. 2.5, where the mn intercept of Fig. 2.4 is drawn at a larger scale. The solid curve corresponds to a target moving with constant radial velocity, and the dotted line to a target at rest.

Figure 2.6 allows for an indefiniteness in the initial phase of the emitted oscillations, which arises if the initial phase of the

generated oscillations is random and not kept in mind in order that it can be eliminated in the reception.

A packet with random phase variation from pulse to pulse (Fig. 2.6) is termed incoherent pulse packet.

The analysis of a radar signal in the case of a nonpoint-like target can be simplified considerably if the diagram of the secondary reradiation having a petaloid form for nonpoint-like targets is introduced. Since the angular position of the target is random, also the signal has a random amplitude. If during the time of irradiation the target is shifted aside relative to the direction toward the radar (Fig. 2.7) the signal suffers an additional modulation, according to the kind of motion and the form of the secondary reradiation diagram. In this case, the envelope of the packet is distorted (Fig. 2.8). The same result can be obtained if the target is replaced by all elementary reflectors distributed over the volume it occupies. The distortion of the packet is here explained by the interference of the elementary packet signals from the point-like radiators superposed on each other. The shift of the target relative to the direction toward the radar gives rise to an inequality of the radial velocities of all target points and, therefore, also of the initial phases of the interfering pulses.

Thus, real radar signals have the following properties:

1. Regular modulation determined by the way in which the transmitter works and by the law of antenna beam formation.
2. Regular variation of the signal phase structure owing to the target moving with fixed velocity.
3. Random amplitude and phase modulation of the signal in the case of secondary radiation or presence of random signal parameters (if during the time of irradiation the target is not shifted remark-

ably relative to the direction toward the radar).

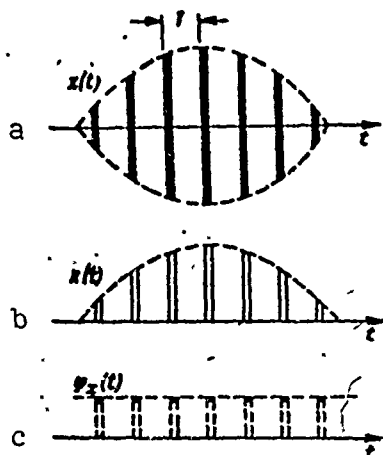


Fig. 2.3. Coherent Packet of reflected radio pulses (a); its envelope (b); time dependence of the initial phase (c) (case of reflector at rest).

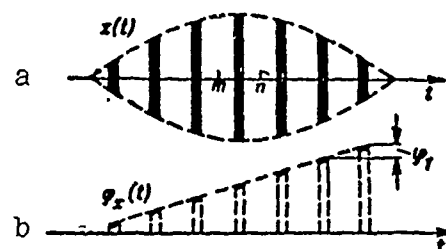


Fig. 2.4. Coherent packet of reflected radio pulses (a); time dependence of the initial phase (b) (case of point-like moving reflector).

It is essential feature that the delay of the signal depends on the distance from the target, and that the phase structure depends on the radial velocity. This fact makes it possible to measure both the distance and the radial velocity.

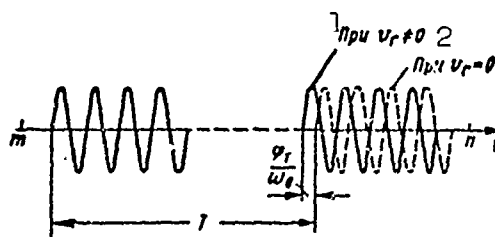


Fig. 2.5. Variation of the phase structure of a coherent packet of radio pulses in the case of a moving point-like reflector. 1) at; 2) at.

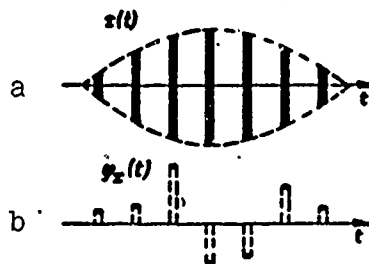


Fig.2.6. Incoherent packet of reflected radio pulses (a) and possible time dependence of the initial phase (b)

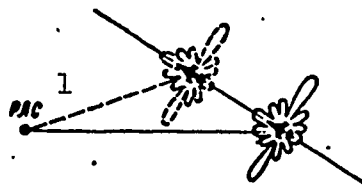


Fig.2.7. Explanation of the random modulation of a reflected signal in the case of a moving nonpoint-like target. 1) RLS.

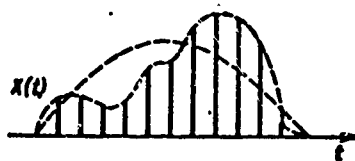


Fig. 2.8. Example showing the distortion of the envelope of a radio-pulse packet due to the motion of a nonpoint-like target.

§2.2. BASIC MODELS OF RADAR SIGNALS

Certain signal models are used in the theory of detection and measurement of parameters. A model must satisfy the contradictory demands of a sufficient similarity to the real signals and simplicity of theoretical analysis. The degree of generality of the results which can be obtained is also of essential significance. According to which of the demands is more important one or another model of radar signal of different degree of complexity is used.

The simplest model is an arbitrary signal with fully known parameters.

$$x(t) = X(t) \cos [\omega_0 t + \varphi_x(t)]. \quad (1)$$

In a detection problem only the fact if this signal is present is considered unknown.

According to the degree of complexity this model is followed by that of a signal with random initial phase

$$x(t, \beta) = X(t) \cos [\omega_0 t + \varphi_x(t) + \beta], \quad (2)$$

where β is a random quantity, uniformly distributed in the interval from 0 to 2π .

Furthermore, the model of a signal with random amplitude and initial phase can be introduced

$$x(t, \beta, B) = BX(t) \cos [\omega_0 t + \varphi_x(t) + \beta], \quad (3)$$

where not only β , but also B is a random quantity. Usually, the latter quantity can be regarded as distributed according to Rayleigh's law

$$p(B) = \frac{B}{B_0^2} e^{-\frac{B^2}{2B_0^2}} \quad (B > 0),$$

where the mean-square value of the amplitude is determined from the condition

$$\overline{B^2} = B_{rms}^2 = 2B_0^2.$$

We may put $B_{skv} = 1$, without loss of generality. Hence

$$p(B) = 2Be^{-B} \quad (B \geq 0). \quad (4)$$

The following model is a signal in the form of a packet non-fluctuating as to the amplitude with random initial phases of the individual nonoverlapping pulses

$$x(t, \beta_1, \beta_2, \dots) = \sum_k X_k(t) \cos[\omega_k t + \varphi_k(t) + \beta_k]. \quad (5)$$

Usually, the β_k are independent random quantities each of which is uniformly distributed in the interval from 0 to 2π . This model corresponds to an incoherent packet of radio pulses.

If all β_k are equal to the same random quantity β , the packet signal reduces to the signal (2) with random initial phase. In fact, expression (5) will go over into expression (2), if we assume within the limits of the k th pulse $X(t) = X_k(t)$, $\varphi_k(t) = \varphi_k(t)$, and in the intervals between the pulses $X(t) = 0$. Such a signal model with the same total phase for all pulses (see Fig. 2.3) is, obviously, a coherent pulse packet.

The expression

$$x(t, \beta_1, \dots, B_1, \dots) = \sum_k B_k X_k(t) \cos[\omega_k t + \varphi_k(t) + \beta_k] \quad (6)$$

contains random factors B_k allowing for the fluctuation of the packet envelope (Fig. 2.8), in contrast to the preceding expression. If all random factors B_k are equal: $B_1 = \dots = B_k = B$, we have the case of "friendly" fluctuations, where only the packet amplitude fluctuates, but the form of its envelope remains unchanged. Another limiting case is the independent fluctuation of the packet pulses, where all B_k are independent random quantities.

Thus, for detection problems the radar signal model can be represented by an expression of the form

$$x(t, \beta_1, \beta_2, \dots). \quad (7)$$

β_1, β_2, \dots are here random parameters whose common distribution law is given. Only the fact whether such a signal is present is considered unknown.

For problems concerning the measurement of parameters the signal can be denoted in an analogous way

$$x(t, \alpha_1, \alpha_2, \dots, \beta_1, \beta_2, \dots), \quad (8)$$

where, additionally, $\alpha_1, \alpha_2, \dots$ are parameters subject to measurement. Among these, e.g., there may be quantities characterizing the distance from the target, its radial velocity, angular coordinates, etc. The same fact whether the signal is present is considered unknown, in this case.

§2.3. FLUCTUATION INTERFERENCES AND THEIR STATISTICAL PROPERTIES

Fluctuation interferences (fluctuation noise) play a special role among the interferences limiting the possibilities of receiving weak radio signals. These interferences may be generated by various phenomena in the input units of the radio receiver, as, e.g., by thermal motion of the electrons in the conductors and resistances, by a short effect in the electronic amplifiers, etc.

Fluctuation noise may also be induced in the receiving antenna by electromagnetic oscillations due to all kinds of electron motions in the surrounding terrestrial or cosmic space. All these sources cannot be fully eliminated, a fact that explains also the particular role played by fluctuation noise among the other kinds of interference.

Fluctuation noise is one of the stationary random processes, i.e., of those processes whose mean statistic characteristics, as, e.g., their mean power, are constant in time.

In order to clarify the statistical laws governing the fluctua-

tion interferences, we shall turn to the simplest arrangement used to observe these interferences (Fig.2.9). This arrangement consists of the noise source, a linear band-pass amplifier, whose pass band Δf is considerably lower than the central frequency f_0 , and the oscillograph. We assume (as is usually the case, in reality) that the pass band of the amplifier is considerably narrower than the spectral width of the noise source.



Fig.2.9. Simplest arrangement used to observe fluctuation noise. A) Noise source; B) band-pass amplifier; C) oscillograph.

Obviously, the individual random random noise pulses will set swinging the oscillatory system of the amplifier. Since the pulses are random, the voltage at the output end of the amplifier will be given by an oscillation with

random amplitude and random initial phase (Fig.2.10)

$$n(t) = U_n(t) \cos[2\pi f_0 t + \varphi_n(t)], \quad (1)$$

since it is obtained by the reaction of the amplifier's oscillatory system superposed on each pulse.

The narrower the pass band Δf , the more time is taken by the transient in the amplifier circuits that is due to each individual pulse, and the more slowly vary the amplitude $U_n(t)$ and the phase $\varphi_n(t)$ compared to the high-frequency oscillations $\cos 2\pi f_0 t$ or $\sin 2\pi f_0 t$. On the other hand, the wider the band Δf , the sooner the reaction after each pulse comes to an end and the more chaotic the oscillation $n(t)$ will be.

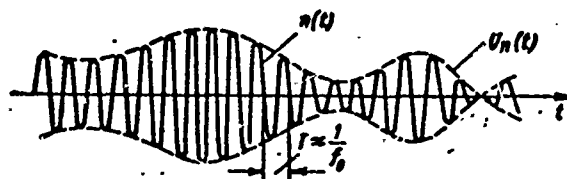


Fig.2.10. Random noise realization at the output of the resonance amplifier tuned to the frequency f_0 .

Let us choose at random a sufficiently great number of instants of time for the purpose of observation t_i ($i = 1, 2, \dots$) in an interval exceeding the value of $1/\Delta f$ by many times. As is well known, the latter quantity characterizes the duration of the transients in the oscillatory system. The position of this interval on the axis of time is unessential since the process is assumed to be stationary.

We shall consider the voltage values $n_i = n_i(t)$ at the chosen instants of time to be the values of a random quantity n characterized by the probability density $p(n)$. Since positive and negative values of n are equally probable, the distribution function $p(n)$ (Fig. 2.11) is symmetric relative to the axis of ordinates $n = 0$, such that the mean value is $\bar{n} = 0$. The probability of the values n_i lying in the interval from n to $n + dn$ will be equal to the crosshatched area $p(n)dn$. The whole area below the curve $p(n)$ is equal to unit. The distribution curve of the instantaneous values of fluctuation noise obeys a normal (Gaussian) law,

$$p(n) = \frac{1}{\sqrt{2\pi}n_0} e^{-\frac{n^2}{2n_0^2}} \quad (2)$$

where n_0^2 is the dispersion.

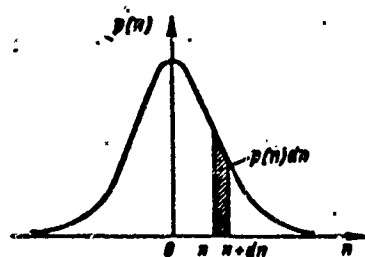


Fig. 2.11. The distribution curve $p(n)$ of the instantaneous values of the fluctuation oscillations.

The applicability of the Gaussian law to the case considered follows immediately from the central limit theorem of the theory of probability. At any instant of time, the voltage n at the amplifier output is composed of the results of a very great number of random effects each of which yields a component of the voltage with sufficiently small dispersion. Under this condition, the law of great numbers is valid and the distribution

of the quantity \underline{n} as well as that of the accidental errors ϵ , (§1.2) is sufficiently close to a normal one.

The distribution law of the instantaneous fluctuation noise values can be observed if the voltage $n(t)$ to be studied is fed from the amplifier output to the vertically deflecting plates of an oscillograph with switched off sweep. In this case, a bright vertical line of high intensity in the center and lower one at the edge will be observed on its screen. The curve of brightness distribution, which, e.g., can be taken by means of a photocell, will correspond to a normal distribution law (2).

Besides by the distribution law of the instantaneous values, the noise can also be characterized by the distribution law of its amplitude U_n and its initial phases φ_n .



Fig. 2.12. Distribution curve of the fluctuation oscillation amplitudes.

The values U_n and φ_n at the instants of time t_i , as well as the values n_i , are random quantities, the first of which is distributed according to Rayleigh's law (Fig. 2.12),

$$p(U_n) = \frac{U_n}{n_0^2} e^{-\frac{U_n^2}{2n_0^2}}, \quad (3)$$

whereas the second quantity has a uniform distribution within the limits from zero to 2π .

The distribution law $p(U_n)$ can be observed by using the same arrangement as in (Fig. 2.9) if a linear envelope detector is inserted between the amplifier and the oscillograph. In this case, a bright vertical line with an asymmetric brightness distribution will be observed on the screen. The brightness curve will, in this case, obey the Rayleigh law (3). The most intense brightness will correspond to the most probable value of the amplitude.

The distribution laws $p(n)$ and $p(U_n)$ characterizing the possible

oscillation amplitude at every instant of time does not make it possible to estimate the statistical connection of the oscillation values $n(t)$ at neighboring instants of time. Thus, they also do not permit a clarification of the general structure of the individual noise realizations (Fig.2.10) determined by the character of the transients in the amplifier circuits.

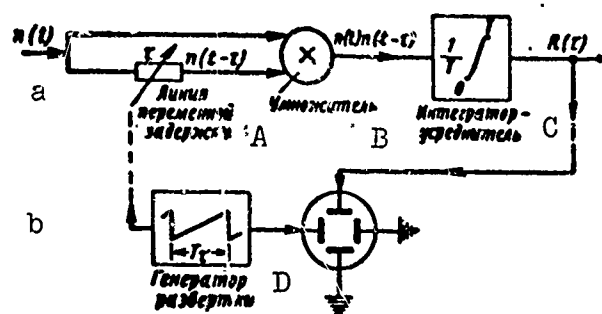


Fig.2.13. Diagram showing the oscillographic observation of the correlation function of fluctuation noise. A) Line of variable delay; B) multiplier; C) integrating averager; D) sweep generator.

To describe this structure it is sufficient to take the curve of the noise correlation function. The latter can be obtained experimentally if the circuit shown in Fig.2.13a is connected with the output of the amplifier (Fig.2.9).

In this circuit provision was made for a delay of the fluctuation voltage $n(t)$ by the time τ , multiplication of the delayed and non-delayed oscillations* and taking the time average which can be realized approximately by means of an RC-type integrating circuit.

As a result, we shall obtain a quantity, which can be adopted approximately as the true value of the noise correlation function, for each fixed delay τ :

$$R(\tau) = \overline{n(t)n(t-\tau)} = \lim_{T \rightarrow \infty} \frac{1}{T} \int_0^T n(t)n(t-\tau) dt. \quad (4)$$

The measured value will be the closer to the true one (4), the longer the period of averaging T compared to the duration of the transient, which can be measured by the quantity $1/\Delta f$.

The correlation function $R(\tau)$ characterizes the statistical connection between the value of the noise $n(t)$ at a given instant of time and its values at the preceding instants of time $n(t - \tau)$. In the general case, the quantity $n(t)$ has a component determinable by the value of $n(t - \tau)$, which can be considered the initial value. The influence of the initial conditions decreases when τ increases and becomes insignificantly weak if τ exceeds the duration of the transients. Consequently, if $\tau \gg 1/\Delta f$ the values of $n(t)$ and $n(t - \tau)$ become independent, and their product $n(t)n(t - \tau)$ a random quantity whose mean value is equal to zero.

Conversely, if τ is sufficiently small compared to the duration of the transients, any value of $n(t)$ is only slightly different from $n(t - \tau)$ and $R(\tau)$ is close to maximum

$$R(0) = \lim_{T \rightarrow \infty} \frac{1}{T} \int_0^T n^2(t) dt.$$

The value of $R(0)$ determines the mean power of the stationary process $n(t)$ for a load resistance of one ohm or, differently, the noise dispersion at the output end of the band-pass amplifier

$$R(0) = n_0^2.$$

The curve of the correlation function $R(\tau)$ can also be observed if the voltage is fed from the circuit output (Fig. 2.13a) to the vertically deflecting plate of the oscillograph (Fig. 2.13b) whose horizontal sweep is synchronized with the periodical variation of the delay time τ . The observed curve of the function $R(\tau)$ will have a shape similar to that drawn in Fig. 2.14b. In this case, the period of the sweep T_τ must exceed the time of integration considerably.

In the given case, the correlation function corresponds to the noise at the output end of the oscillatory system (Fig.2.9). Since the transients in this system are oscillatory, also the correlation function has the shape of a high-frequency oscillation whose amplitude decreases with increasing τ and approaches zero if $\tau \gg 1/\Delta f$. The zeros of the function $R(\tau)$ are separated by time intervals approximately or exactly equal to the natural oscillation period of the system. The damping of the correlation function amplitude for increasing τ is connected with the duration and the character of the transients in the system, which was discussed above.

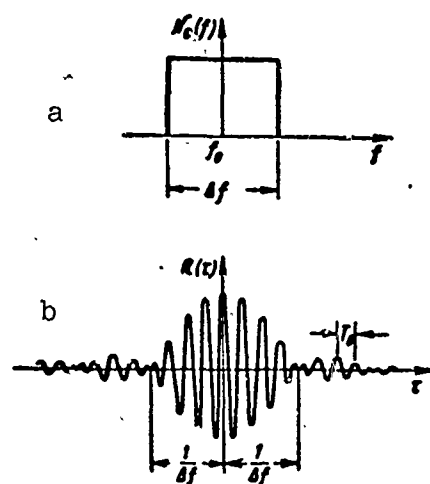


Fig.2.14. Example of a rectangular interference spectrum and the corresponding curve of the correlation function.

The course of the correlation function can also be explained from the spectral point of view.

As is well known from the theory of stationary random processes, the Fourier transform of the correlation function yields the spectral density of the noise or its energy spectrum to be determined in the range $-\infty < f < \infty$,

$$N(f) = \int_{-\infty}^{\infty} R(\tau) e^{-i2\pi f\tau} d\tau. \quad (5)$$

In its turn, the correlation function is given by

$$R(\tau) = \int_{-\infty}^{\infty} N(f) e^{i2\pi f\tau} df. \quad (6)$$

Since $R(\tau)$ is an even function, i.e., $R(\tau) = R(-\tau)$, $N(f)$ is also an even function. Consequently, an expansion in the frequency spectrum $0 < f < \infty$ is frequently used. This expansion is obtained by putting $N(f) = N(-f) = 1/2 N_0(f)$ in Eq. (6). In this case

$$R(\tau) = \int_0^{\infty} N_0(f) \cos 2\pi f \tau df. \quad (7)$$

In its turn, $N_0(f) = 2N(f)$. Using the fact that $R(\tau)$ is even we obtain finally

$$N_0(f) = 2 \int_{-\infty}^{\infty} R(\tau) e^{-j2\pi f \tau} d\tau = 4 \int_0^{\infty} R(\tau) \cos 2\pi f \tau d\tau. \quad (8)$$

Figure 2.14a shows an example of rectangular spectral density distribution of the noise $N_0(f)$ with a spectral width Δf . This case is particularly easy to calculate although the frequency characteristics of real physical systems, i.e., also the spectral density may not be strictly limited as to the frequency.

Carrying out the calculation according to formula (7) we obtain for this case

$$\begin{aligned} R(\tau) &= N_0 \int_{f_1}^{f_2} \cos 2\pi f \tau df = \\ &= N_0 (f_2 - f_1) \frac{\sin \pi (f_2 - f_1) \tau}{\pi (f_2 - f_1) \tau} \cos 2\pi \frac{f_2 + f_1}{2} \tau. \end{aligned} \quad (9)$$

The corresponding curve of $R(\tau)$ is drawn in Fig. 2.14b which illustrates graphically that

1) the curve $R(\tau)$ is symmetric relative to $\tau = 0$, i.e., the correlation function is even;

2) at $\tau = 0$ the correlation function assumes the maximum value

$$R(0) = N_0 (f_2 - f_1) = n_0^2,$$

equal to the noise dispersion or, in other words, to its mean power with a resistance of 1 ohm.

3) the high-frequency filling of the function $R(\tau)$ has the same period

$$T_0 = \frac{1}{f_0}, \text{ где } f_0 = \frac{f_2 + f_1}{2},$$

as the noise at the output end of the band filter.

Thus, if the distribution law of the instantaneous noise values

characterizes the noise statistics at each fixed instant of time the correlation function describes the statistical connection of noise values at instants of time separated by intervals τ . The smaller the ratio $R(\tau)/R(0)$, the weaker the statistical connection between them.

§2.4. White Noise as a Model of Fluctuation Noise

As is well known, the thermal radiation spectrum has different intensities for different frequencies. Within the limits of the radio-frequency range, however, its intensity is practically constant. At any rate, it can be affirmed that within the spectral ranges occupied by radar or other radio signals this intensity is constant. In order to simplify analysis one often passes, therefore, to the model of thermal noise with a perfectly uniform radiation spectrum. In analogy to the white light which is characterized by an equal spectral intensity in the whole frequency range corresponding to the visible part of the spectrum this model of thermal noise is termed white noise.

Let us return to the problem concerning the connection between the spectral density and the correlation function in order to extend this connection to the white noise.

Figure 2.15 shows the transition from noise in the frequency band $f_{\min} < f < f_{\max}$, to noise in the frequency band $0 < f < f_{\max}$, which will be called quasiwhite noise in the following, and, finally, the transition to the case $f_{\max} \rightarrow \infty$, corresponding to the introduction of the white noise model.

Figure 2.16 shows the correlation function of quasiwhite noise. The width of its main petal as taken between the zeros is equal to

$\frac{2}{f_{\max}}$, and its maximum value is equal to the noise dispersion $N_0 f_{\max}$.

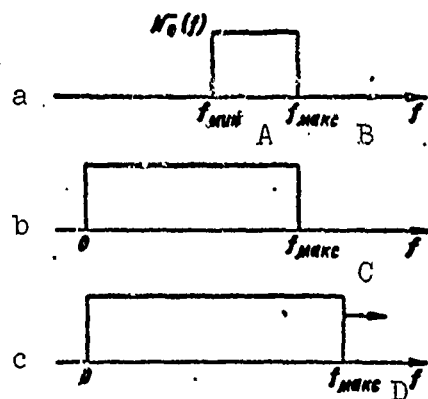


Fig.2.15. Explanation of transition to white noise. A) f_{\min} ; B) f_{\max} ; C) f_{\max} ; D) f_{\max} .

The area surrounded by the curve of the correlation function is determined from the relation [(8) §2.3] if we put $\tau = 0$ in it:

$$\int_{-\infty}^{\infty} R(\tau) d\tau = \frac{N_0}{2}. \quad (1)$$

This area does not depend on the value of f_{\max} .

It is easy to understand what happens with the correlation function if f_{\max} increases. It shrinks relative to the axis of abscissas and is stretched in the direction of the axis of or-

ordinates such that the area surrounded by the curve of the correlation function always remains equal to $N_0/2$. In the limiting case if $f_{\max} \rightarrow \infty$

$$R(\tau) = N_0 \int_{-\infty}^{\infty} \cos 2\pi f \tau df = \frac{N_0}{2} \int_{-\infty}^{\infty} e^{i2\pi f \tau} df,$$

or

$$R(\tau) = \frac{N_0}{2} \delta(\tau). \quad (2)$$

Here

$$\delta(\tau) = \int_{-\infty}^{\infty} e^{i2\pi f \tau} df \quad (3)$$

is the delta function which is equal to zero if $\tau \neq 0$. It becomes infinite for $\tau = 0$ and is characterized by the property that

$$\int_{-\infty}^{\infty} \delta(\tau) d\tau = 1. \quad (4)$$

Thus, the correlation function of white noise is described by a delta function except for a factor $N_0/2$. This implies that two arbi-

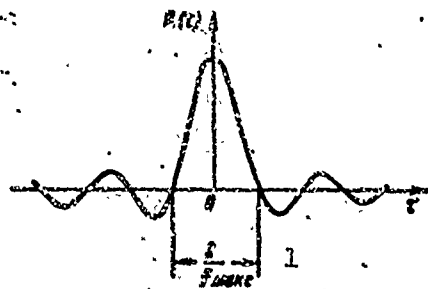


Fig. 2.16. Curve of correlation function for $f_{\min} = 0$. 1) f_{\max} .

trary values of noise corresponding to a finite interval τ between the moments of observation are not correlated with one another.

One says that white noise is delta correlated. This property considerably simplifies the mathematical calculations when white noise is used as an interference model.

§2.5. Approximation of Signals and Interferences

In the example of optimum detection and measurement (§1.5 and 1.6) considered earlier the probability densities $p_p(y)$ and $p_{sp}(y)$ of a one-dimensional random quantity y were used. The introduction of these functions was not difficult: the interference as well as the signal were characterized by only one numerical value y . The situation is completely different if the interference and the signal are functions of time. Obviously, neither of them can be described by one numerical value in the general case. In this connection the problem arises how many independent numerical values must be given in order to describe, e.g., the interference. In other words, how many degrees of freedom has this interference?

This problem is closely connected with the approximation of signals and interferences by series of the form

$$y(t) = \sum_k y_k \psi_k(t), \quad (1)$$

where $\psi_k(t)$ are nonrandom functions, and y_k are the expansion coefficients with respect to these functions, random for the expansion of the interference. If an interference is completely characterized by some set v of independent random coefficients y_k ($k = 1, 2, \dots, v$) one says that it has v degrees of freedom.

Most convenient for practical use are expansions where $\psi_k(t)$ are orthogonal functions of time, and the expansion coefficients of the interference y_k are independent random quantities. In this case, the

approximation (1) is termed canonical expansion.

The entirety of quantities y_k completely characterizing the realization of the interference $y(t)$ is a multidimensional random quantity whose distribution law may be regarded as the distribution law of the realizations. Thus, it is possible to speak of a multidimensional distribution law of one interference $p_p(y_1, y_2, \dots, y_k, \dots)$. If a signal is superposed on the interference, one has, however, to speak of a multidimensional distribution law of signal and interference $p_{sp}(y_1, y_2, \dots, y_k, \dots)$.

We shall not dwell on the general problems of constructing canonical expansions, but rather consider their construction for the quasiwhite noise model, i.e., noise in the limited frequency band $0 < f < f_{maks}$ with constant spectral density $N_0(f) = N_0$ in this band. The passage to the limit $f_{maks} \rightarrow \infty$ makes it possible to pass from the relations obtained in this case to the corresponding relations for the white-noise model.

First of all, we shall consider the properties of functions with limited frequency spectrum for the first time established in 1933 by the Soviet scientist V. A. Kotel'nikov, which equally belongs to random and nonrandom functions describing interferences and signals.

§2.6. KOTEL'NIKOV'S THEOREM

The essential statement of the theorem is the fact that an arbitrary function $y(t)$ whose spectrum is concentrated in the frequency band $0 < f < f_{maks}$ can be expanded in a series of functions of the form $\frac{\sin x}{x}$, i.e.,

$$y(t) = \sum_{k=-\infty}^{\infty} y_k \frac{\sin 2\pi f_{maks} (t - t_k)}{2\pi f_{maks} (t - t_k)} \quad (1)$$

where $y_k = y(t_k)$ are the expansion coefficients having an interesting property insofar as they are equal to the instantaneous values of

the function $y(t)$ at discrete instants of time

$$t_k = k\Delta t \quad (k=0, \pm 1, \pm 2, \dots).$$

Δt is here a time interval whose magnitude is determined by the width of the frequency spectrum of the function $y(t)$

$$\Delta t = \frac{1}{2f_{\max}}. \quad (2)$$

Functions of the form $\frac{\sin x}{x}$ (Fig. 2.17) whose values vary by y_k and are shifted in time by Δt to the left and to the right enter formula (1) as addends. Their summation yields a curve that coincides with the curve $y(t)$ in all points. This is easy to verify immediately for the discrete points $t_k = k\Delta t$, at which all addends of the sum (1) except for one, vanish. For $t = t_k$ the addend different from zero assumes a value equal to the instantaneous value of the function $y(t)$ at the instant of time t_k .

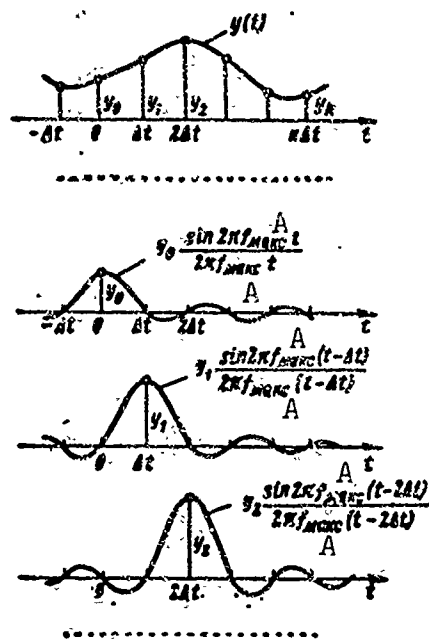


Fig. 2.17. Explanation of Kotel'nikov's theorem A) max.

For the intermediate points of each interval Δt the validity of formula (1) must be proved. It is, however, evident without proof that the sum (1) on an arbitrary interval Δt cannot experience remarkable oscillations since it does not contain any spectral components whose period would be shorter than $\frac{1}{f_{\max}} = 2\Delta t$.

The proof of Kotel'nikov's theorem may be obtained from the Fourier integral

$$y(t) = \int_{-\infty}^{\infty} G(f) e^{j2\pi ft} df = \int_{-f_{\max}}^{f_{\max}} G(f) e^{j2\pi ft} df, \quad (3)$$

if the spectra function $G(f)$ given different from zero in the interval

$-f_{\text{maks}} < f < f_{\text{maks}}$ is replaced by the function $G_1(f)$ with a period $2f_{\text{maks}}$ coinciding with the spectral function in this interval and continued periodically, and the latter is expanded in a Fourier series

$$G_1(f) = \sum_{k=-\infty}^{\infty} D_k e^{-j2\pi \frac{k}{2f_{\text{maks}}} f} \quad (4)$$

The periodical continuation of the function $G(f)$ is illustrated for its modulus $|G(f)|$ by Fig. 2.18. Determining the Fourier coefficients D_k in the usual way and using the formulas (2) and (3) we obtain

$$D_k = \frac{1}{2f_{\text{maks}}} \int_{-f_{\text{maks}}}^{f_{\text{maks}}} G_1(f) e^{j2\pi \frac{k}{2f_{\text{maks}}} f} df = \frac{1}{2f_{\text{maks}}} y(k\Delta t). \quad (5)$$

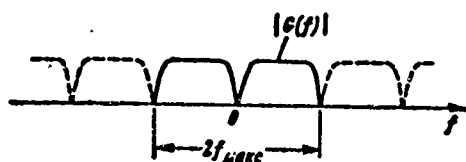


Fig. 2.18. Illustration of the periodical continuation of the spectral density $G(f)$ by the example of its modulus.

Substituting expression (4) for $G_1(f)$ into the right-hand side of Eq. (3) instead of $G(f)$ and using the expression for the coefficients of the series (5) we obtain an interchanging the order of integration and summation

$$y(t) = \sum_{k=-\infty}^{\infty} y(k\Delta t) \frac{1}{2f_{\text{maks}}} \int_{-f_{\text{maks}}}^{f_{\text{maks}}} e^{j2\pi \left(t - \frac{k}{2f_{\text{maks}}}\right) f} df. \quad (6)$$

Carrying out the integration we obtain expression (1) corresponding to Kotel'nikov's theorem,

$$y(t) = \sum_{k=-\infty}^{\infty} y_k \frac{\sin [2\pi f_{\text{maks}}(t - t_k)]}{2\pi f_{\text{maks}}(t - t_k)}.$$

Kotel'nikov's theorem may be considered to be an alternative form of the series expansion

$$y(t) = \sum_k y_k \psi_k(t)$$

with respect to the nonrandom functions,

$$\psi_k(t) = \frac{\sin[2\pi f_{\text{max}}(t - t_k)]}{2\pi f_{\text{max}}(t - t_k)}.$$

It can be shown that these functions are orthogonal to each other in the interval $-\infty < t < \infty$, i.e.,

$$\int_{-\infty}^{\infty} \psi_k(t) \psi_l(t) dt = 0, \text{ if } k \neq l.$$

Thus, Kotel'nikov's theorem permits signals and interferences with a limited spectrum to be expanded in orthogonal nonrandom functions.

§2.7. METHOD OF SOLVING PROBLEMS OF DETECTION AND MEASUREMENT OF RADAR SIGNAL PARAMETERS ON A FLUCTUATION NOISE BACKGROUND

Let us remember the problem of optimum detection of radar signals and measurement of their parameters formulated in §1.4. An oscillation

$$y(t) = n(t) + Ax(t, \alpha_1, \alpha_2, \dots, \beta_1, \beta_2, \dots),$$

is received, where $n(t)$ and $x(t, \alpha_1, \alpha_2, \dots, \beta_1, \beta_2, \dots)$ are the interference and the signal, respectively. The signal is given as a function of the time t , the measurable random parameters $\alpha_1, \alpha_2, \dots$ and the unmeasurable parameters β_1, β_2, \dots . In its turn, A is a discrete random parameter (0 or 1) to be determined in the detection.

On the basis of the received oscillation $y(t)$ and the well known statistics of the interference and all random parameters the estimates $A^*, \alpha_1^*, \alpha_2^*, \dots$ of the discrete and the continuous parameters must be given.

In order to explain the method of solving this problem we shall simplify its conditions to some extent. To start with, we shall assume that there are no unmeasurable random parameters. In this case

$$y(t) = n(t) + Ax(t, \alpha_1, \alpha_2, \dots).$$

In particular, for the detection problem

$$y(t) = n(t) + Ax(t), \quad (1)$$

and for the problem of measurement

$$y(t) = n(t) + x(t, a_1, a_2, \dots). \quad (2)$$

The relations (1) and (2) differ substantially from the corresponding relations for the onedimensional case insofar as functions of time enter into them.

We shall assume that these functions do not contain spectral constants outside the frequency band $0 < f < f_{\text{maks}}$. Meanwhile, we shall consider the quantity f_{maks} to be finite, intending to pass to the limit $f_{\text{maks}} \rightarrow \infty$, finally. According to Kotel'nikov's theorem the functions $n(t)$, $x(t)$, $y(t)$ can be fully characterized by the set of their discrete values

$$n_1, n_2, \dots$$

$$x_1, x_2, \dots$$

$$y_1, y_2, \dots$$

In other words, we may pass over from the random functions of time to multidimensional random quantities. Assuming their distribution to be continuous, these quantities can be characterized by the corresponding multidimensional probability densities, e.g., $p_p(y_1, y_2, \dots)$ and $p_{sp}(y_1, y_2, \dots)$ where as before the subscripts "p" and "sp" denote the conditions that only an interference or a signal with interference are present. When multiplied by $dy_1 dy_2 \dots$ these densities characterize the probability of realizing the values of the first discrete quantity within the limits of y_1 and $y_1 + dy_1$, and those of the second quantity within the limits of y_2 and $y_2 + dy_2$, etc. Moreover, since the quantities y_1, y_2, \dots uniquely determine the whole curve $y(t)$, the total probability $p_p(y_1, y_2, \dots) dy_1 dy_2$ or $p_{sp}(y_1, y_2, \dots) dy_1 dy_2$ determines the probability of realizing the whole curve $y(t)$ in the following sense. If two noninteracting curves (dotted in Fig.2.19) satisfying the conditions of Kotel'nikov's theorem are directed through the points $y_1, y_2 \dots$ and $y_1 + dy_1, y_2 + dy_2 \dots$, the probability of the realization of

$y(t)$ lying between these curves in the presence of solely the interference will be equal to $p_n(y_1, y_2, \dots) dy_1 dy_2 \dots$, and in the presence of signal and interference $p_{cn}(y_1, y_2, \dots) dy_1 dy_2 \dots$.

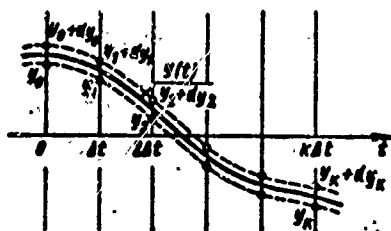


Fig.2.19. Explanation of the concept of the probability density of realising $y(t)$.

It is well known that the onedimensional random quantities are characterized by points on a straight line, the two-dimensional ones by points on a plane, and three-dimensional ones by points in space. The three-dimensional quantity y_1, y_2, y_3 , e.g., can be represented by a point in a Cartesian coordinate system.

If the probability density $p(y_1, y_2, y_3)$ corresponds to each point of the space, the integral

$$\int_{-\infty}^{\infty} \int_{-\infty}^{\infty} \int_{-\infty}^{\infty} p(y_1, y_2, y_3) dy_1 dy_2 dy_3 = 1.$$

Sometimes, one speaks of a multidimensional space, assuming it to be some abstraction that is illustrated plastically by means of a three dimensional, twodimensional(plane) or onedimensional(straight line) space. Each realization y_1, y_2, y_3, \dots may in this case be regarded as a point of a multidimensional space. Obviously, also in this case

$$\int_{-\infty}^{\infty} \dots \int_{-\infty}^{\infty} p(y_1, y_2, \dots) dy_1 dy_2 \dots = 1. \quad (3)$$

The use of a multidimensional-space terminology causes the well known transparency, but sometimes also gives rise to conceptual difficulties. These difficulties can always be avoided if the point of the multidimensional space is interpreted as a conventional name for the realization of the expansion coefficients y_k .

In the case of regular detection on a regular solution must be

adopted for each realization y_1, y_2, \dots . This implies that a solution function $A^*(y_1, y_2, \dots)$ can be introduced, which may assume two values according to its arguments: 1 or 0, to which solutions of present or absent signal correspond. In other words, to each point of the multidimensional space its value A^* - zero or unity, must be ascribed. Thus, this space is split into sections. According to into which section the point corresponding to the received oscillation falls the solution A^* of present or absent signal must be adopted. The choice of the best solution function $A^*_{\text{opt}}(y_1, y_2, \dots)$ or, in other terminology, the best splitting of the multidimensional space into two regions $A^* = 0$ and $A^* = 1$ and represents a problem of the theory of optimum detection.

It is easy to see that there is full analogy to the onedimensional case of detection. There, the solution function of only one variable was involved and the splitting into the regions $A^* = 0, A^* = 1$ was carried out for a straight line. In this case, however, the functions of many variables are considered and the splitting into regions must be carried out for a multidimensional space.

Let us obtain the probabilities of correct detection and false alarm for an arbitrary solution function $A^*(y_1, y_2, \dots)$. In analogy to the relations [(7) §1.5] we may write

$$D = \iint \dots A^*(y_1, y_2, \dots) p_{\text{en}}(y_1, y_2, \dots) dy_1 dy_2 \dots, \quad (4)$$

$$F = \iint \dots A^*(y_1, y_2, \dots) p_{\text{n}}(y_1, y_2, \dots) dy_1 dy_2 \dots \quad (5)$$

In order to choose the optimum method of detection we shall, as before, use the weight criterion which is a consequence of the criterion of the mean risk minimum. The expression $D - \ell_0 F$, corresponding to the weight criterion can be represented in the form

$$D - \ell_0 F = \iint \dots A^*(y_1, y_2, \dots) p_{\text{n}}(y_1, y_2, \dots) [\ell(y_1, y_2, \dots) - \ell_0] dy_1 dy_2 \dots, \quad (6)$$

where

$$l(y_1, y_2, \dots) = \frac{p_{\text{en}}(y_1, y_2, \dots)}{p_{\text{a}}(y_1, y_2, \dots)}. \quad (7)$$

Since a system that maximizes the integral (6) is optimum from the point of view of the weight criterion we obtain as in §1.5

$$A_{\text{opt}}^*(y_1, y_2, \dots) = \begin{cases} 1, & \text{if } l(y_1, y_2, \dots) > l_0, \\ 0, & \text{if } l(y_1, y_2, \dots) < l_0. \end{cases} \quad (8)$$

We note that the quantities y_1, y_2, \dots uniquely depend on the received realization of $y(t)$, for which reason the denotation $l[y(t)]$ may be used instead of the denotation $l(y_1, y_2, \dots)$. In analogy, the denotation $A^*[y(t)]$ may be used for $A^*(y_1, y_2, \dots)$. The solution (8) of the problem of optimum detection may then be written in the form

$$A_{\text{opt}}^*[y(t)] = \begin{cases} 1, & \text{if } l[y(t)] > l_0, \\ 0, & \text{if } l[y(t)] < l_0. \end{cases} \quad (9)$$

Thus, we have established that optimum detection problems can be solved by the following method. The probability ratio (7) for the received oscillation $y(t)$ must be calculated. This probability ratio must further be compared with the threshold l_0 . The solution of present signal is adopted if the probability ratio $l[y(t)] > l_0$ and the solution of absent signal if $l[y(t)] < l_0$. The value of l_0 is chosen such that the probability of false alarm F does not exceed the admissible value F_{dop} .

When solving the problem of optimum measurement of the parameters $\alpha_1, \alpha_2, \dots$, we have to apply, as also in §1.6, to their a-posteriori probability density $p(\alpha_1, \alpha_2, \dots | y_1, y_2, \dots)$, where y_1, y_2, \dots are discrete values of the received realization of $y(t)$.

According to the theorem of probability multiplication we may write

$$\begin{aligned}
p(a_1, a_2, \dots, y_1, y_2, \dots) &= \\
&= p(a_1, a_2, \dots) p(y_1, y_2, \dots | a_1, a_2, \dots) = \\
&= p(y_1, y_2, \dots) p(a_1, a_2, \dots | y_1, y_2, \dots),
\end{aligned} \tag{10}$$

whence we have for a fixed realization of the received signal

$$\begin{aligned}
p(a_1, a_2, \dots | y_1, y_2, \dots) &= \\
&= k_1 p(a_1, a_2, \dots) p(y_1, y_2, \dots | a_1, a_2, \dots),
\end{aligned} \tag{11}$$

where

$$\begin{aligned}
k_1 &= \frac{1}{p(y_1, y_2, \dots)} = \\
&= \frac{1}{\int \dots \int p(a_1, a_2, \dots) p(y_1, y_2, \dots | a_1, a_2, \dots) da_1 da_2 \dots}.
\end{aligned} \tag{12}$$

If the a-posteriori probability density is known the estimates that are optimum from the point of view of the mean risk minimum can be determined. In many cases, the most probable, i.e., those estimates $\alpha_1^*, \alpha_2^*, \dots$, that maximize expression (11) are, in particular, the optimum estimates.

When obtaining the optimum estimates the quantity of the probability ratio can be successfully used, as in the detection problem. In fact, the expression

$$p(y_1, y_2, \dots | a_1, a_2, \dots) = p_{en}(y_1, y_2, \dots | a_1, a_2, \dots)$$

is the probability density of the realization of the expansion coefficients y_1, y_2, \dots under the condition that an interference and a signal with the parameters $\alpha_1, \alpha_2, \dots$ are acting.

The same realization of the values y_1, y_2, \dots may appear also if only an interference with a probability density of

$$p_n(y_1, y_2, \dots)$$

is acting. The ratio of these probability densities is the probability ratio as calculated for completely determined values of the parameters $\alpha_1, \alpha_2, \dots$

$$\frac{p(y_1, y_2, \dots | a_1, a_2, \dots)}{p_n(y_1, y_2, \dots)} = l(y_1, y_2, \dots | a_1, a_2, \dots). \tag{13}$$

Substituting the value of $p(y_1, y_2, \dots | \alpha_1, \alpha_2, \dots)$, found from formula (13) into (11) we obtain

$$\begin{aligned} p(\alpha_1, \alpha_2, \dots | y_1, y_2, \dots) = \\ = K_y p(\alpha_1, \alpha_2, \dots) l(y_1, y_2, \dots | \alpha_1, \alpha_2, \dots), \end{aligned} \quad (14)$$

where

$$K_y = k_y p_\pi(y_1, y_2, \dots). \quad (15)$$

Noting that y_1, y_2, \dots are determined by the realization of $y(t)$ relation (14) may be written in the form

$$p(\alpha_1, \alpha_2, \dots | y(t)) = K_y p(\alpha_1, \alpha_2, \dots) l[y(t) | \alpha_1, \alpha_2, \dots], \quad (16)$$

where

$$K_y = \frac{1}{\int \dots p(\alpha_1, \alpha_2, \dots) l[y(t) | \alpha_1, \alpha_2, \dots] d\alpha_1 d\alpha_2 \dots}. \quad (17)$$

Besides the a-priori parameter distribution expression (16), which is used in obtaining the optimum estimates, contains the probability ratio $l[y(t) | \alpha_1, \alpha_2, \dots]$. If the role of the a-priori information is small compared to that of the information obtained by the experiment the estimates are essentially determined by the probability ratio. Thus, the solution of the problem of measurement, as well as that of detection, proves to be substantially connected with the calculation of the probability ratio.

We note that in the derivation of the relations (7) and (16) the presence of unmeasurable random signal parameters was not taken into account. The presence of these parameters changes the dependence of $p_{c\pi}(y_1, y_2, \dots)$, but has no influence on the form of the final formulas. In this case, it is only necessary to calculate the conditional probability density $p_{c\pi}(y_1, y_2, \dots)$ and the probability ratio in a somewhat more complex manner as will be shown in the third chapter.

In the third chapter we shall calculate the probability ratio under various assumptions on the unmeasurable random parameters. The measurable random parameters are always assumed to be fixed, in this

chapter (such that they will not be discussed). The dependence of the probability ratio on these parameters will be analyzed in the following chapters.

Manu-
script
Page
No.

[Footnotes]

- 40 We do not take account of an additional phase modulation if the antenna is rotated. This is only correct in the case where the axis of rotation passes through the "phase center".
- 41 Thus, a continuous variation of conditions (e.g., the scanning rate of the antenna beam [10]) as a function of the voltage at the receiver input is not considered.
- 52 Various methods of designing multiplying circuits are known. One of these methods consists in obtaining a voltage difference at the output of two diodes with quadratic characteristics and n^2 under the condition that the half sum and the half difference of the multiplied voltages are, respectively, fed to either of them.

[Transliterated Symbols]

- 56 макс = maks = maksimal'nyy = maximum
- 56 мин = min = minimal'nyy = minimum
- 65 опт = opt = optimal'nyy = optimum
- 66 доп = dop = dopustimyy = admissible
- 59 сп = sp = signal s pomekhoy = signal with interference

Chapter 3

THE PROBABILITY RATIO FOR THE FUNDAMENTAL RADAR SIGNAL MODELS IN THE PRESENCE OF FLUCTUATION NOISE IN THE FORM OF WHITE GAUSSIAN NOISE

§3.1. THE PROBABILITY RATIO FOR A SIGNAL WITH COMPLETELY GIVEN PARAMETERS.

The simplest example of calculating the probability ratio refers to the case where the expected signal $x(t)$ has no unknown parameters. In this case, the received oscillation $y(t)$ differs from the random noise oscillation by a given function under the condition of present signal and interference

$$y(t) = n(t) + x(t).$$

The discrete values y_k corresponding to this oscillation satisfy the equations

$$y_k = n_k + x_k,$$

where x_k are given quantities (discrete values of the signal); $k = 1, 2, \dots$

This implies that the presence of a signal shifts the distribution of the values y_k relative to the case where only the interference is acting and $y_k = n_k$. In analogy to relation [(5) §1.5] we may write

$$p_{\Sigma}(y_1, y_2, \dots) = p_n(y_1 - x_1, y_2 - x_2, \dots). \quad (1)$$

Thus, the probability ratio for a signal with completely given parameters can be represented in the form

$$l(y_1, y_2, \dots) = \frac{p_{\Sigma}(y_1 - x_1, y_2 - x_2, \dots)}{p_n(y_1, y_2, \dots)}. \quad (2)$$

In order to calculate the probability ratio, the dependence of $p_n(y_1, y_2, \dots)$, i.e., the total distribution law of the discrete interference values must be established.

The following assumptions were already made on the interference:

1) The interference is a fluctuation interference and its instantaneous values are distributed according to a normal law with an average value equal to zero.

2) The interference is stationary, i.e., its statistical characteristics are constant in time.

3) The interference belongs to the quasiwhite noise with a uniform spectrum in the frequency band $0 < f < f_{\text{max}}$ (in the following, the passage to the limit $f_{\text{max}} \rightarrow \infty$ is intended).

It follows from the first assumption that the probability density of any discrete value of interference is equal to

$$p(y_k) = \frac{1}{\sqrt{2\pi n_{0k}^2}} e^{-\frac{y_k^2}{2n_{0k}^2}},$$

where n_{0k}^2 is the dispersion; $k = 1, 2, \dots$

It follows from the second assumption that the dispersion of the interference is equal for all discrete values: $n_{0k}^2 = n_0^2$.

It follows from the third assumption that the correlation function of the voltage of this noise for a resistance equal to unity is described by the expression [(9) §2.3] for $f_{\text{max}} = 0$, i.e.,

$$\begin{aligned} R(\tau) &= N_0 f_{\text{max}} \frac{\sin(\pi f_{\text{max}} \tau)}{\pi f_{\text{max}} \tau} \cos(\pi f_{\text{max}} \tau) = \\ &= N_0 f_{\text{max}} \frac{\sin(2\pi f_{\text{max}} \tau)}{2\pi f_{\text{max}} \tau}. \end{aligned}$$

Putting the interval τ times the time discretization interval we obtain using Kotelnikov's theorem $\Delta t = \frac{1}{2f_{\text{max}}}$,

$$R(m\Delta t) = N_0 f_{\text{max}} \frac{\sin m\pi}{m\pi} = \begin{cases} 0 & \text{for } m=1, 2, \dots, \\ N_0 f_{\text{max}} & \text{for } m=0. \end{cases}$$

This implies that discrete values y_k with different numbers are uncorrelated random quantities and that the dispersion of these quantities is equal to the product of the spectral noise density and its spectral width

$$n_0^2 = R(0) = N_0 f_{\text{max}}. \quad (3)$$

Using all three assumptions we can write the manydimensional distribution law in the following form:

$$p_n(y_1, y_2, \dots) = p_n(y_1) p_n(y_2) \dots =$$

$$= \left[\frac{1}{\sqrt{2\pi n_0}} e^{-\frac{y_1^2}{2n_0^2}} \right] \left[\frac{1}{\sqrt{2\pi n_0}} e^{-\frac{y_2^2}{2n_0^2}} \right] \dots,$$

where $n_0^2 = N_0 f_{\text{max}}$. Substituting the obtained expression in formula (2) we have

$$l(y_1, y_2, \dots) = \frac{e^{-\frac{(y_1-x_1)^2}{2n_0^2}} e^{-\frac{(y_2-x_2)^2}{2n_0^2}}}{e^{-\frac{y_1^2}{2n_0^2}} e^{-\frac{y_2^2}{2n_0^2}}} \dots \quad (4)$$

Rewriting formula (4) and replacing in it $n_0^2 = N_0 f_{\text{max}} = N_0/2\Delta t$, we obtain

$$l(y_1, y_2, \dots) = e^{-\frac{1}{N_0} \sum_k x_k^2 \Delta t} e^{\frac{2}{N_0} \sum_k x_k y_k \Delta t}. \quad (5)$$

Expression (5) determined the sought probability ratio for a signal with completely given parameters and an interference in the form of quasiwhite noise. It permits a simple limiting transition to the case of white noise if $f_{\text{max}} \rightarrow \infty$, and $\Delta t \rightarrow 0$. In this case, the sum in the exponent of the first factor goes over into an integral that is numerically equal to the energy of the expected signal

$$\lim_{\Delta t \rightarrow 0} \sum_k x_k^2 \Delta t = \int_{-\infty}^{\infty} x^2(t) dt = \mathcal{E}, \quad (6)$$

and the sum in the exponent of the second factor goes over into the integral

$$\lim_{M \rightarrow 0} \sum_k x_k y_k \Delta t = \int_{-\infty}^{\infty} x(t) y(t) dt,$$

which will be termed correlation integral in the following.

Thus, the final expression for the probability ratio can be given in the following form:

$$l = l[y(t)] = e^{-\frac{\vartheta}{N_0}} e^{\frac{z}{N_0}}, \quad (7)$$

where N_0 is the spectral noise density; ϑ is the energy of the expected signal and z is the correlation integral

$$z = \int_{-\infty}^{\infty} x(t) y(t) dt = z[y(t)]. \quad (8)$$

§3.2. THE PROBABILITY RATIO IN THE PRESENCE OF UNMEASURABLE RANDOM PARAMETERS

Let the total oscillation

$$y(t) = n(t) + x(t, \beta_1, \beta_2, \dots).$$

be received under the condition of present signal and interference.

We shall consider the total probability density of the discrete values y_k of the received oscillation and the unmeasurable random parameters β_1 . The considerations are made on the assumption that the measurable random parameters are fixed. According to the multiplication theorem of probabilities we may write

$$\begin{aligned} p(y_1, y_2, \dots, \beta_1, \beta_2, \dots) &= \\ &= p(y_1, y_2, \dots) p(\beta_1, \beta_2, \dots | y_1, y_2, \dots) = \\ &= p(\beta_1, \beta_2, \dots) p(y_1, y_2, \dots | \beta_1, \beta_2, \dots). \end{aligned} \quad (1)$$

On integration of an absolute or conditional probability density within infinite limits we always obtain unity, in particular,

$$\int \int \dots p(\beta_1, \beta_2, \dots | y_1, y_2, \dots) d\beta_1 d\beta_2 \dots = 1.$$

Consequently, we obtain as a result of the integration (1)

$$p(y_1, y_2, \dots) = \int_{-\infty}^{\infty} \dots p(\beta_1, \beta_2, \dots) p(y_1, y_2, \dots | \beta_1, \beta_2, \dots) d\beta_1 d\beta_2 \dots \quad (2)$$

According to the condition $p(y_1, y_2, \dots) = p_{cn}(y_1, y_2, \dots)$ represents the probability density of realizing the values y_k in the presence of signal and interference. Dividing both sides of Eq. (2) by the probability density of the same values y_k in the presence of the interference alone $p_n(y_1, y_2, \dots)$, we shall obtain the sought expression for the probability ratio

$$l(y_1, y_2, \dots) = \int_{-\infty}^{\infty} \dots p(\beta_1, \beta_2, \dots) \frac{p(y_1, y_2, \dots | \beta_1, \beta_2, \dots)}{p_n(y_1, y_2, \dots)} d\beta_1 d\beta_2 \dots$$

The divisor may be written under the integral sign since it is independent of the variables of integration. The quantity

$$\frac{p(y_1, y_2, \dots | \beta_1, \beta_2, \dots)}{p_n(y_1, y_2, \dots)} = l(y_1, y_2, \dots | \beta_1, \beta_2, \dots)$$

is a special value of the probability ratio for fixed values of the unmeasurable random parameters. In other words, this is the probability ratio for a signal with completely given parameters.

Hence it follows that the sought probability ratio is obtained by taking the mean of its special values over the unmeasurable random parameters:

$$l(y_1, y_2, \dots) = \int_{-\infty}^{\infty} \dots p(\beta_1, \beta_2, \dots) l(y_1, y_2, \dots | \beta_1, \beta_2, \dots) d\beta_1 d\beta_2 \dots \quad (3)$$

or

$$l[y(t)] = \int_{-\infty}^{\infty} \dots p(\beta_1, \beta_2, \dots) l[y(t) | \beta_1, \beta_2, \dots] d\beta_1 d\beta_2 \dots \quad (4)$$

According to the results of the preceding section

$$l[y(t) | \beta_1, \beta_2, \dots] = e^{-\frac{p(\beta_1, \beta_2, \dots)}{N_0}} e^{\frac{2}{N_0} y(t) | \beta_1, \beta_2, \dots} \quad (5)$$

where

$$\mathfrak{D}(\beta_1, \beta_2, \dots) = \int_{-\infty}^{\infty} x^2(t, \beta_1, \beta_2, \dots) dt \quad (6)$$

and

$$z[y(t)|\beta_1, \beta_2, \dots] = \int_{-\infty}^{\infty} x(t, \beta_1, \beta_2, \dots) y(t) dt. \quad (7)$$

Finally we have then

$$\begin{aligned} l = l[y(t)] = \\ = \int_{-\infty}^{\infty} \dots \int_{-\infty}^{\infty} p(\beta_1, \beta_2, \dots) e^{-\frac{\mathfrak{D}(\beta_1, \beta_2, \dots)}{N_0}} \frac{2}{e^{N_0}} z[y(t)|\beta_1, \beta_2, \dots] d\beta_1 d\beta_2 \dots \end{aligned} \quad (8)$$

§3.3. PROBABILITY RATIO FOR A SIGNAL WITH RANDOM INITIAL PHASE

As to the degree of complexity, the next model after the signal with completely known parameters is, as was already remarked in §2.2, a signal with random initial phase

$$x(t, \beta) = X(t) \cos[\omega_0 t + \varphi_x(t) + \beta]. \quad (1)$$

It is also just this signal that may be regarded as the simplest example of an application of the general relations of the preceding section.

We consider the initial phase β to be distributed uniformly in the interval from 0 to 2π with a probability density of $p(\beta) = 1/2\pi$.

In order to apply the general formula [(8) §3.2], it is, first of all, necessary to calculate the correlation integral and energy for a fixed value of the parameter β , making use of the relations [(7) and (6) §3.2].

Using the formula of the cosine sum, we obtain from (1) that

$$\begin{aligned} x(t, \beta) &= X(t) \cos[\omega_0 t + \varphi_x(t)] \cos \beta - \\ &- X(t) \sin[\omega_0 t + \varphi_x(t)] \sin \beta. \end{aligned}$$

Introducing the designations

$$\begin{aligned} x_1(t) &= X(t) \cos[\omega_0 t + \varphi_x(t)], \\ x_2(t) &= -X(t) \sin[\omega_0 t + \varphi_x(t)], \end{aligned} \quad (2)$$

we find

$$x(t, \beta) = x_1(t) \cos \beta + x_2(t) \sin \beta. \quad (3)$$

The correlation integral can then be written

$$z[y(t)|\beta] = \int_{-\infty}^{\infty} x(t, \beta) y(t) dt = z_1 \cos \beta + z_2 \sin \beta, \quad (4)$$

where

$$\left. \begin{aligned} z_1 &= \int_{-\infty}^{\infty} x_1(t) y(t) dt = z_1[y(t)]; \\ z_2 &= \int_{-\infty}^{\infty} x_2(t) y(t) dt = z_2[y(t)]. \end{aligned} \right\} \quad (5)$$

Introducing the quantities Z and θ , determined by the relations

$$Z = \sqrt{z_1^2 + z_2^2}, \quad (6)$$

$$\left. \begin{aligned} \cos \theta &= \frac{z_1}{Z}, \\ \sin \theta &= \frac{z_2}{Z}, \end{aligned} \right\} \quad (7)$$

we shall finally write the expression for the correlation integral in the form

$$z[y(t)|\beta] = Z [\cos \beta \cos \theta + \sin \beta \sin \theta] = Z \cos(\beta - \theta).$$

We shall now obtain the energy of the signal $\mathfrak{P}(\beta)$. If its oscillation amplitude $X(t)$ and phase $\varphi_X(t)$ vary only slightly during each high-frequency oscillation period, the energy is practically independent of the initial phase β such that

$$\begin{aligned} \mathfrak{P}(\beta) &= \int_{-\infty}^{\infty} X^2(t) \cos^2[\omega_0 t + \varphi_X(t) + \beta] dt \approx \\ &\approx \frac{1}{2} \int_{-\infty}^{\infty} X^2(t) dt = \mathfrak{P}. \end{aligned} \quad (8)$$

We may now pass over to the calculation of the probability ratio. Using formula (8) of the preceding section we obtain

$$I = e^{-\frac{\mathfrak{P}}{N_0}} \frac{1}{2\pi} \int_0^{2\pi} e^{\frac{2Z}{N_0} \cos(\beta - \theta)} d\beta.$$

We remember that

$$\frac{1}{2\pi} \int_0^{2\pi} e^{u \cos(\beta - \alpha)} d\beta = I_0(u) \quad (9)$$

is a zero-order modified Bessel function (Fig. 3.1).

Thus we have for a signal with random initial phase

$$I = e^{-\frac{3}{N_0}} I_0\left(\frac{2Z}{N_0}\right), \quad (10)$$

where the value of Z is determined from the relations (5) and (6).

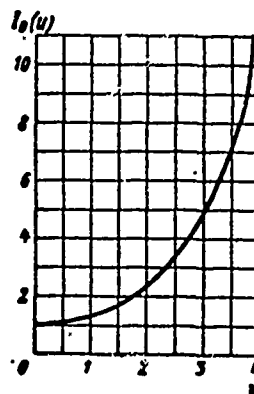


Fig. 3.1. Diagram of the zero-order Bessel function.

§3.4. PROBABILITY RATIO FOR A SIGNAL WITH RANDOM AMPLITUDE AND RANDOM INITIAL PHASE

The model of the signal with random amplitude and random initial phase is written in the form

$$x(t, \beta, B) = BX(t) \cos[\omega_c t + \varphi_x(t) + \beta]. \quad (1)$$

Assuming the initial phase to be equally probable within the limits of 0 to 2π and the coefficient B distributed according to Rayleigh's law with a root-mean-square value equal to unity the probability density of the quantities β and B may be written in the form

$$p(\beta, B) = \frac{1}{2\pi} 2Be^{-B^2} = \frac{B}{\pi} e^{-B^2}, \quad (2)$$

where $B \geq 0$.

Let us pass over to the calculation of the correlation integral $x(y(t)|\beta, B)$ and the energy $\mathfrak{Z}(\beta, B)$ for fixed values of the parameters β and B . In analogy to the way in which this was done the preceding section we may obtain

$$x(y(t)|\beta, B) = BZ \cos(\beta - \theta) \quad (3)$$

and

$$\mathfrak{Z}(\beta, B) = B^2 \mathfrak{Z}, \quad (4)$$

where the expressions for Z , θ and \mathfrak{Z} are the same as in §3.3. It is easy to see that in contrast to the preceding case the energy $\mathfrak{Z}(\beta, B)$ depends on the random factor B . Its mean value is equal to

$$\mathfrak{Z}_0 = \int_0^\infty dB \int_0^{2\pi} \mathfrak{Z}(\beta, B) p(\beta, B) d\beta = \mathfrak{Z} \int_0^\infty 2B^2 e^{-B^2} dB = \mathfrak{Z}, \quad (5)$$

i.e., to the energy of the signal for the special value $B = 1$.

Using the general formula [(8) §3.2] we obtain

$$I = \frac{1}{\pi} \int_0^\infty dB \int_0^{2\pi} B e^{-B^2} e^{-\frac{B^2 \mathfrak{Z}}{N_0}} e^{\frac{2BZ}{N_0} \cos(\beta - \theta)} d\beta.$$

By virtue of Eq. [(9) §3.3] and Eq. (4)

$$I = 2 \int_0^\infty I_0\left(\frac{2BZ}{N_0}\right) e^{-\frac{B^2(\mathfrak{Z} + N_0)}{N_0}} B dB. \quad (6)$$

Using the tabulated integral

$$\int_0^\infty I_0(\mu x) e^{-\mu^2 x^2} x dx = \frac{1}{2\mu} e^{\frac{\mu^2}{4}}, \quad (7)$$

we obtain

$$I = \frac{N_0}{\mathfrak{Z} + N_0} e^{\frac{1}{N_0} \frac{Z^2}{\mathfrak{Z} + N_0}}, \quad (8)$$

where the value of Z is determined from the relations [(2), (5), (6) §3.3.].

§3.5. PROBABILITY RATIO FOR A SIGNAL IN THE FORM OF A RADIOPULSE PACKET WITH RANDOM INITIAL PHASES

The model of a signal in the form of a pulse packet with random initial phases is described by the relation

$$x(t, \beta_1, \beta_2, \dots) = \sum_k X_k(t) \cos[\omega_k t + \varphi_k(t) + \beta_k]. \quad (1)$$

We assume the pulse amplitudes to be nonrandom and the initial phases β_k to be independent random quantities each of which is uniformly distributed within the limits from 0 to 2π . The total probability density of these quantities is described by the relation

$$p(\beta_1, \beta_2, \dots) = p(\beta_1) p(\beta_2) \dots, \quad (2)$$

where

$$p(\beta_1) = p(\beta_2) = \dots = \frac{1}{2\pi}. \quad (3)$$

Using the cosine sum formula as in §3.3, expression (1) may be written in the form

$$x(t, \beta_1, \beta_2, \dots) = \sum_k [x_{1k}(t) \cos \beta_k + x_{2k}(t) \sin \beta_k], \quad (4)$$

where

$$\left. \begin{aligned} x_{1k}(t) &= X_k(t) \cos[\omega_k t + \varphi_k(t)]; \\ x_{2k}(t) &= -X_k(t) \sin[\omega_k t + \varphi_k(t)]. \end{aligned} \right\} \quad (5)$$

Hence

$$\begin{aligned} z[y(t) | \beta_1, \beta_2, \dots] &= \int_{-\infty}^{\infty} x(t, \beta_1, \beta_2, \dots) y(t) dt = \\ &= \sum_k (z_{1k} \cos \beta_k + z_{2k} \sin \beta_k), \end{aligned} \quad (6)$$

where

$$\begin{aligned} z_{1k} &= \int_{-\infty}^{\infty} x_{1k}(t) y(t) dt, \\ z_{2k} &= \int_{-\infty}^{\infty} x_{2k}(t) y(t) dt. \end{aligned}$$

With the denotation

$$\sqrt{z_{1k}^2 + z_{2k}^2} = Z_k,$$

expression (6), as in §3.3, may be written in the form

$$z[y(t)|\beta_1, \beta_2, \dots] = \sum_k Z_k \cos(\beta_k - \theta_k). \quad (7)$$

On the assumption that the packet consists of nonoverlapping pulses its energy can be determined as the sum of the energies of the individual pulses. Assuming the amplitude and the initial phase of each pulse to vary only slightly during a high-frequency oscillation period we obtain

$$\mathcal{E}(\beta_1, \beta_2, \dots) = \sum_k \mathcal{E}_k(\beta_k) \approx \sum_k \frac{1}{2} \int X_k^2(t) dt = \sum_k \mathcal{E}_k, \quad (8)$$

where \mathcal{E}_k is independent of the random initial phase β_k .

To calculate the probability ratio we use, as before, the general formula [(8) §3.2] which by virtue of Eqs. (2), (7), (8) may be written in the form of a product

$$l = \prod_k e^{-\frac{\mathcal{E}_k}{N_0}} \frac{1}{2\pi} \int_0^{2\pi} e^{\frac{2Z_k \cos(\beta_k - \theta_k)}{N_0}} d\beta_k.$$

On integration we obtain according to formula [(9) §3.3]

$$l = \prod_k e^{-\frac{\mathcal{E}_k}{N_0}} I_0\left(\frac{2Z_k}{N_0}\right). \quad (9)$$

It is easy to see that the probability ratio for a packet of nonoverlapping pulses with random independent initial phases is determined as the product of the probability ratios for each pulse of the packet.

§3.6. PROBABILITY RATIO FOR SIGNALS IN THE FORM OF A PACKET OF RADIO-PULSES WITH RANDOM AMPLITUDES AND INITIAL PHASES

For the model of a signal in the form of a packet of nonoverlapping pulses with random amplitudes and initial phases we have

$$x(t, \beta_1, \beta_2, \dots, B_1, B_2, \dots) = \sum_k B_k \chi_k(t) \cos[\omega_k t + \varphi_k(t) + \beta_k]. \quad (1)$$

In this case, we shall restrict our considerations to two limiting cases:

a) the case of independent fluctuations where

$$p(\beta_1, \beta_2, \dots, B_1, B_2, \dots) = p(\beta_1, \beta_2, \dots) p(B_1) p(B_2) \dots \quad (2)$$

b) the case of friendly fluctuations where

$$p(\beta_1, \beta_2, \dots, B_1, B_2, \dots) = p(\beta_1, \beta_2, \dots) \delta(B_1 - B) \delta(B_2 - B) \dots p(\beta). \quad (3)$$

In the first case the amplitude factors B_1, B_2, \dots are independent random quantities. In the second case they are identical random quantities, i.e.,

$$B_1 = B_2 = \dots = B$$

[if they were not equal at least one delta function in the expression (3) would become zero]. As to the distribution function of the initial phases $p(\beta_1, \beta_2, \dots)$, it can be chosen equal to that in the preceding section [formulas (2) and (3) §3.5]. The quantities B_1, B_2, \dots in (2) and B in (3) are assumed to be distributed according to Rayleigh's law

$$p(B) = 2B e^{-B^2}. \quad (4)$$

In analogy to the corresponding relations of the preceding sections we may write for the case of independent fluctuations

$$z[y(t) | \beta_1, \beta_2, \dots, B_1, B_2, \dots] = \sum_k B_k Z_k \cos(\beta_k - \theta_k), \quad (5)$$

$$\mathfrak{Z}(\beta_1, \beta_2, \dots, B_1, B_2, \dots) = \sum_k B_k^2 \mathfrak{Z}_k, \quad (6)$$

where \mathfrak{Z}_k is the mean energy of the k th pulse of the packet.

Substituting the relations (2), (4), (6) into the general formula [(8) §3.2] we obtain

$$I = \prod_k \frac{1}{\pi} \int_0^\infty dB_k \int_0^{2\pi} B_k e^{-B_k^2} e^{-\frac{B_k^2 Z_k}{N_k}} e^{\frac{2B_k Z_k}{N_k} \cos(\beta_k - \alpha_k)} d\beta_k.$$

The same transformations as in the derivation of Eq. [(8) §3.4] may be carried out for each factor of the obtained product. For the case of independent fluctuations of the packet pulses we then obtain, finally,

$$I = \prod_k \frac{N_k}{\beta_k + N_k} e^{\frac{1}{N_k + \beta_k} \frac{Z_k^2}{2}}. \quad (7)$$

For the case of friendly packet fluctuations we may obtain, similarly

$$I = 2 \int_0^\infty B e^{-\frac{B^2(\beta_t + N_k)}{N_k}} \left[\prod_k I_0\left(\frac{2\beta_k Z_k}{N_k}\right) \right] dB, \quad (8)$$

where β_t is the mean packet energy

$$\beta_t = \sum_k \beta_k.$$

The formula for the probability ratio is considerably simpler for independent packet fluctuations (7) than formula (8) for the case of friendly fluctuations.

We must note that formula (7) is not only applicable to a packet of pulse signals nonoverlapping in time, but also in several other cases. It is also correct in the case where the signal overlap, but have nonoverlapping spectra, and their fluctuations are independent. In several works on radar these signals are recommended for reducing the influence of target fluctuations (the case that signal fading on one of the carrier frequencies will be accompanied by fading on another frequency is not very probable if the frequency separation is great enough). It is easy to see that the calculations carried out will remain correct also for the aforementioned class of signals if in Eq. (1) the phase $\omega_0 t + \varphi_k(t)$ is replaced by $\omega_k t + \varphi_k(t)$. In this case, also Eqs. (5), (6)

and, consequently, also Eq.(7) will remain valid.

Manu-
script
Page
No.

[Transliterated Symbols]

70	$c\pi = sp = \text{signal } s \text{ pomekhoy} = \text{signal with interference}$
70	$\pi = p = \text{pomekha} = \text{interference}$
71	$\text{makc} = \text{maks} = \text{maksimal'nyy} = \text{maximum.}$

Chapter 4

THEORY AND PRINCIPLES OF DESIGNING DEVICES FOR OPTIMUM DETECTION AND MEASUREMENT OF PARAMETERS

§4.1. GENERAL CONSIDERATIONS CONCERNING THE CONSTRUCTION OF DEVICES FOR OPTIMUM DETECTION AND MEASUREMENT OF PARAMETERS

As shown before, the problem of optimum detection may be solved in the following way: the probability ratio for the received oscillation $y(t)$ is calculated; it is then compared with some threshold l_0 , whose value is determined such that the probability of false alarm F does not exceed an admissible value F_{dop} . Not only the probability ratio, but also any quantity connected monotonically with it can be compared with the threshold. The calculations of this quantity may be automatized or not, but it is just the automatized calculations realizable by means of optimum receivers that are most interesting for present-day radar.

The situation occurring in the solution of the problem concerning optimum measurement of parameters is analogous. An optimum receiver must calculate the a-posteriori probability density [(16) §2.7] or any quantity connected with it monotonically as a function of the possible values of the measurable parameters. As a result, some optimum estimates, e.g., the most probable estimates corresponding to the maximum of the a-posteriori probability density must be worked out. The optimum measurement devices must carry out the calculation of these estimates, depending on the high-frequency oscillations entering the input of the receiver, in which case it is desirable to carry out these calculations

automatically.

The purpose of this chapter is to consider the possibilities of synthesizing detection and measurement -- revealed by theory. The values of the probability ratios obtained in the preceding chapter for fundamental signal models in the presence of an interference in the form of white Gaussian noise will be the starting point in the synthesis of these devices.

§4.2. SIMPLEST CORRELATION CIRCUITS OF OPTIMUM RECEIVERS

To start with, we shall consider the problem of synthesizing optimum receivers as applied to detection devices for the three simplest radar signal models: a signal with completely given parameters, a signal with random initial phase and a signal with random amplitude and random initial phase. The probability ratios for these signals read, respectively:

$$l = e^{-\frac{\beta}{N_0}} e^{\frac{2z}{N_0}}, \quad (1)$$

$$l = e^{-\frac{\beta}{N_0}} I_0\left(\frac{2z}{N_0}\right), \quad (2)$$

$$l = \frac{N_0}{\beta + N_0} e^{\frac{1}{N_0} \frac{z^2}{\beta + N_0}}. \quad (3)$$

Here

$$z = \int_{-\infty}^{\infty} x(t) y(t) dt, \quad (4)$$

$$z = \sqrt{z_1^2 + z_2^2}, \quad (5)$$

where, in its turn,

$$z_{1,2} = \int_{-\infty}^{\infty} x_{1,2}(t) y(t) dt, \quad (6)$$

and

$$x_{1,2}(t) = \pm X(t) \begin{cases} \cos \\ \sin \end{cases} \{\omega_c t + \varphi_x(t)\}. \quad (7)$$

For a signal with completely given parameters the probability ratio (1) is a monotonic function of the correlation integral z to be determined from relation (4). The comparison of the probability ratio with the threshold z_0 is equivalent to the comparison of the correlation integral with the corresponding threshold z_0 , which is illustrated by Fig. 1.7, except for the designations.

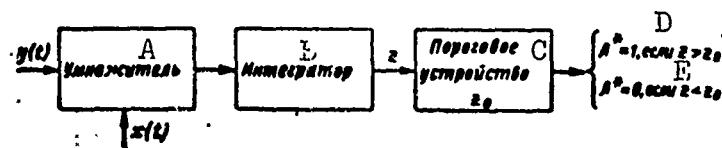


Fig. 4.1. Structural diagram of the simplest correlation detector. A) Multiplier; B) integrator; C) threshold device; D) if; E) if.

Thus, the device for optimum detection of a signal with completely given parameters must calculate the correlation integral (4) and compare it with the threshold z_0 .

Figure 4.1 shows the structural diagram of such an optimum detector. It consists of a multiplier, an integrator and a threshold device (a minimum limiter). A reference oscillation $x(t)$ corresponding to the expected signal and the received signal $y(t)$ are fed to the multiplier. Immediate integration of the product $x(t)y(t)$ yields the correlation integral. Such a receiver is termed a correlation receiver. The value of the correlation integral is compared with the threshold z_0 in the limiter circuit. The threshold level is chosen such that if there is no useful signal the probability of exceeding the threshold (the probability of false alarm F) is not greater than the admissible one.

For signals with random initial phase and signals with random amplitude and initial phase either of the probability ratios [(2) or (3)] is a monotonic function of the quantity $Z = \sqrt{z_1^2 + z_2^2}$. $z_{1,2}$ are here the correlation integrals to be determined from Eq. (6). Thus, in

these cases the optimum detector circuit must calculate the correlation integrals z_1 and z_2 . After the $\sqrt{z_1^2 + z_2^2}$ operation the comparison of the obtained quantity Z with the threshold z_0 which is chosen by the same considerations as in the first case must be made. Figure 4.2 shows the structural diagram of the corresponding device. The oscillations $x_1(t)$ and $x_2(t)$, which are phases shifted by 90° are fed to its multipliers as reference vibrations. In radio engineering such oscillations are usually called quadrature oscillations. Consequently, also the diagram shown in Fig. 4.2 may be termed correlation diagram with two quadrature channels.

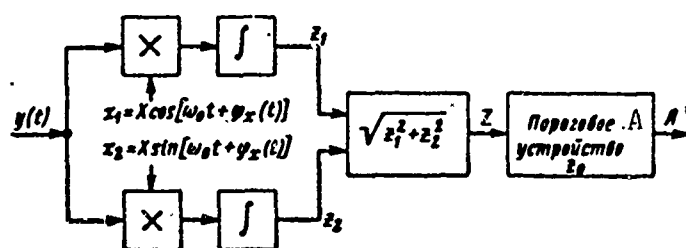


Fig. 4.2. Diagram of a correlation detector with two quadrature channels. A) Threshold device.

The existence of two channels excludes the possibility of losing the useful signal owing to the fact that its initial phase is unknown. If, e.g., the useful signal does not yield an increase of the correlation integral in the first channel on account of a phase shift by 90° relative to the reference voltage, it certainly yields an increase of the correlation integral in the second quadrature channel. As can be seen from the expressions (5)-(7), the result of reception in the presence of two quadrature channels is independent of the random initial phase. It is remarkable that this rule is taken into account by theory on the basis of general considerations on the optimum way of processing, without previously analyzing the circuit solutions.

The circuits (Fig. 4.1 and 4.2) are only optimum if the position of

the expected signal on the axis of time is known. The case where the delay time of the signal is unknown was not analyzed here in detail owing to difficulties of computational character. An answer to the problem whether a signal with unknown delay time is present may, however, be given if the fact of presence or absence of this signal is established for different values of the delay time, the interval between which does not exceed the corresponding resolving power. Hence we can apply a multichannel correlation circuit in which each channel or each pair of quadrature channels is calculated as to its delay time (Fig. 4.3). Multichannel correlation circuits may be used to receive signals differing not only by the delay time, but also by their carrier frequency (e.g., on account of the Doppler effect).

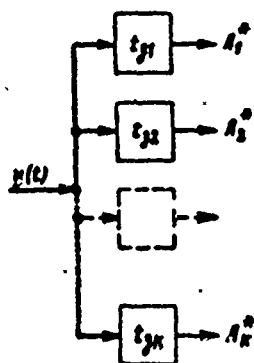


Fig. 4.3. Principle of constructing a multichannel correlation circuit.

We have to note that the reception of signals with arbitrary time delay is particularly widespread and important in radar. The fact that a correlation reception circuit must have a great number of channels for scanning the whole range proves to be its drawback. In the following sections we shall familiarize ourselves with the circuit of optimum reception permitting optimum detection in a wide range of delay times using one receiving channel.

§4.3. USE OF OPTIMUM LINEAR FILTERS IN THE CONSTRUCTION OF OPTIMUM RECEIVERS. PULSE RESPONSE OF THE OPTIMUM FILTER.

We require that a circuit element of optimum reception should compute the correlation integral for arbitrary delay time of the expected signal

$$x(t) = u(t - t_s), \quad (1)$$

where $u(t)$ is the function describing the signal with vanishing time de-

lay. We shall assume that this function is completely known.

In this case the correlation integral is not only a function of the realization of the received oscillation $y(t)$, but also of the delay time of the expected signal. i.e.,

$$z = z[y(t)|t_z] \quad (2)$$

or, rewriting it in a slightly different way.

$$z = z(t_z) = \int_{-\infty}^{\infty} y(t) u(t - t_z) dt. \quad (3)$$

Thus, a circuit realizing the mathematical operation (3) for an arbitrary given function $u(t)$ and an arbitrary parameter t_z must be designed.

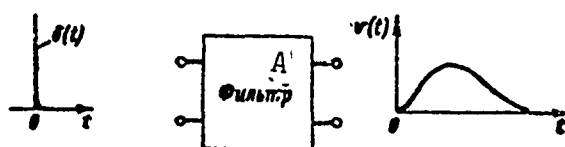


Fig. 4.4. Explanation of Pulse response Determination. A) Filter.

It is easy to see that Eq. (3) is a convolution integral. It is wellknown from the theory of linear electric circuits that the convolution integral expresses the voltage at the output end of the linear filter. Consequently, in order to carry out the mathematical operation (3) it is also possible to use a filter which yields a convolution integral of the required form. In the following such a filter will be called optimum, since it carries out the basic operation of optimum processing - the calculation of the correlation integral.

One of the fundamental characteristics of an arbitrary linear filter is its pulse response, or weight function, $v(t)$. It is wellknown that the pulse response describes the reaction of the system on an input voltage in the form of a single pulse $\delta(t)$, supplied at the instant of time $t = 0$ (Fig. 4.4). Of course, the pulse response assumes values

different from zero only at $t \geq 0$, since the effect cannot precede its cause.

The reaction of the filter on an arbitrary action $y(t)$ is given as the convolution integral of the function $y(t)$ and the pulse response $v(t)$

$$w(t) = \int_{-\infty}^{\infty} v(t-s)y(s)ds. \quad (4)$$

The derivation of relation (4) is illustrated by Fig. 4.5. The action of the oscillation $y(t)$ at the instants of time from s to $s + ds$ is equivalent to the input of a very short pulse with an "area" of $y(s)ds$. The reaction on this pulse at an arbitrary instant of time $t > s$ is equal to $v(t-s)y(s)ds$ and zero if $t < s$. Using the superposition principle we obtain

$$w(t) = \int_{-\infty}^t v(t-s)y(s)ds$$

and

$$0 = \int_t^{\infty} v(t-s)y(s)ds.$$

Summing up these expressions term by term we obtain Eq. (4).

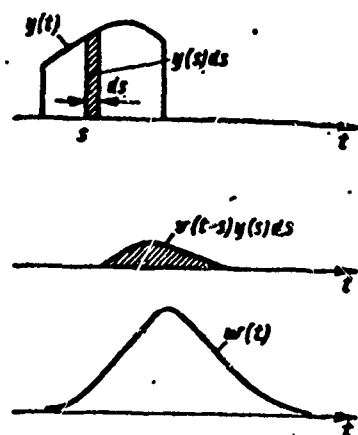


Fig. 4.5. Explanation concerning the calculation of the voltage at the output end of an optimum filter.

As follows from Eq. (4), the voltage at the output end of the filter at an arbitrary instant of time t depends not only on the supplied voltage $y(t)$, but also on the pulse response $v(t)$.

In order to determine the pulse response of the optimum filter we shall require that the voltage at its output end at the instant of time

$t = t_z + t_0$ (t_0 is some constant va-

lue) except for a real factor C should be equal to the value of the correlation integral, i.e.,

$$w(t_0 + t_2) = Cz(t_2). \quad (5)$$

This requirement boils down to the demand that the values of the correlation integral should be reproduced at the output end of the filter one after another with some constant delay t_0 . In this case, the use of the time base permits the fact of exceeding the threshold level to be determined for any delay time of the signal. The greater the delay time, the later the correlation integral will be formed. This corresponds to the picture usually observed on the amplitude marker when the signal from the target is placed at a distance from the base head that grows with the distance from the target.

By virtue of Eqs. (3), (4) and (5) we obtain

$$\int_{-\infty}^{\infty} v(t_0 + t_2 - s)y(s)ds = C \int_{-\infty}^{\infty} u(s - t_2)y(s)ds. \quad (6)$$

Eq. (6) is identically fulfilled if

$$v(t_2 + t_0 - s) = Cu(s - t_2). \quad (7)$$

Introducing a new independent variable $t = t_2 + t_0 - s$, we obtain the final expression for the pulse response of an optimum filter

$$v(t) = v_{\text{opt}}(t) = Cu(t_0 - t), \quad (8)$$

where C and t_0 are constants to be determined by its parameters.

At any instant $t_2 + t_0$ such a filter yields the value of the correlation integral $z(t_2)$ at the output (except for a factor C), i.e., it may serve as the sought element of the optimum reception circuit.

Expression (8) shows that the pulse response of the optimum filter is obtained from the function $u(t)$ describing the signal with zero time delay, by replacing its argument t by $t_0 - t$. Such a transformation corresponds to a mirror reflection of the function $u(t)$ relative to the straight line $t = t_0/2$. The latter is easy to verify if in Eq. (8) the

substitution of variables $t = t_0/2 + \xi$ is carried out. In this case, Eq. (8) may be rewritten in the form

$$v_{\text{opt}}\left(\frac{t_0}{2} + \xi\right) = Cu\left(\frac{t_0}{2} - \xi\right),$$

which attests to the fact that the transformation (8) is a mirror reflection relative to the straight line $t_0/2$. As follows from all these considerations set forth, the mirror pulse response of the optimum filter guarantees the best signal detection on a white Gaussian noise background.

Figure 4.6 a, b, c, d, illustrates the considerations made above. In particular, Fig. 4.6a shows a signal with definite delay time $x(t) = u(t - t_3)$ as superposed on fluctuation noise. The wider the frequency band in which the noise is acting the greater is its dispersion. For white noise the dispersion is infinite. Consequently, the figure shows a noise whose spectral width is about the same as with the useful signal.

Figure 4.6b shows a signal $u(t)$ analogous to a useful one but with zero delay time and without noise. Figure 4.6c shows the corresponding pulse response at $C = 1$. The values of the pulse response and the signal for points on the time axis lying on opposite sides of $t_0/2$ at a distance of the same magnitude ξ coincide.

Figure 4,6c shows the result of optimum filtration as a function of the time t . It was calculated with the help of formula (4) under the condition that the pulse response $v(t)$ is determined by Eq. (8), i.e., that

$$w(t) = C \int_{-\infty}^{\infty} u(t_0 - t + s) y(s) ds. \quad (9)$$

In this case

$$w(t_0 + t_1) = C \int_{-\infty}^{\infty} u(s - t_1) y(s) ds = Cz(t_1).$$

The envelope of the useful signal oscillations at the output end of the filter (in case there is no noise) is shown by the dotted line in Fig. 4.6d.

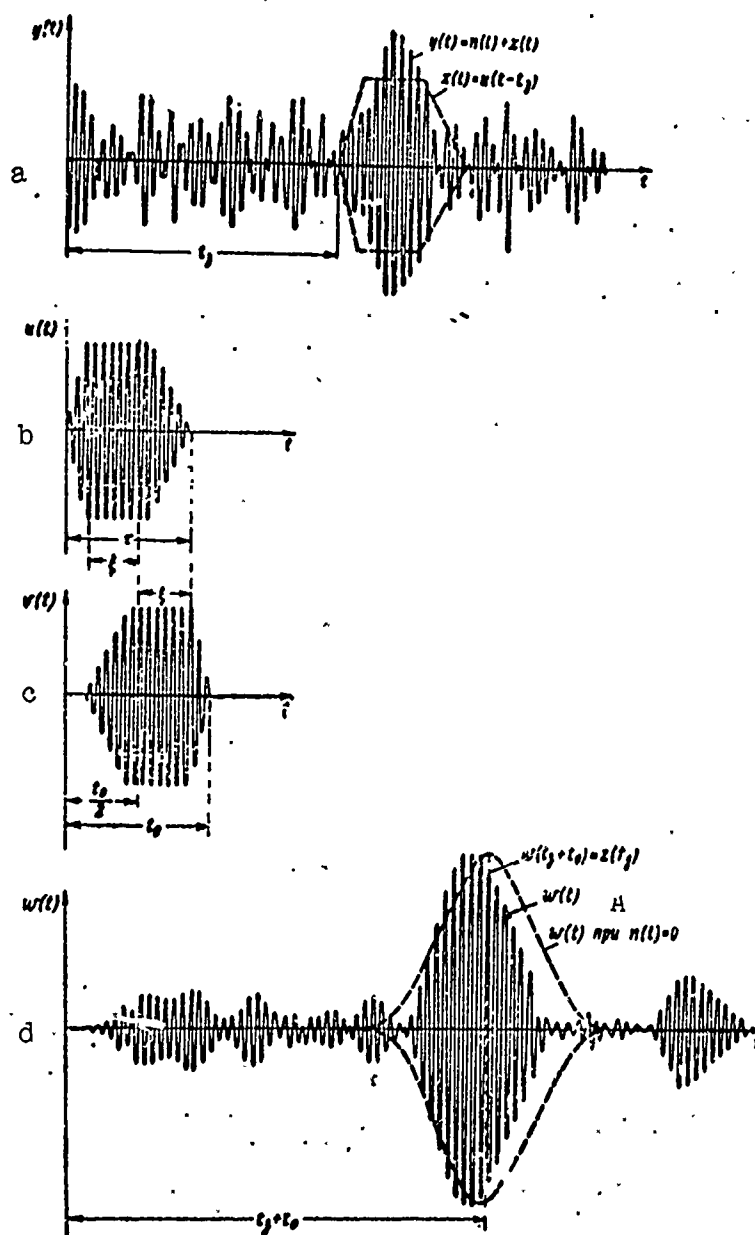


Fig. 4.6. Explanation of the determination and the principle of action of an optimum filter. a) Total voltage $y(t)$ of noise and useful signal at the input end of the filter; b) expected signal $u(t)$ with zero delay time; c) pulse response $v(t) = v_{\text{opt}}(t)$; d) total voltage $w(t)$ of noise and useful signal at the output end of the filter. A) At.

In this case, the maximum corresponds to the time $t_z + t_0$.

The noise distorts the useful signal. Thus, the total voltage of signal and noise at the output end of the filter $w(t)$ at the instant of time $t = t_z + t_0$ will not be maximum, in all probability. The value of $w(t_z + t_0) = C_z(t_z)$, however, always corresponds to the value of the correlation integral for a given signal with an expected delay time t_z . This value appears the later the greater the value of t_0 which, in this way, characterizes the delay of oscillations in an optimum filter.

It can be seen from the figure that after the filtration (Fig. 4.6d) the separation of the signal from the noise background is better than before the filtration (Fig. 4.6a). The difference will be still more remarkable if the interference acts in a wide frequency band, similar to the white noise model.

We must pay attention to the constant quantities C and t_0 which enter Eq. (8) for the pulse response. They permit the demands which must be fulfilled in the realization of optimum processing of the received oscillations with the help of a filter to be taken into account.

As a matter of fact, if the signal amplitude is small the transfer constant of the circuit must be chosen to be great, which is allowed for by a factor $C \neq 1$ in relation (5). At the same time, the corresponding level of the limiting threshold must be determined in order to guarantee the given probability level of false alarm.

Furthermore, a filter cannot be realized by choosing the value of t_0 in an arbitrary way. By way of example, for the signal $u(t)$ (Fig. 4.6b) at $t_0 = 0$ the pulse response of the filter $v(t)$ will lie in the region $t < 0$. Such a response cannot be realized.

Thus, the value of t_0 must be chosen such that the values of the pulse response $v(t)$ different from zero lie in the region $t > 0$. Hence it follows that the duration of the delay in an optimum filter t_0 cannot be shorter than the duration of the signal τ_1 .

§4.4. SIGNAL-TO-NOISE RATIO AT THE OUTPUT END OF AN OPTIMUM FILTER

Owing to the linearity of the filter the voltage at its output end is the sum of the results of the independently acting voltages of the useful signal $x(t)$ and the fluctuation noise $n(t)$. As a matter of fact, carrying out the substitution

$$y(s) = n(s) + u(s - t_2), \quad (1)$$

in Eq. [(9) §4.3] we obtain

$$w(t) = w_c(t) + w_n(t), \quad (2)$$

where

$$w_c(t) = C \int_{-\infty}^{\infty} u(t_0 - t + s) u(s - t_2) ds, \quad (3)$$

$$w_n(t) = C \int_{-\infty}^{\infty} u(t_0 - t + s) n(s) ds. \quad (4)$$

The voltage of the useful signal $w_s(t)$ is a nonrandom function of time. This function attains a maximum at $t = t_z + t_0$ (Fig. 4.6d, dotted line) if both factors of the expression under the integral sign in Eq. (3) are identical functions superposed in time. In this case, the value of the maximum proves to be proportional to the energy of the expected signal and independent of its form:

$$w_c(t_z + t_0) = C \int_{-\infty}^{\infty} u^2(s - t_2) ds = C\mathcal{E} = w_{c \text{ max}}. \quad (5)$$

We may, by the way, conclude from this fact that the instant $t_z + t_0$ of reading off the correlation integral from the output voltage is quite justified. The correlation integral is read off at the moment of maximum expected voltage of the useful signal at the output end of the filter.

This noise voltage $w_p(t)$ is a random function of time. Its mean value is equal to zero since $\overline{n(s)} = 0$. In fact,

$$\overline{w_n(t)} = C \int_{-\infty}^{\infty} u(t_0 - t + s) \overline{n(s)} ds = 0. \quad (6)$$

The noise dispersion is, therefore, equal to the mean square of the voltage $w_p(t)$:

$$\overline{w_p^2(t)} = \left[C \int_{-\infty}^{\infty} u(t_0 - t + s) n(s) ds \right]^2. \quad (7)$$

Replacing the square of the integral by the product of two identical integrals with different variables of integration and passing over to a double integral we obtain

$$\overline{w_p^2(t)} = C^2 \int_{-\infty}^{\infty} u(t_0 - t + s) ds \int_{-\infty}^{\infty} u(t_0 - t + r) \overline{n(s)n(r)} dr. \quad (8)$$

For a stationary interference $n(t)$ with a mean value equal to zero the value of the product $\overline{n(s)n(r)}$ is a correlation function of a difference argument

$$\overline{n(s)n(r)} = R(s-r).$$

As to an interference in the form of white noise with a spectral density N_0 we have by virtue of Eq. [(2) §2.4]

$$\overline{n(s)n(r)} = \frac{N_0}{2} \delta(s-r). \quad (9)$$

Substituting expression (9) into (8) and using the general property of integrals with delta functions

$$\int_{-\infty}^{\infty} \varphi(r) \delta(s-r) dr = \varphi(s),$$

we obtain

$$\overline{w_p^2(t)} = \frac{C^2 N_0}{2} \int_{-\infty}^{\infty} u^2(t_0 - t + s) ds = C^2 \frac{N_0}{2} \mathcal{A}. \quad (10)$$

The effective (root-mean square) interference voltage $w_{p \text{ ef}}$ is, thus, equal to

$$w_{p \text{ ef}} = \sqrt{\overline{w_p^2(t)}} = C \sqrt{\frac{N_0}{2} \mathcal{A}}. \quad (11)$$

The ratio of the maximum value of the signal to the effective value of the interference $w_{s \text{ maks}}/w_{p \text{ ef}}$ is called signal-to-noise voltage ratio. Its value is found with the help of Eqs. (5) and (11),

$$\frac{w_{\text{с max}}}{w_{\text{ш}}} = \frac{C\beta}{c\sqrt{N_0\beta}} = \sqrt{\frac{2\beta}{N_0}}. \quad (12)$$

It is characteristic that the signal-to-noise voltage ratio at the output of the optimum filter depends only on the energy of the useful signal and the spectral noise density N_0 and not on the form of the signal. The same holds for the signal-to-noise power ratio

$$\frac{w_{\text{с max}}^2}{w_{\text{ш}}^2} = \frac{2\beta}{N_0}. \quad (13)$$

There is no filter which can yield a greater signal-to-noise ratio than the optimum filter. In fact, let us assume that such a filter exists. In this case, putting it before the threshold circuit instead of the optimum one a greater probability of correct detection D can be obtained if the probability of false alarm F is given. But it is just the optimum receiver that yields the highest probability D for a given probability F . This implies that also the optimum filter of this receiver under given conditions yields a signal-to-noise ratio which is the highest compared to other linear filters.

§4.5. FREQUENCY CHARACTERISTIC OF AN OPTIMUM FILTER

Besides the pulse-response characteristics of filters the use of their frequency characteristics is very widespread. The frequency characteristics are particularly convenient if signal filtration from noise by means of resonance oscillatory systems is considered. But they can also be used in other cases.

The frequency characteristic $K(f)$ of a linear circuit (in complex form) is determined in the following way. We assume that a harmonic oscillation

$$y(t) = e^{j2\pi ft}. \quad (1)$$

is fed to the input end of the circuit.

In this case, the voltage at its output must be equal to

$$w(t) = K(f) e^{j2\pi ft}. \quad (2)$$

Or, the frequency characteristic is, by definition, the relation

$$K(f) = \frac{w(t)}{y(t)} \text{ for } y(t) = e^{j2\pi ft}. \quad (3)$$

Substituting expression (1) into formula [(4) §4.3] for the voltage at the output end of the filter and replacing $w(t)$ according to formula (2) we obtain

$$K(f) e^{j2\pi ft} = \int_{-\infty}^{\infty} v(t-s) e^{j2\pi fs} ds.$$

Dividing both sides of the equation by the factor $e^{j2\pi ft}$ and carrying out the substitution of variables $t - s = \tau$, we find an expression for the frequency characteristic in terms of the pulse-response characteristic:

$$K(f) = \int_{-\infty}^{\infty} v(\tau) e^{-j2\pi f\tau} d\tau. \quad (4)$$

Equation (4) shows that the frequency characteristic is the Fourier transform of the pulse-response characteristic.

Making use of relation (4) we find the frequency characteristic of the optimum filter. In view of

$$v_{\text{opt}}(t) = Cu(t_0 - t),$$

we obtain

$$K_{\text{opt}}(f) = C \int_{-\infty}^{\infty} u(t_0 - \tau) e^{-j2\pi f\tau} d\tau.$$

Carrying out the substitution of variables $t_0 - \tau = t$, we find

$$K_{\text{opt}}(f) = C \int_{-\infty}^{\infty} u(t) e^{j2\pi ft} dt e^{-j2\pi ft_0}. \quad (5)$$

Hence it follows that the frequency characteristic of the optimum filter $K_{\text{opt}}(f)$ will be

$$K_{\text{opt}}(f) = C g^*(f) e^{-j2\pi ft_0}. \quad (6)$$

Here C and t_0 are real constants (as also in §4.3), $g^*(f)$ is the

complex conjugate value of the spectral density $g(f)$ of the expected signal $u(t)$,

$$g(f) = \int_{-\infty}^{\infty} u(t) e^{-j2\pi ft} dt. \quad (7)$$

The expression $g^*(f)$ differs from expression (7) only by the sign in front of the factor j in the power exponent.

We shall pass over to a more detailed analysis of relation (6) determining the frequency characteristic of an optimum filter.

Evidently, this characteristic is described by the complex conjugate spectral density $g^*(f)$ of the expected signal $u(t)$, except for an arbitrary real factor C and the delay factor $e^{-j2\pi f t_0}$.

We shall rewrite the spectral density of the expected signal in terms of its modulus and its argument

$$g(f) = |g(f)| e^{j \arg g(f)}, \quad (8)$$

where $|g(f)|$ corresponds to the amplitude frequency spectrum of the expected signal, and $\arg g(f)$ to its phase-frequency spectrum. Obviously,

$$g^*(f) = |g(f)| e^{-j \arg g(f)}, \quad (9)$$

i.e., in the conjugate spectrum the modulus is the same, but the argument has the opposite sign.

Substituting expression (9) into formula (6) we obtain

$$K_{\text{opt}}(f) = C |g(f)| e^{-j \arg g(f)} e^{-j2\pi f t_0}. \quad (10)$$

Taking the modulus and the argument of both sides of Eq. (10) it is possible to go over to the amplitude-frequency and the phase-frequency characteristics of the optimum filter, respectively.

To start with, we shall deal with the modulus. Noting that $|e^{j\alpha}| = 1$, we obtain

$$|K_{\text{opt}}(f)| = C |g(f)|. \quad (11)$$

This implies that the amplitude-frequency characteristic of an op-

timum filter is proportional to the amplitude-frequency spectrum of the expected signal. An optimum filter must, therefore, be most permeable for those spectral components which are most distinctly expressed in the spectrum. Weak spectral components of the signal are suppressed by the filter since in the opposite case besides them intense noise components would pass through in a wide frequency range. The shape of the amplitude-frequency spectrum at the output end of the filter is distorted, which is one of the reasons for the distortion of the signal (e.g., Fig. 4.6d). The problem of filtration in the given case is, however, the best discrimination of this signal on the noise background rather than an exact reproduction of the signal shape.

Taking the argument of both sides of Eq. (10) we obtain

$$\arg K_{\text{opt}}(f) = -\arg g(f) - 2\pi ft_0. \quad (12)$$

Equation (12) shows that the argument of the frequency characteristic of the optimum filter is the sum of the argument of the expected signal spectrum, taken with the reverse sign, and the argument of the delay $-2\pi ft_0$. Such a choice of the phase-frequency characteristic is, obviously, very valuable from the viewpoint of guaranteeing an optimum filtration effect.

In order to convince ourselves of this fact, we shall express the signal component of the voltage at the output end of the filter in terms of the corresponding frequency characteristics. If a useful signal $u(t - t_z)$ enters the input end of the filter, and the spectral density of the function $u(t)$ is equal to $g(f)$, the spectral density of the signal $u(t - t_z)$ will be $g(f)e^{-j2\pi ft_z}$, according to the delay theorem. The corresponding spectral density at the output end of the filter is equal to

$$K_{\text{opt}}(f)g(f)e^{-j2\pi ft_z}$$

and the voltage of the useful signal at the output end of the filter at an arbitrary instant of time t will be

$$w_o(t) = \int_{-\infty}^{\infty} K_{opt}(f) g(f) e^{-j2\pi f t_0} e^{j2\pi f t} df. \quad (13)$$

according to the superposition principle.

Substituting here instead of $K_{opt}(f)$ its expression (10) we obtain the relation

$$w_o(t) = C \int_{-\infty}^{\infty} |g(f)|^2 e^{j2\pi f (t - t_0 - t_0)} df, \quad (14)$$

which is the spectral analog of the preceding expression [(3) §4.4].

Using the Euler formula and the oddness of the function $\sin[2\pi f(t - t_0 - t_0)]$, we find finally,

$$w_o(t) = C \int_{-\infty}^{\infty} |g(f)|^2 \cos[2\pi f(t - t_0 - t_0)] df.$$

It is evident from the expression obtained that the voltage at the output end of the filter, which is a superposition of harmonic components of different frequencies, is determined by the amplitude-frequency spectrum of the signal. It does not depend on the phase-frequency spectrum since the latter is compensated by the phase-frequency characteristic of the filter. Consequently, all harmonic components simultaneously attain the amplitude values at the instant of time $t = t_0 + t_0$, and these values are superposed on each other (Fig. 4.7). At this instant of time the voltage maximum of the useful signal at the output end of the filter

$$w_{o \max} = w_o(t_0 + t_0) = C \int_{-\infty}^{\infty} |g(f)|^2 df.$$

occurs.

By virtue of Parseval's theorem

$$\int_{-\infty}^{\infty} |g(f)|^2 df = \int_{-\infty}^{\infty} u^2(t) dt,$$

i.e., this maximum is determined by the value of the energy of the useful signal

$$\omega_{\text{с макс}} = C\beta.$$

It is easy to understand the results of deviations from an optimum phase-frequency characteristic. If the latter does not compensate the phase shifts, the maxima of the harmonic components (Fig. 4.7) will move apart, and the peak of the total oscillation of the useful signal will begin to fade away. This fact aggravates the conditions of discriminating the signal on the noise background.

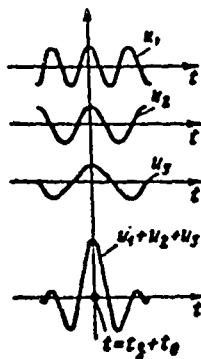


Fig. 4.7. Superposition of the maxima of the useful signal's harmonic components at the output end of the filter in the case of an optimum phase-frequency characteristic.

§4.6. APPLICATION OF THE METHOD OF ENVELOPES IN THE ANALYSIS OF THE OPTIMUM FILTRATION PROCESS

In the case of high-frequency oscillations with slowly varying amplitude and initial phase the relations used for calculation may be simplified considerably by using the so-called method of envelopes.

We shall represent the oscillations at the input end of the filter in complex form

$$y(t) = Y(t) \cos[\omega_c t + \varphi_y(t)] = \operatorname{Re}[Y(t)e^{j\omega_c t}]. \quad (1)$$

$\bar{Y}(t)$ is here the envelope of the amplitudes, and $\bar{Y}(t)$ is the complex amplitude (complex envelope) including the initial phase

$$Y(t) = Y(t) e^{j\omega_0 t}. \quad (2)$$

In an analogous way, the complex amplitudes $\vec{X}(t)$, $\vec{U}(t)$, $\vec{V}(t)$, $\vec{W}(t)$ may be introduced.

All relations for the complex amplitudes follow from the corresponding relations for the instantaneous values $y(t)$, $x(t)$, $u(t)$, $v(t)$, $w(t)$, as can be shown by several examples.

As the first example, we shall consider the expression for an expected signal arriving with some delay:

$$x(t) = u(t - t_0)$$

or

$$x(t) = X(t) \cos[\omega_0 t + \varphi_x(t)] = U(t - t_0) \cos[\omega_0(t - t_0) + \varphi_u(t - t_0)].$$

Introducing complex amplitudes we obtain

$$\operatorname{Re}[X(t) e^{j\omega_0 t}] = \operatorname{Re}[U(t - t_0) e^{-j\omega_0 t_0} e^{j\omega_0 t}].$$

Since this equation is correct for arbitrary values of the complex quantity $e^{j\omega_0 t}$, also the complex factors with $e^{j\omega_0 t}$ are equal to one another, i.e.,

$$X(t) = U(t - t_0) e^{-j\omega_0 t_0}. \quad (3)$$

We pass to the corresponding expression for the pulse-response characteristic of the optimum filter

$$v_{\text{opt}}(t) = Cu(t_0 - t).$$

Introducing complex amplitudes we obtain

$$\operatorname{Re}[V_{\text{opt}}(t) e^{j\omega_0 t}] = \operatorname{Re}[CU(t_0 - t) e^{j\omega_0(t_0 - t)}]. \quad (4)$$

It is still inconvenient to use this expression to compare the complex amplitudes since the factor $e^{j\omega_0 t}$ enters the left-hand side of Eq. (4), whereas the factor $e^{-j\omega_0 t}$ enters the right-hand side. We shall, therefore, replace the complex expression the right-hand side of Eq. (4) by its complex conjugate value: in this case the real part will not change and the equation

$$\operatorname{Re}[V_{\text{opt}}(t)e^{j\omega_0 t}] = \operatorname{Re}[CU^*(t_0 - t)e^{-j\omega_0 t}e^{j\omega_0 t}].$$

remains correct.

The obtained relation holds for arbitrary values of $e^{j\omega_0 t}$. Consequently,

$$V_{\text{opt}}(t) = CU^*(t_0 - t)e^{-j\omega_0 t}. \quad (5)$$

Expression (5) establishes the connection between the complex amplitudes of the pulse-response characteristic and the expected signal.

We shall now consider the connection of the complex amplitudes at the input and output ends of the optimum filter. As before, we shall choose the corresponding expression for the instantaneous values [(4) §4.3], to be the basis. Introducing complex amplitudes into it, we obtain

$$\operatorname{Re}[W(t)e^{j\omega_0 t}] = \int_{-\infty}^{\infty} \operatorname{Re}[V(t-s)e^{j\omega_0(t-s)}] \operatorname{Re}[Y(s)e^{j\omega_0 s}] ds. \quad (6)$$

In order to transform (6) we use an auxiliary relation that is well-known from the theory of complex numbers,*

$$\operatorname{Re} a \operatorname{Re} b = \operatorname{Re} \left[\frac{ab}{2} + \frac{ab^*}{2} \right]. \quad (7)$$

Besides, we shall take account of the fact that the real part of the sum is equal to the sum of the real parts and that this relation remains correct if we go over from sums to integrals. The right-hand side of expression (6) may then be rewritten in the form

$$\operatorname{Re} \left[\frac{1}{2} \int_{-\infty}^{\infty} ab ds + \frac{1}{2} \int_{-\infty}^{\infty} ab^* ds \right],$$

where

$$\begin{aligned} a &= V(t-s)e^{j\omega_0(t-s)}, \\ b &= Y(s)e^{j\omega_0 s}. \end{aligned}$$

As a result of transforming (6) we obtain

$$\operatorname{Re} [W(t) e^{j\omega_0 t}] = \operatorname{Re} \{ [W_1(t) + W_2(t)] e^{j\omega_0 t} \}, \quad (8)$$

where

$$W_1(t) = \frac{1}{2} \int_{-\infty}^{\infty} V(t-s) Y(s) ds, \quad (9)$$

$$W_2(t) = \frac{1}{2} \int_{-\infty}^{\infty} V(t-s) Y^*(s) e^{-j2\omega_0 s} ds. \quad (10)$$

It follows from relation (8) that the expression for the complex voltage amplitude at the output end of the filter may be written in the form

$$W(t) = W_1(t) + W_2(t), \quad (11)$$

where the quantities $W_1(t)$ and $W_2(t)$ are determined in terms of the complex input voltage amplitude by Eqs. (9) and (10).

In the case of a sufficiently high carrier frequency (compared to the spectral width of the signal) the complex amplitudes vary slowly whereas the factor $e^{-j2\omega_0 s}$ in expression (10) oscillates rapidly, compared to them. Consequently, on integrating expression (10) we obtain a negligibly small value of the second term in (11) compared to the first one, i.e.,

$$W(t) \approx W_1(t) = \frac{1}{2} \int_{-\infty}^{\infty} V(t-s) Y(s) ds. \quad (12)$$

Formula (12) is a very convenient calculational aid for analyzing linear electric filters.

In particular, we obtain for an optimum filter by virtue of relation (5)

$$W_{\text{opt}}(t) \approx \frac{1}{2} C e^{-j\omega_0 t} \int_{-\infty}^{\infty} U^*(t_0 - t + s) Y(s) ds. \quad (13)$$

If a useful signal without any interference $Y(t) = X(t)$ [relation (3)] acts on the input end of the optimum filter

$$W_e(t) = \frac{1}{2} C e^{-j\omega_0(t-t_0)} \int_{-\infty}^{\infty} U^*(t_0 - t + s) U(s - t_0) ds.$$

The envelope of the useful voltage at the output end of the filter can be found as the modulus of the corresponding complex amplitude

$$W_e(t) = |W_e(t)| = \frac{1}{2} C \left| \int_{-\infty}^{\infty} U^*(s - t + t_0) U(s - t_0) ds \right|. \quad (14)$$

It is characteristic that factors oscillating with high frequency do not enter relation (14), for which reason the calculation of the envelope is simpler than that with the help of the formula for the instantaneous values [(4) §4.3.].

By way of example, let us calculate the result of the action of a radio pulse with constant instantaneous frequency on the optimum filter. We assume the shape of the envelope to be similar to a rectangular one, supposing the duration of the fronts to be small compared to the pulse duration τ_1 (but great compared to the oscillation period). For numerous calculations we shall restrict ourselves to the rectangular approximation, on the assumption that the function

$$u(t - t_0) = \cos \omega_0(t - t_0) = \text{Re}[e^{j\omega_0(t - t_0)}],$$

if $t_0 < t < t_0 + \tau_1$, and that this function is equal to zero for all other t . Hence it follows that its complex amplitude

$$U(t - t_0) = \begin{cases} 1, & \text{if } t_0 \leq t \leq t_0 + \tau_1, \\ 0, & \text{if } t < t_0 \text{ or } t > t_0 + \tau_1. \end{cases} \quad (15)$$

In the given case, the complex amplitude is described by the real function $U(t - t_0) = U(t - t_0)$. In this case, also each factor in the expression under the integral sign of relation (14) will be real:

$$U^*(s - t + t_0) = U(s - t + t_0),$$

$$U(s - t_0) = U(s - t_0).$$

The diagrams of these factors and their products as functions of the integration variable s are shown in Fig. 6. a, b, c, , which correspond to the following four cases:

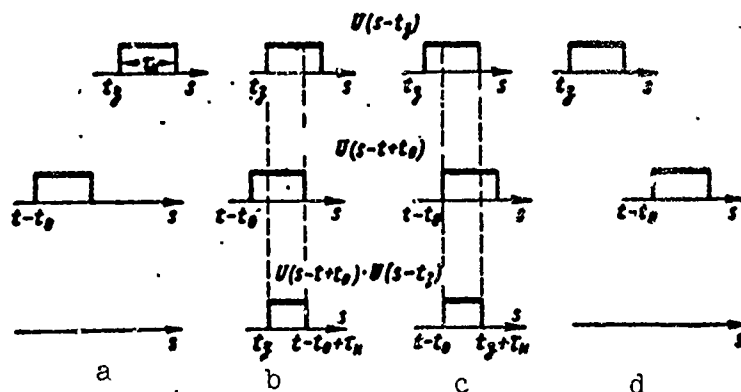


Fig. 4.8. Typical calculation of voltage envelope at optimum-filter output.

- a $t - t_0 + \tau_n < t_2$ (Fig. 4.8a),
 b $t_0 < t - t_0 + \tau_n < t_2 + \tau_n$ (Fig. 4.8b)
 c $t_2 < t - t_0 < t_2 + \tau_n$ (Fig. 4.8c).
 d $t_2 + \tau_n < t - t_0$ (Fig. 4.8d).

It is easy to see that for the cases a and d the integral (14) is equal to zero since the expression under the integral sign vanishes identically.

For the cases b and c we find, respectively:

$$W_0(t) = \frac{1}{2} C \int_{t_2}^{t-t_0+\tau_n} ds = \frac{1}{2} C [\tau_n + (t-t_0-t_2)],$$

$$-\tau_n < (t-t_0)-t_2 < 0,$$

$$W_0(t) = \frac{1}{2} C \int_{t-t_0}^{t_2+\tau_n} ds = \frac{1}{2} C [\tau_n - (t-t_0-t_2)],$$

$$0 < (t-t_0)-t_2 < \tau_n.$$

or else,

$$W_0(t) = \begin{cases} \frac{1}{2} C [\tau_n - |(t-t_0)-t_2|], & \text{if } |(t-t_0)-t_2| < \tau_n, \\ 0, & \text{if } |(t-t_0)-t_2| > \tau_n. \end{cases} \quad (16)$$

Figure 4.9a and b show diagrams of the envelope of the useful signal voltages at the input and output ends of the filter as functions of

time. Analogous diagrams of the instantaneous values of the same voltages are drawn in Fig. 4.9c and d. The maximum of the output voltage envelope corresponds to the instant of time $t_z + t_0$. The filter realizability condition $t_0 \geq \tau_1$ corresponds to the fact that the voltage peak at the output end of the optimum filter cannot be obtained before the pulse has come to an end. In the opposite case, it would be quite impossible to make use of all its energy.

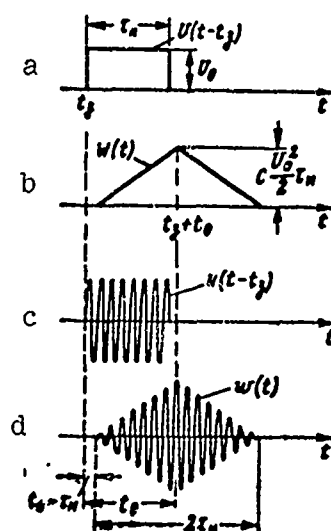


Fig. 4.9. Diagrams showing the envelopes and instantaneous values of a useful signal at the input and output ends of an optimum filter for a rectangular radio pulse with constant carrier frequency.

§4.7. RECEIVER WITH OPTIMUM FILTER IN THE CASE OF RANDOM INITIAL PHASE OF THE SIGNAL

We may approach the problem of designing a receiver with optimum filter in the case of random initial phase of the signal from two points of view.

It is, e.g., possible to analyze the behavior of the voltage at the output end of the filter if the initial phase is random and hence to provide for the corresponding modifications in optimum processing.

More rigorous will, however, be the synthesis of a processing

device with optimum filter immediately from the probability ratio for a signal with random initial phase or with random amplitude and initial phase. We shall, therefore, begin with the analysis of the probability ratio.

It follows from expressions [(2) and (3) §4.2] that the probability ratios are monotonic functions of the quantity $Z = \sqrt{z_1^2 + z_2^2}$ for these cases. It was just this fact which was chosen to be the basis of designing a correlation reception circuit with two quadrature channels. When using an optimum filter it is not necessary to have a circuit with two quadrature channels. We shall confirm this by appropriate mathematical calculations.

From Eqs. [(7) §4.2] we obtain

$$x_1(t) = \operatorname{Re}[X(t)e^{j\omega t}] = \operatorname{Re}[X^*(t)e^{-j\omega t}], \quad x_2(t) = -\operatorname{Im}[X(t)e^{j\omega t}] = \operatorname{Im}[X^*(t)e^{-j\omega t}],$$

where $X(t) = X(t)e^{j\varphi_X(t)}$. Hence by virtue of [(6) §4.2]

$$z_1 = \operatorname{Re} \left[\int_{-\infty}^{\infty} y(t) X^*(t) e^{-j\omega t} dt \right],$$

$$z_2 = \operatorname{Im} \left[\int_{-\infty}^{\infty} y(t) X^*(t) e^{-j\omega t} dt \right].$$

Let us remember that for any complex number $a = \operatorname{Re} a + j\operatorname{Im} a$ the equation

$$\sqrt{(\operatorname{Re} a)^2 + (\operatorname{Im} a)^2} = |a|,$$

is valid.

Consequently,

$$Z = \sqrt{z_1^2 + z_2^2} = \left| \int_{-\infty}^{\infty} y(t) X^*(t) e^{-j\omega t} dt \right|. \quad (1)$$

Using the obvious equation

$$y(t) = Y(t) \cos[\omega_0 t + \varphi_Y(t)] = \frac{1}{2} Y(t) e^{j\omega_0 t} + \frac{1}{2} Y^*(t) e^{-j\omega_0 t}, \quad (2)$$

we rewrite the expression under the integral sign (1) as the sum of two

terms

$$\frac{1}{2} Y(t) X^*(t) + \frac{1}{2} Y^*(t) X(t) e^{-j\omega_0 t},$$

the second of which is rapidly oscillating with the high frequency $2\omega_0$. Neglecting its integral we obtain

$$Z \approx \left| \frac{1}{2} \int_{-\infty}^{\infty} Y(t) X^*(t) dt \right| \quad (3)$$

or, owing to Eq. [(3) §4.6]

$$Z(t_z) \approx \left| \frac{1}{2} \int_{-\infty}^{\infty} Y(t) U^*(t - t_z) e^{j\omega_0 t} dt \right|. \quad (4)$$

Putting the constant factor $e^{j\omega_0 t}$ in front of the integral sign and realizing that its modulus is equal to unity we obtain

$$Z(t_z) = \left| \frac{1}{2} \int_{-\infty}^{\infty} Y(s) U^*(s - t_z) ds \right|. \quad (5)$$

Let us compare the obtained expression with expression [(13) §4.6] for the voltage at the output end of the optimum filter as calculated for a given signal $u(t)$ with arbitrarily chosen initial phase. We substitute into [(13) §4.6] the value of $t = t_z + t_0$ corresponding to reading off the amplitude peak of the useful signal at the output end of the filter. Passing over to the modulus and taking into account that $|e^{-j\omega_0 t}| = 1$, we obtain

$$|W_{out}(t_z + t_0)| = \frac{1}{2} C \left| \int_{-\infty}^{\infty} Y(s) U^*(s - t_z) ds \right| \quad (6)$$

or

$$W_{out}(t_z + t_0) = CZ(t_z) \cdot * \quad (7)$$

Thus, the voltage amplitude at the output end of the optimum filter at the instant $t_z + t_0$ represents, except for a factor, the quantity $Z(t_z)$, which also has to be compared with the threshold for each trial delay time. Thus, in order to obtain the quantity $Z(t_z)$, it is sufficient to have only one channel. In order to go over from the in-

stantaneous voltage values at the output end of the filter to the amplitude values an envelope detector must be set up. In other words, an optimum receiver must contain a detector, besides the filter.

We may come to the same conclusion by directly analyzing the voltage at the output end of the optimum filter in the case of a random initial phase of the signal, which was remarked at the beginning of the section. The phase of the input voltage is also random in this case. Information on the presence of a signal is, therefore, only yielded by the envelope, which may be obtained by amplitude detection.

The voltage after the detector must be compared with the threshold whose level is chosen by taking account of the transmission factor C of the filter. One channel of optimum processing (Fig. 4.10) permits targets differing by the delay time to be detected.

The significance of the results obtained is sufficiently general. The processing system consisting of the optimum filter and the amplitude detector may be used, as will be shown in the following, as an element of the system of optimum delay time measurement for the type of signal under consideration. Besides, the conclusions obtained for signals with random initial phase may also be applied to more complex signal models.

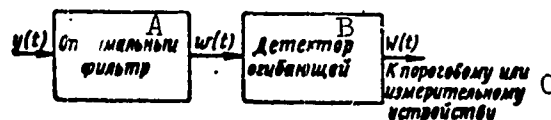


Fig. 4.10. Principle of designing a single-channel receiver with optimum filter for a signal with random initial phase. A) Optimum filter; B) envelope detector; C) toward the threshold and measuring device.

§4.8. CORRELATION-FILTRATION RECEPTION

Considering various versions of optimum processing we satisfied ourselves of the fact that in each of them we encountered on the calculation of the correlation integral

$$z = \int_{-\infty}^{\infty} x(t)y(t)dt. \quad (1)$$

In §4.2 the computation of this integral by means of direct multiplication and integration with the help of a correlator was considered: In §4.3-4.7 we intended to obtain this integral as the voltage at a certain instant of time at the output end of a linear optimum filter.

A combined method of calculating this integral is also possible, in which both multiplication of the voltages and filtration of the oscillation obtained in doing so are used. We will call a receiver designed according to this principle a correlation-filtration receiver.

Let us assume that the expected oscillation $x(t)$ can be represented as the product of two functions

$$x(t) = x_1(t)x_2(t). \quad (2)$$

Figure 4.11 shows that the computation of the correlation integral (1) is carried out in two stages. First, the received oscillation $y(t)$ is immediately multiplied by $x_1(t)$. The received oscillation

$$y_1(t) = y(t)x_1(t) \quad (3)$$

is fed to the filter which is optimum for the oscillation $x_2(t)$. At a certain instant of time the correlation integral

$$\int_{-\infty}^{\infty} y_1(t)x_2(t)dt = \int_{-\infty}^{\infty} y(t)x_1(t)x_2(t)dt. \quad (4)$$

is formed at the output end of the filter.

By virtue of relation (2) this integral coincides with the given correlation integral (1).

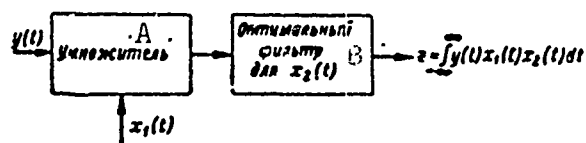


Fig. 4.11. Structural diagram of the simplest correlation-filtration receiver. A) Multiplier; B) optimum filter for $x_2(t)$.

Figure 4.12 shows a coherent sequence of rectangular radio pulses $x(t)$ as an example illustrating the representation of a real signal by means of relation (2). It is represented as the product of two functions - the function $x_1(t)$, which corresponds to a sequence of video pulses, and the function $x_2(t)$ corresponding to a single radio pulse of long duration.

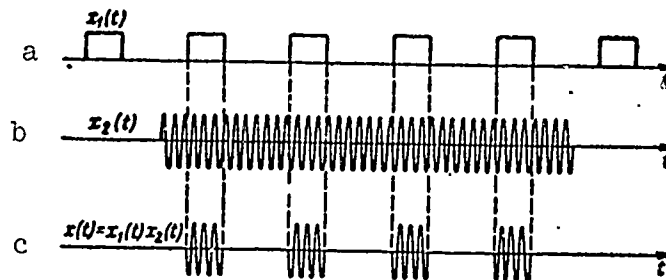


Fig. 4.12 Representation of a coherent sequence of pulses as a product of two functions.

The multiplication of an arbitrary function $y(t)$ by $x_1(t)$ (Fig. 4.12a) is equivalent to a gating of the oscillation $y(t)$ by means of rectangular, selecting video pulses $x_1(t)$. In its turn, designing a filter for a single radio pulse $x_2(t)$ (Fig. 4.12b) is a simpler problem than designing it for a series of pulses (Fig. 4.12c).

The simplest approximation to an optimum filter for a radio pulse of long duration $x_2(t)$ is a narrow-band circuit whose band is inversely proportional to the duration of the pulse.

We must, however, mention that the reduction of the demands made on the filter is achieved on account of a limitation of the possibilities of using the circuit. Optimum work of the circuit is only possible if the gated pulses coincide with the pulses subject to processing. In the opposite case transition to multichannel circuits is necessary as shown in Fig. 4.3.

For the example under consideration the receiver (Fig. 4.11), thus, proves to be a device with gating of the pulses to be processed and their coherent storage in the narrow-band system on the high frequency applied.

Let us consider another important but, compared to the preceding one, modified case of correlation-filtration reception which leads to optimum processing making use of filtering systems on an intermediate frequency. Let

$$x(t) = X(t) \cos[\omega_0 t + \varphi_x(t)],$$

where

$$X(t) = X_1(t) X_2(t), \quad \omega_0 = \omega_1 + \omega_2, \\ \varphi_x(t) = \varphi_1(t) + \varphi_2(t).$$

If the functions $x_1(t) = X_1(t) \cos[\omega_1 t + \varphi_1(t)]$ and $x_2(t) = X_2(t) \cos[\omega_2 t + \varphi_2(t)]$ are introduced, their product yields $x(t)$ up to a difference frequency term $\omega_1 - \omega_2$ and an unimportant factor $1/2$:

$$x_1(t) x_2(t) = \frac{1}{2} X_1(t) X_2(t) \cos[\omega_0 t + \varphi_x(t)] + \\ + \frac{1}{2} X_1(t) X_2(t) \cos[(\omega_1 - \omega_2)t + \varphi_1(t) - \varphi_2(t)].$$

Let the sum and the difference frequency terms have nonoverlapping spectra, and the frequency interval $\omega_0 - \Delta\omega/2 < \omega < \omega_0 + \Delta\omega/2$ completely cover all components of the spectrum of the sum frequency ω_0 .

In this case, the oscillation $x(t)$ can be formed by filtering the product $x_1(t)x_2(t)$ with the help of a filter which does not distort in the $\Delta\omega$ band and suppresses the oscillations outside this band.

Let us denote the pulse-response characteristic of such a filter by $v_f(t) = 2x_3(t - t_f)$, where t_f characterizes the delay time in the filter. The expression for $x(t)$ can then be represented by a convolution integral

$$x(t) = 2 \int_{-\infty}^{\infty} x_1(s) x_2(s) x_3(t - t_f - s) ds.$$

Eq. (5) is a generalization of Eq. (2) and goes over into (2) for $x_3(t) = \delta(t)$ and $t_f = 0$.

If $x(t)$ is represented by Eq. (5), the calculation of the correlation integral reduces to the operation

$$z = \int_{-\infty}^{\infty} y(t) \left[2 \int_{-\infty}^{\infty} x_1(s) x_2(s) x_3(t - t_0 - s) ds \right] dt.$$

On interchanging the order of integration this operation may be replaced by the following operations:

1) we calculate

$$y_1(s) = 2 \int_{-\infty}^{\infty} y(t) x_3(t - t_0 - s) dt;$$

2) we calculate

$$y_2(s) = y_1(s) x_1(s);$$

3) we calculate

$$z = \int_{-\infty}^{\infty} y_2(s) ds.$$

The first operation may be carried out with the help of a filter, the second one by multiplying by $x_1(s)$ and the third one by means of a filter, as well.

In particular, if we put $\omega_2 = \omega_{pr}$, $\omega_1 = \omega_0 - \omega_{pr}$, $X_2(t) = X(t)$, $\varphi_2(t) = \varphi_X(t)$, $X_1(t) = 1$, $\varphi_1(t) = 0$, the indicated operations will reduce to the following ones:

1) preselection of the high-frequency oscillation spectrum before heterodyning.

2) heterodyning with the help of a heterodyne whose frequency is $\omega_1 = \omega_0 - \omega_{pr}$, and whose amplitude and phase are not modulated.

3) optimum filtration of the signal on an intermediate frequency.

Thus, the given case corresponds the ordinary superheterodyne reception method.

If we put $\omega_2 = \omega_{pr}$, $\omega_1 = \omega_0 - \omega_{pr}$, $X_1(t) = X(t)$, $\varphi_1(t) = \varphi_X(t)$,

$X_2(t) = 1$ (in a section greater than the signal duration) $\varphi_2(t) = 0$, the processing operations will reduce to the following ones:

- 1) preselection before heterodyning.
- 2) heterodyning with the help of a heterodyne whose law of modulation corresponds to the modulation law of the signal,* and whose carrier frequency is $\omega_1 = \omega_0 - \omega_{pr}$.
- 3) optimum storage on an intermediate frequency ω_{pr} with the help of a narrow-band circuit.

If we put $\omega_2 = \omega_{pr}$, $\omega_1 = \omega_0 - \omega_{pr}$, $X_2(t) = X(t)$, $\varphi_2(t) = 0$, $X_1(t) = 1$, $\varphi_1(t) = \varphi_X(t)$, this implies that the heterodyne voltage on the carrier frequency $\omega_1 = \omega_0 - \omega_{pr}$ must take account of the phase modulation law of the signal, and the characteristic of the optimum filter on the intermediate frequency must allow for the amplitude modulation law of the signal.

In the latter two cases we are concerned with modified operations of superheterodyne reception differing by the distribution of the functions between correlation and filtration processing. It is easy to realize that very many variants of this distribution are possible.

§4.9. RECEIVER WITH OPTIMUM FILTER FOR A PACKET OF RADIO PULSES WITH RANDOM INDEPENDENT INITIAL PHASES

Let us pass on to the synthesis of optimum receivers for a signal in the form of a radio pulse packet with random initial phases. We shall choose the expressions for the probability ratios (§3.5, 3.6) to be the starting point:

- a) in the case of a nonfluctuating packet

$$I = \prod_k e^{-\frac{\sigma_k}{N_0}} I_0\left(\frac{2Z_k}{N_0}\right); \quad (1)$$

- b) in the case of independent fluctuations of the pulse packet

$$l = \prod_k \frac{N_0}{\vartheta_k + N_0} e^{\frac{1}{N_0} \frac{z_k^2}{\vartheta_k + N_0}}. \quad (2)$$

We shall not consider the case of friendly fluctuations. Taking the logarithm of these expressions we obtain

$$\ln l = \sum_k \ln I_0 \left(\frac{2Z_k}{N_0} \right) - \sum_k \frac{\vartheta_k}{N_0}. \quad (3)$$

$$\ln l = \frac{1}{N_0} \sum_k \frac{z_k^2}{\vartheta_k + N_0} + \sum_k \ln \frac{N_0}{\vartheta_k + N_0}. \quad (4)$$

In doing so, the operations of multiplication are replaced by the simpler operations of addition.

It is essential that the logarithmic functions is monotonic. Consequently, instead of calculating the probability ration l and comparing it with the threshold l_0 it suffices to calculate the quantity $\ln l$ and to compare it with its threshold $\ln l_0$, which simplifies the realization of optimum detection devices. When realizing optimum detection devices it is possible to start from the obvious relation $l = e^{\ln l}$. Substituting $\ln l$ into it from relation (3) or (4) the values of l needed to calculate the aposteriori probability density of the parameters to be measured may be obtained.

Thus, we may assume that in detection and measuring systems, the cascades of an optimum receiver, except for the terminal ones, must carry out the mathematical operations;

$$\sum_k \ln I_0 \left(\frac{2Z_k}{N_0} \right) \quad (5)$$

in the processing of a nonfluctuating packet and

$$\sum_k \frac{z_k^2}{\vartheta_k + N_0} \quad (6)$$

in the processing of a packet with independent pulse fluctuations.

In both cases, the initial stage of processing is the calculation

of the quantities Z_k for each pulse separately

$$Z_k \approx \left| \frac{1}{2} \int_{-\infty}^{\infty} Y(t) X_k^*(t) dt \right|, \quad (7)$$

where $X_k(t) = X_k(t)e^{j\varphi_k(t)}$ is a given function, depending on the time position of the k th pulse, its amplitude and its law of modulation (it does not depend on the random unmeasurable parameters β_k and B_k , see §3.5, 3.6).

Let us introduce amplitude factors S_k characterizing the shape of an undistorted packet. For the greatest pulse of the undistorted packet $S = 1$. Denoting the k th pulsing moment by t_k , and its delay time by t_{zk} we represent the function $X_k(t)$ in the form

$$X_k(t) = S_k U(t - t_k - t_{zk}) e^{-j\omega(t_k + t_{zk})}. \quad (8)$$

In this case,

$$Z_k = S_k Z_{0k}, \quad (9)$$

where for any pulse number

$$Z_{0k} = \left| \frac{1}{2} \int_{-\infty}^{\infty} Y(t) U^*(t - t_k - t_{zk}) dt \right|. \quad (10)$$

This implies that all quantities Z_{0k} may be obtained with the help of the circuit diagram considered earlier (Fig. 4.10) for a signal with random initial phase. This circuit consists of an optimum filter, intended to process the pulse $\bar{U}(t)$, and the envelope detector. In order to obtain the quantities X_k after the detector it is necessary to add a circuit introducing weight factors S_k .

Thus, a weighted packet of video pulses is obtained as the result of the first stage of processing an incoherent packet of radio pulses.

For a nonfluctuating packet the following processing reduces to the calculation of the values of $\ln I_0 \left(\frac{2S_k Z_{0k}}{N_0} \right)$ and their summation. The result of summation does not depend on the initial phases of the high-frequency oscillations since video pulses are summed. Such a summation

is called incoherent. The whole diagram of optimum processing is shown in Fig. 4.13. It consists of an optimum filter for the single radio pulse, a linear detector, the circuit of multiplication by the factors of the packet envelope S_k , a nonlinear element with a characteristic of the form $\ln I_0(u)$ and an incoherent summation and storing device realizing the actions of combining video pulses which do not act at the same time and of summing them. Judging by its outside this diagram reminds somewhat of a correlation-filtration diagram. It differs, however, from it insofar as the multiplication by S_k is carried out after the detector.*

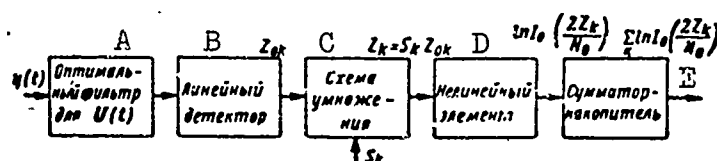


Fig. 4.13. Structural diagram of optimum processing of a packet of radio pulses with random initial phases. A) Optimum filter for $\bar{U}(t)$; B) linear detector; C) multiplier circuit; D) nonlinear element; E) summation and storing device.

For the limiting cases of weak and strong signals the diagram in Fig. 4.13 may be simplified in an essential way. In fact, for small values of the argument $u = 2S_k Z_{0k} / N_0$ the function $\ln I_0(u)$ is well approximated by the first term of its power series expansion in u

$$\ln I_0(u) \approx \frac{1}{4} u^2, \quad u \ll 1, \quad (11)$$

i.e., it has a parabolic initial part. For great values of the argument its asymptotic representation can be used

$$\ln I_0(u) \approx u, \quad u \gg 1, \quad (12)$$

which corresponds to the linear region in its diagram (Fig. 4.14).

This implies that for a packet of pulses whose amplitudes are

small compared to the noise

$$\sum_k \ln I_0 \left(\frac{2S_k Z_{0k}}{N_0} \right) \approx \sum_k \frac{S_k^2 Z_{0k}^2}{N_0^2} \quad (13)$$

and for great amplitudes

$$\sum_k \ln I_0 \left(\frac{2S_k Z_{0k}}{N_0} \right) \approx \sum_k \frac{2S_k Z_{0k}}{N_0} \quad (14)$$

Thus, the summation of logarithms is replaced by the summation of linear or quadratic functions of the quantity Z_{0k} . The incoherent summation proves to be weighted. The weight coefficients are quantities proportional to the square or first power of the expected value of the pulse amplitude S_k , respectively. This summation, as well as the formation of the correlation integral may be realized with the help of a special filter.

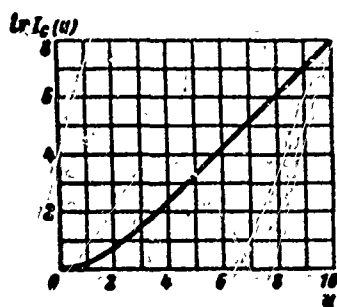


Fig. 4.14. Diagram of the function $\ln I_0(u)$.

In this connection, the schematic diagram of Fig. 4.15 shows the optimum filter of post-detector processing (its possible realizations as well as the realizations of pre-detector filters will be considered in Chapter 5). In the diagram of Fig. 4.15 a

linear detection is provided in order to realize processing in accordance with relation (14). If the processing (13) is needed the detector is replaced by a quadratic one. In this case, also the necessary pulse response characteristic of the post-detector processing filter is changed.

Let us pass on to the construction of a circuit for optimum processing of a packet with independent fluctuations of the pulse amplitudes. By virtue of Eqs. (6) and (9) this circuit must realize the mathematical operation

$$\sum_k \frac{S_k^2 Z_{0k}^2}{S_k^2 + N_k/\vartheta_k} = \frac{1}{\vartheta_k} \sum_k \frac{S_k^2 Z_{0k}^2}{S_k^2 + N_k/\vartheta_k}, \quad (15)$$

where $\vartheta_k = \vartheta_k/S_k^2$ is the mean energy of the greatest pulse of the undistorted packet. As in the preceding case (13), the mathematical operation reduces to the weighted summation of squares of the quantities Z_{0k} . Consequently, the circuit diagram of Fig. 4.15 in which the linear detector is replaced by a quadratic one is adequate also in the given case. But in contrast to the case (13) the quadratic detection is optimum also for strong and for weak signals, and the weight factors are proportional to $\frac{S_k^2}{S_k^2 + N_k/\vartheta_k}$. For a pulse packet with rectangular envelope the weighted summation is equivalent to a nonweighted one since all weight coefficients are equal to each other.

Thus, the considered circuits solve the problem of optimum processing of signals in the form of packets of pulses with random initial phases without fluctuations and with independent fluctuations from pulse to pulse. In order to guarantee optimum detection on the basis of these circuits it is sufficient to set up the last element in the form of a threshold circuit. To realize the optimum measurement of a parameter also an appropriate last element is necessary. An example of designing such an element for measuring the delay time $t_z = \text{const}$ is given in the following section.



Fig. 4.15. Simplified circuit diagram of optimum processing of an incoherent packet of great-amplitude radio pulses. A) Optimum filter for $U(t)$; B) linear detector; C) post-detector processing filter.

§4.10 OPTIMUM MEASUREMENT OF DELAY TIME

The expression for the a-posteriori probability density (§2.7)

$$p[t_0|y(t)] = K_0 p(t_0) l[y(t)|t_0] \quad (1)$$

is represented in the form

$$p[t_0|y(t)] = K_0 p(t_0) e^{\ln l[y(t)|t_0]} \quad (2)$$

For a packet of radio pulses with independent initial phases the logarithm of the probability ratio will be

$$\ln l(t_0) = \sum_k \ln l_k \left[\frac{2S_k Z_{0k}(t_0)}{N_0} \right] - \sum_k \frac{\theta_k}{N_0} \quad (3)$$

The quantity $Z_{0k}(t_0)$ is here determined from the value of the voltage envelope at the output end of the optimum filter

$$W(t_k + t_0 + t_0) = CZ_{0k}(t_0), \quad (4)$$

where t_k is the instant at which the corresponding sounding pulse is given.

Taking account of the results of the preceding section we obtain the circuit suitable to determine the a-posteriori probability density of the delay time (Fig. 4.15) with the addition of a terminal device (Fig. 4.16).

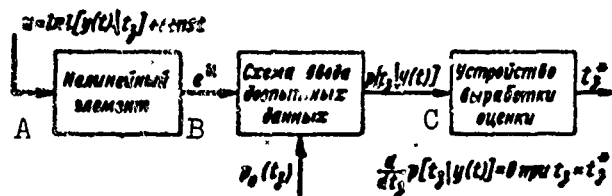


Fig. 4.16. Circuit diagram of a terminal device for obtaining the most probable a-posteriori estimate. A) Nonlinear element; B) Circuit introducing a-priori data; C) device for working out the estimate.

This device contains:

- 1) a nonlinear element with exponential characteristic.
- 2) a circuit introducing a-priori data. At the output end of the latter the a-posteriori probability density $p[t_0|y(t)]$ is obtained ex-

cept for a factor.

The circuit introducing a-priori data is an element realizing the multiplication of the probability ratio and the a-priori probability density as functions of a possible value of the measurable parameter delay time $\alpha = t_z$. In particular, if the distribution of the distance from the target is equally probable in some interval $r_1 < r < r_2$, an ordinary gate amplifier which is turned on for an interval of delay time values of $t_{z1} < t_z < t_{z2}$,

$$t_{z1,2} = \frac{2r_{1,2}}{c}.$$

may serve as the circuit introducing a-priori data.

The estimate of the measurable parameter may be carried out from the curve of the a-posteriori distribution of this parameter in accordance with the criterion of the mean risk minimum. In analogy to the case of one-dimensional measurement the center of gravity of the a-posteriori distribution curve

$$\alpha_{\text{opt}}^* = M_1\{\alpha|y(t)\} = \int_{-\infty}^{\infty} \alpha p[\alpha|y(t)] d\alpha$$

proves to be the optimum estimate, or, by virtue of [(16) and (17) §2.7]

$$\alpha_{\text{opt}}^* = \frac{\int_{-\infty}^{\infty} \alpha p(\alpha) l[y(t)|\alpha] d\alpha}{\int_{-\infty}^{\infty} p(\alpha) l[y(t)|\alpha] d\alpha}. \quad (5)$$

As was already shown before, frequently the most probable estimate, i.e. an estimate $\alpha^* = t_z^*$ such that

$$\frac{d}{dt_z} p[t_z|y(t)] = 0 \text{ for } t_z = t_z^*. \quad (6)$$

is chosen to be the optimum estimate. This estimate corresponds to the maximum of the a-posteriori distribution curve of the parameter t_z . The device for working out this estimate is also the output stage of the

circuit in Fig. 4.16.

In those cases where the a-priori probability distribution in the interval of measurable values of the delay time $t_{z1} < t_z < t_{z2}$ may be assumed constant the optimum measurement circuit is simplified considerably. By virtue of (1) and (2) one of the following two conditions is sufficient to fulfill Eq. (6):

$$\frac{d}{dt_s} l[y(t)|t_s] = 0 \text{ for } t_s = t_s^* \quad (7)$$

$$\frac{d}{dt_s} \ln l[y(t)|t_s] = 0 \text{ for } t_s = t_s^* \quad (8)$$

Using Eqs. [(3)-(6) §4.9] we conclude that in this case the most probable estimate corresponds to the voltage maximum at the output of the summation circuit (Fig. 4.13 or 4.15). Otherwise, the structural diagram of the device (Fig. 4.16) for working out the estimate can be replaced by a simpler one (Fig. 4.17).

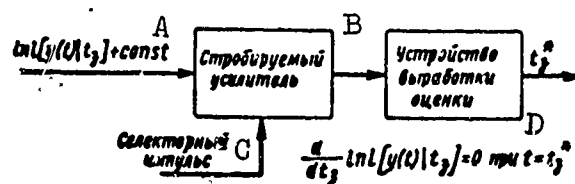


Fig. 4.17. Modification of the circuit of Fig. 4.16 for a rectangular law of a-priori distribution in the case of delay time measurement.
A) Gate amplifier; B) device for working out the estimate; C) gate;
D) at.

Since the values of the functions $Z_{Ok}(t_z)$ are working out for various expected t_z in chronological succession they may be estimated by means of the voltage envelope of the individual pulses at the output of the optimum filter. The same successive inflow of data usually takes place also after an incoherent summation circuit. Consequently, the differentiation (8) practically boils down to the determination of the instant of time at which the maximum of the strongest voltage pulse arrives at the output of the incoherent summation circuit.

If each individual pulse of the packet is remarkably discriminated from the noise after the detector one may do without an incoherent summation circuit when working out the optimum estimate t_z^* . In doing so, the necessary accuracy of measurement can be secured by taking the mean of the delay time estimates obtained independently from each pulse of the chosen packet, a fact that follows from Eq. (8). Using [(3) and (14) §4.9] we obtain

$$\frac{d}{dt_z} \sum_k S_k Z_{ok}(t_z) = 0 \text{ при } t_z = t_z^* = \text{const.} \quad (9)$$

In its turn, when estimating the delay time of only the kth pulse of the packet we have

$$\frac{d}{dt_z} Z_{ok}(t_z) = 0 \text{ при } t_z = t_{zk}^*, \quad (10)$$

where t_{zk}^* is the optimum estimate of the delay time t_z , obtained after receiving only the kth pulse.

Expanding each of the functions $Z_{ok}(t_z)$ in a Taylor series in the neighborhood of the corresponding estimate t_{zk}^* we obtain by virtue of Eq. (10)

$$Z_{ok}(t_z) \approx Z_{ok}(t_{zk}^*) + \frac{1}{2} Z_{ok}''(t_{zk}^*)(t_z - t_{zk}^*)^2, \quad (11)$$

where

$$Z_{ok}''(t_{zk}^*) = -|Z_{ok}''(t_{zk}^*)|.$$

Substituting (11) into (9) we find

$$\sum_k S_k |Z_{ok}''(t_{zk}^*)| (t_z^* - t_{zk}^*) = 0,$$

whence

$$t_z^* = \frac{\sum_k t_{zk}^* S_k |Z_{ok}''(t_{zk}^*)|}{\sum_k S_k |Z_{ok}''(t_{zk}^*)|}, \quad (12)$$

i.e., the optimum estimate of the delay time measured once for the whole packet is the weighted sum of the results of independent measure-

ments for the individual pulses. The weight coefficients are quantities that are the reciprocals of the dispersions of the independent measurements, a fact one may realize after studying Chapter 6.

The following modification of the calculation carried out which is particularly interesting in case one object is observed for a long time while tracking it is possible. Aiming merely at the explanation of the ideas and results of the modified calculation we maintain the assumption that the true delay time is the same as measured from $(m-1)$ and from m pulses (a somewhat more complete consideration is contained in Chapter 8).

We denote the sum entering (9) for $m-1$ pulses by

$$\sum_{k=1}^{m-1} S_k Z_{0,k}(t_s) = Z_{\Sigma(m-1)}(t_s), \quad (13)$$

and the optimum delay time estimates from all $(m-1)$ and m pulses by $t_{\Sigma(m-1)}^*$ and $t_{\Sigma m}^*$, respectively (in contrast to the estimate t_{Om}^* from the m th pulse only).

The conditions for determining these optimum estimates will then assume the form, owing to (9) and (13),

$$\frac{d}{dt_s} Z_{\Sigma(m-1)}(t_s) = 0 \text{ for } t_s = t_{\Sigma(m-1)}^*, \quad (14)$$

$$\frac{d}{dt_s} [Z_{\Sigma(m-1)}(t_s) + S_m Z_{0,m}(t_s)] = 0 \text{ for } t_s = t_{\Sigma m}^*. \quad (15)$$

Using the Taylor expansion for the functions $Z_{\Sigma(m-1)}(t_z)$ and $Z_{Om}(t_z)$ for the neighborhoods of the corresponding optimum estimates we find

$$Z_{\Sigma(m-1)}(t_s) \approx Z_{\Sigma(m-1)}(t_{\Sigma(m-1)}^*) - \frac{1}{2} |Z_{\Sigma(m-1)}''(t_{\Sigma(m-1)}^*)| \times (t_s - t_{\Sigma(m-1)}^*)^2, \quad (16)$$

$$Z_{0,m}(t_s) \approx Z_{0,m}(t_{0,m}^*) - \frac{1}{2} |Z_{0,m}''(t_{0,m}^*)| (t_s - t_{0,m}^*)^2. \quad (17)$$

On the assumption that the corresponding neighborhoods overlap and substituting (16), (17) into (15) we may obtain

$$t_{zm}^* = t_{z(m-1)}^* + A_m(t_{0m}^* - t_{z(m-1)}^*), \quad (18)$$

where

$$A_m = \frac{S_m |Z_{0m}'(t_{0m}^*)|}{|Z_{zm}'(t_{zm}^*)| + S_m |Z_{0m}'(t_{0m}^*)|}. \quad (19)$$

Eq. (18) shows that the optimum delay time estimate from m pulses is the sum of the preceding estimate from (m - 1) pulses and the time signal of the error ($t_{0m}^* - t_{zm}^*$), multiplied by some weight factor A_m .

Differentiating (17) and substituting $t_z = t_{zm}^*$, the time signal of the error may be determined

$$t_z - t_{0m}^* = - \frac{Z_{0m}'(t_z)}{|Z_{zm}'(t_{zm}^*)|} \text{ for } t_z = t_{zm}^*.$$

Expression (18) then reduces to the form

$$t_{zm}^* = t_{z(m-1)}^* + a_m Z_{0m}'(t_{z(m-1)}^*), \quad (20)$$

where

$$a_m = \frac{S_m}{|Z_{zm}'(t_{zm}^*)| + S_m |Z_{0m}'(t_{0m}^*)|}. \quad (21)$$

The quantity $Z_{0m}'(t_z)$ characterizes the voltage of the error signal. Owing to (17) it vanishes at the point $t_z = t_{0m}^*$, and passing through this point with increasing t_z the sign changes from positive to negative.

If in the case of prolonged observation the quantities A_m and a_m which vary from reading to reading are replaced by constants in (18) and (20) the operations (18), (20) will reduce to the wellknown operations for the range self-tracking (see Chapter 8). The operation of obtaining the voltage of the error signal in the form of the derivative $Z_{0m}'(t_z)$ corresponds to time discrimination with selecting pulses of short duration since only under this condition the derivative will be taken at the point t_z as a result of the discrimination.

The latter conclusion was obtained from the found calculational relations as the consequence of the assumption on the small scatter of

the values of $t_{\Sigma(m-1)}^*$ and t_{Om}^* . In the opposite case one usually aims at increasing the duration of the selecting pulses in order to reduce the probability of a tracking collapse.

§4.11. THE PRINCIPLE OF BROAD-BAND RADIO PULSE COMPRESSION

All preceding discussions were concerned with the optimum processing of radio signals of arbitrary form. Let us now deal with the properties of optimum processing of signals having the form of broad-band radio pulses, i.e., of radio pulses the product of whose spectral width the duration is essentially greater than unity. It is assumed that processing is realized by optimum filtration on a high or intermediate frequency. The pulse parameters are assumed to be given except for the amplitude, the initial phase and the delay time which is the same during the whole duration of the pulse (a somewhat more general case will be considered in Chapter 7).

As was shown in §4.5 the shape of the signal voltage at the output of the filter which is optimum for it

$$w_c(t) = C \int_{-\infty}^{\infty} |g(f)|^2 \cos[2\pi f(t - t_s - t_0)] df \quad (1)$$

depends only on the amplitude-frequency spectrum of the signal. By definition, the spectral density of an arbitrary real function of time $u(t)$ is

$$g(f) = \int_{-\infty}^{\infty} u(t) e^{-i2\pi ft} dt = g^*(-f).$$

The amplitude-frequency spectrum is, therefore, symmetric relative to the axis of ordinates $f = 0$, i.e., $|g^*(-f)| = |g(f)|$ and the expression (1) reduces to the form

$$w_s(t) = 2C \int_0^{\infty} |g(f)|^2 \cos[2\pi f(t - t_s - t_0)] df. \quad (2)$$

We introduce the function $G(f)$ describing the distribution of the spectral density around the carrier frequency on the semiaxis of positive

frequencies

$$G(f) = \begin{cases} g(f_0 + F) & \text{for } f_0 + F \geq 0, \\ 0 & \text{for } f_0 + F < 0. \end{cases}$$

After replacing the variable of integration $f = f_0 + F$ in (2) we find

$$w_e(t) = 2C \int_{-\infty}^{\infty} |G(F)|^2 \cos[2\pi(f_0 + F)(t - t_s - t_0)] dF.$$

Using the formula for the cosine of a sum we obtain

$$w_e(t) = W_1(t) \cos[2\pi f_0(t - t_s - t_0)] - W_2(t) \sin[2\pi f_0(t - t_s - t_0)], \quad (3)$$

where

$$W_{1,2}(t) = 2C \int_{-\infty}^{\infty} |G(F)|^2 \begin{matrix} \cos \\ \sin \end{matrix} [2\pi F(t - t_s - t_0)] dF. \quad (4)$$

Or

$$w_e(t) = W(t) \cos[2\pi f_0(t - t_s - t_0) + \Phi(t)], \quad (5)$$

where

$$W(t) = \sqrt{W_1^2(t) + W_2^2(t)}, \quad \Phi(t) = \arctg \frac{W_2(t)}{W_1(t)}. \quad (6)$$

The expressions (6) describe the law of amplitude and phase modulation of a radio pulse at the output of an optimum filter.

As can be seen from expression (4-6) the function $\Phi(t)$ vanishes if the amplitude-frequency spectrum is symmetric relative to the carrier frequency f_0 and the output pulse

$$w_e(t) = W_1(t) \cos[2\pi f_0(t - t_s - t_0)] \quad (7)$$

proves to be nomodulated as to the phase (even if the input pulse is phase modulated). The phase of the output pulse may also vary by π if the sign of the function $W_1(t)$ describing the envelope changes.

The envelope $W_1(t)$ is the narrower the broader the amplitude-frequency spectrum of the signal. In particular, if a spectrum of the width Δf is approximated by the rectangle

$$G(F) = \begin{cases} 1 & \text{for } |F| < \frac{\Delta f}{2}, \\ 0 & \text{for } |F| > \frac{\Delta f}{2}. \end{cases} \quad (8)$$

we have, according to (4)

$$W_1(t) = W_m \frac{\sin \pi \Delta f (t - t_0 - t_d)}{\pi \Delta f (t - t_0 - t_d)}, \quad (9)$$

where $W_m = 2C\Delta f$. Hence it follows that the pulse duration at the output of the optimum filter is $2/\Delta f$ on the first zeros, and $1/\Delta f$ on the level $\frac{2}{\pi} \approx 0,64$. Thus, the duration of the output radio pulse is not determined by the duration of the input pulse, but by its spectral width.

The spectral width of a radio pulse may, generally, be considerably greater than the quantity which is the inverse of its duration. Only if the pulse is not phase modulated the spectral width is inversely proportional to the duration of the radio pulse.

Using internal pulse modulation as to phase (frequency) or even amplitude it is possible to broaden the spectrum remarkably compared to $1/\tau_1$ if the duration τ_1 is given, i.e., to achieve substantial compression of the output radio pulse compared to the input radio pulse.

Since the compression takes place in a linear system the superposition principle is applicable. The compression of two overlapping broad-band radio pulses that are shifted in time is realized independently, for which reason it is possible to receive the compressed radio pulses separately even if the reflected radio pulses arriving at the input of the optimum filter overlap considerably.

Hence it follows that using compression of broad-band radio pulses in optimum filters the resolving power as to delay time and range is determined by the duration of the compressed rather than by that of the sounding signal and inversely proportional to its spectral width.

Thus, an increase of the duration of the sounding radio pulses

without impairing (or even with considerable improvement of the resolving power of a pulse radar as to range is made possible.

The increase of the duration permits the energy of the radio pulses and the radar range to be increased without raising the peak power which is usually limited by the conditions of generating and breakdowns in the transmission lines.

The increase in the resolving power in the case of spectral broadening and optimum signal processing is a property of the latter and may be realized not only in case the pulses are compressed in optimum filters. Let us, e.g., turn to a correlation circuit of optimum processing (Fig. 4.1 or 4.2). We shall feed a radio pulse with a spectral width of $\Delta f \gg 1/\tau_1$ into its input. Evidently, there will not be any compression in this circuit. The correlation will, however, be disturbed providing this pulse is shifted relative to the reference voltage by a time $|\tau| = 1/\Delta f \ll \tau_1$. Hence it follows that among all overlapping identical broad-band radio pulses at the input of the correlation circuit only the pulse for which this processing is optimum will be discriminated.

Thus, the pulse compression in optimum filters must be considered to be one of the variants of raising the resolving power on account of spectral broadening.

Manu-
script
Page
No.

[Footnotes]

- 104 As a matter of fact, $ab = (\text{Re } a + j \text{Im } a) (\text{Re } b + j \text{Im } b)$, from which $\text{Re } ab = \text{Re } a \text{Re } b - \text{Im } a \text{Im } b$. Similarly, $\text{Re } ab^* = \text{Re } a \text{Re } b^* - \text{Im } a \text{Im } b^* = \text{Re } a \text{Re } b + \text{Im } a \text{Im } b$. The half of the sum of the given relations yields expression (7).
- 110 The character of relation (7) is more general than that of (3) since it can be proved without neglecting the rapidly oscillating terms in the expression under the integral sign.
- 116 When heterodyning in the case of discrete signals the func-

tions of gating are carried out at the same time.

119 Multiplication is also possible before the detector; in this case it is, however, possible to join a linear detector and a nonlinear element.

Manu-
script
Page
No.

[Transliterated Symbols]

84	доп = dop = dopustimyy = admissible
88	з = z = zapazdyvaniye = delay
91	опт = opt = optimal'nyy = optimum
95	с = s = signal = signal
95	п = p = pomekha = interference
95	с макс = s maks = signal, maksimal'nyy = signal, maximum
96	п эф = p ef = pomekha, effektivnyy = interference, effective
96	и = i = impul's = pulse
114	ф = f = fil'ter = filter

Chapter 5

THE ELEMENTS OF OPTIMUM DETECTION AND PARAMETER MEASURING DEVICES

§5.1. THE ELEMENTS OF OPTIMUM DEVICES UNDER CONSIDERATION

Among the elements of Optimum detection and measuring devices there are: optimum filters, incoherent storing devices, threshold devices, signal delay and memory devices, etc. Specific selective elements are, in particular, the optimum filters; we have established only the general rules by which they are governed, but did not discuss the principles of their construction, as yet.

In widespread types of radar receivers the main selectivity and amplification are guaranteed by resonance amplifiers of intermediate frequency containing a great number of cascades. The problem arises as to what extent these amplifiers can simultaneously perform the functions of optimum filters. Moreover, it must be clarified how to design optimum filters in case their functions are not performed by resonance amplifiers.

Let us pass on to a consideration of the problems posed.

§5.2. CONDITIONS UNDER WHICH MULTISTAGE RESONANCE AMPLIFIERS CAN BE APPLIED IN ORDER TO ACHIEVE OPTIMUM FILTRATION

The selective properties of resonance amplifiers are characterized by their amplitude-frequency and their phase frequency characteristics. The main approximations of these characteristics are:

1) The bell-shaped for the amplitude-frequency, and the linear approximation for the phase-frequency characteristic (Fig. 5.1a);

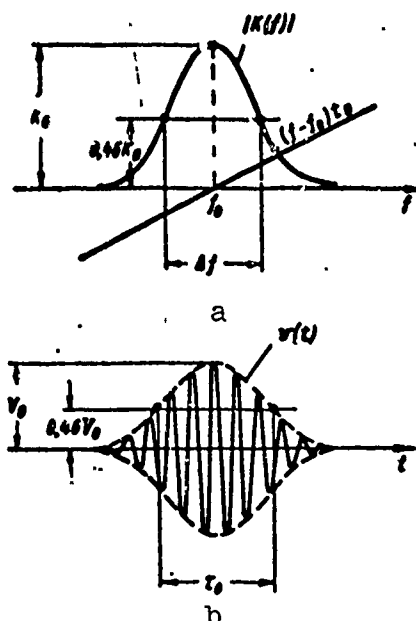


Fig. 5.1. Bell-shaped approximation of the amplitude-frequency and linear approximation of the phase-frequency characteristic (a); corresponding pulse-response characteristic (b).

2) The rectangular for the amplitude-frequency and the linear approximation for the phase-frequency characteristic (Fig. 5.2a).

The corresponding frequency characteristics $K(f)$ will be written in complex form for the frequency range $f > 0$. For the range $f < 0$ it is implied that

$$K(f) = K^*(-f). \quad (1)$$

In this case we obtain: for the bell-shaped approximation

$$K_1(f) = K_0 e^{-\left(\frac{f-f_0}{\Delta f}\right)^2} e^{-j2\pi(f-f_0)t_0}, \quad (2)$$

and for the rectangular one

$$K_2(f) = \begin{cases} K_0 e^{-j2\pi(f-f_0)t_0}, & \text{if } |f-f_0| < \frac{\Delta f}{2}, \\ 0 & \text{if } |f-f_0| > \frac{\Delta f}{2}. \end{cases} \quad (3)$$

Here f_0 is the carrier frequency;

K_0 is the transmission factor on the carrier frequency;

t_0 is the slope coefficient of the phase-frequency characteristic;

Δf is the transmission band (for the bell-shaped characteristic on a level of $e^{-\frac{1}{4}} \approx 0,46$) .

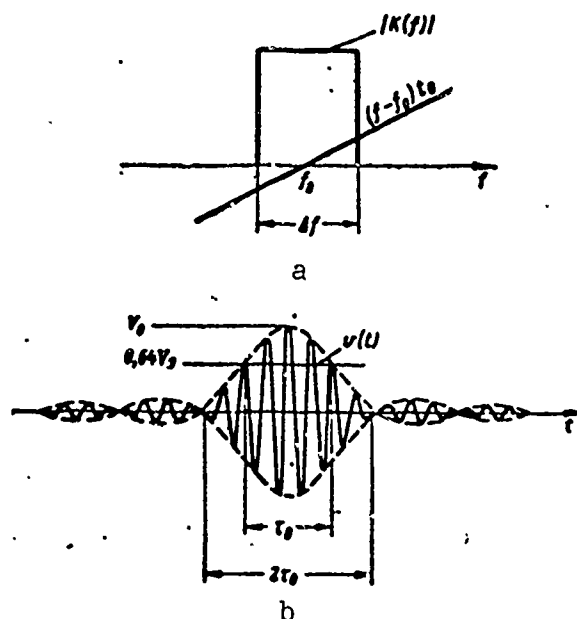


Fig. 5.2. Rectangular approximation of the amplitude-frequency and linear approximation of the phase-frequency characteristic (a); corresponding pulse-response characteristic (b).

The corresponding pulse-response characteristics are determined from the Fourier transformation

$$v(t) = \int_{-\infty}^{\infty} K(f) e^{j2\pi f t} df \quad (4)$$

and will be

$$v_1(t) = V_0 e^{-\pi \left(\frac{t-t_0}{\tau_0} \right)^2} \cos 2\pi f_0 t, \quad (5)$$

$$v_2(t) = V_0 \frac{\sin \pi \frac{t-t_0}{\tau_0}}{\pi \frac{t-t_0}{\tau_0}} \cos 2\pi f_0 t. \quad (6)$$

$V_0 = 2K_0\Delta f$ is here the maximum value of the pulse-response characteristic amplitude, and $\tau_0 = 1/\Delta f$ is a quantity characterizing its duration. The value of τ_0 is measured on a level of $e^{-\frac{1}{4}} \approx 0,46$ for the first characteristic and on a level of $\frac{2}{\pi} \approx 0,64$ for the second one (in the

latter case it is, besides, the half-width of the characteristic with respect to the first zeroes). The pulse-response characteristics (5) and (6) are shown in Fig. 5.1b and 5.2b. It follows from these figures that the characteristics (5) and (6) can only be realized for sufficiently great (theoretically infinite) values of t_0 since otherwise the condition $v(t) = 0$ for $t < 0$ is not satisfied. This fact is a drawback of the chosen approximations. It is, however, in agreement with the fact that real systems satisfy well the approximations (2) or (3) with a great number of stages. The more stages the greater is the slope coefficient of the resulting phase-frequency characteristic of t_0 , at the same time characterizing the delay time in the amplifier.

Using the expression for the optimum pulse-response characteristic

$$v_{\text{opt}}(s) = Cu(t_0 - s), \quad (7)$$

we shall pass over to the explanation of the shape of signals $u(t)$ for which the considered approximations (2) and (3) of the frequency characteristics are optimum. Substituting $t_0 - s = t$ we obtain

$$u(t) = \frac{1}{C} v_{\text{opt}}(t_0 - t). \quad (8)$$

Thus, the sought signals are the mirror reflection of the corresponding pulse-response characteristics (Fig. 5.1b and 5.2b)

$$u_1(t) = U_0 e^{-\pi \left(\frac{t}{\tau_0}\right)^2} \cos(2\pi f_0 t - \varphi), \quad (9)$$

$$u_2(t) = U_0 \frac{\sin \pi \frac{t}{\tau_0}}{\pi \frac{t}{\tau_0}} \cos(2\pi f_0 t - \varphi), \quad (10)$$

where $U_0 = V_0/C$ and $\varphi = 2\pi f_0 t_0$ are arbitrary constants.

As we see, an amplifier with a bell-shaped amplitude-frequency and a linear phase-frequency characteristic is an optimum filter for a bell-shaped radio pulse of the resonance frequency f_0 (without phase modulation). The pulse duration τ_0 and the transmission band Δf on the level $\tau^{-\frac{1}{2}} \approx 0.46$ must satisfy the condition

$$\tau_0 \Delta f = 1. \quad (11)$$

In its turn, a band amplifier with a rectangular amplitude-frequency and a linear phase-frequency characteristic is an optimum filter for a radio pulse with an envelope of the form $\sin x/x$. The pulse duration τ_0 on the level $2/\pi \approx 0.64$ is connected with the transmission band of the amplifier by relation (11). The shorter the pulse duration the broader the transmission band must be, and vice versa.

In the general case, agreement of the pulse shape with the pulse-response characteristic of the filtering system is required. If there is no exact agreement, the system will not be an optimum filter, rigorously speaking. Its characteristics may, however, be similar to optimum characteristics. Let us consider the following practically important case in order to satisfy ourselves of this fact.

Let the frequency characteristic of the resonance system be approximated by expression (3), and the input pulse $u(t)$ have a rectangular envelope and a constant carrier frequency f_0 :

$$u(t) = \begin{cases} U_0 \cos 2\pi f_0 t & \text{for } |t| < \frac{\tau_0}{2} \\ 0 & \text{for } |t| > \frac{\tau_0}{2} \end{cases} \quad (12)$$

i.e., there is no exact agreement between the pulse-response characteristic of the system and the input pulse $u(t)$.

Let us calculate the signal-to-noise energy ratio at the output of the system and compare it with the optimum.

We shall represent the voltage at the output of the system in the form of a convolution integral

$$w(t) = \int_{-\infty}^{\infty} v(t-s) u(s) ds.$$

Using expressions (6) and (12)

$$w(t) = 2K_0 U_0 \Delta f \int_{-t_0/2}^{t_0/2} \frac{\sin \pi \Delta f (t-s-t_0)}{\pi \Delta f (t-s-t_0)} \times \\ \times \cos 2\pi f_0 (t-s) \cos 2\pi f_0 s ds.$$

In view of the equation

$$\cos 2\pi f_0 (t-s) \cos 2\pi f_0 s = \frac{1}{2} \cos 2\pi f_0 t + \frac{1}{2} \cos 2\pi f_0 (t-2s)$$

and the fact that the second term of the right-hand side oscillates with a high frequency of $2f_0 \gg \Delta f$ as a function of the variable of integration s we neglect the integral of this term. In this case

$$w(t) = W(t) \cos 2\pi f_0 t,$$

where $W(t)$ is the voltage envelope at the output of the system

$$W(t) = \frac{1}{\pi} K_0 U_0 \left[-\text{Si} \pi \Delta f \left(t - \frac{t_0}{2} - t_0 \right) + \right. \\ \left. + \text{Si} \pi \Delta f \left(t + \frac{t_0}{2} - t_0 \right) \right]. \quad (13)$$

The function $\text{Si } y$ is here the integral sine

$$\text{Si } y = \int_0^y \frac{\sin x}{x} dx.$$

The maximum of the envelope $W(t)$ is attained at the instant of time t_m where $W'(t_m) = 0$. Thus, t_m is determined as the root of the equation

$$\frac{\sin \pi \Delta f \left(t_m - \frac{t_0}{2} - t_0 \right)}{\pi \Delta f \left(t_m - \frac{t_0}{2} - t_0 \right)} - \frac{\sin \pi \Delta f \left(t_m + \frac{t_0}{2} - t_0 \right)}{\pi \Delta f \left(t_m + \frac{t_0}{2} - t_0 \right)} = 0.$$

This root is $t_m = t_0$, which follows from the evenness of the function $\sin x/x$. By virtue of Eq. (13) the maximum of the envelope will be

$$W_{\text{max}} = W(t_0) = \frac{2}{\pi} K_0 U_0 \text{Si} \frac{\pi \Delta f t_0}{2}. \quad (14)$$

The effective noise voltage referred to a resistance of 1 ohm is determined by the relation

$$W_{\text{eff}}^2 = \int_0^\infty |K(f)|^2 N_s(f) df = K_0^2 N_s \Delta f.$$

The integration will here be carried out only on the positive semi-axis since $N_0(f) = N_0$ is the spectral density for positive frequencies.

Thus, the sought signal-to-noise energy ratio will be

$$\frac{W_{\text{с макс}}^2}{W_{\text{шф}}^2} = \frac{4}{\pi^2} \frac{U_0^2}{N_0} \frac{\text{Si}^2\left(\frac{\pi \Delta f \tau_n}{2}\right)}{\Delta f}. \quad (15)$$

the obtained expression has a maximum for the optimum value of the product $\Delta f \tau_n = 1.37$. In this case

$$\left(\frac{W_{\text{с макс}}}{W_{\text{шф}}}\right)_{\text{макс}}^2 = \frac{4}{\pi^2} \frac{U_0^2 \tau_n}{N_0} \frac{\text{Si}^2\left(\frac{1.37\pi}{2}\right)}{1.37}.$$

Noting that $\frac{1}{2} U_0^2 \tau_n = \mathcal{E}$ is the energy of the radio pulse also referred to the resistance of 1 ohm we obtain after carrying out the calculation

$$\left(\frac{W_{\text{с макс}}}{W_{\text{шф}}}\right)_{\text{макс}}^2 = 0.83 \frac{2\mathcal{E}}{N_0}. \quad (16)$$

This value is attained with the optimum band of the rectangular frequency characteristic

$$\Delta f_{\text{опт}} = \frac{1.37}{\tau_n}. \quad (17)$$

Comparing (17) with expression [(13) §4.4] we satisfy ourselves of the fact that a band filter with a nonoptimum frequency characteristic, but an optimum band yields a loss in the signal-to-noise energy ratio of 17% or by $1/0.83 \approx 1.2$ times, for the type of signal under consideration.

The last conclusion is only correct for the type of signal under consideration if the initial phase is unmodulated. If the initial phase is considerably modulated the band filter cannot yield results that are so similar to the optimum.

§5.3. USE OF DELAY LINES IN THE SYNTHESIS OF OPTIMUM FILTERS

An optimum filter with a given pulse-response or frequency characteristic may be realized by using a delay line. Different methods of

this realization are possible. Fig. 5.3 shows one of the methods of designing an optimum filter. The use of a delay line with branches serves as its basis. Amplifiers with amplification factors K_1, K_2, \dots, K_m are connected to the branches, and the outputs of all amplifiers are fed to the total load.

Let the distance between the connection points of the branches correspond to a delay by Δt . We shall feed a rectangular pulse of the same duration Δt to the output of this line. In this case we obtain the oscillation $v(t)$ consisting of a sequence of rectangular pulses at the output end. Taking a sufficiently great number of branches from the delay line and choosing amplification factors K_1, K_2, \dots, K_m as well as their signs any step-like curve may be obtained. Continuous oscillations, among them also one that is similar enough to the mirror-reflection of the given signal may be formed by smoothing this curve. In the limit if $\Delta t \rightarrow 0$ we may assume that the input pulses approximates a delta function, and the output oscillation the pulse-response characteristic.

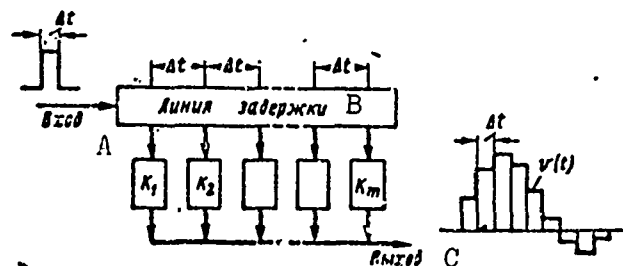


Fig. 5.3. Principle of forming the pulse-response characteristic by using a delay line with branches. A) Input; B) delay line; C) output.

Thus, it is possible, in principle, to form a pulse-response characteristic that is sufficiently similar to the given one. Obviously, the circuit (Fig. 5.3) will practically be an optimum filter in the latter case. The shorter, however, Δt the more branches from the delay

line are required, and the limiting case $\Delta t \rightarrow 0$ corresponds to a continuous extraction of oscillations from this line.*

The number of branch lines from the line of delay may be reduced if before it an additional filter of low frequencies $0 < f < F_{\max}$ is inserted (Fig. 5.4), and the delay Δt is chosen equal to $\Delta t = 1/2F_{\max}$ (see §2.6). Such a filter converts a unit pulse to an oscillation of the type $\sin x/x$ with a duration of $2\Delta t$ as measured between the zeroes. Summing these oscillations any function with a limited spectrum may be reproduced according to Kotel'nikoy's theorem (except for boundary effects). It is here implied that the duration of the pulse-response characteristic $\tau_i \gg \Delta t$. Instead of an ideal low-frequency filter an ordinary filter which is similar to it may be used, but in this case a denser spacing of branches may be necessary.

In several cases the necessary characteristics can be obtained comparatively simply by combining a delay line and a resonance filtering system. Let us, e.g., assume that it is necessary to form the pulse-response characteristic in the form of a rectangular radio pulse of the duration $\tau_i = mT_0$ where m is a great number of periods T_0 . It turns out that such a pulse-response characteristic may be formed with the help of a line of delay by the time τ_i with two branches and an oscillatory circuit with a great quality factor. Figure 5.5a, b show different forms of the corresponding circuits. The pulse-response characteristic is obtained as the result of subtracting two free oscillations- an undelayed one and one which is delayed by τ_i . Owing to the great quality factor of the circuit it represents the required radio pulse of a duration τ_i similar to a rectangular one.

The frequency characteristic of an optimum filter corresponds to the spectrum of this pulse. In particular, the amplitude-frequency characteristic has the form $\sin x/x$; its width as measured between the

zeroes is equal to $2/\tau_1$.

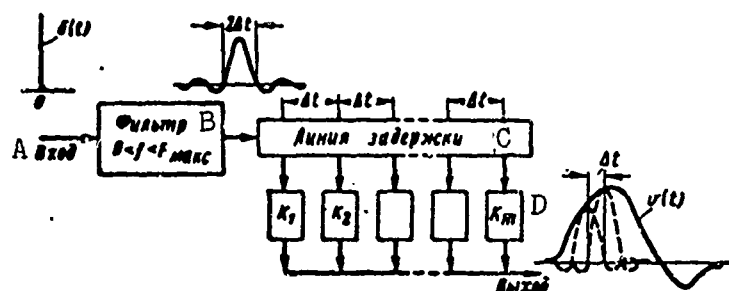


Fig. 5.4. Formation of the pulse-response characteristic $v(t)$ with a limited frequency spectrum $0 < f < F_{\max}$. A) Input; B) filter; C) delay line; D) output.

If a rectangular radio pulse acts on the input of the filter a rhombiform radio pulse is obtained at the output as it must be according to Fig. 4.9. In this case a linear increase of the voltage amplitude during the duration of the pulse and a very slow damping of the oscillations after it has come to an end takes place in the high quality circuit. As a result of subtracting the two transient processes, the undelayed and the delayed one, a rhombiform radio pulse of the duration of $2\tau_1$ (Fig. 5.6) is obtained at the output.

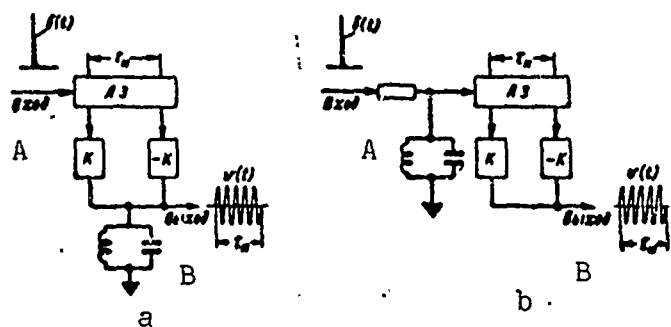


Fig. 5.5. Formation of a pulse-response characteristic in the form of a rectangular radio pulse. A) Input; B) output.

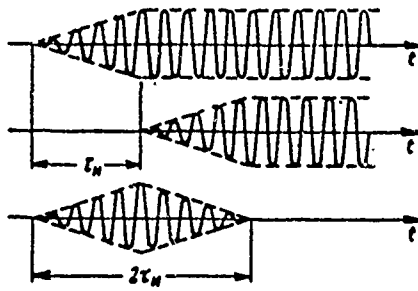


Fig. 5.6. Optimum filtering process for square radio pulse in circuit of Fig. 5.5.

§5.4. OPTIMUM FILTER FOR A COHERENT SEQUENCE OF RADIO PULSES

We shall pose the problem of synthesizing an optimum filter for an expected signal in the form of a packet of coherent radio pulses, i.e., pulses whose phases are rigidly connected with each other. Only the initial phase of the first radio pulse of the packet may be random. For the sake of definiteness, we will assume that all pulses have the same initial phase. We shall assume the period with which the pulses arrive at the input of the receiver to be equal to T .

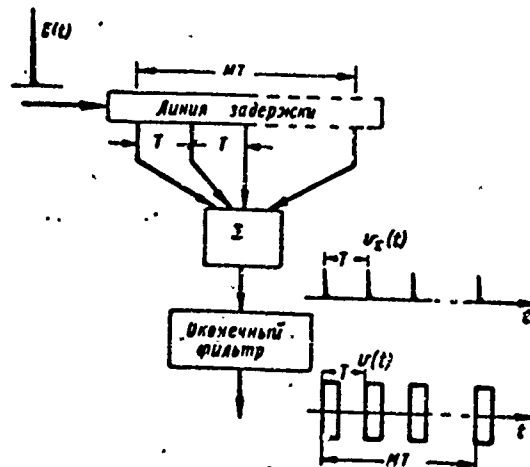


Fig. 5.7. Shaping of pulse characteristic in form of coherent packet of square radio pulses. 1) Delay line; 2) final filter.

Applying the method set forth above we shall choose a line (Fig. 5.7) with branches of a distance T and a total delay time MT where M is the number of pulses in the packet. The branches are connected to the summation device. We shall establish a terminal filter at its output end (Fig. 5.5.a or b) which is optimum for a single radio pulse.

Let us consider the formation of the pulse-response characteristic of the filter. If a unit pulse acts on the input of the delay line a sequence of unit pulses is picked up from the output of the summation device. Each of them generates its own rectangular radio pulse at the output of the end filter. As a result the required pulse-response characteristic is formed.

Let us track the result of an expected coherent packet of pulses acting on an optimum filter. Fig. 5.8a shows the voltages as picked up from the branches of the line, and Fig. 5.8b the voltage at the output of the summation device. As we see, the optimum filtration of the packet boils down to a coherent summation of the mutually shifted pulses of the packet. This leads to an improvement of the signal-to-noise ratio at the output of the filter since the pulses are added in phase, and the interferences with random phases. Instead of the term coherent summation also the term coherent integration of the packet pulses is used.

The end filter that is located after the summation device performs optimum filtration of each of these radio pulses.

As a whole, the voltage that is schematically drawn in Fig. 5.8c is obtained at the output of the optimum filter.

The result of filtration will not be changed if the order of optimum filtration of a single pulse and optimum summation of the packet pulses is interchanged.

As shown in §5.2, replacing the optimum filter for a single radio

pulse by a band filter leads only to a small loss of threshold signal energy.

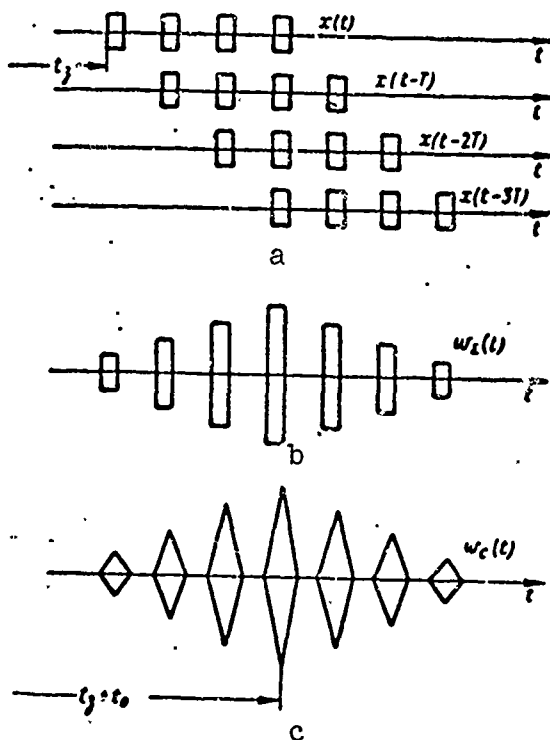


Fig. 5.8. Optimum filtration process of a coherent packet of rectangular radio pulses.

It makes, therefore, sense to distinguish the optimum summation circuit as a basic element of the device for optimum processing of the packet.

The frequency characteristic of the optimum summation circuit may be calculated from the formula

$$K(f) = \frac{u_{\Sigma\Sigma}(f)}{u_{\Sigma\Sigma}(f)} = \frac{\sum_{k=0}^{M-1} u_{\Sigma\Sigma}(f - kT)}{u_{\Sigma\Sigma}(f)} \text{ for } u_{\Sigma\Sigma}(f) = e^{j2\pi f t}.$$

Summing up the geometrical series with the terms $e^{j2\pi f (t-kT)}$ and using the Euler formula we obtain

$$K(f) = \frac{\sin \pi f M T}{\sin \pi f T} e^{-j\pi f T (M-1)}.$$

Figure 5.) shows the amplitude-frequency characteristic of the optimum summation circuit. It consists of a number of peaks and is, therefore termed comb-shaped. Taking account of an optimum filter for a single radio pulse the resulting comb-shaped characteristic shown in Fig. 5.10a is obtained. If instead of an optimum filter a band filter is used the shape of the envelope of the amplitude-frequency characteristic will be changed (Fig. 5.10b).

Filters using optimum summation of the packet pulses are often called comb-filters (more accurately, band-pass comb filters).

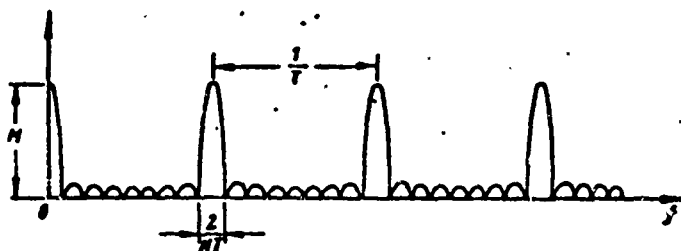


Fig. 5.9. Comb-shaped amplitude-frequency characteristic for an optimum summation circuit.

Comb filters can also be designed by not only using a delay line, but also oscillator circuits tuned to the comb frequencies. As can be seen from Fig. 5.10 however, a considerable number of circuits is necessary such that this method is only appropriate for systems of low pulse ratio.

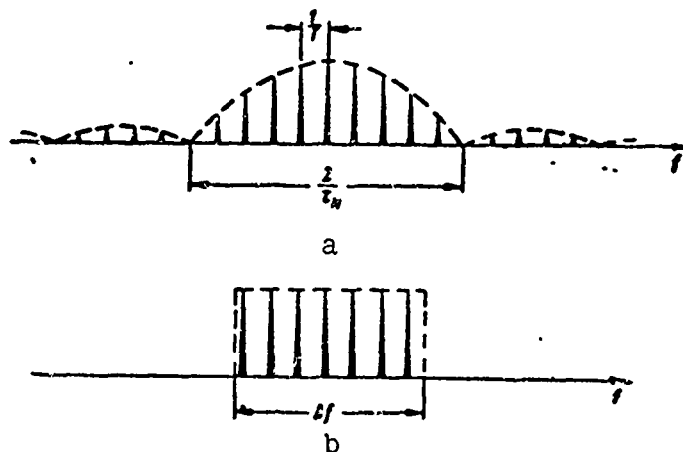


Fig. 5.10. Comb-shaped amplitude-frequency characteristics for an optimum summation circuit, together with a filter of a single radio pulse of the packet. a) In case this filter is optimum; b) if it is replaced by a band filter.

§5.5. AN EXAMPLE OF SYNTHESIZING AN OPTIMUM FILTER FOR THE COMPRESSION OF A RADIO PULSE WITH A COMPLEX LAW OF MODULATION

Let us consider a radio pulse of a duration of τ_1 with a complex law of modulation characterized by the fact that it consists of elementary pulses of the duration $\tau_0 = \tau_1/n$ (Fig. 5.11a). In the course of each time interval τ_0 oscillations of the same frequency f_0 with constant initial phase which may change by a jump by π when passing over to the following elementary pulse are emitted. In other words, if the initial phase is constant and the same for all oscillations some of the elementary pulses are multiplied by $+1$, and some by -1 , which is shown schematically in Fig. 5.11b.

The optimum pulse-response characteristic corresponding to this signal is schematically represented in Fig. 5. 11c. In order to design an optimum filter with such a characteristic a delay line with branches and a general summation device to which some of the branches are connected via inverse cascades may be used (Fig. 5.12). The output voltage of the summation device is fed to the end filter which is optimum for an

elementary pulse of the duration $\tau_0 = \tau_1/n$ (see §5.3).

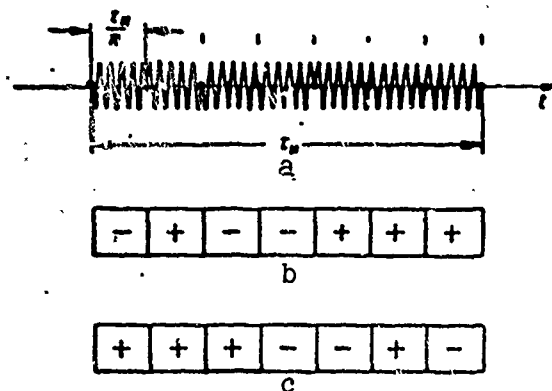


Fig. 5.11. Radio pulse with complex law of modulation-phase-manipulated radio pulse (a); conventional representation of a phase-manipulated radio pulse (b); conventional representation of an optimum pulse-response characteristic (c).

Let us track the process of optimum filtration of a pulse (Fig. 5.11a) with a complex law of modulation. Figure 5.13a shows schematically the input radio pulses shifted in time allowing for the presence of inverse cascades. The result of their summation is shown in Fig. 5.13b, and the output voltage of the optimum filter, as a whole, in Fig. 5.13c.

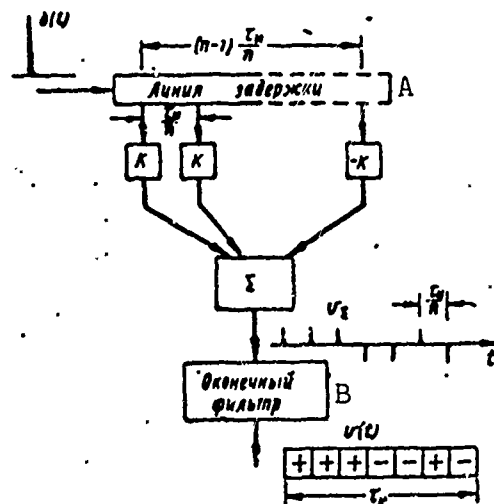


Fig. 5.12. Formation of a pulse-response characteristic which is optimum for a phase-manipulated radio pulse. A) Delay line; B) end filter.

The considered example is interesting from two points of view. On the one hand, it shows the possibilities of synthesizing optimum filters with rather complex pulse-response characteristics. On the other hand, it illustrates the afore-mentioned effect of compression of a pulse with a complex law of modulation in the case of optimum processing. It is easy to see that the duration of the main overshoot of the output signal can be made essentially shorter compared to the duration of the signal at the input.

We note that also a band-pass filter with an optimum band $1.37/\tau_0 = 1.37/\tau_1$ may be used as the end filter of the circuit (Fig. 5.12). In this case, the band-pass filter transforms the elementary rectangular radio pulses (Fig. 5.13b) into radio pulses the shape of whose envelope is somewhat different from the rhombiform one (Fig. 5.13c). Although as a whole the processing will not be optimum, the loss in the signal-to-noise energy ratio is only 17%.

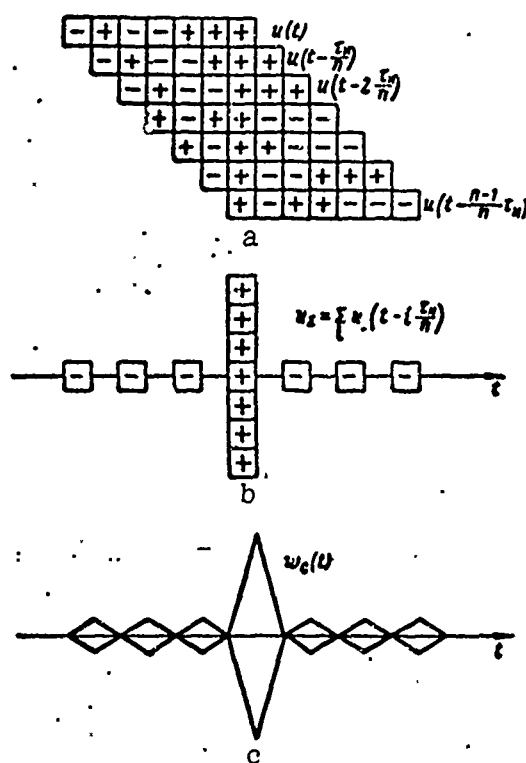


Fig. 5.13. Optimum filtration process of a phase-manipulated radio pulse.

§5.6. SIGNAL DELAY (MEMORY) DEVICES

In order to design devices for optimum processing the received signals must be recorded (remembered). The latter is necessary both in designing optimum filters and incoherent storing devices. Delay lines, potentialoscopes, magnetic recording devices, etc., are used to solve numerous problems. There are electrical and ultrasonic delay lines.

In the electrical delay lines the effect of finite time of propagation of electromagnetic oscillations in a system containing storing devices of electric and magnetic energy (capacity and inductance) is used. The delay lines may have concentrated and distributed storing devices. Besides the distributed inductance of the winding there is a distributed capacity between this winding and the screen in lines with distributed storing devices. Usually, the screen consists of longitudinal conductors that are insulated among each other in order that the transverse currents do not shunt the distributed inductance of the winding nor give rise to excessive losses. On the edges the conductors are joined with each other.

Electric delay lines guarantee a delay of the order of some microseconds (in several cases also of the order of several tens of microseconds). The greater the time delay the narrower is the frequency band.

With the help of the ultrasonic delay lines a delay up to some milliseconds for a frequency band of the order of some megahertz (or even tens of can be obtained. Such a great delay is guaranteed by the fact that, first of all, the electric oscillations are transformed into ultrasonic ones. The latter are delayed, and then again transformed into electric ones. With the limited dimensions of the lines great delay is achieved since sonic speed is considerably lower than the velocity of light. The direct and the inverse piezoelectric effects appearing in the case of quartz crystals, barium titanate, etc., are used to

transform electric oscillations into mechanic ones, and vice versa.

The direct piezoelectric effect lies in the fact that when there are electric charges on the surface of a crystal capacitor it is compressed or stretched depending on the sign of the charge. Inversely, the compression or stretching of a crystal gives rise to electric charges (inverse piezoelectric effect). Consequently, applying a variable electric field along the axis of a crystal capacitor mechanic oscillations of the crystal, which are then transferable to a sound-conducting medium, can be generated. Inversely, if mechanic oscillations arrive from a sound-conducting medium electric oscillations can be obtained. Special amplifiers will be inserted in the channel of the delay line in order to amplify these oscillations.

The magnetostrictive effect is sometimes used to excite ultrasonic oscillations in thin sound-conducting bodies. This effect consists in the fact that mechanic oscillations which will then be propagated in the sound-conducting medium are excited if a variable magnetic field acts along a sound-conducting body made of an appropriate kind of metal (e.g., nickel). Thus, the magnetostrictive delay line is a modification of the ultrasonic one, in which the oscillations are excited by the magnetostrictive rather than by the piezoelectric effect. The inverse magnetostrictive effect may be used to pick up oscillations.

Recently, the piezoresistive effect, i.e., an effect which lies in the variation of the resistance of the transition layer at the boundary with a semiconductor if the latter is compressed or stretched began to be used to transform electric oscillations into ultrasonic ones. This fact permits ultrasonic oscillations of super-high frequencies to be delayed with small energy losses and guarantees the transmission of broad-band signals.

Potentialoscopes are devices in which electric oscillations are

recorded on a dielectric target in the form of a potential relief. For this purpose the target surface must have the property of secondary emission. This implies that more than one electron leaves the target if a high-energy electron falls on it. The more electrons hit the target the more electrons will leave it and, consequently, the greater is the positive charge remaining on the target. If the electron beam arises along the surface of the dielectric target and at the same time the intensity of the electron flow varies also the charge distribution at the target surface will vary accordingly. This means also that the electric oscillations are recorded on the dielectric target in the form of a potential relief. If the electric conductivity of the target is sufficiently small, the potential relief is maintained all the time needed for optimum processing. The measurement of the potential relief may be carried out by various methods, among them with the help of a special counting electron beam.

If magnetic recording is used the electric signal remains in the form of a magnetic relief on the magnetic tape or drum, which move in the neighborhood of the magnetic field of the recording coil. In contrast to the electric recording, the magnetic one permits an infinitely great time delay to be obtained. The magnetic recording may be kept for many years. The frequency band of this recording is, however, usually narrower than that of the electric one.

§5.7. INCOHERENT STORING DEVICES

When processing radio pulse packets with independent random initial phases we must be concerned with the summation of these pulses after the detector, or, in other words, with incoherent summation. Incoherent summation takes place already in case the data are put out visually from a radar indicator since afterglow occurs. In the case of automatized output it can be realized with the help of delay lines, potentialoscopes,

etc.

In the case of visual output the pulses acting in different scanning periods successively excite the same point of the screen. In its effect, such a summation approximates the quadratic one though it is, of course, different from the optimum.

The fact that there is no incoherent storing in the case of automatized output may considerably raise the level of the threshold signal, even compared to visual output. Consequently, when designing an automatized detection (or measurement) system one must try to make it similar to an optimum processing system. As will be shown in Chapter 6, the deviation from optimum summation in details, e.g., the replacement of quadratic summation by linear one and vice versa, has no substantial influence on the level of the threshold signal. On the other hand, it is quite inadmissible to give up incoherent summation completely.

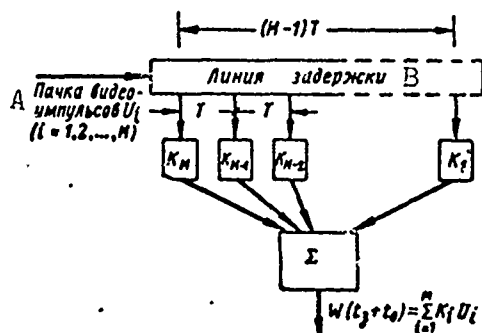


Fig. 5.14. Principle of constructing a post-detector filter on a delay line with branches. A) Packet of video pulses; B) delay line.

In order to realize incoherent summation in an approximate way successive recording on a potentialoscope with readout, magnetic recording, etc., may be used.

A circuit of post-detector filters with delay lines can be used for incoherent summation.

Thus, e.g., a filter in the form of a delay line with a finite number

of branches connected to the summation device may be used for post-detector processing of a signal having the form of a packet of radio pulses. The number of branches from the delay line must be equal to the number M of pulses in the packet, and the delay between the connection points must be equal to the pulse repetition period T (Fig. 5.14).

At some instant of time a voltage (Fig. 5.15) equal to

$$\sum_i K_i U_i, \quad (1)$$

is obtained at the output of the summation device, where U_i is the voltage of the i th pulse at the output of the detector, and K_i is the amplification factor of the i th weight amplifier.

For $U_i = Z_{0i}^2$ and $K_i = S_i^2/N_0^2$ expression (1) reduces to expression [(13) §4.9]; for $U_i = Z_{0i}^2$ and $K_i = S_i^2/(S_i^2 + N_0/\theta_0)$ expression (1) corresponds to expression [(15) §4.9].

It is, however, rather difficult to realize an ultrasonic line with a delay time to be measured by the duration of the pulse packet. Consequently, sometimes a delay only for one pulsing period is used, but a positive feedback from the output of the line to its input is introduced (Fig. 5. 16).

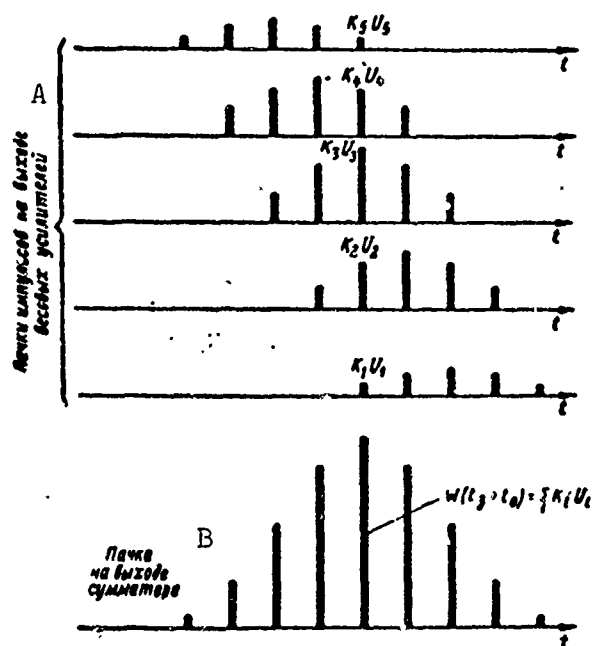


Fig. 5.15. Process of optimum processing in a post-detector filter. A) Pulse packets at the output of the weight amplifiers; B) packet at the output of the summation device.

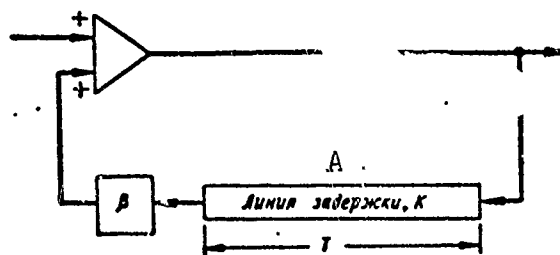


Fig. 5.16. Recirculator. A) Delay line.

The feedback factor β is chosen such that the pulse is only slightly weakened when returning to the input of the line after running through a delay line with a transmission factor K . The process is then repeated (recirculation).

If the delay time of the line is equal to the pulsing period the signal will be stored if a packet of pulses is fed to its input. In this case the quantity $K\beta$ must be chosen such that the first pulse is not damped very strongly until the instant when the last pulse of the packet arrives. On the other hand, if the quantity $K\beta$ is too close to unity the superposition of noise will be amplified considerably whereas no additional superposition of packet pulses will occur. Usually, one chooses $K\beta = 0.8-0.95$.

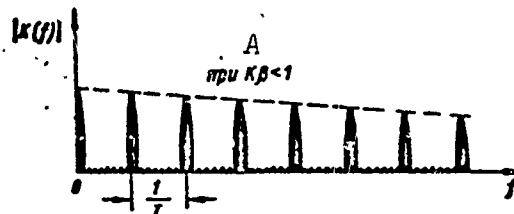


Fig. 5.17. Amplitude-frequency characteristic of a recirculator. A) For.

The amplitude-frequency characteristic of such a device is comb-like (Fig. 5.17); it may be called comb band-pass filter for a packet of video pulses.

We note that the recirculator (Fig. 5.16) may not only be used for incoherent storage. If it guarantees stable work for sufficiently high frequencies it can also be used for coherent storage as may be seen by comparing Figs. 5.17 and 5.9.

A practically important realization of incoherent storage is the digital storage. In this case, the quantities to be summed are rounded

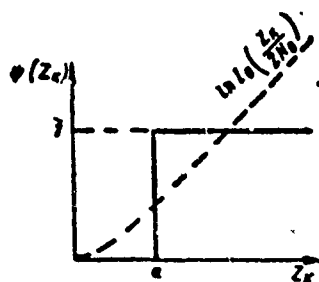


Fig. 5.18. On replacing optimum incoherent summation by digital summation.

off, first of all, in order that they can be expressed in terms of one or several binary discharges. The simplest method of rounding off lies in feeding the pulses to be summed into a threshold circuit with a characteristic (Fig. 5.18)

$$\psi(Z_k) = \begin{cases} 1, & \text{if } Z_k > a, \\ 0, & \text{if } Z_k < a. \end{cases}$$

The voltage at the output of this circuit is expressed in terms of only one binary discharge (0 or 1). For the purpose of comparison the optimum characteristic [see (5) §4.9] approximated by the characteristic $\psi(Z_k)$ is represented by the dotted line in Fig. 5.18.

The threshold circuit may be considered an additional nonlinear element; if it is switched on the whole circuit of processing will not become fully optimum. On the other hand, the operations of processing may be realized with the help of digital devices — memory and summation devices. This permits information from a great number of integrated pulses from a single gated target to be stored. The digital memory of a binary discharge (0 or 1) may be realized with the help of triggered circuits in electron tubes or transistors having two stable states of equilibrium. Recently, the use of ferrites and ferromagnetic films has become widespread, for this purpose.

In order to detect a target the number obtained after summation must be compared with the corresponding threshold, i.e., as a whole, the detection circuit will have two thresholds (Fig. 5.19a).

The diagram of Fig. 5.19a shows that, first of all, the detected pulses enter the first threshold circuit. To its output an M-pulse digital summation device is connected. It is implied that it realizes the

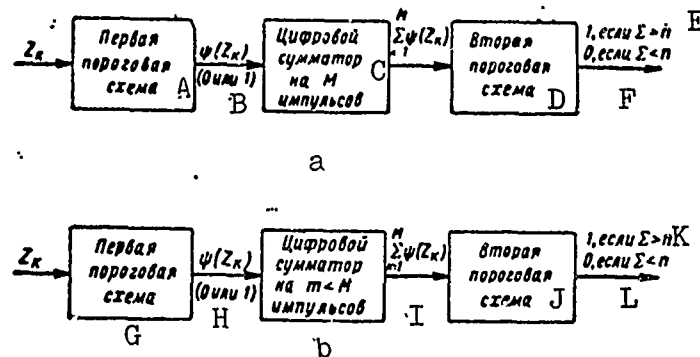


Fig. 5.19. Double-threshold circuits of digital storage. a) With conservation of information on all M pulses of the packet; b) with conservation of information on a number of pulses $m < M$. A) First threshold circuit; B) or; C) digital summation device for M pulses; D) second threshold circuit; E, F) if; G) first threshold circuit; H) or; I) digital summation device for $m < M$ pulses; J) second threshold circuit; K) if; L) if.

memory and summation operations and is analogous to a circuit with delay line as to the functions it performs (Fig. 5.14), but, in contrast to the latter, requires compulsory dropping of obsolete data. After the summation device there is a second threshold circuit with a figure threshold \underline{n} .

As a whole, the detection of a whole packet by means of a double-threshold circuit is recorded if and only if the threshold level of the first circuit is exceeded by, at least, \underline{n} pulses of the M pulses that are possible. M possible pulses are here understood to be the entirety of all successive pulses of the packet which correspond to a certain range section.

Figure 5.19b shows a simplified variant of a double-threshold circuit. As before, the digital summation device is intended to the memory and summation of the excesses over the first threshold, but for the smaller number $m < M$ of the successive pulses of the packet. This implies that the solution on the presence of a target is adopted even if only during the duration of the packet the level of the first threshold

is exceeded by n pulses of the m pulses that are possible.

The choice $m < M$ considerably simplifies the circuit, particularly if m is small (e.g., $m = 2, 3$); this means, however, a certain deviation from optimum processing.

It is in place here to carry on the analogy of the work of the digital summation device (Fig. 5.19) and the summation circuit (Fig. 5.14). The replacement $m < M$ is equivalent to an appropriate reduction of the number of branches and the length of the line in this circuit. In this case the peaks of its frequency characteristic (see, e.g., Fig. 5.17) are broadened, which impairs the signal-to-noise ratio. Or else, we may say that the signal-to-noise ratio is impaired since the energy of the packet is not fully made use of ($m < M$), which gives rise to energy losses. These losses are, however, partly filled up (see §6.4). As a matter of fact, in order to detect a packet it is sufficient to exceed the second threshold if only for one group m of successive pulses, for a total number of pulses in the packet $M > m$.

§5.8. ON THE USE OF THE PHENOMENON OF DISPERSION IN DELAY LINES IN THE CASE OF OPTIMUM FILTRATION OF BROAD-BAND RADIO PULSES

In §§ 5.3-5.7 a number of examples of the use of delaying devices and, in particular, of delay lines aiming at pre- and post-detector optimum processing was given. It was understood that distortions of the signals are undesirable. In this section the possibilities of a profitable use of phase-frequency distortions in delay lines will be mentioned.

Before analyzing the application of distorting lines it is expedient to premise a brief consideration of the frequency characteristics of nondistorting lines. A delay line for which the input and output voltages are connected by the relation

$$u_{\text{out}}(t) = cu_{\text{in}}(t - t_0),$$

where c and t_0 are constants will be called perfect.

The corresponding spectral densities are connected by the relation

$$g_{\text{out}}(f) = cg_{\text{in}}(f)e^{-j2\pi ft_0},$$

from which the complex frequency characteristic $K(f) = g_{\text{vykh}}(f)/g_{\text{vkh}}(f)$ is determined. The amplitude-frequency characteristic of the perfect delay line corresponding to it is uniform

$$|K(f)| = \text{const},$$

and the phase-frequency characteristic is linear and passes through zero (Fig. 5.20a).

$$\arg K(f) = -2\pi ft_0.$$

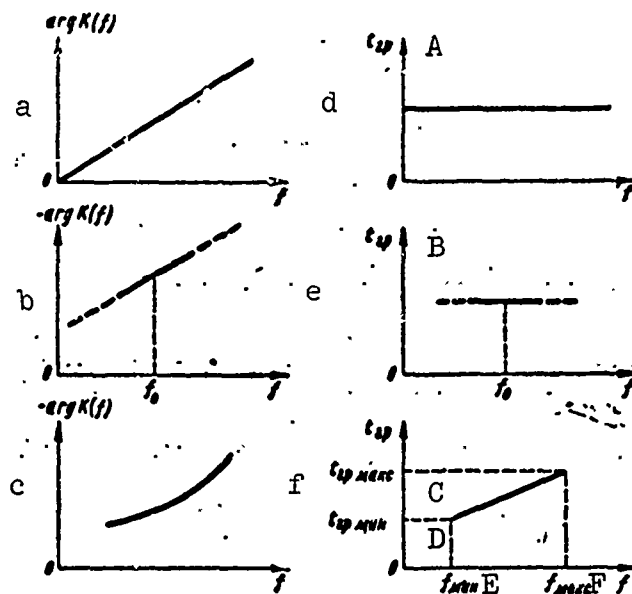


Fig. 5.20. Phase-frequency characteristics and frequency characteristics of the group delay time of nondistorting (a, b, d, e) and distorting (c, f) delay lines. A) gr; B) gr; C) gr maks; D) gr min; E) min; F) maks.

In the case of a high-frequency delay line working in a comparatively narrow frequency spectrum around the carrier frequency f_0 undistorted reproduction is usually understood in a narrower sense. The requirement of reproducing the delayed envelope except for a constant

initial phase ψ without distortion

$$U_{out}(t) = cU_{in}(t - t_0)e^{i\psi};$$

is made; the requirement, however, that the initial phase of the vibrations should be conserved for an arbitrarily chosen initial point of the envelope is not made. Such a delay is obtained in the case of an amplitude-frequency characteristic which is uniform in the neighborhood of the carrier frequency f_0 (within the limits of the signal spectrum), and in the case of a linear (within the same limits) phase-frequency characteristic. The phase-frequency characteristic itself does not necessarily pass through zero (Fig. 5.20b) such that

$$\arg K(f) = \arg K(f_0) - 2\pi t_0(f - f_0), \quad (1)$$

where, generally,

$$\arg K(f_0) \neq 2\pi t_0.$$

The extremely narrow spectrum around an arbitrary frequency f_0 is called a group of frequencies, and the delay time of the envelope corresponding to it the group delay time t_{gr} . Within the limits of a frequency group a linear approximation of any phase-frequency characteristic $\arg K(f)$ may be used. Keeping only the first two terms of the Taylor expansion

$$\arg K(f) = \arg K(f_0) + (f - f_0) \frac{d}{df} \arg K(f_0), \quad (2)$$

comparing (1) and (2) and identifying t_{gr} with t_0 we obtain

$$-2\pi t_{gr} = \frac{d}{df} \arg K(f_0).$$

Replacing the arbitrary frequency f_0 by f we find the following final expression for the group delay time

$$t_{gr} = -\frac{1}{2\pi} \frac{d}{df} \arg K(f). \quad (3)$$

The preceding result (1) may now be treated in the following way. In order to reproduce the signal envelope without distortion the group

delay time must remain unchanged within the limits of the whole frequency spectrum of the signal (Fig. 5.20d, e).

In the case of optimum filtration it is not always admissible to strive for an undistorted reproduction of the envelope. A nonlinear phase-frequency characteristic of the delay line may be used to compensate immediately the phase-frequency spectrum of the signal, without use of any intermediate branches from the delay line.

For this purpose the group delay time in the line must vary in the frequency range of the signal according to some law, e.g., to a linear one (Fig. 5.20c, f).

The inconstancy of the group delay time for different spectral components is classed among the phenomena of dispersion of propagation velocity. Delay lines with variable group delay time are, therefore, termed dispersion delay lines.

As is known from §4.11, optimum filtration of broad-band radio pulses gives rise to their compression in time. The compensation of the phase-frequency spectrum, being part of this filtration, is also connected with pulse compression. Moreover, it is just the compensation of the phase-frequency spectrum of the signal which is the main reason for the compression, since it leads to a simultaneous superposition of the harmonic components (Fig. 4.7) and to the formation of a peak of the compressed radio pulse. But the choice of an optimum amplitude-frequency characteristic, while reducing the individual spectral components of the signal (in order to weaken the noise), may even lead to a contraction of the spectrum and to a widening of the compressed pulse. In the case of broad-band radio pulses this broadening is substantially overlapped by the compression owing to the considerable compensating action of the phase-frequency characteristic $\chi(f)$.

The concept of a variable group delay time permits the compression

mechanism of broad-band radio pulses also be treated in another way, i.e., as that of pulses whose spectral widening is achieved by frequency modulation within the pulse. A line with a characteristic $t_{gr} = t_{gr}(f)$ as shown in Fig. 5.20f, delays high frequencies to a greater extent than low ones. Let us feed to it a pulse whose instantaneous frequency varies from a higher one at the beginning to a lower one at the end of the pulse. Thus, higher frequencies act earlier in the given case, but are delayed to a higher degree, and lower frequencies appear later, but are delayed to a lower degree. This yields the reason for the combination of all frequency groups and the formation of the compressed pulse. Obviously,

$$t_v(f) + t_{cp}(f) = \text{const.} \quad (4)$$

is the condition for such a combination, where $t_v(f)$ is the moment at which the instantaneous frequency acts; for the sake of simplicity, we assume that its variation is monotonic.* The duration of the compressed pulse in case the phase shifts are fully compensated is inversely proportional to the width of the frequency spectrum.

The dispersion delay lines may be described not only with the help of the characteristics of Fig. 5.20, but, as before, also with the help of pulse-response characteristics. Since the delta function acting in taking up this characteristic may be considered the superposition of groups of different frequencies these groups are delayed relative to the instant of action by different times, in the case of a dispersion line. For the example considered (Fig. 5.20f) groups of high frequencies are delayed to a higher degree and groups of low frequencies are delayed to a lower degree.

The pulse-response characteristic proves to be frequency-modulated: at the beginning it is followed by lower, and finally by higher frequencies. At the beginning there are higher frequencies in the pulse

of the signal for which this characteristic is the mirror image, but at the end there are lower frequencies, which corresponds to the conclusion on the character of the signal compressed by the line which we have obtained earlier.

The different dispersion delay devices yield characteristics $t_{gr}(f)$ differing by the operating frequency band $f_{maks}-f_{min}$ and by the drop of the group delay time $t_{gr maks}-t_{gr min}$ within the limits of this band.

The super-high frequency dispersion delay systems in radio waveguides may guarantee very broad frequency bands $f_{maks}-f_{min}$, but with a comparatively small drop in the group delay time $t_{gr maks}-t_{gr min}$. The latter is explained by the fact that the values of the group delay time are determined by the duration of the high-frequency oscillation period and by the number of oscillation periods relative to which the delay takes place. Since the latter is usually limited it is difficult to guarantee a great group delay time in the case of very small values of the high-frequency oscillation period.

Greater variable time delays may be obtained with the help of electric delay lines with distributed or concentrated parameters working in an intermediate frequency range.

Still greater variable time delays, but for smaller frequency bands, may be achieved by making use of ultrasonic waveguides having the shape of tapes or cylindrical wires and made of an ultrasound-conducting material.

§5.9. CORRECTION OF THE SHAPE OF THE COMPRESSED RADIO PULSE ENVELOPE

If the nonlinearity of the phase-frequency spectrum of a radio pulse is compensated by the phase-frequency characteristic of an optimum filter or a dispersion delay line the envelope of the output volt-

age is completely determined by the shape of the output amplitude-frequency spectrum. As was shown in §4.11 an effective pulse compression takes place in the optimum filter in the case of a rectangular amplitude-frequency spectrum of a width of $\Delta f \gg \frac{1}{\tau}$. Minor lobes, however, appear besides the major one. The level of the greatest of them is about 22%. The same situation is, apparently, given in the case of a linearly frequency-modulated radio pulse whose spectrum is similar to a rectangular one (see §7.7). The existence of minor lobes of the envelope ("residues") may sometimes aggravate the resolution of two targets that are close to one another.

The level of the minor lobes may be lowered by changing the shape of the amplitude-frequency spectrum. In particular, if the amplitude-frequency spectrum is almost bell-shaped the compressed pulse also has a bell-shaped envelope whose duration is inversely proportional to the spectral width.

It is not advantageous to pass over immediately from a rectangular spectrum to a bell-shaped one at the expense of suppressing a considerable part of the spectral components of the signal owing to losses in the signal-to-noise ratio and to a considerable widening of the shortened pulse. Consequently, the amplitude-frequency spectrum is partly rounded off in order to suppress the minor lobes, but, if possible, without considerable widening of the shortened pulse or impairing of the signal-to-noise ratio.

By way of example, the passage of a rectangular amplitude-frequency spectrum with a band of Δf on a carrier frequency f_0 through a filter with a linear phase-frequency characteristic and an amplitude-frequency characteristic of the form

$$K(f) = a + 2b \cos 2\pi \frac{f - f_0}{\Delta f} \quad (1)$$

(where $a = 0.5$ and $b = 0.25$) leads to energy losses of 1.72 db (the calculation is analogous to that given in §5.1) and to a widening of the major lobe of the compressed pulse by 1.2 times. In this case a calculated minor lobe level of 2.4% is already guaranteed. For $a = 0.54$ and $b = 0.23$ the calculated level of the minor lobes is reduced to 0.16% with losses of only 1.34 db, but with a widening of the major lobe by 1.5 times.

A pulse-response characteristic of the form

$$v(t) = a\delta(t - t_0) + b\delta\left(t - t_0 - \frac{1}{\Delta f}\right) + b\delta\left(t - t_0 + \frac{1}{\Delta f}\right)$$

corresponds to the frequency characteristic (1) or if $t_0 = 1/\Delta f$

$$v(t) = b\delta(t) + a\delta\left(t - \frac{1}{\Delta f}\right) + b\delta\left(t - \frac{2}{\Delta f}\right). \quad (2)$$

The characteristic (2) is realized with the help of a summation device to which the input and the branches of a nondistorting line of delay by, respectively, $1/\Delta f$ and $2/\Delta f$ are connected, in which case the summation will be carried out with weights equal to, respectively, b, a and b. A device with a pulse characteristic (2) is, therefore, called a weight processing device.

A weight processing device for a radio pulse with a complex rectangular spectrum may be replaced by a resonance amplifier with a characteristic similar to a bell-shaped one and a band on the level (0.05-0.1) which is somewhat broader than the frequency band Δf of a rectangular spectrum.

Weight processing may be used not only in the compression of frequency-modulated, but also in that of phase-manipulated radio pulses.

- 141 By way of example, in the case of an electric nondispersive delay line a continuous capacity output whose shape corresponds to the given pulse-response characteristic (or to a pair of mutually supplementing outputs connected as a differential circuit) may be used.
- 162 Condition (4) may be obtained more rigorously from [(12) §4.4], using the asymptotic principle of the stationary phase.

[Transliterated Symbols]

- 136 опт = opt = optimal'nyy = optimum
- 138 с = s = signal = signal
- 138 п = p = pomekha = noise
- 138 эф = ef = effektivnyy = effective
- 138 и = i = impul's = pulse
- 138 макс = maks = maksimal'nyy = maximum
- 145 з = z = zapazdyvaniye = delay
- 145 вых = vykh = vykhod = output
- 145 вх = vkh = vkhod = input
- 159 гр = gr = gruppa = group
- 162 в = v = vozdeystviye = action
- 163 мин = min = minimal'nyy = minimum

Chapter 6

QUALITATIVE INDICES OF OPTIMUM PARAMETER DETECTION AND MEASUREMENT DEVICES

§6.1. STATEMENT OF THE PROBLEM

The best qualitative detection and measurement indices (in a statistical sense) can be obtained only by optimum processing of the received oscillations.

In the case of detection, such an index, in particular, is the correct detection probability D , calculated for different ratios of signal energy and spectral noise density at the fixed false alarm probability F . With optimum detection this has the highest value.

In the case of measurement, a typical qualitative index is the root mean square error, which can also be calculated for different values of the signal energy to spectral noise density ratio. For a given signal modulation law, the optimum measurement device gives the minimum root mean square error.

The increasing demands made on detection and measurement enforce a continuous improvement of the quality of the processing of the received signals. Hence the qualitative indices of optimum systems are of great interest because they are the limit which one must strive to attain by approximating the non-optimum processing to optimum. The material in Chapters 4 and 5 shows that such an approximation is entirely possible.

In the analysis of the qualitative indices we shall start out with the assumption that optimum processing is achieved. The qualitative in-

dices are then independent of the concrete method of which this processing is achieved. In view of the fact a great number of calculations requires an enormous effort, we shall carry out in detail only the simplest ones, with the aim of illustrating the method of analysis. The most simple case in detection theory is that of a signal with completely known parameters. We shall begin the analysis of the qualitative detection indices with an examination of the simplest case.

§6.2. CHARACTERISTICS OF OPTIMUM DETECTION OF A SIGNAL WITH COMPLETELY KNOWN PARAMETERS

Optimum detection of a signal with completely known parameters consists in a comparison of the correlation integral with the threshold. In the absence of noise the correlation integral

$$z = \int_{-\infty}^{\infty} x(t)y(t)dt$$

can be assumed only two values:

$$z = \begin{cases} \int_{-\infty}^{\infty} x^2(t)dt = \mathfrak{E} & \text{in the presence of a signal,} \\ 0 & \text{in the absence of a signal,} \end{cases}$$

and the detection will always be error-free.

If noise is present, the correlation integral is a random quantity which can assume any values independently of the presence of a signal. The case of signal transmission and false detection then becomes possible. In order to calculate the corresponding probabilities, we determine the distribution law of the random quantity z under condition that signal and noise or noise only are present.

First let us point out that the correlation integral, being the limit of the linear combination of Gaussian random quantities, is also a Gaussian random quantity.

In order to ascertain the distribution law of this quantity we

must find its mathematical expectation $\overline{M}\{z\}=\bar{z}$ and scatter $D\{z\}=v_0^2$ under two conditions, the presence and absence of a useful signal.

The mathematical expectation of the correlation integral we find as the integral of the integrand of the mathematical expectation

$$\bar{z}=M\{z\}=\int_{-\infty}^{\infty} \overline{x(t)y(t)} dt = \int_{-\infty}^{\infty} x(t)\overline{y(t)} dt.$$

The scatter of the correlation integral, in turn, will be

$$v_0^2 = D\{z\} = M\{(z - \bar{z})^2\} = \left[\int_{-\infty}^{\infty} x(t)[y(t) - \overline{y(t)}] dt \right]^2.$$

Under condition of the presence of a useful signal we have

$$\overline{y(t)} = x(t) + \overline{n(t)} = x(t)$$

and

$$\bar{z} = \int_{-\infty}^{\infty} x^2(t) dt = \mathcal{E}, \quad (1)$$

and in its absence $\overline{y(t)} = \overline{n(t)} = 0$ and $\bar{z} = 0$. It is obvious that in both cases $y(t) - \overline{y(t)} = n(t)$ applies.

By replacing in the expression for $D\{z\}$ the second power of the integral by the product of two identical integrals and then proceeding to derive the double integral, we find

$$v_0^2 = D\{z\} = \int_{-\infty}^{\infty} dt \int_{-\infty}^{\infty} x(t)x(s)\overline{n(t)n(s)} ds.$$

By substituting the value of the correlation function for white noise $\overline{n(t)n(s)} = \frac{N_0}{2} \delta(t-s)$ and carrying out the integration, we finally obtain

$$v_0^2 = D\{z\} = \frac{N_0}{2} \int_{-\infty}^{\infty} x^2(t) dt = \frac{N_0}{2} \mathcal{E}. \quad (2)$$

The value $v_0^2 = D\{z\}$ thus obtained is valid not only in presence but also in absence of a useful signal. It depends on the energy of the expected signal in either case because the expression of the correlation integral contains the expected signal $x(t)$.

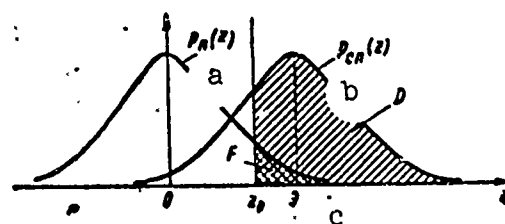


Fig. 6.1. Curves of the conditional probability densities $p_p(z)$ and $p_{sp}(z)$ of the values of the correlation integral. a) p; b) sp; c) E.

Knowing the mathematical expectation and scatter, it is easy to write the conditional probability densities of the Gaussian random quantity z in absence and presence of the useful signal

$$p_n(z) = \frac{1}{\sqrt{2\pi}\sigma_0} e^{-\frac{z^2}{2\sigma_0^2}}, \quad (3)$$

$$p_{cn}(z) = \frac{1}{\sqrt{2\pi}\sigma_0} e^{-\frac{(z-s)^2}{2\sigma_0^2}}. \quad (4)$$

The two distribution laws $p_p(z)$ and $p_{sp}(z)$ are represented in Fig. 6.1. The decision on the presence of a signal is taken if $z > z_0$, which is possible not only in presence of a signal but also in its absence. The probability of the threshold value z_0 being exceeded in absence of a signal is the false alarm probability

$$F = P_n(z > z_0) = \int_{z_0}^{\infty} p_n(z) dz. \quad (5)$$

The probability of the same event in presence of a signal is the correct detection probability

$$D = P_{cn}(z > z_0) = \int_{z_0}^{\infty} p_{cn}(z) dz. \quad (6)$$

The areas in Fig. 6.1 corresponding to these probabilities, are shaded.

The expression for the calculation of F and D with an accuracy corresponding to the specification are solutions of a one-dimensional

problem. This is due to the fact that after the calculation of the correlation integral the multidimensional problem is reduced to a one-dimensional problem. Applying the normal distribution law, the formulas for F and D can be expressed via the probability integral

$$F = 0,5 \left[1 - \Phi \left(\frac{z_0}{v_0} \right) \right]. \quad (7)$$

$$D = 0,5 \left[1 - \Phi \left(\frac{z_0 - \vartheta}{v_0} \right) \right]. \quad (8)$$

The expression (7) shows that the false alarm probability F is unequivocally defined by the ratio of the threshold level z_0 and the root mean square value

$$v_0 = \sqrt{\frac{N_0}{2} \vartheta}$$

of the noise component v of the correlation integral

$$v = \int_{-\infty}^{\infty} n(t) x(t) dt.$$

It follows from the expression (8) that the correct detection probability D depends also on the magnitude of the relation

$$\frac{\vartheta}{v_0} = \sqrt{\frac{2\vartheta}{N_0}} = q. \quad (9)$$

In the following we shall term this quantity detection parameter. We recall that the quantity q is numerically equal to the signal-noise voltage ratio at the output of the optimum filter.

Introducing now the parameter

$$q_0 = \frac{z_0}{v_0}$$

and using the relation

$$\Phi(-u) = -\Phi(u),$$

we bring the expression for the correct detection probability D into the form

$$D = 0,5 [1 + \Phi(q - q_0)]. \quad (10)$$

The family of curves $D(q)$ at different values of q_0 is shown in Fig. 6.2. It is readily seen that the family of Fig. 6.2 is analogous to the family of Fig. 1.9 for the one-dimensional case. At $q = q_0$ the value is $D = 0.5$ and at $q = 0$, $D = F$. The magnitude of F depends only on q_0 ; hence the curves $q_0 = \text{const}$ are at the same time the curves $F = \text{const}$. The correct detection probability D at a given false alarm probability F is the greater, the greater the detection parameter q . A decrease in the attainable value of F , due to an increase in the threshold level, results in a shift of the detection curve to the right.

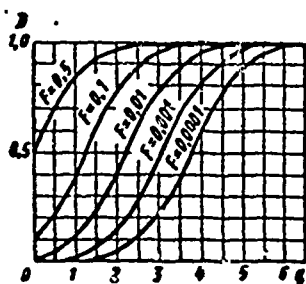


Fig. 6.2. Detection curves for a signal with completely known parameters.

Using the detection curves, we can find the threshold signal. A signal is termed threshold signal when it can be detected at a given false alarm probability F_0 with a given correct detection probability D_0 . The threshold signal is characterized by its energy (or power) which can be calculated if we know the threshold value q_{porog} of the detection parameter. The magnitude of q_{porog} is determined by means of the detection curves.

Assuming, for example, that we wish to achieve the probability $D_0 = 90\%$ at $F = F_0 = 10^{-3}$ at optimum detection of a square radio pulse with the duration τ_1 with a completely known parameter. By means of the curves of Fig. 6.2 we find $q_{\text{porog}} = 4.4$, which corresponds to an energy of the threshold signal of

$$\mathcal{E}_{\text{porog}} = \frac{1}{2} N_0 q_{\text{porog}}^2 = 9.7 N_0.$$

The power of the threshold signal then is

$$P_{\text{porog}} = \frac{\mathcal{E}_{\text{porog}}}{\tau_n} = \frac{1}{2\tau_n} N_0 q_{\text{porog}}^2 = 9.7 \frac{N_0}{\tau_n}.$$

If the power of the signal $P \geq P_{\text{porog}}$ or its energy is $\mathfrak{E} \geq \mathfrak{E}_{\text{porog}}$, then at $F = F_0$ the value is $D \geq D_0$.

The detection parameter $q = \sqrt{2\mathfrak{E}/N_0}$ depends solely on the signal energy and the spectral noise density. Hence it is immaterial which form the signal has, pulsed or continuous, and by which law it is modulated, and the possibility of detecting it at optimum reception with given values of D and F is determined only by the ratio of signal energy to spectral noise density.* The latter conclusion is of fundamental significance.

§6.3. CHARACTERISTICS OF OPTIMUM DETECTION OF SIGNALS WITH RANDOM INITIAL PHASE AND RANDOM AMPLITUDE AND INITIAL PHASE

With optimum detection of a signal of the above discussed form the quantity $z = \sqrt{z_1^2 + z_2^2}$ is calculated and compared with the threshold Z_0 . Then we have

$$z_{1,2} = \int_{-\infty}^{\infty} y(t) x_{1,2}(t) dt,$$

where, in turn,

$$\begin{aligned} y(t) &= Bx(t, \beta) + n(t); \\ x(t, \beta) &= x_1(t) \cos \beta + x_2(t) \sin \beta, \end{aligned}$$

where $p(B) = \delta(B-1)$ is valid in presence of a signal with random initial phase ($B = 1$); $p(B) = 2Be^{-B^2}$ in presence of a signal with random amplitude and phase ($B^2 = 1$); $p(B) = \delta(B)$ in absence of a signal ($B = 0$).

For any fixed B we find in analogy to the results of the preceding section

$$\begin{aligned} \overline{z_{1,2}} &= B \int_{-\infty}^{\infty} x(t, \beta) x_{1,2}(t) dt = \begin{cases} B\mathfrak{E} \cos \beta, \\ B\mathfrak{E} \sin \beta, \end{cases} \\ D\{z_{1,2}\} &= \left[\int_{-\infty}^{\infty} n(t) x_{1,2}(t) dt \right]^2 = \frac{N_0}{2} \mathfrak{E} = v_0^2. \end{aligned}$$

The random quantities z_1 and z_2 are not correlated, because their

mixed central moment

$$\overline{(z_1 - \bar{z}_1)(z_2 - \bar{z}_2)} = \int_{-\infty}^{\infty} dt \int_{-\infty}^{\infty} \overline{n(t)n(s)} x_1(t) x_2(s) ds$$

is practically zero. In fact, by using [(9) §4.4] and integrating over s , the double integral thus found can be reduced to an expression of the form

$$\frac{N_0}{2} \int_{-\infty}^{\infty} x_1(t) x_2(t) dt,$$

which contains as cofactor the integral of the product of the two oscillations phase-shifted by $\pi/2$ with slowly varying amplitudes and phases, which is practically zero.

Using the uncorrelated condition of the quantities z_1 and z_2 and the normal law of their distribution, we obtain the two-dimensional conditional probability density

$$\begin{aligned} p(z_1, z_2 | \beta, B) &= p(z_1 | \beta, B) p(z_2 | \beta, B) = \\ &= \frac{1}{2\pi\sigma_0^2} e^{-\frac{(z_1 - \bar{z}_1)^2 + (z_2 - \bar{z}_2)^2}{2\sigma_0^2}}. \end{aligned}$$

Assuming that $z_1 = Z \cos \varphi$ and $z_2 = Z \sin \varphi$, where $Z = \sqrt{z_1^2 + z_2^2}$, we go over to the new variables of the two-dimensional probability density

$$p(Z, \varphi | \beta, B) = p(z_1, z_2 | \beta, B) \frac{\partial(z_1, z_2)}{\partial(Z, \varphi)},$$

where

$$\frac{\partial(z_1, z_2)}{\partial(Z, \varphi)} = \begin{vmatrix} \cos \varphi & \sin \varphi \\ -Z \sin \varphi & Z \cos \varphi \end{vmatrix} = Z$$

which is the Jacobian of the transformation.

This probability density will be

$$p(Z, \varphi | \beta, B) = \frac{Z}{2\pi\sigma_0^2} e^{-\frac{Z^2 + B^2\sigma_0^2 - 2BZ\sigma_0 \cos(\varphi - \beta)}{2\sigma_0^2}}. \quad (1)$$

Integrating it over φ and using [(9) §3.3] we find the one-dimensional conditional probability density Z in presence of a signal with fixed

parameters β and B

$$p(Z|\beta, B) = \int_0^{2\pi} p(Z, \varphi|\beta, B) d\varphi = \frac{Z}{\sigma_0^2} I_0\left(\frac{BZ\vartheta}{\sigma_0^2}\right) e^{-\frac{Z^2 + B^2\vartheta^2}{2\sigma_0^2}}. \quad (2)$$

Averaging with respect to β and B , we find the expression for the sought-for probability density

$$p(Z) = \frac{1}{2\pi} \int_0^{2\pi} d\beta \int_0^\infty p(Z|\beta, B) p(B) dB. \quad (3)$$

Actually this probability density is conditional because its form varies depending on the distribution $p(B)$. Hence the further calculations must be carried out separately depending on the condition of presence or absence of signal and the form of the signal. By substituting the corresponding expressions for $p(B)$ and carrying out the integration, we obtain:

a) in presence of a signal with random initial phase [$p(B) = \delta(B - 1)$]

$$p_{\text{on}}(Z) = \frac{Z}{\sigma_0^2} e^{-\frac{Z^2 + \vartheta^2}{2\sigma_0^2}} I_0\left(\frac{Z\vartheta}{\sigma_0^2}\right); \quad (4)$$

b) in presence of a signal with random amplitude and initial phase [$p(B) = 2Be^{-B^2}$]

$$p_{\text{on}}(Z) = \frac{2Z}{2\sigma_0^2 + \vartheta^2} e^{-\frac{Z^2}{2\sigma_0^2 + \vartheta^2}}; \quad (5)$$

c) in absence of a signal [$p(B) = \delta(B)$]

$$p_{\text{off}}(Z) = \frac{Z}{\sigma_0^2} e^{-\frac{Z^2}{2\sigma_0^2}}. \quad (6)$$

We observe that under the conditions b the integration is carried out by using the table formula [(7) §3.4].

Figure 6.3 shows the curve $p_{\text{sp}}(Z)$ of the distribution Z in presence of a signal and noise and the curve for $p_p(Z)$ corresponding to the

presence of noise only. The curve $p_{sp}(Z)$ has been plotted for the relatively small $q = 2$. The greater the detection parameter q , the more do the curves $p_{sp}(Z)$ and $p_p(Z)$ differ.

The shaded areas under the curves in Fig. 6.3 to the right of the abscissa Z_0 correspond to the correct detection probability D and the false alarm probability F . Then

$$D = \int_{Z_0}^{\infty} p_{sp}(Z) dZ = \int_{q_0}^{\infty} s I_0(qs) e^{-\frac{q^2+s^2}{2}} ds, \quad (7)$$

$$F = \int_{Z_0}^{\infty} p_n(Z) dZ = \int_{q_0}^{\infty} s e^{-\frac{s^2}{2}} ds = e^{-\frac{q_0^2}{2}}, \quad (8)$$

where $q_0 = \frac{Z_0}{\sigma}$.

The relations (7) and (8) respectively define the family of the detection curves $D(q)$ and the connection between the parameter of this family q_0 and the false alarm probability F . If, using (8) we express q via F , we obtain an expression for the family of detection curves, whose direct parameter is the false alarm probability F :

$$D = \int_{\frac{Z_0}{\sqrt{2\ln(1/F)}}}^{\infty} s I_0(qs) e^{-\frac{q^2+s^2}{2}} ds. \quad (9)$$

Figure 6.4 shows the curve $p_{sp}(Z)$ of the distribution of Z in presence of a signal with random amplitude and initial phase and noise and also the curve $p_p(Z)$ which corresponds to the presence of noise only. The correct detection and false alarm probabilities correspond to the shaded areas and will be:

$$D = \int_{Z_0}^{\infty} p_{sp}(Z) dZ = e^{-\frac{q_0^2}{1+q^2/2}}, \quad (10)$$

$$F = \int_{Z_0}^{\infty} p_n(Z) dZ = e^{-\frac{q_0^2}{2}}. \quad (11)$$

Excluding q_0 from the relation (10) by means of (11), we obtain

$$D = F^{\frac{1}{1+\eta/2}}. \quad (12)$$

Figure 6.5 presents the calculated detection curves for three cases: 1) a signal with completely known parameters; 2) a signal with random initial phase; 3) a signal with random amplitude and initial phase.

The curves for the second and third case were calculated by means of the formulas (9) and (12); the curves for the signal with completely known parameters correspond to the curves presented earlier in Fig.

6.2. The curves for the signal with random initial phase are shifted

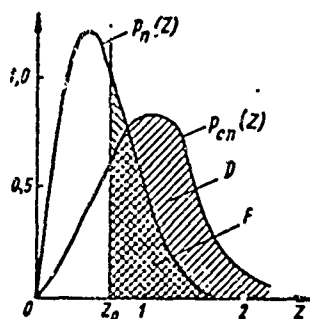


Fig. 6.3. Curves of the conditional probability densities $p_p(Z)$ and $p_{sp}(Z)$ corresponding to the detection of a signal with random initial phase.

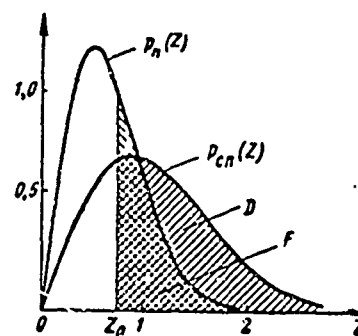


Fig. 6.4. Curves of the conditional probability densities $p_p(Z)$ and $p_{sp}(Z)$ corresponding to the detection of a signal with random amplitude and initial phase.

relatively to them to the right, i.e., in this case a greater signal energy is required for achieving the desired qualitative detection indices.

The curves for the signal with random amplitude and initial phase are particularly strongly shifted to the right in the range of large values of correct detection probability. This is connected with possible fading in presence of random signal amplitudes. In order to attain

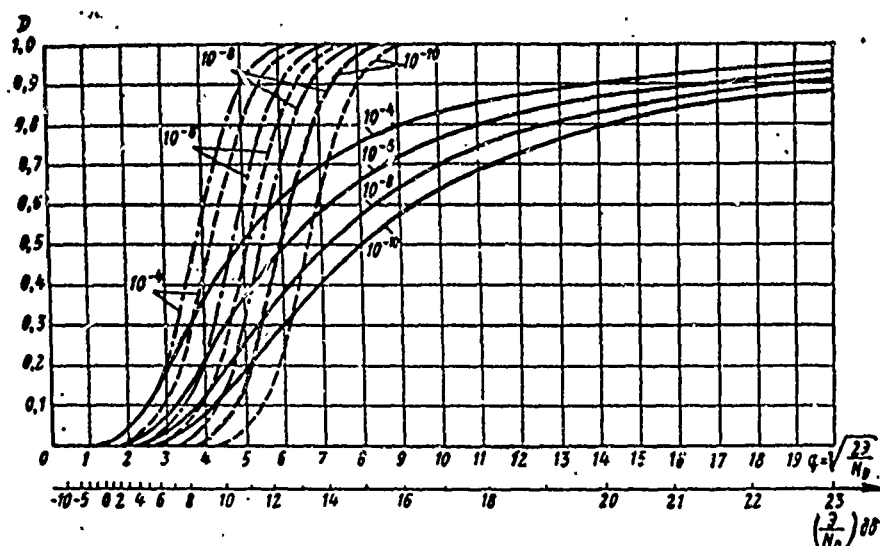


Fig. 6.5. Detection curves for the signals: with completely known parameters (dash line), with random initial phase (dotted line) and with random amplitude and initial phase (thick lines).

sufficiently high correct detection probabilities in presence of such fading, a considerable increase in the mean signal energy is required.* Conversely, at low correct detection probabilities ($D \leq 0.2$) amplitude fluctuations facilitate detection and the curves are shifted to the left.

§6.4. DETECTION CHARACTERISTICS OF AN INCOHERENT PULSE PACKET WITH LINEAR- QUADRATIC AND DIGITAL SUMMATION

Let us turn to the detection characteristics for a signal in the form of a packet of incoherent radio pulses.

It was shown in §4.9 that the law of optimum post-detection processing for a nonfluctuating packet can be approximated to a quadratic or linear relationship. The quadratic approximation is correct for low signal-noise ratios for every pulse, for example, when their energy is of the same order (or even less) than the spectral noise density. Conversely, the linear approximation is closer to the optimum for large

excess of the energy of each pulse over the noise energy.

Quadratic processing is always optimum for a fluctuating signal.

We observe that a widely used summator such as the screen of an electron beam tube approximates the square processing to a certain degree. The nature of the processing depends also on the operating regime of the detector (linear, quadratic).

The voltage at the output of an ideally quadratic summator can be represented in the form

$$U = U_1^2 + U_2^2 + \dots + U_M^2,$$

and that for a linear summator

$$U = U_1 + U_2 + \dots + U_M.$$

Here U_1, U_2, \dots, U_M are the amplitudes of the first, second and M th pulse, respectively. In the absence of a signal these amplitudes are independent random quantities, obeying the Rayleigh law. In the presence of a signal the distribution of each of these amplitudes varies.

Knowing the distribution law for each amplitude, we can find the probability densities $p_{sp}(U)$ and $p_p(U)$ for the magnitude of U in presence and absence of a signal, respectively.*

Integrating the probability densities $p_{sp}(U)$ and $p_p(U)$ within the limits from the threshold value U_{porog} to ∞ , we can find the correct detection and false alarm probabilities and estimate the gain obtained by incoherent summation of M pulses as compared with the case of single pulse reception.

The calculation curves for the estimation of the gain from incoherent summation of a nonfluctuating packet with a rectangular envelope are presented in Fig. 6.6a. These curves have been plotted for the fixed values $D = 0.5$ and $F = 10^{-10}$, the thick line for linear, and the dotted line for quadratic summation. The number of summed (integrated) pulses M (from $M = 1$ to $M = 10^4$) is plotted on the ordinate, and the

necessary excess energy of a single pulse over the spectral noise density at the optimum filter input on the abscissa. The amount of the excess of 13.5 db at $M = 1$ corresponds to the point $F = 10^{-10}$ and $D = 0.5$ on the detection curve for the single signal with random initial phase (Fig. 6.5).

The slight difference between the thick and dotted curves in Fig. 6.6a shows that at a low false alarm and high correct detection probability the transition from quadratic to linear summation practically does not alter the threshold signal. This means that both above-considered forms of nonoptimum processing approximate the optimum processing

$$\sum_k \ln I_k(CU_k).$$

at high signal levels to the linear and at low ones, to quadratic summation, respectively (see §4.9). Here C is a constant depending on the noise level.

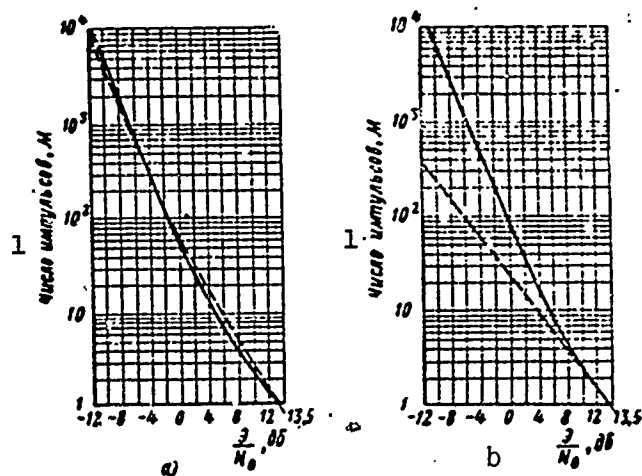


Fig. 6.6. Curves connecting the values of the threshold energy of a single pulse of a rectangular packet with the number of pulses M : a) For linear (thick line) and quadratic (dotted line) summation ($D = 0.5$, $F = 10^{-10}$); b) for incoherent (thick line) and coherent (dotted line) summation ($D = 0.9$, $F = 10^{-7}$). 1) Number of pulses, M .

The use of integration of a large number of pulses lowers the threshold level of the energy of every pulse in the packet. For example, if we go over from a single pulse to 10, the threshold level is lowered by 8 db, if we go over to 100 pulses, by 15.5 db and to 10,000 pulses in a packet, by 25.5 db.

An analogous curve for the estimation of the gain from incoherent integration is given in Fig. 6.6b for the probabilities $D = 0.9$ and $F = 10^{-7}$. As comparison of the curves in Fig. 6.6a and b shows, the requirement $D = 50\%$ and $F = 10^{-10}$, on the one hand* and $D = 90\%$ and $F = 10^{-7}$ on the other, are practically equivalent. In either case, the incoherent integration gives almost the same gain in the threshold energy of each pulse, i.e., the corresponding curves in Fig. 6.6a and b practically coincide. It is found that if we use one of them, we can plot an approximate analogous curve for any values of D and F by shifting it relative to the point 13.5 db to the right or left. The shift should correspond to the change in the threshold energy of a single pulse when passing from $D_0 = 0.9$ and $F_0 = 10^{-7}$ to new values of D and F . In other words, the relative change of the threshold energy due to a change of D and F is practically independent of the number of pulses in a packet. Writing the function relation between the threshold energy and the quantities D , F and M as

$$\left(\frac{\partial}{\partial N_0}\right)_{D,F,M} = \varphi(D, F, M), \quad (1)$$

we can use the approximation

$$\frac{\varphi(D, F, M)}{\varphi(D_0, F_0, M)} \approx \frac{\varphi(D, F, 1)}{\varphi(D_0, F_0, 1)} \quad (2)$$

or in decibels

$$\Delta\varphi(M)_{db} \approx \Delta\varphi(1)_{db}. \quad (3)$$

Formula (3) can also be used for an approximate estimate of the influence of harmonious fluctuations, i.e., to make a correction for

these fluctuations at given D and F from the curves Fig. 6.5.

A comparison between incoherent and coherent integration is of interest. It is easy to see that coherent integration gives a greater gain because the possibility of detection in this case is defined by the ratio of the energy of the entire packet to N_0 . Hence when going over from a single pulse to 10, the threshold energy of each pulse is reduced 10 times (i.e., by 10 db and not by 8 db, as with incoherent summation), upon transition to 100 pulses, 100 times (i.e., by 20 db instead of 15.5 db), etc. The corresponding straight line for coherent integration is shown in Fig. 6.6b by a dotted line.

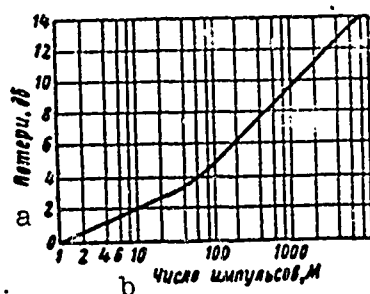


Fig. 6.7. Energy losses in decibels with incoherent integration as compared with coherent ($D = 0.9$, $F = 10^{-7}$). a) Loss, db; b) number of pulses, M.

Figure 6.7 is a diagram of the losses in decibels during incoherent integration. Whilst the losses are still relatively small with a small number of pulses, they can become quite marked if the number of pulses in the packet increases. For example, for 10 pulses the loss is equal to 2 db, and for 100 pulses, the losses amount to 4.5 db.

This notwithstanding, the gain from incoherent integration of the pulse packet must be used in all cases where coherent in-

tegration is not possible.

In conclusion let us examine the detection characteristics of an incoherent packet of radio pulses with digital accumulation.

We shall assume that the detection is achieved by means of a two-threshold circuit working in accordance with the law \underline{n} out of \underline{m} , where the number \underline{m} is equal to the number M of pulses in a packet. This means that the decision concerning the presence of a target is taken if more than \underline{n} pulses from M possible exceeds a certain amplitude thresh-

old. In other words, the linear or quadratic pulse summation is replaced by counting the number of pulses exceeding the threshold.

Assuming the pulse packet to be rectangular, we designate the probability of the threshold value D_0 by any pulse of the packet being exceeded and the probability of this threshold being exceeded by a false pip F_0 . We observe that all packets are detected in which the number of threshold exceeding pulses is $k \geq n$. For every k there can be C_M^k such packets, and the probability of the threshold being exceeded by k pulses from one such packet or of the threshold not being exceeded by the other $M - k$ pulses will be $D_0^k (1 - D_0)^{M-k}$. Hence the probability of correct detection is

$$D = \sum_{k=n}^M C_M^k D_0^k (1 - D_0)^{M-k}. \quad (4)$$

For $n = 0$, D is always 1 because in accordance with the binomial formula the above-written sum changes to

$$[D_0 + (1 - D_0)]^M = 1.$$

Analogously,

$$F = \sum_{k=n}^M C_M^k F_0^k (1 - F_0)^{M-k}, \quad (5)$$

where the quantity n must be larger than zero because otherwise $F = 1$.

If the pulse packet does not fluctuate, the quantities D_0 and F_0 , entering into the formulas (4), (5), can be found by means of the detection curves for a single signal with random initial phase. Then, if the energy of the entire packet is equal to E , one must introduce the energy E/M into the calculation when determining D_0 on the basis of the detection characteristics.

Let us illustrate the above-given relationships by means of the simplest examples.

Assuming the detection is carried out for a number of pulses in

the packet $M = 2$ according to the rule "two from two" which is the case, for example, when a coincidence circuit is used. In this case

$$D = D_0^2 \text{ and } F = F_0^2.$$

Then, for $F = 10^{-10}$ and $D = 0.5$, we should have $F_0 = 10^{-5}$ and $D_0 \approx 0.7$. By means of the diagram (Fig. 6.5) we find $\left(\frac{\partial}{\partial N_s}\right)_{\text{dB}} \approx 11.5$ db, i.e., $\left(\frac{\partial}{\partial N_s}\right)_{\text{dB}} \approx 11.5 + 3 = 14.5$ db.

Thus, the same qualitative detection indices $D = 0.5$ and $F = 10^{-10}$ are achieved with a threshold signal of 14.5 db as against 13.5 db with coherent integration. In this case the losses incurred by digital incoherent processing amount to only 1 db.

If for a number of pulses $M = 2$ detection were carried out in accordance with the rule "one out of two," somewhat inferior results would be obtained. In fact, in this case

$$D = 2D_0 - D_0^2, \quad F = 2F_0 - F_0^2.$$

applies.

Then for $F = 10^{-10}$ and $D = 0.5$ we should have $F_0 = 0.5 \cdot 10^{-10}$ and $D_0 \approx 0.3$. By means of the curve (Fig. 6.5) we determine $\left(\frac{\partial}{\partial N_s}\right)_{\text{dB}} \approx 13$ db or $\left(\frac{\partial}{\partial N_s}\right)_{\text{dB}} \approx 16$ db, i.e., the losses have increased.

Let us present the analogous relations for the rule "n out of three":

for the rule "one out of three"

$$D = 3D_0(1 - D_0)^2 + 3D_0^2(1 - D_0) + D_0^3;$$

for the rule "two out of three"

$$D = 3D_0^2(1 - D_0) + D_0^3;$$

for the rule "three out of three"

$$D = D_0^3.$$

As a more detailed analysis shows there exists for each M an optimum value of n_{opt} , for which the gain as compared with coherent inte-

gration is a minimum. Figure 6.8 shows the loss curves for digital post-detection integration as a function of the number of integrated pulses for $n = n_{\text{opt}}$ $n = 1$ at $F = 10^{-6}$ and $D = 0.5$. The dotted line indicates the design loss curve for quadratic pulse accumulation. Using these curves one can estimate the losses in digital post-detection integration at $m = M$.

If the number of accumulated pulses is $m < M$, there will be other losses in addition to those connected with the application of the rule " n out of m ." These losses can be roughly estimated in the following manner. The relation $m' = M/m$ gives the number of independent observations, at each of which detection is carried out. The situation is

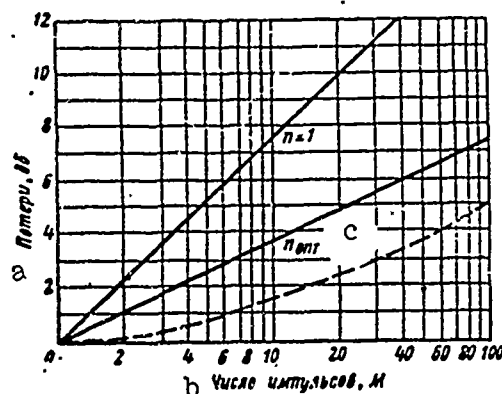


Fig. 6.8. Energy losses in decibels during digital (thick lines) and quadratic (dotted) accumulation. a) Losses; db; b) number of pulses, M ; c) opt.

somewhat analogous to that obtaining with detection according to the rule " 1 out of m' ." Hence a rough estimate of the additional losses can be obtained from the diagram Fig. 6.8 if $m' = M/m$ is plotted on the abscissa and the count is carried out along the line $n = 1$.

§6.5. QUALITATIVE INDICES OF OPTIMUM MEASUREMENT OF THE PARAMETERS OF A SIGNAL WITH RANDOM INITIAL PHASE (GENERAL CONSIDERATIONS)

The mean risk equal to the root mean square of the measurement error,

$$\bar{r} = \epsilon_{\text{opt}}^2 = \overline{|\alpha_{\text{opt}}^* - \alpha|^2}. \quad (1)$$

has been chosen as the basic qualitative index of optimum measurement of the parameter α .

Because a systematic error is absent with optimum measurement, the expression (1) characterizes at the same time the magnitude of the error scatter.

The formulation (1) implies an averaging of a double kind (see §1.6), namely: with respect to the possible values of the parameter α and the possible values of the estimate of α^* . The precise value of the optimum estimate corresponds to the center of gravity of the post-experimental distribution

$$\alpha_{\text{opt}}^* = M\{\alpha|y(t)\}. \quad (2)$$

The averaging (1) can be carried out in any desired sequence. If we carry it out first with respect to α for the fixed realization $y(t)$, and this means, also for the estimate of α_{opt}^* , the root mean square error thus obtained will be equal to the scatter of the post-experimental distribution $D\{\alpha|y(t)\}$, as in §1.6. By averaging this value with respect to the possible realization $y(t)$ we can obtain the quantity ϵ_{skv}^2 .

Let us limit consideration to signals with random initial phase against the background of a superposed white Gaussian noise. The equation [(16) §2.7] of the curve of the post-experimental probability density during the measurement of the parameter α of such a signal can be represented in the form (see §3.3)

$$p\{\alpha|y(t)\} = K_y p(\alpha) e^{-\frac{Z(\alpha)}{N_s}} I_0\left(\frac{2Z}{N_s}\right). \quad (3)$$

Here the quantity $Z=Z[y(t)|\alpha]$ is equal to the modulus of the complex correlation integral

$$Z = \frac{1}{2} \left| \int_{-\infty}^{\infty} Y(t) X^*(t, \alpha) dt \right|. \quad (4)$$

Substituting

$$Y(t) = X(t, \alpha_0) + N(t),$$

where α_0 is the true value of the parameter, unknown to the observer, into this integral, we can separate the signal and noise parts

$$Z_s = \frac{1}{2} \int_{-\infty}^{\infty} X(t, \alpha_0) X^*(t, \alpha) dt, \quad (5)$$

$$Z_n = \frac{1}{2} \int_{-\infty}^{\infty} N(t) X^*(t, \alpha) dt. \quad (6)$$

Then

$$Z = |Z_s + Z_n|. \quad (7)$$

One of the possible relations of Z and α for a certain realization $y(t)$ is shown in Fig. 6.9a. This diagram corresponds to the case in which the detection parameter is $q = \sqrt{\frac{2Z}{N_0}} > 1$. If it is assumed, for example, that the lag time is measured, the curve (Fig. 6.9a) can be regarded as the envelope of the summary signal and noise voltage at the optimum filter output as a function of time. The corresponding curve of the post-experimental probability density is shown in Fig. 6.8b. The signal peak which is already noticeable in Fig. 6.9a is more pronounced in Fig. 6.9b. This is in consequence of the fact that the relation $I_0(u)$ is close the exponential, and $u = 2Z/N_0$ in the region of the peak is considerably greater than unity.

The corresponding curves for the case $q < 1$ are shown in Fig. 6.10a and b. Here we have in mind that the signal is weak and hardly visible among the noise pips. In expression (3) we then have $e^{-\frac{3}{N_0}} \approx 1$. It is important that there is also $I_0(u) \approx 1$ because $u = 2Z/N_0 \ll 1$ is

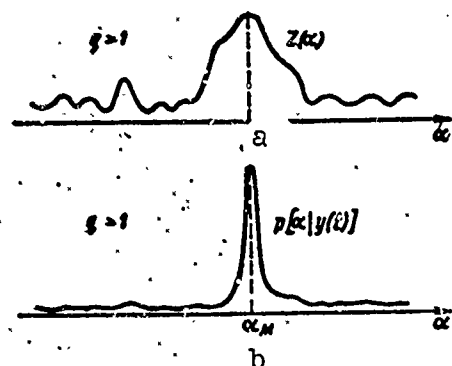


Fig. 6.9. Example of the relationships $Z[y(t)|\alpha] = Z(\alpha)$ and $p[\alpha|y(t)]$ at $q > 1$.

valid owing to the smallness of the expected values of $X(t, \alpha)$ in relation (4). Hence the small pips $Z(\alpha)$ are almost completely obliterated after the operation $I_0(u)$ (Fig. 6.11).

It follows from this that the approximate equality $p[\alpha|y(t)] \approx K_y p(\alpha)$, where the magnitude of the constant K_y is found from the standardizing condition, is fulfilled at very small values of the expected signal $q \leq 1$. Integrating the right and left parts of the equality within infinite limits, we obtain $K_y \approx 1$. This means that the post-experimental probability density is equal to the pre-experimental:

$$p[\alpha|y(t)] \approx p(\alpha). \quad (8)$$

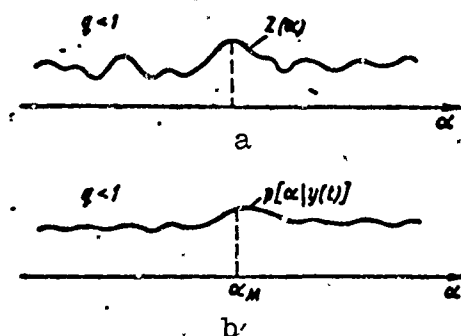


Fig. 6.10. Example of the relations $Z[y(t)|\alpha] = Z(\alpha)$ and $p[\alpha|y(t)]$ at $q < 1$.

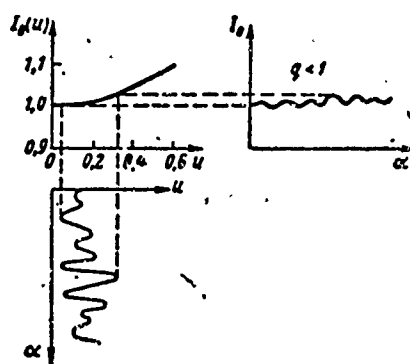


Fig. 6.11. Explanation of the smoothing out of the pips in the curve $p[\alpha|y(t)]$ at $q \ll 1$.

i.e., a very weak signal practically does not give any information increment. The scatter of the post-experimental distribution also coincides with the scatter of the pre-experimental distribution. For rectangular approximation of these distributions, as in §1.6, it is equal to

$$D\{\alpha|y(t)\} = \frac{(\alpha_2 - \alpha_1)^2}{12}. \quad (9)$$

Because the magnitude of the scatter is independent of the realization $y(t)$, we obtain after averaging for the realizations that we also have

$$\sigma_{\alpha\alpha}^2 = \frac{(\alpha_2 - \alpha_1)^2}{12}.$$

Let us now go on to an analysis of the post-experimental distribution for another extreme case, the case of a very strong signal ($q \gg \gg 1$). The area under the post-experimental distribution curve (see, for example, Fig. 6.9b for $q > 1$) is divided into the area in the region of the peak ($\alpha \approx \alpha_0$) and the area along the "noise track." Reliable measurements are possible only if the first area is considerably larger than the second, which is the case with a fairly strong signal. Because of this circumstance, we can use of approximation of the entire curve $p[\alpha|y(t)]$ its approximation in the vicinity of the peak, which de-

creases fairly rapidly on both sides of it.

In this vicinity, the argument of the modified Bessel function is $u = 2Z/N_0 \gg 1$, so that we can use its asymptotic expression

$$I_0(u) \approx \frac{e^u}{\sqrt{2\pi u}}. \quad (10)$$

By virtue of the exponential nature of the relation (10), relatively small increments of the argument u can lead to considerable modifications of the function $I_0(u)$. As is evident from Fig. 6.12, a small section of the apex of the curve $Z(\alpha)$ is transformed almost into the whole curve $I_0\left[\frac{2}{N_0}Z(\alpha)\right]$. For such a small section of the curve it is easy to obtain a suitable approximation. If the function $Z(\alpha)$ is analytical, it is sufficient to limit this to three terms of the Taylor expansion

$$Z(\alpha) \approx Z(\alpha_0) + Z'(\alpha_0)(\alpha - \alpha_0) + \frac{1}{2} Z''(\alpha_0)(\alpha - \alpha_0)^2, \quad (11)$$

which corresponds to an approximation of the apex of the parabola. The quantity $Z''(\alpha_0)$ is expressed by a negative number because the apex is convex.

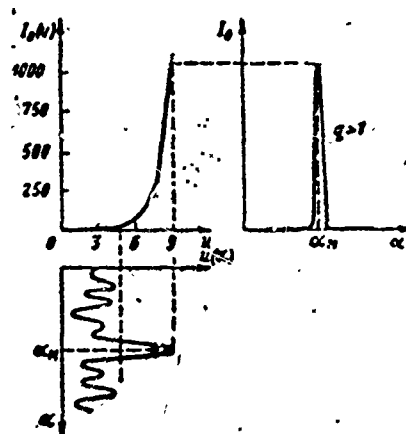


Fig. 6.12. Explanation of the transformation of the apex of the curve $u = 2Z(\alpha)/N_0$ into the main part of the curve $p[\alpha|y(t)]$ at $q \gg 1$.

Completing the second and third addends in (11) to the complete square, we transform the equation of the approximate parabola into the canonical form

$$Z(\alpha) = -A(\alpha - \alpha_M)^2 + B. \quad (12)$$

Here are:

$A = (1/2)|Z''(\alpha_0)|$ the coefficient which characterizes the curvature of the apex of the parabola;

$\alpha_M = \alpha_0 + Z'(\alpha_0)/|Z''(\alpha_0)|$ the abscissa of the maximum (of the apex of the curve) which is slightly shifted with respect to α_0 because of the action of noise;

$B = Z(\alpha_0) + [Z'(\alpha_0)]^2/2|Z''(\alpha_0)|$ is the ordinate of the apex.

The abscissa α_M corresponds to the most probable estimate of $\alpha_{opt}^* = \alpha_M$.

Using the approximation (12) and the asymptotic expression (10), we transform the post-experimental probability distribution (3). Owing to the narrowness of the peak of the curve ($q \gg 1$) we may neglect the variation of the denominator of the asymptotic expression (10) and consider that $p(\alpha) = \text{const}$. We stipulate further that the quantity $\mathfrak{Z}(\alpha) = 3$ is constant, which corresponds, for example, to the case of measurement of the lag time (or the Doppler shift of the frequency). The post-experimental distribution of the probability (3) is then reduced to a normal distribution

$$p[\alpha|y(t)] = Ce^{-\frac{2A}{N_0}(\alpha - \alpha_M)^2}. \quad (13)$$

The coefficient C is determined on the basis of the standardizing condition

$$C = \frac{1}{\sqrt{2\pi}\sigma},$$

where σ is the standard deviation. Its square (the scatter) is found from the relation

$$\frac{1}{\sigma^2} = -\frac{4A}{N_0} = -\frac{2}{N_0} Z''(\alpha_0). \quad (14)$$

In the general case the dependence of the signal energy $\mathfrak{Z}(\alpha)$ on the measured parameter must be considered. The post-experimental density

(3) is then proportional to the exponential function $e^{\frac{Z(\alpha) - \frac{1}{2}\mathfrak{Z}(\alpha)}{N_0}}$, i.e., it is a function of the difference $Z(\alpha) - \frac{1}{2}\mathfrak{Z}(\alpha)$. If this difference is expanded into a Taylor series, the relation (14) is replaced by the relation

$$\frac{1}{\sigma^2} = -\frac{2}{N_0} \left[Z''(\alpha_0) - \frac{1}{2} \mathfrak{Z}'(\alpha_0) \right]. \quad (15)$$

If the signal is sufficiently strong ($q \gg 1$), the modulus of the correlation integral $Z(\alpha)$ can be replaced by the modulus of its signal part $Z_s(\alpha) = |Z_s(\alpha)|$, which is determined from the relation (5). The relation (15) then assumes the form

$$\frac{1}{\sigma^2} = -\frac{2}{N_0} \left[Z_s''(\alpha_0) - \frac{1}{2} \mathfrak{Z}'(\alpha_0) \right]. \quad (16)$$

Let us illustrate the use of the relation (16) in the case of the measurement of the amplitude of a fairly strong signal. In this case

$X(t, \alpha) = a U_s(t)$, where the function $U_0(t)$ describes a signal with a single amplitude. If we designate the energy of the latter by

$$\mathfrak{Z}_s = \frac{1}{2} \int_{-\infty}^{\infty} |U_s(t)|^2 dt,$$

the modulus of the signal part of the correlation integral will be

$$Z_s(\alpha) = \frac{1}{2} \left| \int_{-\infty}^{\infty} a_s U_s(t) a U_0'(t) dt \right| = a_s a \mathfrak{Z}_s,$$

and the energy of the expected signal $\mathfrak{Z}(\alpha) = a^2 \mathfrak{Z}_s$.

From the relation (16) we obtain

$$\frac{1}{\sigma^2} = \frac{2\mathfrak{Z}_s}{N_0},$$

from which follows

$$\sigma = \sqrt{\frac{N_c}{29}}. \quad (17)$$

The right part of the equality (17) represents the signal-noise ratio at the optimum filter output at single amplitude. The result is not altered by the averaging of σ^2 with respect to the realizations.

§6.6. ERROR SCATTER OF THE OPTIMUM MEASUREMENT OF THE LAG TIME OF A SIGNAL WITH RANDOM INITIAL PHASE AT $q \gg 1$

Assuming that $X(t, \alpha) = U(t - \alpha)e^{-j2\pi f_s \alpha}$, i.e., that the lag time is the measured parameter α . We consider that $\vartheta(\alpha) = \vartheta$, i.e., we do not take into account the energy signal as a function of the lag time. Then at $q \gg 1$, by virtue of [(16) §6.5], we have

$$\frac{1}{\sigma^2} = -\frac{2}{N_s} Z_c''(\alpha_s). \quad (1)$$

Taking into account [(5) §6.5] and noting that $|e^{j2\pi f_s(\alpha - \alpha_s)}| = 1$, we have

$$Z_c(\alpha) = \frac{1}{2} \left| \int_{-\infty}^{\infty} U(t - \alpha_s) U^*(t - \alpha) dt \right|. \quad (2)$$

We introduce the spectral density $G(f)$ of the complex amplitude $\bar{U}(t)$

$$G(f) = \int_{-\infty}^{\infty} U(t) e^{-j2\pi f t} dt.$$

Then

$$\int_{-\infty}^{\infty} U(t - \alpha) e^{-j2\pi f t} dt = G(f) e^{-j2\pi f \alpha},$$

i.e., the lag α is taken into account as the lag factor $e^{-j2\pi f \alpha}$. To the convolution (2) of the time functions corresponds the integral of the product of the spectral densities. Hence

$$Z_c(\alpha) = \frac{1}{2} \left| \int_{-\infty}^{\infty} G(f) G^*(f) e^{j2\pi f(\alpha - \alpha_s)} df \right|. \quad (3)$$

In order to avoid long operations, we find the second derivative function $Z_s(\alpha)$ directly from its Taylor expansion. We obtain the required terms of this expansion by representing the exponential function by a series and limiting the expansion to the member of the second power

$$e^{j2\pi(\alpha - \alpha_0)} \approx 1 + j2\pi(\alpha - \alpha_0) + \frac{1}{2} [j2\pi(\alpha - \alpha_0)]^2. \quad (4)$$

We introduce the signal energy

$$\mathcal{E} = \frac{1}{2} \int_{-\infty}^{\infty} |G(f)|^2 df \quad (5)$$

and the above-given moments of its energy spectrum, the first and second

$$M_1 = M_1\{f\} = \frac{\int_{-\infty}^{\infty} f |G(f)|^2 df}{\int_{-\infty}^{\infty} |G(f)|^2 df}, \quad (6)$$

$$M_2 = M_2\{f\} = \frac{\int_{-\infty}^{\infty} f^2 |G(f)|^2 df}{\int_{-\infty}^{\infty} |G(f)|^2 df}. \quad (7)$$

By substituting (4) into (3) and using (5)-(7) we obtain the approximation of the integral by the first terms of the series

$$Z_s(\alpha) \approx \mathcal{E} \left[1 + j2\pi(\alpha - \alpha_0) M_1 + \frac{1}{2} [j2\pi(\alpha - \alpha_0)]^2 M_2 \right].$$

By recalculating the modulus, we find

$$Z_s(\alpha) \approx \mathcal{E} \sqrt{[1 - 2\pi^2 M_2 (\alpha - \alpha_0)^2]^2 + 4\pi^2 M_1^2 (\alpha - \alpha_0)^2}.$$

Limiting the expansion to the second-order terms and using the formula for the approximate extraction of the root, we find

$$Z_s(\alpha) \approx \mathcal{E} [1 - 2\pi^2 (M_2 - M_1^2) (\alpha - \alpha_0)^2].$$

By comparing the expression thus obtained with the sum of the first terms of the Taylor expansion [(11) §6.5] we find

$$Z_c(\alpha) = \mathfrak{D}, \quad Z'_c(\alpha) = 0$$

and

$$Z''_c(\alpha) = -4\pi^2 \mathfrak{D} (M_s - M_1^2). \quad (8)$$

The difference $M_s\{f\} - M_1^2\{f\}$ in relation (8) is analogous to the scatter $D\{\alpha\} = M_s\{\alpha\} - M_1^2\{\alpha\}$ and characterizes the width of the energy spectrum of the signal. If the frequency f_0 is taken as carrier, corresponding to "the center of gravity" of the amplitude-frequency spectrum, then $M_1\{f\} = 0$. The width of the spectrum is then characterized only by the second distribution moment.

On this assumption, we have

$$\frac{1}{\sigma^2} = 4\pi^2 M_s \frac{2\mathfrak{D}}{N_s}.$$

The expression (1) for the scatter of the post-experimental error can then be transformed

$$\sigma^2 = \frac{1}{q^2 (\Delta f_s)^2}, \quad (9)$$

where Δf_s is the effective width of the signal spectrum

$$\Delta f_s = 2\pi \sqrt{M_s\{f\}}. \quad (10)$$

Thus the standard deviation σ of the measured lag time is inversely proportional to the detection parameter q and the effective spectral width of the signal Δf_s .

$$\sigma = \frac{1}{q \Delta f_s}. \quad (11)$$

The relation (11) is valid for $q \gg 1$ if the relation $Z(\alpha)$ is analytical in the vicinity of its maximum value, i.e., for a wide class of signals. The degenerate case of measurement in the case of a discontinuous signal will be examined in §6.7.

By way of an example, let us calculate the standard deviation σ of the measured lag time for a bell-shaped radio pulse with complex envelope $U(t) = e^{-\pi \left(\frac{t}{T}\right)^2}$. The spectral density of this envelope is described by

an expression of the form

$$G(f) = \tau_n e^{-\pi \tau_n^2 f^2}.$$

Then

$$M_s(f) = \frac{\int_{-\infty}^{\infty} f^2 e^{-2\pi \tau_n^2 f^2} df}{\int_{-\infty}^{\infty} e^{-2\pi \tau_n^2 f^2} df} = \frac{1}{4\pi \tau_n^2}.$$

Here, we have $\Delta f_0 = \sqrt{\pi}/\tau_n = \sqrt{\pi} \Delta f$ and

$$\sigma = \frac{\tau_n}{q \sqrt{\pi}} = \frac{1}{q \Delta f \sqrt{\pi}},$$

where τ_n and Δf , respectively, are the pulse duration and width of its spectrum at the level $e^{-1/2} \approx 0.46$.

For example, at $\tau_n = 2$ microseconds ($\Delta f = 0.5$ Mc) and $q = 8$, the root mean square error of the optimum measurement of the lag time of a single bell-shaped pulse is $\sigma = \frac{2}{8 \sqrt{\pi}} = 0.14$ microseconds.

§6.7. DEGENERATE CASE OF LAG TIME MEASUREMENT AT $q \gg 1$

Assuming that the lag time of a radio pulse with a rectangular envelope is measured. In this case we cannot use the parabolic approximation [(11) §6.5] because the function $Z_s(\alpha)$ corresponds to a rhombic envelope at the optimum filter output and has an inflexion at the apex. We can, however, introduce the linear broken approximation (Fig. 6.13)

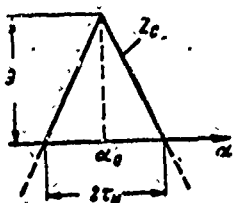


Fig. 6.13. Linear broken approximation of $Z_s(\alpha)$.

$$\begin{aligned} |Z(\alpha) \approx Z_s(\alpha) = Z_s(\alpha_0) \left[1 - \frac{|\alpha - \alpha_0|}{\tau_n} \right] = \\ = 2 \left[1 - \frac{|\alpha - \alpha_0|}{\tau_n} \right]. \end{aligned} \quad (1)$$

The principle of this approximation consists in neglecting the noise component. Moreover, the description of the apex in the region $|\alpha - \alpha_0| \leq \tau_n$ is extended to the region $|\alpha - \alpha_0| > \tau_n$. The values of the post-experimental probability density in this re-

gion are still small. However, the approximation (1) for this region gives a negative value. The exponential function of this quantity tends to zero in proportion to the increase in the ratio $\frac{|a-a_0|}{\tau_n}$.

Using approximation (1), the expression for the post-experimental probability density can be represented in the form

$$p[a|y(t)] = Ke^{-\frac{2\beta}{N_0} \frac{|a-a_0|}{\tau_n}},$$

where the coefficient K is determined by the standardizing conditions.

The scatter of the post-experimental distribution then is

$$\sigma^2 = \frac{\int_{-\infty}^{\infty} (a-a_0)^2 e^{-q^2 \frac{|a-a_0|}{\tau_n}} da}{\int_{-\infty}^{\infty} e^{-q^2 \frac{|a-a_0|}{\tau_n}} da}$$

or

$$\sigma^2 = \frac{\tau_n^2 \int_0^{\infty} u^2 e^{-u} du}{q^2 \int_0^{\infty} e^{-u} du} = \frac{2\tau_n^2}{q^2} \quad (2)$$

Thus, the standard deviation $\sigma = \frac{\tau_n \sqrt{2}}{q}$ in this case proves to be inversely proportional to the square of the detection parameter $q^2 = \frac{2\beta}{N_0}$. Replacing the pulse energy β by its power P and the duration τ_1 , we find

$$\sigma = \frac{\tau_n N_0 \sqrt{2}}{2\beta} = \frac{\sqrt{2}}{2} \frac{N_0}{P} \quad (3)$$

The quantity σ thus obtained which characterizes the potential errors of the measurement, is independent of the pulse duration and is determined only by its power.

The above-described relation must be treated with a certain caution when the rectangular approximation of the envelope is applied to real radio pulses with flat fronts. The smaller the calculated quantity σ , the greater are the requirements for the steepness of the fronts, i.e., the closeness of the real to an ideal pulse.

§6.8. THRESHOLD EFFECT IN MEASUREMENT

If the detection parameter q is fairly large, the peak area of the post-experimental distribution curve exceeds considerably the area along the "noise track." The magnitude of the standard deviation σ then varies relatively slowly as a function of q (as $1/q$ in the nondegenerate case and $1/q^2$ in the degenerate case). If q decreases, the area

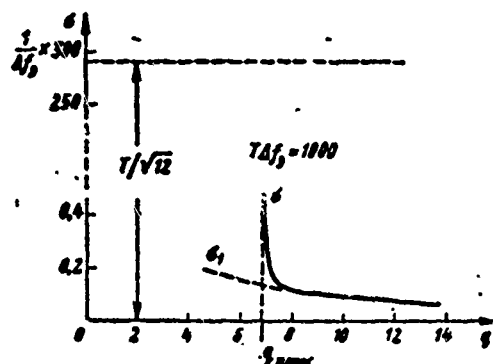


Fig. 6.14. The relations $\sigma = \sigma(q)$ (thick line) and $\sigma_1 = \sigma_1(q)$ (dotted line), plotted with and without taking into account the noise tracks.

along the "noise track" becomes commensurable with the peak area. The measurements become unreliable, the magnitude of σ increases rapidly, considerably exceeding the values calculated in §§ 6.6-6.7. The measurement errors are then due not so much to the superposition of the noise on the signal as to the effect of the spurious noise pips, i.e., the effect of false alarm. This effect is the more noticeable, the wider the possible limits of parameter measurement.

Assuming a rectangular law for the pre-experimental distribution of the parameter α , the measurement limits can be characterized by the difference $\alpha_2 - \alpha_1$. Having in mind the measurement of the lag time, we designate the difference $\alpha_2 - \alpha_1 = T$. Whilst at a large q the standard deviation σ is of the order of $1/q\Delta f_e$, at small q it is close to $T/\sqrt{12}$

i.e., it varies approximately $qT\Delta f_e$ times. This quantity can be very large and thus at relatively small changes of q , a sudden variation of σ is observed (Fig. 6.14) as soon as q comes near to its threshold value q_{porog} .

In order to estimate this phenomenon quantitatively, we approximate the resulting post-experimental distribution curve

$$p\{\alpha | y(t)\} = p_\alpha(\alpha) = P_1 p_1(\alpha) + P_2 p_2(\alpha) \quad (1)$$

Here the probability density $p_1(\alpha)$ approximates the distribution law in the vicinity of the peak, and the probability density $p_2(\alpha)$ the distribution law which applies to the "noise track." The probabilities P_1 and P_2 , whose sum is equal to unity, describe the ratio of the areas in the region of the peak and the "noise track." The approximation $p_2(\alpha)$ can be taken as rectangular and without break in the peak area, because in this region $p_2 \ll p_1$ even at $q \approx q_{\text{porog}}$, provided that $T\Delta f_e \gg 1$.

Let us connect the scatter of the resulting distribution with the scatter of the partial distributions $\sigma^2 = D\{\alpha\}$. To this end we calculate the first and second moments of the resulting distribution

$$M_1\{\alpha\} = \int_{-\infty}^{\infty} \alpha p_\alpha(\alpha) d\alpha = P_1 M_{11}\{\alpha\} + P_2 M_{12}\{\alpha\},$$

$$M_2\{\alpha\} = \int_{-\infty}^{\infty} \alpha^2 p_\alpha(\alpha) d\alpha = P_1 M_{21}\{\alpha\} + P_2 M_{22}\{\alpha\}.$$

Here M_{11} and M_{12} are the first, and M_{21} and M_{22} the second moments of the corresponding partial distribution. By means of the first two moments we can calculate the scatter

$$D\{\alpha\} = M_2 - M_1^2 = (P_1 M_{21} + P_2 M_{22}) - (P_1 M_{11} + P_2 M_{12})^2.$$

Introducing the scatter of the partial distributions $D_1\{\alpha\} = M_{21} - M_{11}^2$, $D_2\{\alpha\} = M_{22} - M_{12}^2$ and using the obvious equality $P_2 = 1 - P_1$, we obtain

$$D\{\alpha\} = (1 - P_1) D_1\{\alpha\} + P_2 D_2\{\alpha\} + (1 - P_1) P_2 [M_{11}\{\alpha\} - M_{12}\{\alpha\}]^2. \quad (2)$$

If $q \gg 1$, then $P_2 = 0$ and $D\{\alpha\} = D_1\{\alpha\}$; however, if $q \ll 1$, then $P_2 \approx 1$ and $D\{\alpha\} = D_2\{\alpha\}$, i.e., the measurement is entirely unreliable. Hence the quantity P_2 is termed measurement unreliability coefficient.

In order to estimate the unreliability coefficient P_2 , we proceed in the following manner. Starting out with the relation [(3) §6.5] we represent P_2 in the form

$$P_2 = \lambda \overline{I_0\left(\frac{2Z}{N_0}\right)} \quad (3)$$

where the factor is $\lambda = K_p P_0 e^{-\frac{3}{N_0}}$ and $\overline{I_0\left(\frac{2Z}{N_0}\right)}$ is the mean value of the modified Bessel function within the interval of the "noise track." The factor λ is found from the standardizing condition $P_1 + P_2 = 1$. Taking into account [(3), (10), (12) §6.5], we represent the quantity P_1 in the form

$$P_1 = \lambda \sqrt{\frac{N_0}{4\pi B}} \int_{-\infty}^{\infty} e^{\frac{Z^2}{N_0} (1 - e^{-u^2})} du$$

or

$$P_1 = \lambda \frac{N_0}{2\sqrt{2AB}} e^{\frac{2R}{N_0}}$$

The mean value $\overline{I_0\left(\frac{2Z}{N_0}\right)}$ within the interval we replace by the mean of the set $\overline{I_0\left(\frac{2Z}{N_0}\right)}$ at an arbitrary point of the interval, which can be done by virtue of the stationary nature of the process on "noise track." Using the expression of the Rayleigh law $p_z(Z) = \frac{Z}{v_0^2} e^{-\frac{Z^2}{v_0^2}}$, where $v_0 = \sqrt{2N_0/2}$, and the integral representation of the Bessel function [(9) §3.3], we obtain after substitution of $u = Z/v_0$

$$\overline{I_0\left(\frac{2Z}{N_0}\right)} = \int_0^{\infty} I_0\left(\frac{2Z}{N_0}\right) p_z(Z) dZ = \frac{1}{2\pi} \int_0^{2\pi} d\theta \int_0^{\infty} e^{i\theta \cos \varphi - \frac{u^2}{2}} u du.$$

Going over from the polar to Cartesian coordinate, we find finally

$$\overline{I_0\left(\frac{2Z}{N_0}\right)} = \overline{I_0\left(\frac{2Z}{N_0}\right)} = \frac{1}{2\pi} \int_{-\infty}^{\infty} \int_{-\infty}^{\infty} e^{-\frac{(x-y)^2 - \eta^2 + \eta^2}{2}} d\eta dx dy. \quad (3')$$

Thus,

$$P_2 = \lambda e^{\frac{q}{2}}. \quad (4)$$

For the calculation of λ we have the equation

$$\lambda \left[T e^{\frac{q}{2}} + \frac{N_0}{2\sqrt{2AB}} e^{\frac{2B}{N_0}} \right] = 1, \quad (5)$$

where the coefficients A and B are determined in correspondence with §6.5. Assuming tentatively in the region of the peak $Z(q) \approx Z_c(q)$, and taking into account that $Z'_c(q_0) = 0$, we obtain [see (8), (10) §6.6]

$$A \approx \frac{1}{2} |Z''_c(q_0)| = \frac{1}{2} \beta(\Delta f_e)^2.$$

$$B \approx Z_c(q_0) = \beta.$$

Determining from (5) the factor λ and substituting it into (4), we find the final expression for the unreliability coefficient

$$P_2 = \frac{T \Delta f_e q^2 e^{-q/2}}{1 + T \Delta f_e q^2 e^{-q/2}}. \quad (6)$$

The curve for the unreliability coefficient in the function q for two values of the product $T \Delta f_e$ is represented in Fig. 6.15.

Fig. 6.15. Curves of the unreliability coefficient $P_2 = P_2(q)$ for two values of the produce $T \Delta f_e$.

Because normally $T \Delta f_e \gg 1$, the reception threshold is reached even at small values of the unreliability coefficient, when $T \Delta f_e q^2 e^{-q/2} \ll 1$. In this case the expression for P_2 can be represented in the form

$$P_2 \approx T \Delta f_e q^2 e^{-q/2}. \quad (7)$$

Making use of the relation (7), we estimate the increase in the scatter, due to the increase in the unreliability coefficient. Supposing for the sake of simplicity that the measured value corresponds to the center of the range of expected values, we assume in the formula (2)

$$M_{11}(a) = M_{11}(a).$$

Substituting in this formula

$$D_1\{\sigma\} = \sigma_1^2 = \frac{1}{q^2(\Delta f_e)^2}, \quad D_2\{\sigma\} = \sigma_2^2 = \frac{T^2}{12}.$$

we find

$$\sigma^2 = D\{\sigma\} \approx \frac{1}{q^2(\Delta f_e)^2} + \frac{T^2}{12} \Delta f_e^2 e^{-q\Delta f_e}$$

or

$$\frac{\sigma^2}{\sigma_1^2} \approx 1 + \frac{(T\Delta f_e)^2}{12} q^2 e^{-q\Delta f_e}. \quad (8)$$

The curves $\sigma^2/\sigma_1^2 = \text{const}$ are shown in Fig. 6.16 in the coordinates $T\Delta f_e$ and q . These curves attest to the presence of a threshold because relatively small changes of q can lead to marked changes in σ^2 . For example, a variation of q from 7.5 to 6.8 at $T\Delta f_e = 1000$ results in a variation of the ratio σ^2/σ_1^2 from 1.1 to 10.

The presence of a threshold is due to the exponential nature of the dependence of the ratio of the peak area to the area along the noise track, which follows directly from the graph (Fig. 6.12). The level of the threshold depends on the product $T\Delta f_e$ characterizing the number of resolved elements. This relationship is nearly logarithmic.

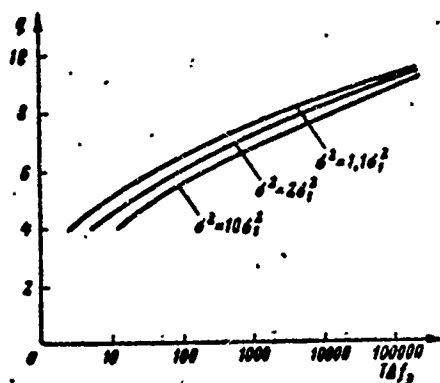


Fig. 6.16. The curves $q = q(T\Delta f_e)$ for different values of the relative increase in the scatter σ^2/σ_1^2 due to the influence of the noise track.

The above-given analysis refers only to the simplest single signal with random initial phase, but the regularities which have been demonstrated apply to signals of a wider class, including signals in the form of packets of radio pulses with independent initial phases.

§6.9. ERROR SCATTER OF THE OPTIMUM MEASUREMENT OF THE DOPPLER FREQUENCY FOR A SIGNAL WITH RANDOM INITIAL PHASE

Let us examine the case in which the measured parameter of a signal with random initial phase is a Doppler frequency, i.e., $X(t, \alpha) = U(t)e^{-j2\pi\alpha t}$. Assuming that $q > q_{\text{porog}}$ and that the measurement is nondegenerate, i.e., that the second derivative $Z''(\alpha)$ exists and is a finite quantity, we find the error scatter of the optimum measurement from the relation [(14) §6.5].

The calculation results are analogous to [(7), (10), (11) §6.6]. The standard deviation of the measured value is determined by means of the formula

$$\sigma_F = \frac{1}{2\Delta t_{\text{ekv}}}, \quad (1)$$

where Δt_{ekv} is the equivalent signal duration.

At $M_1(t) = 0$, i.e., when the time reading is carried out from the "center of gravity" of the envelope $U(t)$, we have

$$\Delta t_{\text{ekv}} = 2\pi / M_2(t). \quad (2)$$

Here $M_2(t)$ is the reduced second moment of the signal energy distribution in time

$$M_2(t) = \frac{\int_{-\infty}^{\infty} t^2 |U(t)|^2 dt}{\int_{-\infty}^{\infty} |U(t)|^2 dt}. \quad (3)$$

The greater the signal duration, the greater is the quantity $M_2(t)$ and Δt_{ekv} , i.e., the smaller is the standard deviation of the measured value of the Doppler frequency.

As an example we calculate the standard deviation of the Doppler frequency in the reception of a bell-shaped pulse with the envelope

$U(t) = e^{-\frac{t^2}{\tau_1^2}}$, where τ_1 is the pulse duration at the level $e^{-\frac{1}{2}} \approx 0.46$. In this case we have

$$M_s(t) = \frac{\int_{-\infty}^{\infty} t^2 e^{-\frac{t^2}{\tau_1^2}} dt}{\int_{-\infty}^{\infty} e^{-\frac{t^2}{\tau_1^2}} dt} = \frac{\tau_1^2}{2\pi}.$$

and

$$\Delta t_s = \sqrt{2\pi\tau_1^2}.$$

Then

$$\sigma_F = \frac{1}{q\tau_1\sqrt{2\pi}}.$$

For example, if $\tau_1 = 1$ msec and $q = 8$, then $\sigma_F = 50$ cps.

We must pay attention to the fact that all the relations given in this section refer to a case in which the lag time is accurately known. If the lag time and the Doppler frequency are unknown, the measurement result depends essentially on the structure of the so-called ambiguity diagram of the corresponding radar signal. These diagrams will be considered in the next chapter, which begins with a detailed analysis of the required calculation relations. An analysis of the errors in simultaneous measurement of two parameters is given in Appendix 2.

Manu-
script
Page
No.

[Footnotes]

- 173 If $F_m \approx mF = \text{const} \ll 1$ (§1.1) is given, and if F decreases with increasing m , then q increases but only logarithmically (see Figs. 6.2, 6.5).
- 178 Or a transition to the emission of a main signal at two or more carrier frequencies (see §3.6 and Appendix 1).

- 179 An example of the calculation for quadratic summation is given in Appendix 1.
- 181 The probability $F = 10^{-10}$ corresponds to a single microsecond false noise pip in three hours of continuous operation.
- 194 Replacing $G(f)$ by its expression via $U(t)$ we can also show that

$$M_s = \frac{\int_{-\infty}^{\infty} |U(t)|^2 dt}{\int_{-\infty}^{\infty} |U(t)|^2 dt}.$$

[Transliterated Symbols]

- 170 $\pi = p = \text{pomekha} = \text{noise}$
- 170 $c = s = \text{signal} = \text{signal}$
- 172 $\text{порог} = \text{porog} = \text{threshold}$
- 172 $\text{и} = i = \text{impul's} = \text{pulse}$
- 185 $\text{опт} = \text{opt} = \text{optimal'nyy} = \text{optimum}$
- 186 $\text{скв} = \text{skv} = \text{srednekvadratic'hnyy} = \text{rms}$
- 194 $\mathcal{E} = E = \text{energiya} = \text{energy}$
- 195 $\mathfrak{e} = e = \text{effektivnyy} = \text{effective}$
- 203 $\text{екв} = \text{ekv} = \text{ekivalentnyy} = \text{equivalent}$

Chapter 7

AMBIGUITY DIAGRAMS OF RADAR SIGNALS

§7.1. FORMULA FOR OPTIMUM PROCESSING OF THE RADAR SIGNAL WITH TARGET MOTION CONTROL

Let us examine the expression for the reflected signal from a point target

$$x(t) = u(t - t_{zt}) = U(t - t_{zt}) \cos [\omega_s(t - t_{zt}) + \varphi(t - t_{zt}) + \theta], \quad (1)$$

where

t_{zt} is the present lag time,

$U(t)$ and $\varphi(t)$ are non-random functions,

θ is the random initial phase.

The quantity $t_{zt} = \frac{2r}{c}$ is a function of time if the distance $r(t)$ to the target varies during the sweep interval. The expected functional relationship can be conveniently expressed by using the Taylor expansion for $r(t)$

$$t_{zt} = \frac{2}{c} \left[r(0) + r'(0)t + \frac{1}{2} r''(0)t^2 + \dots \right]$$

or

$$t_{zt} = t_z + \frac{2v_r}{c}t + \frac{a_r}{c}t^2 + \dots \quad (2)$$

Here we use the initial moment of the target sweep as the time reading reference $t = 0$; the quantities t_z , v_r and a_r are the initial signal lag time, the initial target velocity and its initial acceleration in a radial direction, respectively.

For most radar signals the functions $U(t)$ and $\varphi(t)$ vary slowly as compared with the high-frequency oscillations $\cos \omega_0 t$ or $\sin \omega_0 t$. Hence

the present lag time variation t_{zt} does not vary greatly during the sweep:

$$U(t-t_s) = U\left(t-t_s - \frac{2v_r}{c}t - \frac{a_r}{c}t^2 - \dots\right) \approx U(t-t_s),$$

$$\varphi(t-t_s) = \varphi\left(t-t_s - \frac{2v_r}{c}t - \frac{a_r}{c}t^2 - \dots\right) \approx \varphi(t-t_s).$$

Assuming further by virtue of the short duration of the sweep that

$$a_r t^2 \ll \lambda_s = \frac{2\pi c}{\omega_s},$$

we can neglect the influence of the acceleration on the phase of the high-frequency oscillations. Expression (1) then assumes the form

$$x(t) = U(t-t_s) \cos[(\omega_s - \Omega_d)t + \varphi(t-t_s) + \beta], \quad (3)$$

where $\Omega_d = \omega_s \frac{2v_r}{c}$ is the Doppler frequency, and $\beta = \theta - \omega_s t_s -$ is the initial phase which is generally a random equal probability quantity. The expression thus obtained describes the signal with a random initial phase and two unknown measurable parameters t_z and Ω_d .

The expression (3) can be transformed thus

$$x(t) = x_1(t) \cos \beta + x_2(t) \sin \beta, \quad (4)$$

where

$$x_{1,2}(t) = \frac{1}{\sqrt{2}} X(t) \begin{matrix} \cos \\ \sin \end{matrix} [\omega_s t + \varphi_x(t)]. \quad (5)$$

In the case under consideration

$$\left. \begin{aligned} X(t) &= U(t-t_s), \\ \varphi_x(t) &= \varphi(t-t_s) - \Omega_d t. \end{aligned} \right\} \quad (6)$$

For optimum detection and measurement, the magnitude

$$Z = \left| \frac{1}{2} \int_{-\infty}^{\infty} Y(t) X^*(t) dt \right|, \quad (7)$$

must be calculated.

Here $Y(t) = Y(t)e^{j\varphi_y(t)}$ and $X(t) = X(t)e^{j\varphi_x(t)}$ are the complex amplitudes of the received and expected oscillations. Taking into account (6), we present the expression for $\bar{X}(t)$ in the form

$$X(t) = U(t - t_0) e^{j\Omega_d(t-t_0)} e^{-j\Omega_d t} = U(t - t_0) e^{-j\Omega_d t}. \quad (8)$$

By substituting this expression in (7), we obtain the formula for the optimum signal processing with the target motion being taken into account

$$Z = \left| \frac{1}{2} \int_{-\infty}^{\infty} Y(t) U^*(t - t_0) e^{j\Omega_d t} dt \right|. \quad (9)$$

It must be remembered that the quantity $Y(t)$ represents the sum of the complex amplitudes of signal and noise

$$Y(t) = U(t - t_0) e^{-j\Omega_d t} + N(t), \quad (10)$$

where t_{z0} and Ω_{d0} are the true lag time and Doppler frequency of the useful signal (at the moment $t = 0$).

In order to decide on the presence of a target, it is necessary to compare for every pair of expected values t_z and Ω_d the quantity $Z = Z(t_z, \Omega_d)$ with a certain threshold level. If the threshold is exceeded for any range of the values t_z and Ω_d , the presence of a target is assumed. For the evaluation of the true values of the measured parameters those values of t_z and Ω_d are then used for which the magnitude of Z is a maximum. The operations which are essential for the computation can be carried out automatically, by means of correlators or optimum filters or both simultaneously.

Depending on the actual signal shape, the degree of accuracy of the estimation of the lag time and Doppler frequency will differ. For some signals the function $Z(t_z, \Omega_d)$ will be more smooth, for others it will have a sharp peak. If noise is present, the measurement in the first case will not be very accurate, in the second case it will have a considerably greater accuracy. This function characterizes not only the measurement accuracy but also the resolving power with respect to

distance and speed.*

The problem is to determine the properties of the function $Z(t_z, \Omega_d)$ for signals with different shape, which will be referred to in the following as ambiguity function.

§7.2. AMBIGUITY FUNCTION AND NORMALIZATION OF THE AMBIGUITY FUNCTION

We transform the expression [(9) §7.1] for the function $Z(t_z, \Omega_d)$ by substituting in it [(10) §7.1] as has been done in chapter 6:

$$Z(t_z, \Omega_d) = |Z_c(t_z, \Omega_d) + Z_n(t_z, \Omega_d)|. \quad (1)$$

Here

$$Z_c(t_z, \Omega_d) = \frac{1}{2} \int_{-\infty}^{\infty} U(t - t_{z0}) U^*(t - t_z) e^{j(\Omega_d - \Omega_{d0})t} dt, \quad (2)$$

$$Z_n(t_z, \Omega_d) = \frac{1}{2} \int_{-\infty}^{\infty} N(t) U^*(t - t_z) e^{j\Omega_d t} dt. \quad (3)$$

In the relation (2) we carry out a substitution of the variables

$$\left. \begin{aligned} t_z &= t_{z0} + \tau, \\ \Omega_d &= \Omega_{d0} + 2\pi F, \end{aligned} \right\} \quad (4)$$

and examine the functions

$$\Psi(\tau, F) = |Z_c(t_{z0} + \tau, \Omega_{d0} + 2\pi F)|, \quad (5)$$

$$\rho(\tau, F) = \frac{\Psi(\tau, F)}{\Psi(0, 0)}. \quad (6)$$

The functions $\Psi(\tau, F)$ and $\rho(\tau, F)$, calculated for signals of different shape, we shall term ambiguity functions and normalized ambiguity functions, respectively, of these signals. In place of the term ambiguity function, the term auto-correlation function of the signal (sometimes modulation correlation function) is also used.

Using the relations (2), (5), we have

$$\Psi(\tau, F) = \left| \frac{1}{2} \int_{-\infty}^{\infty} U(t - t_{z0}) U^*(t - t_{z0} - \tau) e^{j2\pi Ft} dt \right|.$$

After substitution of the variables $t = t_{z0} + s$ and substitution of

$|e^{j2\pi Ft}| = 1$ it becomes obvious that the function $\Psi(\tau, F)$ is independent of the initial values t_{z0} and Ω_{d0} :

$$\Psi(\tau, F) = \left| \frac{1}{2} \int_{-\infty}^{\infty} U(s) U^*(s - \tau) e^{j2\pi F s} ds \right|. \quad (7)$$

The ambiguity function $\Psi(\tau, F)$ has the important property of central symmetry

$$\Psi(-\tau, -F) = \Psi(\tau, F). \quad (8)$$

This can be verified by replacing in (7) $-\tau$ for τ , $-F$ for F and substituting the variables $t = s + \tau$. Nothing that $|e^{j2\pi F \tau}| = 1$, we obtain

$$\Psi(-\tau, -F) = \left| \frac{1}{2} \int_{-\infty}^{\infty} U(t - \tau) U^*(t) e^{-j2\pi F t} dt \right|. \quad (9)$$

The right parts of the equations (9) and (7) are identically equal as modules of complex conjugate expressions, which leads to formula (8).

The normalized ambiguity function $\rho(\tau, F)$ is determined by the relation (6) and in correspondence with (7) assumes the form

$$\rho(\tau, F) = \frac{\left| \int_{-\infty}^{\infty} U(s) U^*(s - \tau) e^{j2\pi F s} ds \right|}{\int_{-\infty}^{\infty} |U(s)|^2 ds}. \quad (10)$$

The normalized ambiguity function $\rho(\tau, F)$ also has the property of central symmetry

$$\rho(-\tau, -F) = \rho(\tau, F). \quad (11)$$

In addition to the normalized ambiguity function $\rho(\tau, F)$, the normalized ambiguity function $\rho^2(\tau, F)$ is used sometimes. The values of this function do not exceed $\rho^2(0, 0) = 1$, and it also has the property of symmetry, i.e., $\rho^2(-\tau, -F) = \rho^2(\tau, F)$. As will be shown in §7.4, the function $\rho^2(\tau, F)$ has one very important property and its study is thus of special interest.

§7.3. GRAPHIC REPRESENTATION OF THE AMBIGUITY FUNCTIONS $\rho(\tau, F)$ and $\rho^2(\tau, F)$

In the Cartesian system of ρ , τ and F coordinates, the ambiguity function $\rho(\tau, F)$ is represented in the form of a surface. Such a surface for the radio pulse with bell shape and constant instantaneous frequency is shown in Fig. 7.1. In this special case, we have not only $\rho(-\tau, -F) = \rho(\tau, F)$ but also $\rho(-\tau, F) = \rho(\tau, F)$.

We shall term the surface corresponding to the ambiguity function, ambiguity surface. The geometrical solid bounded by the surface $\rho = 0$ and the ambiguity surface, we shall term ambiguity solid.

The ambiguity surfaces and solids can be constructed not only for the functions $\rho(\tau, F)$ but also for the functions $\rho^2(\tau, F)$ (in the latter case it is preferable to use the Cartesian coordinates system ρ^2 , τ , F). The form of the ambiguity solid $\rho(\tau, F)$ or $\rho^2(\tau, F)$ depends only on the signal shape.

It is important that during the construction of the ambiguity solid the noise term in formula [(1), §7.2] is excluded. If it were retained, the form of the ambiguity solid would be altered upon transition from one actual noise to another. At the same time one would also observe a displacement of the apex of the solid, or, with sufficiently intense noise, the appearance of false apices. However, if the ratio of the spectral noise density to the signal energy is fixed and sufficiently small, the nature of the ambiguity solid in the absence of noise has the decisive influence on the accuracy of the parameter measurement. The more concentrated the ambiguity body is along the axis τ , the more accurately can the lag time and the distance to the target be measured. The more concentrated the ambiguity solid is along the axis F , the more accurately can the Doppler frequency and the radial velocity of the relative motion of the target be measured.

Hence when we study the influence of the signal form on the accuracy of measurement of the parameters, we shall be interested in ambiguity solids, plotted without taking the noise term into account in formula [(1) §7.2]. The latter is analogous to the replacement of the quantity $Z(\alpha)$ by $Z_s(\alpha)$ in §6.5.

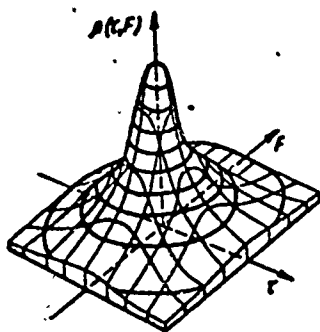


Fig. 7.1. Example of ambiguity surface and solid (case of bell-shaped radio pulse with constant instantaneous oscillation frequency).

In addition to the clinographic representation ambiguity solids one can use the representation of their outline by means of equal-level lines as is done, for example, in topography. Such a representation for the solid shown in Fig.

7.1 is given in Fig. 7.2, where the projections of the constant level lines $\rho = \text{const}$ (or $\rho^2 = \text{const}$) are drawn on the plane τ, F . In this case only the two

lines of equal level $\rho = 0.5$ and $\rho = 0.1$

have been drawn. The region encompassed by the lines $\rho = 0.5$ for which $\rho > 0.5$, is regarded as a "high correlation" region of the received and expected signals. This region is shown in black in the diagram. The region $0.1 < \rho < 0.5$ can be considered as a "low correlation" region and is shown in the diagram by shading. The area of the received and expected signals with zero correlation has been left without shading or darkening. The outline of the ambiguity solid is thus represented by three level gradations forming the ambiguity diagram.

The number of gradations can be increased, but there is no need for this in a qualitative analysis. Hence we shall limit ourselves in the following to the use of three gradations.

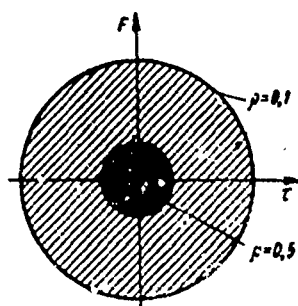


Fig. 7.2. Standard representation of the outline of the ambiguity solid means of level grading.

§7.4. VOLUME OF THE AMBIGUITY SOLID $\rho^2(\tau, F)$

It follows from the preceding discussion that it is sufficient for the simultaneous decrease in the indeterminacy of the metering of the lag time and Doppler frequency that the ambiguity solid has the form of a sharp peak in the vicinity of the values $\tau = 0$ and $F = 0$. Of interest in this connection is the magnitude of the volume V_ρ or V_{ρ^2} of the ambiguity solid $\tau(\tau, F)$ or $\rho^2(\tau, F)$ and the dependence of the form of these solids on the signal shape.

Of the quantities V_ρ and V_{ρ^2} we shall be interested in the following only in V_{ρ^2} , which is defined by the simple relation

$$V_{\rho^2} = \int_{-\infty}^{\infty} \int_{-\infty}^{\infty} \rho^2(\tau, F) d\tau dF. \quad (1)$$

It is found that the volume of the ambiguity solid V_{ρ^2} is a quantity which does not depend on the signal duration or on the law of modulation of its amplitude or phase. This quantity is equal to unity for any signal.

This can be proved by direct calculation of the volume V_{ρ^2} . By substituting in (1) the quantity $\rho^2(\tau, F)$ from [(10) §7.2], taking into account the obvious relationship

$$|\int A(s) ds|^2 = \int A(s) ds \int A^*(u) du = \int \int A(s) A^*(u) ds du,$$

in which the right side no longer contains the module sign, we obtain

$$V_p \left[\int_{-\infty}^{\infty} |U(s)|^2 ds \right]^2 = \\ = \int_{-\infty}^{\infty} \int_{-\infty}^{\infty} \int_{-\infty}^{\infty} \int_{-\infty}^{\infty} U(s) U^*(s-\tau) U^*(u) U(u-\tau) e^{j2\pi F(s-u)} \times \\ \times ds du d\tau dF,$$

where the integral over F is reduced to the delta function.

$$\int_{-\infty}^{\infty} e^{j2\pi F(s-u)} dF = \delta(s-u).$$

Using the properties of the delta function, we find

$$V_p \left[\int_{-\infty}^{\infty} |U(s)|^2 ds \right]^2 = \\ = \int_{-\infty}^{\infty} \int_{-\infty}^{\infty} \int_{-\infty}^{\infty} U(s) U^*(s-\tau) U^*(u) U(u-\tau) \delta(s-u) ds du d\tau = \\ = \int_{-\infty}^{\infty} \int_{-\infty}^{\infty} U(u) U^*(u-\tau) U^*(u) U(u-\tau) du d\tau.$$

Integration over τ within infinite limits gives

$$\int_{-\infty}^{\infty} U(u-\tau) U(u-\tau) d\tau = \int_{-\infty}^{\infty} |U(u-\tau)|^2 d\tau = \\ = \int_{-\infty}^{\infty} |U(s)|^2 ds,$$

hence

$$V_p \left[\int_{-\infty}^{\infty} |U(s)|^2 ds \right]^2 = \\ = \int_{-\infty}^{\infty} |U(u)|^2 du \int_{-\infty}^{\infty} |U(s)|^2 ds = \left[\int_{-\infty}^{\infty} |U(s)|^2 ds \right]^2$$

or

$$V_p = 1. \quad (2)$$

Because no limitations have been imposed on the form of the function $U(t)$ in the derivation of the relation (2), it holds true for any signal shape.

The relation (2) is a rigorous mathematical formulation of the indeterminacy principle in radio location, according to which the volume

of the ambiguity solid V_{ρ_2} cannot be altered by any method of modulation. This solid is like a heap of sand: by altering the form of the signal, we alter the shape of the heap "but cannot get rid of a single grain of sand" [15].

It is important that with unit volume of the ambiguity solid, its height does not exceed unity. Hence, if we compress the ambiguity solid along the axis τ , it flattens out along the axis F ; if we compress it along the axis F , it will inevitably flatten out along the axis τ .

If it is required, for example, to have a narrow peak of the ambiguity solid at the origin of the coordinates $\tau = 0$ and $F = 0$, the entire remaining volume must be distributed along the plane τ, F in the form of a series of peaks or in a thin layer on a large area.

§7.5. CROSS SECTION OF AMBIGUITY SOLIDS AND CHARACTERISTICS OF OPTIMUM RECEPTION CIRCUITS

Among the basic circuits for the optimum reception of a signal with random initial phase are the correlators and optimum filters, for the given signal form. Several important characteristics of these circuits are closely connected with the ambiguity solids of the corresponding signals.

In the correlation circuit (Fig. 4.2) with two quadrature channels the received oscillation $y(t)$ and the 90° phaseshifted reference oscillations $x_1(t)$ and $x_2(t)$ are fed into the multiplier of these channels. If a signal with the parameters $t_z \Omega_d$ is expected, then

$$x_{1,2}(t) = \pm U(t - t_s) \frac{\cos}{\sin} [(\omega_s - \Omega_s)t + \varphi(t - t_s)].$$

applies. Depending on the adopted realization of $y(t)$ the fully determined voltage

$$z = \sqrt{z_1^2 + z_2^2},$$

is produced at the output of the circuit, which is expressed by complex

amplitudes in accordance with the relation [(9) §7.1].

The performance of the circuit can be evaluated by supplying its input with oscillations without noise with the parameters t_{z0} and Ω_{d0} , which are generally different from t_z and Ω_d . The initial phase of the oscillations may be random, because it does not affect the output. With an accuracy limited by a factor which depends on the amplitude of the supplied oscillation, the output effect is characterized by the quantity

$$Z = \left| \frac{1}{2} \int_{-\infty}^{\infty} U(t-t_{z0}) U^*(t-t_z) e^{i(\Omega_d - \Omega_{d0})t} dt \right|.$$

This is nothing but the value of the ambiguity function calculated for fixed maladjustments of the parameters $\tau = t_z - t_{z0}$ and $2\pi F = \Omega_d - \Omega_{d0}$ supplied to the input of the circuit and the reference oscillations.

Hence the ambiguity solid $\rho(\tau, F)$ of the signal characterizes the dependence of the output effect for its optimum correlation circuit on the misadjustment of the two parameters.

If one of the maladjustments is fixed, the dependence of the output effect on the other is characterized by a curve which is a cross section of the surface of the solid by a plane. Fig. 7.3. shows the curves ρ as a function of τ at $F = \text{const}$, which are cross sections of the surface $\rho(\tau, F)$ by the planes $F = \text{const}$. Figure 7.4 shows the curves ρ as a function of F at $\tau = \text{const}$ which are cross section of the surface of the solid by planes $\tau = \text{const}$.

In contrast to the correlator, the output voltage of the optimum filter is described by the time function $w(t)$ and not by the single numerical value Z . The performance of the filter is naturally characterized by the shape of the envelope of the output voltage in the absence of noise for different values of Ω_d and Ω_{d0} of the expected and received

Doppler frequency. By virtue of [(12) §4.6] we have for the envelope

$$W(t) = \left| \frac{1}{2} \int_{-\infty}^{\infty} Y(s) V(t-s) ds \right|. \quad (1)$$

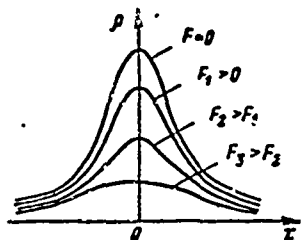


Fig. 7.3. Cross section of the ambiguity solid by the planes $F = \text{const.}$

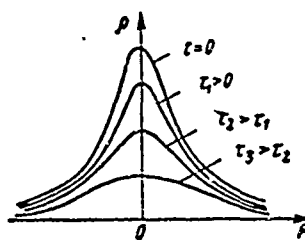


Fig. 7.4. Cross section of the ambiguity solid by the planes $\tau = \text{const.}$

In analogy to [(5) §4.6] we find the magnitude of $V(t) = V_{\text{opt}}(t)$ by means of the relation

$$\text{Re}[V_{\text{opt}}(t) e^{j\omega_d t}] = \text{Re}[CU^*(t_0 - t) e^{-j(\omega_0 - \Omega_d)(t_0 - t)}],$$

where ω_0 in the right part of the equation has been replaced by $\omega_0 - \Omega_d$.

Hence

$$V_{\text{opt}}(t) = CU^*(t_0 - t) e^{j[\Omega_d(t_0 - t) - \omega_d t]}. \quad (2)$$

Considering that the input of the filter is acted on by a signal without noise with a lag time t_{z0} and the Doppler correction Ω_{d0} , we have

$$\text{Re}[Y(t) e^{j\omega_d t}] = \text{Re}[U(t - t_{z0}) e^{j(\omega_0 - \Omega_{d0})t}],$$

hence

$$Y(t) = U(t - t_{z0}) e^{-j\Omega_{d0} t}. \quad (3)$$

By substituting (2) and (3) into (1) and noting that

$$|e^{j[\Omega_d(t_0 - t) - \omega_d t]}| = 1,$$

we find

$$W(t) = \frac{1}{2} C \left| \int_{-\infty}^{\infty} U(s-t_{z0}) U^*(s-t+t_0) e^{j(\omega_A - \omega_{A0})s} ds \right|. \quad (4)$$

After substitution of the variables $s = t_{z0} + \theta$ we obtain

$$W(t) = \frac{1}{2} C \left| \int_{-\infty}^{\infty} U(\theta) U^*(\theta - t + t_{z0} + t_0) e^{j(\omega_A - \omega_{A0})\theta} d\theta \right|$$

or

$$W(t) = C \Psi(t - t_{z0} - t_0, F). \quad (5)$$

The relation (5) indicates that the shape of the signal envelope at the optimum filter output in the absence of noise is described by the cross section of the ambiguity solid in the plane $F = \text{const}$, corresponding to the given difference F of the true and expected Doppler frequencies. The greater the true lag time t_{z0} the later appears the maximum of the voltage envelope at the filter output.

In the absence of a frequency separation of F , the maximum of the voltage envelope corresponds to the moment of time $t_{z0} + t_0$, and the envelope itself is determined by the cross section $F = 0$. The more distant the target, the later the pulse at the filter output appears (Fig. 7.5). With frequency separation of F the shape of the pulse envelope generally changes because the filter becomes non-optimum, the maximum of the envelope is decreased and its displacement is possible (dotted line in Fig. 7.5).

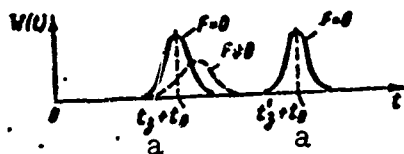


Fig. 7.5. Voltage envelope at the output of the optimum filter for different values of lag time and Doppler frequency. a) z.

§7.6. AMBIGUITY SOLID OF A RECTANGULAR RADIO PULSE WITH CONSTANT INSTANTANEOUS OSCILLATION FREQUENCY

As a first example, let us calculate and analyze the ambiguity solid for the radio pulse $u(t) = \text{Re}[U(t)e^{j2\pi ft}]$ with the rectangular envelope

$$U(t) = U(t) = \begin{cases} 1, & \text{if } 0 \leq t \leq \tau_R, \\ 0, & \text{if } t < 0 \text{ or } t > \tau_R. \end{cases} \quad (1)$$

For the calculation of the normalized ambiguity function we use the formula [(10) §7.2]. Noting that the denominator in this formula is τ_1 , we find

$$\rho(\tau, F) = \frac{1}{\tau_R} \left| \int_{-\infty}^{\infty} U(s) U^*(s - \tau) e^{j2\pi F s} ds \right|. \quad (2)$$

When we calculate the definite integral (2), like in the conclusion [(16) §4.6] we consider the following four cases separately:

a) $\tau < -\tau_R$; b) $-\tau_R \leq \tau < 0$; c) $0 \leq \tau \leq \tau_R$; d) $\tau \geq \tau_R$.

The diagrams for the shifted cofactors $U(s)$, $U(s - \tau)$ and their derivatives are shown in Fig. 7.6.

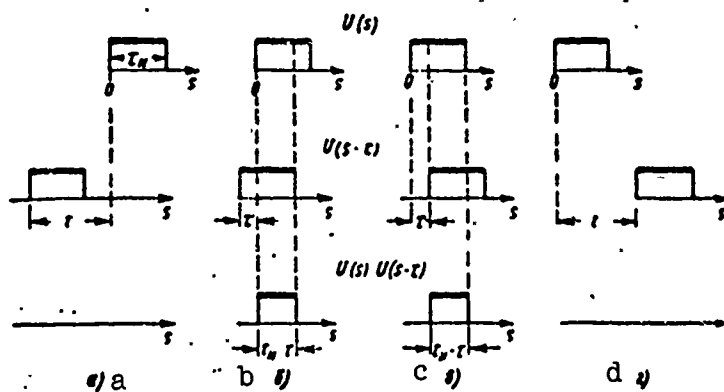


Fig. 7.6. Explanation of the calculation of the normalized ambiguity function of a rectangular radio pulse with constant instantaneous oscillation frequency.

Combining the results for the cases "a" and "d" we have

$$\rho(\tau, F) = 0 \text{ for } |\tau| > \tau_u.$$

For the cases $-\tau_1 \leq \tau \leq 0$ and $0 \leq \tau \leq \tau_1$ we obtain, respectively

$$\rho(\tau, F) = \frac{1}{\tau_u} \left| \int_0^{\tau_u - |\tau|} e^{j2\pi Ft} dt \right| = \left| \frac{\sin \pi F(\tau_u - |\tau|)}{\pi F \tau_u} \right|,$$

$$\rho(\tau, F) = \frac{1}{\tau_u} \left| \int_0^{\tau_u} e^{j2\pi Ft} dt \right| = \left| \frac{\sin \pi F(\tau_u - \tau)}{\pi F \tau_u} \right|.$$

All these results can be combined in a single notation

$$\rho(\tau, F) = \begin{cases} \left| \frac{\sin \pi F(\tau_u - |\tau|)}{\pi F \tau_u} \right| & \text{for } |\tau| \leq \tau_u, \\ 0 & \text{for } |\tau| > \tau_u. \end{cases} \quad (3)$$

At $F = 0$ we must evaluate the indeterminacy in formula (3). Replacing for small values of F the sine by its argument, we obtain

$$\rho(\tau, 0) = \begin{cases} 1 - \frac{|\tau|}{\tau_u} & \text{for } |\tau| \leq \tau_u, \\ 0 & \text{for } |\tau| > \tau_u. \end{cases} \quad (4)$$

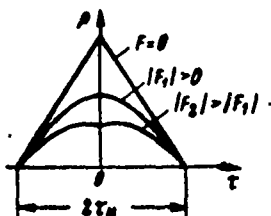


Fig. 7.7. Cross section along the planes $F = \text{const}$ of the ambiguity solid of a rectangular radio pulse with constant instantaneous oscillation frequency.

On the basis of these relationships, Fig. 7.7. shows ρ as a function of τ for different $F = \text{const}$. These may be regarded as voltage envelope curves at the output of the optimum filter at a frequency separation of F in the carrier frequency. The detuning results in a decrease in the peak value and a distortion of the shape of the envelope.

Figure 7.8 shows the corresponding relationships, giving ρ as a function of F for different $\tau = \text{const}$.

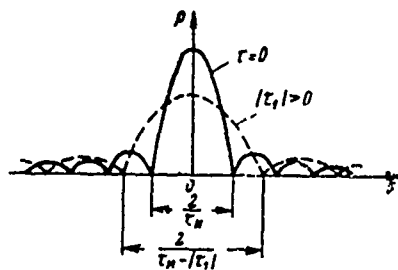


Fig. 7.8. Cross section along the planes $\tau = \text{const.}$ of the ambiguity solid of a rectangular radio pulse with constant instantaneous oscillation frequency.

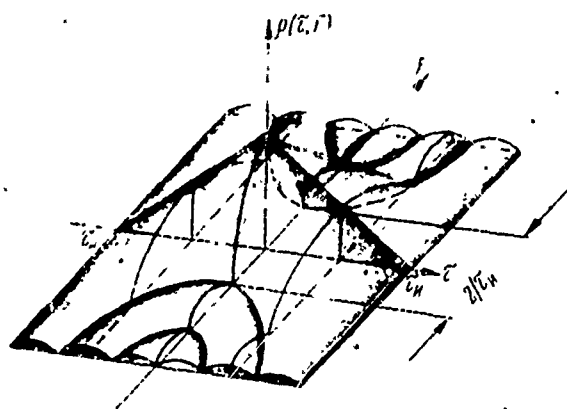


Fig. 7.9. Contour of the ambiguity solid of a rectangular radio pulse with constant instantaneous oscillation frequency.

Each of these curves corresponds to the spectrum of a rectangular video pulse with a duration of $\tau_H - |\tau|$.

Both series of curves can be regarded as cross section of the surface of an ambiguity solid (Fig. 7.9) by the surfaces $\tau = \text{const}$ and $F = \text{const}$. Representations of the ambiguity solid by means of level gradations for two different durations of the main pulse are shown in Fig. 7.10 and 7.11. Compression of the ambiguity solid along the axis

τ causes a spreading along the axis F and vice versa.

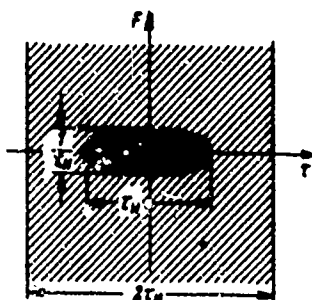


Fig. 7.10. Standard representation of the contour of the ambiguity solid of a rectangular radio pulse with constant instantaneous oscillation frequency.

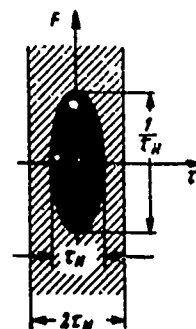


Fig. 7.11. Standard representation of the contour of the ambiguity solid at a pulse duration τ_1 which is shorter than in Fig. 7.10.

§7.7. AMBIGUITY SOLID OF A RECTANGULAR RADIO PULSE WITH LINEAR MODULATION OF THE OSCILLATION FREQUENCY

Let us now pass on to the radio pulse (Fig. 7.12) with linear modulation of the high-frequency oscillation $u(t) = \text{Re}[U(t)e^{j2\pi f t}]$, having a complex amplitude

$$U(t) = \begin{cases} e^{jbt}, & \text{if } 0 \leq t \leq \tau_n, \\ 0, & \text{if } t < 0 \text{ or } t > \tau_n. \end{cases} \quad (1)$$

The instantaneous frequency of such a pulse

$$f = \frac{1}{2\pi} \frac{d}{dt} (2\pi f_0 t + bt^2)$$

varies linearly from f_0 at $t = 0$ to $f_0 + \Delta f = f_0 + b\tau_n$ at $t = \tau_n$, where Δf is the frequency deviation.

The coefficient b in the formula (1) is thus expressed via the frequency deviation Δf and the duration τ_n of the pulse:

$$b = \frac{\pi \Delta f}{\tau_n}. \quad (2)$$

The calculation of $\rho(\tau, F)$ by means of formula [(10) §7.2] we shall carry out by using the diagrams in Fig. 7.6, because the envelope

remains rectangular. As in the preceding case, $\rho(\tau, F) = 0$ at $|\tau| > \tau_n$.

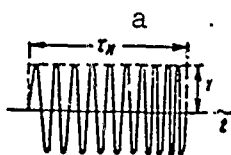
At $-\tau_n < \tau < 0$ and $0 < \tau < \tau_n$, respectively, we obtain

$$\begin{aligned} \rho(\tau, F) &= \frac{1}{\tau_n} \left| \int_0^{\tau_n - |\tau|} e^{j(b\tau - b(t-\tau)^2 + 2\pi F t)} dt \right| = \\ &= \left| \frac{\sin[(b\tau + \pi F)(\tau_n - |\tau|)]}{(b\tau + \pi F)\tau_n} \right|, \\ \rho(\tau, F) &= \frac{1}{\tau_n} \left| \int_{\tau}^{\tau_n} e^{j(b\tau - b(t-\tau)^2 + 2\pi F t)} dt \right| = \\ &= \left| \frac{\sin[(b\tau + \pi F)(\tau_n - \tau)]}{(b\tau + \pi F)\tau_n} \right|. \end{aligned}$$

Combining the results thus obtained and using the relation (2), we find

$$\rho(\tau, F) = \begin{cases} \left| \frac{\sin \left[\pi \left(F + \Delta f \frac{\tau}{\tau_n} \right) (\tau_n - |\tau|) \right]}{\pi \left(F + \Delta f \frac{\tau}{\tau_n} \right) \tau_n} \right| & \text{for } |\tau| \leq \tau_n, \\ 0 & \text{for } |\tau| > \tau_n. \end{cases} \quad (3)$$

Fig. 7.12 Rectangular radio pulse with linear oscillation - frequency modulation. a) i.



On the basis of the relations (3),

Fig. 7.13 is a plot of ρ as a function of τ for two values $F = \text{const}$, each of which can be regarded as the voltage envelope at the output of the optimum filter with detuning of F with regard to the carrier frequency.

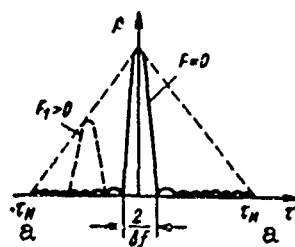


Fig. 7.13. Cross section along the planes $F = \text{const}$ of the ambiguity solid of a rectangular radio pulse with linear oscillation frequency modulation. a) i.

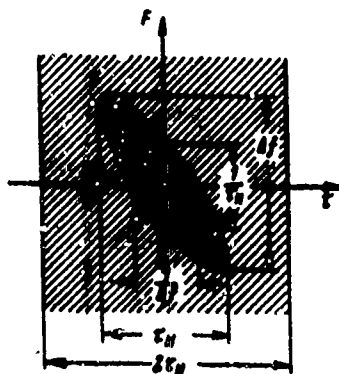


Fig. 7.14. Standard representation of the contour of the ambiguity solid of a rectangular radio pulse with linear oscillation frequency modulation. a) 1.

Figure 7.14 shows a representation of the ambiguity solid by means of level gradations. It is evident from a comparison with Fig. 7.11 that the ambiguity solid of a frequency-modulated radio pulse is rotated relative to the ambiguity solid of a radio pulse without frequency modulation by a certain angle, whose magnitude increases with increase in the frequency deviation Δf .

Let us examine the cross section of the ambiguity solid along the plane $F = \text{const}$ which characterizes the voltage envelope at the output of the optimum filter. This envelope is considerably more narrow than the envelope of the main pulse. At zero separation $F = 0$ and the condition $\Delta f \tau_H \gg 1$, the width of the compressed pulse at zero is $2/\Delta f$.

It can be seen in Fig. 7.13 that a shifting of the compressed pulses in time is possible at the frequency separation F . In absolute magnitude this shift is $\Delta \tau = \frac{\tau_H F}{\Delta f}$ and characterizes the velocity error in the measurement of the lag time at the moment when the main pulse begins to sweep the target. Velocity errors are typical for any processing which amounts to taking the correlation integral. If $\tau_1 F_{\max} \ll \ll 1$ the shift is considerably less than the half width $1/\Delta f$ of the

compressed pulse and is thus not of any importance.*

§7.8. AMBIGUITY SOLID OF COHERENT PACKETS OF

One of the most widely used radar signals is a signal in the form of a coherent packet of radio pulses. As an example let us consider a packet with a rectangular envelope (Fig. 7.15, a). In this diagram τ_1 is the duration of each pulse; T is their repetition interval, and M , the number of pulses in a packet.

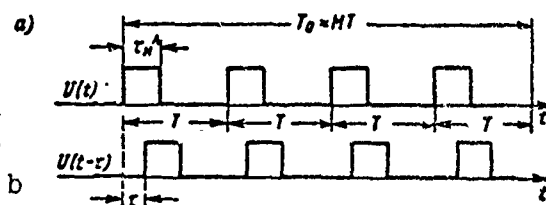


Fig. 7.15. Explanation for the analysis of the convolution integral in the plotting of the ambiguity solid of a rectangular coherent packet of radio pulses. 1) 1.

Let us determine the nature of the surface of the ambiguity solid

$$\rho(\tau, F) = \frac{1}{M\tau_1} \left| \int_{-\infty}^{\infty} U(t) U^*(t-\tau) e^{j2\pi Ft} dt \right|, \quad (1)$$

limiting ourselves to a qualitative analysis of the relation (1) and Fig. 7.15. We shall give special attention to a packet without modulation of the phase or frequency of the carrier.

If the signals $U(t)$ and $U(t-\tau)$ are shifted by the time $|\tau| > T_0 = MT$, the function $\rho(\tau, F)$ will be zero. The same happens when $|\tau| < T_0$, but the pulses of the shifted packets do not overlap.

Within the limits $-T_0 < \tau < T_0$ the ambiguity solid possesses a series of peaks with a width of $2\tau_1$ along the axis τ , which are shifted by the pulse packet period T . At $F = 0$ every peak of the packet and the envelope of these peaks have a triangular shape (Fig. 7.16) which can easily be proved.

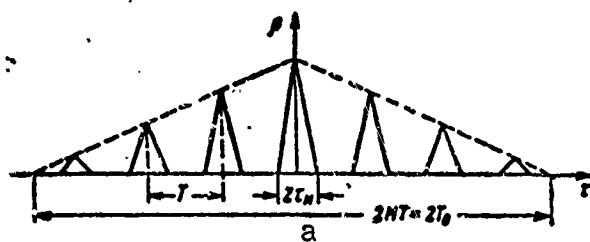


Fig. 7.16. Cross section along the plane $F = 0$ of the ambiguity solid of a rectangular coherent train of radio pulses with constant instantaneous oscillation frequency. a) 1.

The presence of a large number of peaks of the function $\rho(\tau, F)$ along the axis τ can lead to an ambiguity in the distance measurement. However, if the period of the pulse packet $T > t_z$ maks, the ambiguity is eliminated.

Let us consider the behavior of the function $\rho(\tau, F)$ along the axis F . At $\tau = \text{const}$, the function $\rho(\tau, F)$ is the modulus of the Fourier transformation of the product $U(t)U(t - \tau)$. If $\tau \neq 0$ this product coincides within the accuracy of a factor with the signal envelope $U(t)$ and, consequently, the function $\rho(\tau, F)$ describes its amplitude-frequency spectrum.

As we know, the spectrum of the envelope of a packet of radio pulses consists of several peaks which correspond to frequencies which are multiples of the packet frequency $F_{\pi} = 1/T$. The width of each peak at zero is determined by the duration of the packet and is equal to $2/T_0$, while the width of the peak envelope is determined by the duration of a single pulse and is equal to $2/\tau_1$.

Thus, along the axis F at $\tau = 0$, the ambiguity function also consists of a large number of peaks (Fig. 7.17). The same will be the case at $|\tau| = T, |\tau| = 2T$, etc.

The presence of a large number of peaks along the axis F can result in an ambiguity of the measurement of the radial velocity of the

target, if the maximum Doppler frequency is greater than the recurrence frequency of the pulses.

The ambiguity solid of a coherent packet of radio pulses without frequency modulation consists of a number of relatively narrow peaks, distributed along the axis τ as well as the axis F . Its contour is shown in Fig. 7.18; by means of three level gradations. Because the volume of the ambiguity solid $V_{\rho_2} = \text{const}$, the volume of each peak decreases in inverse proportion to their total number but the ambiguity of the target distance and velocity reading remains. This ambiguity can be eliminated by a priori data ($\tau < \tau_{\text{max}}$, $F < F_{\text{max}}$) or as a result of later processing of the radar information.

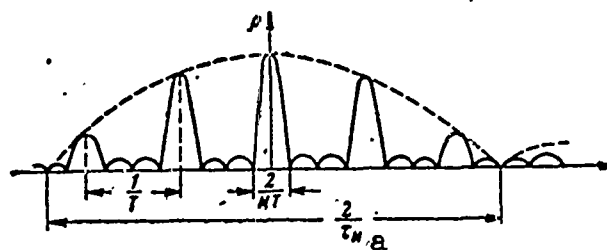


Fig. 7.17. Cross section by the plane $\tau = 0$ of the ambiguity solid of a rectangular coherent packet of radio pulses with constant instantaneous oscillation frequency $\tau = 0$. a) 1.

For a coherent packet of frequency modulated radio pulses the blackened regions of high correlation are slightly sloped (analogous to Fig. 7.14) remaining on the shaded vertical bands of Fig. 7.18. If the frequency deviation Δf is sufficiently large, the slope within the represented section of the axis F is negligible. The length of the peaks along the axis τ then is no longer τ_1 , but $\frac{1}{\Delta f} \ll \tau_n$ (as in Fig. 7.14). Compared with Fig. 7.14 the ambiguity solid is divided into narrower peaks which reduces the ambiguity with respect to τ .

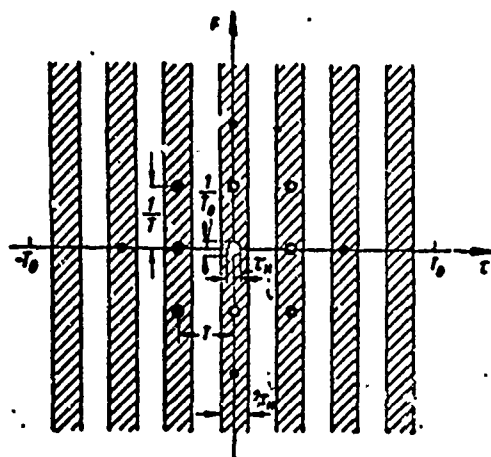


Fig. 7.18. Standard representation of the contour of the ambiguity solid of a coherent packet of radio pulses with constant instantaneous oscillation frequency. a) 1.

§7.9. AMBIGUITY SOLID OF A NOISELIKE SIGNAL

In addition to the splitting up of the ambiguity solid into a multiplicity of narrow peaks, another form of its modification is of interest. The ambiguity solid is compressed into a sharp peak with a single height with the apex at $\tau = 0$ and $F = 0$ and the remainder of the volume spread out over the maximum possible area of the plane τ, F (Fig. 7.19).

Substituting the volume of the ambiguity solid V_{ρ^2} by the sum of the volumina of the peak V_1 and the spread-out part V_2 , we obtain $V_s < 1$ from the condition $V_{\rho^2} = V_1 + V_2 = 1$.

If we could spread the ambiguity solid equally over the area of the rectangle $2\tau_s 2\Delta f$, then

$$V_s = 2\tau_s 2\Delta f \rho^2 < 1,$$

hence the height of the layer of the dispersed part of the volume is

$$\rho < \frac{1}{2\sqrt{\tau_s \Delta f}}. \quad (1)$$

The quantity τ_1 which enters into this formula, we can regard as

the total signal duration, and the quantity Δf as the width of its spectrum. These quantities determine the limits of the ambiguity solid. In fact, when the received and expected signals are shifted by more than $\pm \tau_1$, the function $\rho(\tau, F)$ vanishes; at a Doppler shift greater than the width of the spectrum, the correlation between the signals is also disturbed.

The above reasoning must be considered as approximate because not any signal can be simultaneously limited in time and in frequency. However, if the product $\tau_1 \Delta f$ is large. It is desirable that this product $\tau_1 \Delta f$ should be fairly large.

Let us discuss the possible methods of approximating this idealized pattern.

As has been previously established, a signal of the above considered type should, on the one hand, have a duration in time and, on the other, should extend over a wide band. The shifts of the signal parameters τ, F (relative to the expected) should in itself disintegrate the peak. A signal with linear frequency modulation, of a regular and relatively simple type, does not satisfy this requirement. While the time shift with such modulation destroys the peak, the corresponding frequency shift may re-establish it. In order to obtain an ambiguity solid as in Fig. 7.19, a certain randomness in the modulation law is necessary.

Such a randomness can be observed for the noise section with the duration τ_1 with a frequency band $\Delta f \gg \frac{1}{\tau_1}$. However, with a pure noise signal, it is hardly possible to achieve a constant level of ρ over the entire rectangle $2\tau_1 2\Delta f$ (with the exception of the peak). A pure noise signal also has a variable amplitude which is undesirable from the point of view of the performance of the generators at the optimum power level.

Hence the "noiselike" nature of the signal is preferably achieved by a regular phase change within the limits of the radio pulse, i.e., by nonlinear frequency modulation or phase manipulation.

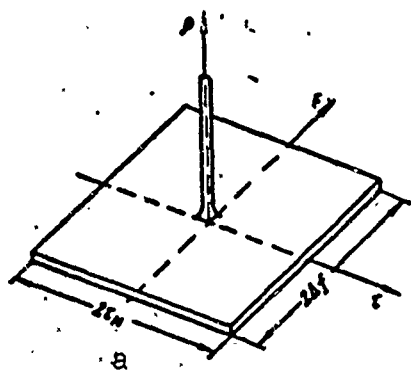


Fig. 7.19. Contour of the ambiguity solid of a noiselike signal. a) 1.

Special codes have been developed recently which enable an approximation to a noiselike signal to be achieved. Let the emitted signal consist (as in Fig. 5.11a) of closed rectangular radio pulses with a duration τ_0 with high-frequency oscillations

$$(-1)^{\xi_k} \cos 2\pi f_s t \quad (k=1, 2, 3, \dots), \quad (2)$$

where ξ_k assumes values of 0 or 1. The sequence of these figures ξ_k characterizes the law of the phase manipulation.

In order to obtain noiselike signals, the establishment of ξ_k codes by means of "logic algebra" (Boolean algebra) has been proposed. An example is the code described by the relation

$$\xi_k = \xi_{k-1} \oplus \xi_{k-2} \oplus \xi_{k-3} \oplus \xi_{k-4}, \quad (k \geq 5). \quad (3)$$

The symbol \oplus indicates "summation over the modulus two" which is defined by the following Table, where the values of the components are given in the upper line and left column and the result in the corresponding diagonals:

\oplus	0	1
0	0	1
1	1	0

i.e., $0 \oplus 0 = 0, 0 \oplus 1 = 1, 1 \oplus 0 = 1$ and $1 \oplus 1 = 0$. (The last relation corresponds to the clearing of the binary adder in connection with the transfer of the binary unit to the following discharge).

As example we assume $\xi_1 = \xi_2 = \xi_3 = \xi_4 = 0$, and $\xi_5 = 1$, and we obtain all the other values of ξ_k by using the formula (3). We then have

$$\xi_6 = \xi_1 \oplus \xi_2 \oplus \xi_3 \oplus \xi_4 = 1$$

etc. The corresponding code has the form

0000111001101111101000100101011.*

If the law on which the construction of the code is based, has been established correctly, then we obtain on the basis of m initial elements (in this example $m = 5$) a code consisting of $n = 2^m - 1$ elements ($n = 31$). The further application of the law for $k \geq n$ leads to a periodic repetition of the code elements. Such codes have been given the special designation zero sequence code with maximum duration or binary pseudorandom codes.

Although the noiselike signals have the desired structure of an ambiguity solid, they also have certain disadvantages. The same optimum filter, without division into channels, cannot eliminate noiselike signals which differ strongly in their Doppler frequency. In order to make the reception of such signals feasible, the scheme must be multi-channel.

Outside the peak the level ρ of the zero sequence code (at products $\tau_n \Delta f$ which are not too large) is relatively high. It is bigger, for example, than for a signal with linear frequency modulation. However, it decreases with increase of n , approximately as $1/\sqrt{n}$.

The noiselike signals must be distinguished from the phase-manipulated signals with lower residue level ($\rho = 1/n$) on the time axis τ with optimum processing. The latter are known up to $n = 13$ and can be used for the separation of frequencies $< \frac{1}{\tau} = \frac{1}{n\tau_0}$. An example of such a signal and its optimum processing is given in Figs. 5.11-5.13.

Because noiselike signals have a residue level which decreases only as $1/\sqrt{n}$, their use is rational only at a fairly large number of

elements n . For zero sequence codes a residue level $(20+30)$ db or $(1/\sqrt{n})^2 = 10^{-2} + 10^{-3}$ occurs only for $n = 2^m - 1 \gg (100+1000)$, i.e., at a number of elements of 127, 255, 511, 1023 and over. This circumstance causes great difficulties in the design of the optimum filter.

Hence modified pseudorandom codes have been proposed with a number of elements $n = 2^m$, characterized by the fact that the pulse characteristic of the filter for these codes can be designed by using only $m = \log_2 n$ delay lines without any additional branches. For $n = (128+1024)$ the number is $m = (7+10)$. The filter is built of single-type elements. Fig. 7.20 shows the system of one (the k th) element of such a filter. This element has two independent inputs and outputs and can be regarded as a six-pole network. Every element contains a delay line for the time $2^{k-1} \tau_0$ (where k is the number of the element and τ_0 the duration of the elementary code pulse) and two algebraic adding on circuits which give sum and difference.

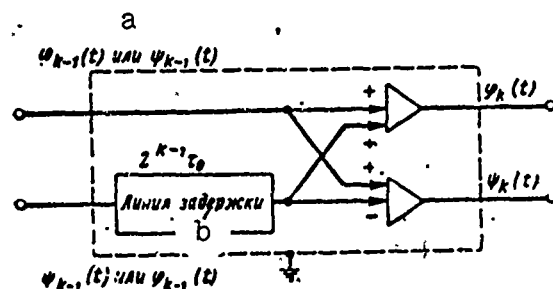


Fig. 7.20. Device of the k th element of the optimum filter for a modified pseudorandom code. a) or; b) delay line.

Let us connect the inputs of the first element ($k = 1$ and $2^{k-1} \tau_0 = \tau_0$) and supply them with a radio pulse of the duration τ_0 (Fig. 7.21 a).

At the output of the first and second adders we obtain two closed pulses of equal duration and respectively equal and different po-

larity (Fig. 7.21 b).

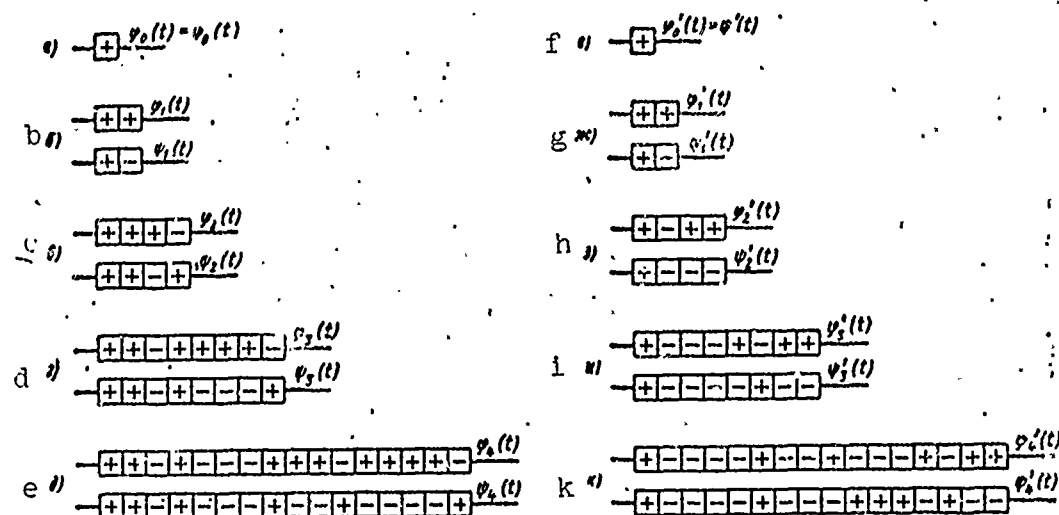


Fig. 7.21. Explanation of the performance of the optimum filter and the forming circuit for the modified pseudorandom code.

Let us supply these pulses to the second element.

Two methods of connection are possible: without inversion (upper output of the first to the upper input of the second, lower output of the first to the lower input of the second) and with inversion. Fig. 7.21, c describes the output voltages of the second element when the connection is made without inversion.

The output voltages of the second element with inversion or without inversion are fed into the third element, etc. Figs. 7.21, d and e describe the voltages at the outputs of the third and fourth elements in presence of inversion in both cases. The corresponding connection scheme four elements is shown in Fig. 7.22, a.

It is found that the elements of the same filter can be used for filtering as well as for the shaping of the main signal. This is useful because the generation and reception take place at different times. For the transition from one operating condition to the other it is suf-

efficient to carry out an additional inversion at the output of the first element and an additional inversion of the pickup from the last element. The corresponding voltages φ'_1 and ψ'_1 after such an inversion are shown in Fig. 7.21 f, g, h, i, k and the connection scheme for the elements in Fig. 7.22, b. It is readily seen that $\varphi_1(t) = -\psi'_1(-t)$ and $\psi_1(t) = \varphi'_1(-t)$, which confirms the possibility of using the elements of such a filter for transmission as well as reception.

§7.10. ON THE CONDITIONAL NATURE OF THE AMBIGUITY DIAGRAMS

The ambiguity diagrams which are examined in §7.1-7.9 were found under condition that the lag time and distance reading is carried out for the moment of time corresponding to beginning of the target sweep by the main pulse. However, not only the target position at the moment of the sweep may be of interest but also its position during the beginning of the sounding, the arrival of the reflected signal, the formation of the peak of the compressed pulse or at any other moment of time shifted any amount relatively to any of the above-indicated moments.

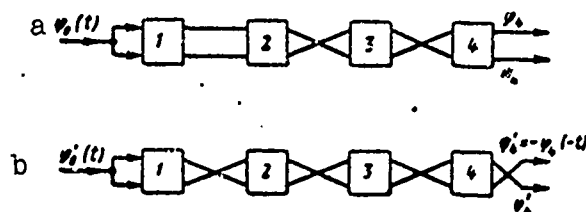


Fig. 7.22. Connection schemes for four modified pseudorandom code elements: a) operation as filter; b) operating as main signal former.

It is found that the ambiguity diagrams are modified thereby even if it is assumed that the target moves uniformly during the time interval between the sweep and the distance reading. This attests to the conditional nature of the ambiguity diagrams.

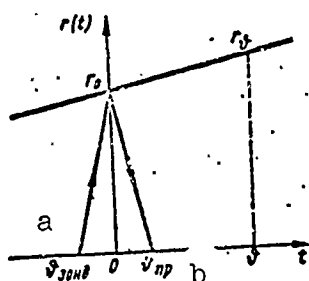


Fig. 7.23. Explanation of the shifting of the moment of distance reading. a) zond; b) pr.

Let us evaluate the possible modifications of the ambiguity diagrams due to the change in the moment of reading the distance to the target.

Fig. 7.23 shows a diagram of uniform target motion from the moment of the beginning of the sweep $t = 0$ to a certain moment $t = t$. Provisionally, without observing the velocity scale,

the diagram of the propagation of the radar signal is plotted, beginning with the moment of the start of the sounding $t_{\text{zond}} = -r_0/c$ to the moment of the beginning of the reception $t_{\text{pr}} = r_0/c$, where r_0 is the distance to target at the moment of the sweep.

Expressing the distance r_0 at the moment of the sweep $t = 0$ by the distance r_t at any arbitrary moment $t = t$, we have

$$r_0 = r_t - v \cdot t. \quad (1)$$

Multiplying the relation (1) by the factor $2/c$ and introducing the equivalent lag time $t_{z,t}$, corresponding to the distance to target r_t , we obtain

$$t_{z,t} = t_{z,0} - \frac{2}{c} v \cdot t. \quad (2)$$

We shall regard the pair of values $t_{z,t}$ and Ω_d as the expected values of the measured quantities (instead of t_z and Ω_d). Replacing in (2) the expected values by the true values, we have

$$t_{z,t} = t_{z,0} - \frac{2}{c} v \cdot t. \quad (3)$$

The signal part of the correlation integral for the simultaneous estimation of the quantities $t_{z,t}$ and Ω_d can be found without repeating the entire analysis of §7.1-7.2 in the following manner. Designating the new functional relationship $Z_c(t_{z,t}, \Omega_d)$ in analogy to the old one, we

obtain the expression for it by substituting the quantities t_z and t_{z0} in the right part of the equation [(2)§7.2] by their values (2), (3)

$$Z_0(t_{z0}, \Omega_{z0}) = \frac{1}{2} \int_{-\infty}^{\infty} U\left(t - t_{z0} + \frac{\theta}{\omega_0} \Omega_{z0}\right) \times \\ \times U^*\left(t - t_{z0} + \frac{\theta}{\omega_0} \Omega_{z0}\right) e^{i(\omega_0 t - \Omega_{z0} t)} dt. \quad (4)$$

Designating $t_{z0} = t_{z0} + \tau$ and $\Omega_{z0} = \Omega_{z0} + 2\pi F$, we introduce the ambiguity function of the pair of measured quantities t_{z0} and Ω_{z0} , namely

$$\Psi_0(\tau, F) = |Z_0(t_{z0} + \tau, \Omega_{z0} + 2\pi F)|. \quad (5)$$

Carrying out the substitution of the integration variable in (4), we find for the introduced function the following expression:

$$\Psi_0(\tau, F) = \left| \frac{1}{2} \int_{-\infty}^{\infty} U(s) U^*\left(s - \tau + \frac{\theta}{f_0} F\right) e^{i2\pi F s} ds \right|. \quad (6)$$

Comparing the new expression (6) with the expression found earlier [(7) §7.2] for the ambiguity function $\Psi(\tau, F)$ of the quantities t_z and Ω_d , we have

$$\Psi_0(\tau, F) = \Psi\left(\tau - \frac{\theta}{f_0} F, F\right). \quad (7)$$

In particular,

$$\Psi_0(0, 0) = \Psi(0, 0). \quad (8)$$

We divide termwise each of the parts of equation (7) by (8). Then we obtain an expression analogous to (7) for the normalized ambiguity function

$$\rho_0(\tau, F) = \rho\left(\tau - \frac{\theta}{f_0} F, F\right). \quad (9)$$

Using the expression (9) we estimate the effect of the variation of the moment of distance reading θ on the shape of the ambiguity solid.

Let the original ambiguity solid $\rho(\tau, F)$ be the ambiguity solid of a rectangular radio pulse with constant carrier (see Fig. 7.11). The transformation (9) slopes the ambiguity solid (at $\theta > 0$ in the clock-

wise direction).

The latter fact is easily explained by the following reasoning. Let the true, but not accurately known Doppler frequency be $\Omega_{d0} = 0$ (case of immobile target). The ambiguity (Fig. 7.11) permits the assumption $\Omega_k = \Omega_{d0} + 2\pi F > 0$, which corresponds to $v_r > 0$. At such a radial speed of the target the ambiguity section along τ , corresponding to the ordinate F , is shifted within the time δ to the side of the greater lag time by $\frac{2}{c} v_r \delta$ or $\frac{\delta}{f_0} F$. In an analogous manner we find that the section, corresponding to the ordinate $F < 0$, is displaced towards the left.

Of interest is the fact that the previously sloped diagrams $\rho(\tau, F)$ (Fig. 7.14) as a result of the additional sloping (9) can be straightened in some cases.

Manu-
script
Page
No.

[Footnotes]

- 209 See Appendix 3.
- 225 See also Appendix 2 and §7.10.
- 231 If we introduce $\eta_k = (-1)^k$, the coding operation in the considered example can be reduced to the use of the normal product $\eta_k = \eta_{k-1} \eta_{k-2} \eta_{k-3} \eta_{k-4} \eta_{k-5}$ ($k \geq 5$) at the initial condition $\eta_1 = \eta_2 = \eta_3 = \eta_4 = 1$ and $\eta_5 = -1$. The sequence η_k then has the form 1111-1-1-111.

[Transliterated Symbols]

- 206 $\tau = z = \text{zapazdyvaniye} = \text{lag time}$
- 207 $d = d = \text{dopplerovskaya} = \text{Doppler}$
- 217 $\text{opt} = \text{opt} = \text{optimal'nyy} = \text{optimum}$
- 219 $i = i = \text{impul's} = \text{pulse}$
- 227 $\text{maks} = \text{maks} = \text{maksimal'nyy} = \text{maximum}$

Manu-
script
Page
No.

235 . зонд = zond = zondirovaniye = sounding

235 пр = pr = priyem = reception.

Chapter 8

CONSECUTIVE REPEATED MEASUREMENTS

§8.1. SIMPLEST MODELS OF TARGET MOTION (MODELS WITH INDEPENDENT INCREMENTS)

In order to increase the measurement accuracy, the initial data can be obtained repeatedly. The more readings are taken, the less is normally the error scatter due to the influence of noise.

However, the measurement process always takes time, and during this time the quantity to be measured can vary. This may result in an additional error, which is usually termed dynamic error. In order to decrease this error, one must make use during the processing of the readings of certain hypotheses concerning the law of variation in time of the random quantity $\alpha = \alpha(t)$ which can be measured, or else, one must introduce a model of target motion. Optimisation of the processing then consists in ensuring the root mean square deviation of the selected motion model. Hence it is obvious that the choice of the target motion model is of great importance for the optimization of the processing.

We shall start out with the fact that the model, even though it is very rough, should take into account the special features of the target maneuvers and at the same time, without complicating the calculation, result in practically realizable solutions in terms of a circuit diagram. These requirements are satisfied by the statistical motion models with random and independent increments, on the basis of which the further analysis will be constructed.

Hence we shall introduce into the analysis the concept of increments of the true values of the measured quantity during the time between readings.

For a more concrete definition we shall assume that the distance to target is measured with a certain repetition period T (for example, T is equal to the scanning period of the station or, if the antenna is always aimed at the target, the pulsing period).*

The first increment of the measured quantity α (distance) during the time between readings we shall term the difference

$$\delta_m = \alpha_m - \alpha_{m-1}. \quad (1)$$

The first distance increment characterizes the radial speed of motion of the target, averaged for the time between readings.

The second increment of the measured quantity α we shall term the corresponding variation of the first increment

$$\gamma_m = \delta_m - \delta_{m-1}. \quad (2)$$

The second distance increment characterizes the acceleration of the target.

Figure 8.1 shows a possible diagram of the measured quantity α as a function of time for a maneuvering target. If the measurement is effected extremely rarely (Fig. 8.1, a) the connection between the discrete values of α_m is disturbed to such a degree that they can be regarded as independent random quantities. Hence the results of the previous readings cannot be used for improvement of the accuracy of the current estimate, i.e., the repeated measurement procedure does not give an accuracy advantage.

With more frequent measurements the scatter of the first increments δ_m decrease and the quantities α_m are no longer independent parameters. In this case the results of the previous measurements can be used for an improvement of the accuracy of the running estimate of

α_m^* . However, when the measurements are not too frequent, the increments δ_m vary from one reading to another in a random manner and they can be considered to be independent random quantities, which simplifies the analysis.

If the measurements are carried out often (Fig. 8.1, b) the connection between the successive values of the first increments must also be taken into account, i.e., the more or less smooth nature of the change in the rate of motion must be taken into account. This means that the δ_m are dependent quantities. At the same time, the second increments γ_m can still be considered to be independent random quantities.

Finally, at very frequent measurements one could also consider the gradual nature of the change of the acceleration, considering, for example, the third and also the fourth increments of the measured quantity as independent random quantities.

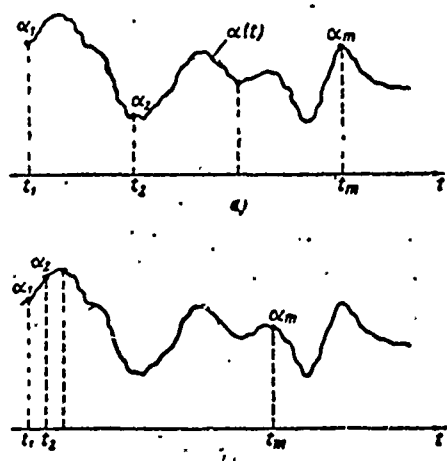


Fig. 8.1. Explanation of the nature of the increments of the measured quantity α at different recurrence frequency of the readings.

Models of motion with random and independent first and second increments naturally do not reflect all the peculiarities of the motion of a real target. Nonetheless they permit a considerable improvement of the results of processing for a maneuvering target as compared with a single measurement.

In the processing of the results of observations on non-maneuvering ballistic targets, the equation of their trajectory (see, for example, [35]) is used to increase the accuracy of numerous measurements as a model of motion.

Figures 8.2 and 8.3 present diagrams which characterize the possible laws of change of the quantity α_m for a motion model with independent first and second increments (thick lines). The scatter and mathematical expectation of the corresponding increments are considered to be invariant with time which characterizes their stationary nature. The mathematical expectations of the corresponding independent increments in this case are considered to be zero.

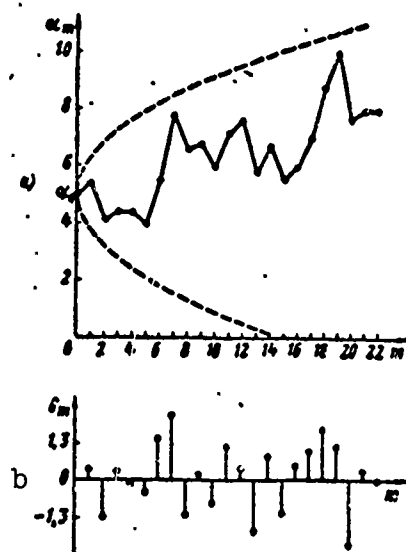


Fig. 8.2. One of the possible realizations of motion models with independent and stationary first increments: a) plot of the variation of the quantity α from one reading to the next; b) discrete values of δ_m of the first increments.

The motion model shown in Fig. 8.2 is convenient for very diverse laws of motion of an intermittent nature, one of which is shown in Fig. 8.2, a. The dotted lines in the same diagram shows the limits of the region within which the possible motion diagrams are situated with a probability of 0.8 on condition that the initial coordinate is α_0 , that the initial speed is characterized by the magnitude of the first increment, equal to zero, and that the scatter of the first increment at all points $D_{\delta_m} = 1$. The increase in the scatter α with time charac-

terizes the nonstationary nature of the discrete values of α_m (stationary are only the first increments δ_m).

The second motion model (Fig. 8.3), in contrast to the first, makes it possible to take into account the gradual nature of the change of the coordinate α , connected with the more smooth change of the first increments δ_m (of the speed). The limits of the corresponding regions for the same probability 0.8 in Fig. 8.3, a and b are indicated by a dotted line (on the basis of the known initial coordinate α_0 , the initial first increment $\delta_0 \neq 0$, the initial second increment $\gamma_0 = 0$ and the scatter $D_1 = 1$).

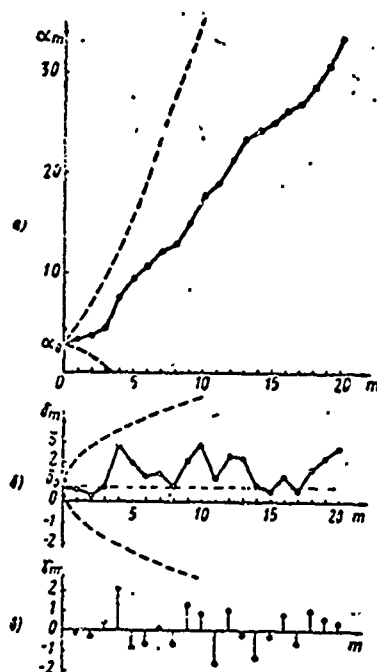


Fig. 8.3. One of the possible realizations of the motion model with independent and stationary second increments; a) curve of the variation of the quantity α from one reading to the next; c) discrete values of γ_m of the second increment.

A certain deficiency of the model of Fig. 8.3 is the fact that it does not take into account the limitation of the maximum rate of motion, which is typical for real targets.

§8.2. OPTIMUM SUCCESSIVE PROCESSING OF THE OBSERVATION RESULTS FOR MOTIONS WITH INDEPENDENT FIRST INCREMENTS

Assuming that preexperimental data on the measured quantity α are lacking and that its first reading $\alpha_{1\text{lotsch}}$ is obtained with a scatter of $D_{1\text{lotsch}}$. Assuming that the uncertainties are due only to the presence of noise and that the signal energy considerably exceeds the threshold value (see chapter 6), we consider the law of error distribution normal and the systematic error as zero.

The law of the postexperimental probability distribution of the measured parameter α_1 then will be

$$p(\alpha_1 | \alpha_{1\text{отсч}}) = \frac{1}{\sqrt{2\pi D_{1\text{отсч}}}} e^{-\frac{(\alpha_1 - \alpha_{1\text{отсч}})^2}{2D_{1\text{отсч}}}} \quad (1)$$

or with different symbols

$$p(\alpha_1 | \alpha_{1\text{отсч}}) = p_1(\alpha_1) = \frac{1}{\sqrt{2\pi D_1}} e^{-\frac{(\alpha_1 - \alpha_1^*)^2}{2D_1}} \quad (2)$$

Here the subscript "1" of the letter p means that the probability density $p_1(\alpha_1)$ is conditional (the condition is the presence of one and only one first reading); $\alpha_1^* = \alpha_{1\text{lotsch}}$ is the optimum estimate; $D_1 = D_{1\text{lotsch}}$ is the corresponding scatter (see 1.6).

Using the relation

$$\alpha_2 = \alpha_1 + \delta_2, \quad (3)$$

we can predict the value of α_2 on the basis of the first reading.

We shall assume that δ_2 like α_1 has a normal distribution. Then, α_2 is also a normally distributed random quantity characterized by its mathematical expectation and scatter. The mathematical expectation of the quantity α_2 we designated by $\alpha_{2\text{pr}}$. It is equal to the sum of the mathematical expectations

$$M\{\alpha_1\} = \alpha_{1\text{отсч}} \quad M\{\delta_2\} = 0,$$

i.e.,

$$\alpha_{2np} = \alpha_1^* \quad (4)$$

The dispersion of α_2 we designate by D_{2pr} . According to the theorem on the scatter of the sum of independent quantities

$$D_{2np} = D_1 + D_{2pr} \quad (5)$$

where $D_{2pr} = D\{\delta_2\}$ is determined only by the law of the target motion.

The distribution of the quantities α_2 predicted on the basis of the results of the first reading satisfy the relation

$$p_1(\alpha_2) = \frac{1}{\sqrt{2\pi D_{2np}}} e^{-\frac{(\alpha_2 - \alpha_{2np})^2}{2D_{2np}}} \quad (6)$$

In analogy with the expression (2) we can conclude that α_{2pr} is the predicted estimate and D_{2pr} the scatter. It is readily seen that the distribution (6) is preexperimental for the following reading α_2 .

Let then the second reading α_{2otsch} arrive. Now we can introduce the probability density of α_2 under conditions of two readings

$$p_2(\alpha_2) = p_1(\alpha_2 | \alpha_{2otsch})$$

In accordance with the previously known results of measurement theory (§1.6) we can write

$$p_1(\alpha_2 | \alpha_{2otsch}) = K p_1(\alpha_2) p(\alpha_{2otsch} | \alpha_2) \quad (7)$$

Using the expression for normal distributions, we find after taking of the logarithms

$$\frac{(\alpha_2 - \alpha_1^*)^2}{2D_1} = -\frac{(\alpha_2 - \alpha_{2np})^2}{2D_{2np}} + \frac{(\alpha_{2otsch} - \alpha_2)^2}{2D_{2otsch}} + \text{const.} \quad (8)$$

Making the coefficients of α_2^2 and α_2 , respectively, equal in the left and right part of equation (8), we obtain

$$\frac{1}{D_1} = \frac{1}{D_{2np}} + \frac{1}{D_{2otsch}},$$

$$\alpha_1^* = \alpha_{2np} \frac{D_2}{D_{2np}} + \alpha_{2otsch} \frac{D_1}{D_{2otsch}}.$$

Using (4) and (5), we find the final expressions for the optimum estimate and scatter of the second reading

$$\hat{\alpha}_2 = \hat{\alpha}_1 + \frac{D_2}{D_1 + D_2} (\alpha_{2 \text{ otcy}} - \hat{\alpha}_1),$$

$$\frac{1}{D_2} = \frac{1}{D_1 + D_2} + \frac{1}{D_2 \text{ otcy}}.$$

In an analogous manner we can find the expressions for the optimum estimate and scatter of the third and generally mth reading

$$\hat{\alpha}_m = \hat{\alpha}_{m-1} + \frac{D_m}{D_{m-1} + D_m} (\alpha_{m \text{ otcy}} - \hat{\alpha}_{m-1}), \quad (13)$$

$$\frac{1}{D_m} = \frac{1}{D_{m-1} + D_m} + \frac{1}{D_m \text{ otcy}}. \quad (14)$$

Utilizing these expressions and introducing the results of the readings, we can consecutively find the distribution parameters for the second, third, etc., measurements and thus determine also the corresponding optimum estimates.

Every subsequent estimate (13) is composed of the estimate predicted on the basis of the preceding reading ($\alpha_{m \text{ pr}} = \alpha_{m-1}^*$) and error signal ($\alpha_{m \text{ otcy}} - \alpha_{m-1}^*$) multiplied with the weight factor

$$A_m = \frac{D_m}{D_{m-1} + D_m}. \quad (15)$$

Thus, the results of the readings are introduced consecutively and up to the moment of obtaining the mth estimate it is not necessary to store in the memory of the computer the results of all the preceding estimates but it is sufficient to store the optimum estimate α_{m-1}^* and its scatter D_{m-1} .

Let us point out that the abovedescribed processing sequence is not the only possible one. One could, for example, obtain m estimates $\alpha_1^*, \alpha_2^*, \dots, \alpha_m^*$ at once. The estimates of the parameters from α_1^* to α_{m-1}^* then will, generally speaking, be more accurate than those obtained on the basis of a smaller number of readings. However, the estimate α_m^* , as can be shown, is exactly the same as with the consecutive processing procedure. Because in radar the accurate determination of the preceding estimates is usually not of independent interest, it is best

to use consecutive processing.

§8.3. CONTINUOUS AND INTERRUPTED REGIMES OF CONSECUTIVE PROCESSING FOR MOTIONS WITH INDEPENDENT AND STATIONARY FIRST INCREMENTS

In order to illustrate the realtions of §8.2 and to trace the accumulation of information on the distance α , let us first consider the simplest case in which $D_{1m}=0$ for an arbitrary m . This case under the condition $M\{\tilde{z}_m\}=0$ corresponds to an unchanged distance to the target.

By virtue of the relation [(14) §8.2] we then find

$$\frac{1}{D_m} = \frac{1}{D_{m-1}} + \frac{1}{D_{m \text{ over}}}. \quad (1)$$

The quantity $\frac{1}{D_{m-1}}$ entering into the right part of the equation we can find from a relation, analogous to (1) in which m is replaced by $(m-1)$. Repeating this procedure and taking into account that $D_0 = \infty$ (pre-experimental data on the measured quantity α are lacking as stipulated) we can find

$$\frac{1}{D_m} = \sum_{n=1}^m \frac{1}{D_{n \text{ over}}}. \quad (2)$$

The relation (2) corresponds to the wellknown situation in which the scatter of the estimate is calculated on the basis of the known scatter of observations with different accuracy. In particular, if the scatter of all readings is the same, the scatter of the m th estimate is m times less than the scatter of each reading.

Further, we can obtain from the relations [(13) §8.2] that

$$\alpha_m = \frac{\frac{\alpha_{m-1}}{D_{m-1}} + \frac{\alpha_{m \text{ over}}}{D_{m \text{ over}}}}{\frac{1}{D_m}}, \quad (3)$$

i.e., that the m th estimate is combined of the $(m-1)$ th and the result of the m th reading with weights which are inverse to the respective scatters. Using the formula (3) consecutively for the calculation

of $\frac{c_n}{D_n}$ ($n=m-1, m-2, \dots, 1$) and taking into account (2), we obtain

$$\alpha_m^* = \frac{\sum_{n=1}^m \frac{c_n}{D_n}}{\sum_{n=1}^m \frac{1}{D_n}} \quad (4)$$

i.e., the estimate α_m^* the weighted average. It is composed of the results of all the preceding readings with weights, which are inverse to the scatters of these readings. If the scatters are equal, the weighted average estimate is transformed into the arithmetic mean of the results of the readings.

It is clear from the expression (2) that at $D_i=0$ the scatter D_m of the estimate α_m^* decreases consecutively with an increase in the number of readings. For example, at equal scatters of the readings $D_{n \text{ oTCY}} = D_{\text{oTCY}}$ we shall have $D_m = \frac{D_{\text{oTCY}}}{m}$. It would seem that with a sufficiently large number of measurements one could reduce the errors as much as desired. This is really true for absolutely immobile targets. However, the usually existing position ambiguity expressed in the fact that $D_i \neq 0$, limits the process of error minimization.

Let, for example, the scatter of all readings be the same $D_i = \infty$, and the magnitude D_0 be $\frac{1}{6} D_{\text{oTCY}}$. Then, consecutively using formula [(14) §8.2], we obtain:

$$\begin{aligned} D_1 &= D_{\text{oTCY}}, \\ D_2 &= \frac{7}{13} D_{\text{oTCY}} \approx 0,54 D_{\text{oTCY}}, \\ D_3 &= \frac{55}{133} D_{\text{oTCY}} \approx 0,41 D_{\text{oTCY}}, \\ D_4 &= \frac{463}{1261} D_{\text{oTCY}} \approx 0,37 D_{\text{oTCY}}, \\ D_5 &= \frac{4039}{11605} D_{\text{oTCY}} \approx 0,35 D_{\text{oTCY}}, \\ &\dots \end{aligned}$$

It is evident from the above-presented calculations that with optimum processing a stabilization of the error scatter takes place.

The stabilized value of the error scatter can be obtained from

Eq. [(14) §8.2] on the assumption for the case of periodic measurements at a certain interval T , that

$$D_m = D_{m-1} = D,$$

$$D_{m \text{ otcy}} = D_{\text{otcy}},$$

$$D_{\text{sm}} = D_s.$$

The equation for the scatter of the stabilized process has the form

$$\frac{1}{D} = \frac{1}{D + D_s} + \frac{1}{D_{\text{otcy}}} \quad (5)$$

or

$$D^2 + D_s D - D_s D_{\text{otcy}} = 0,$$

hence we have for $D > 0$

$$D = \frac{1}{2} \left(-D_s + \sqrt{D_s^2 + 4D_s D_{\text{otcy}}} \right). \quad (6)$$

In particular, for the above-considered example the stabilized value is

$$D = \frac{1}{3} D_{\text{otcy}} \approx 0,33 D_{\text{otcy}}.$$

Simultaneously with the stabilization of the value of D_m the stabilization of the magnitude of the ratio $\frac{D_m}{D_{m \text{ otcy}}} = A_m$, takes place, which characterizes the algorithm of the consecutive method of obtaining estimates [(13) §8.2].

For the stabilized regime is value

$$A = \frac{D}{D_{\text{otcy}}}. \quad (7)$$

where D is determined from (6).

It follows from the relations [(13), (14) §8.2] and (7) that in the stationary regime any following estimate α_m^* is obtained from the preceding α_{m-1}^* and the result of the last reading $\alpha_m \text{ otcy}$ by the same rule, regardless of the number of the observation:

$$\dot{\alpha}_m^* = \dot{\alpha}_{m-1}^* + A(\alpha_{m,otsch} - \alpha_{m-1}^*). \quad (8)$$

§8.4. REALIZATION OF THE OPTIMUM CONSECUTIVE PROCESSING FOR A STABLE MOTION WITH STATIONARY FIRST INCREMENT

The circuit of the computer corresponding to the optimum processing rule [(8). §8.3] is represented in Fig. 8.4. The operations of algebraic summation are carried out by the adders 1 and 2. The first adder calculates the signal error on the basis of the result of the last reading α_{otsch} and the preceding estimate α_{m-1}^* .

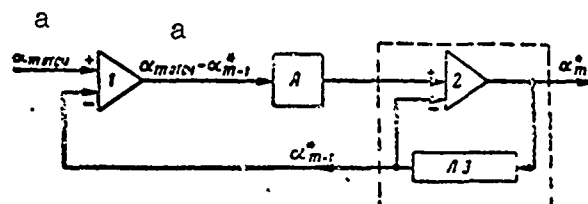


Fig. 8.4. Circuit scheme of the device for the consecutive elaboration of optimum estimates in the stationary regime with independent and stationary first increments of the measured quantity α . a) otsch.

The estimate α_m^* is given by the second adder, whose input has been supplied with α_{m-1}^* and the signal error, multiplied by the constant weighting coefficient A . The preceding estimate is taken from the delay line, connected with the output of the second summator.* The delay in the line is assumed to be exactly equal to the repetition period of the readings. The multiplication with the constant weighting coefficient A can be carried out in a potentiometer, amplifier, etc., circuit.

The computer circuit scheme thus obtained contains two closed circuits with feedback. One of these is outlined by a dotted line and is simply a recirculator circuit (see Fig. 5.16).

In order to give another important interpretation of the processing scheme derived above (Fig. 8.4) let us introduce the transmission characteristics of the recirculator from its input to the output of the summator $K_1(p)$ and from its input to the output of the delay line $K_2(p)$. This means that if the voltage e^{pt} (in the operator form) arrives at the recirculator input, the voltage $K_1(p)e^{pt}$ is taken off from the output of the summator 2 and the voltage $K_2(p)e^{pt}$ from the output of the delay line. Hence, taking into account the peculiarities of the summing operation and the delay in this circuit, we have

$$\begin{aligned} e^{pt} + K_2(p)e^{pt} &= K_1(p)e^{pt}, \\ K_1(p)e^{p(t-T)} &= K_2(p)e^{pt}, \end{aligned}$$

hence

$$\begin{aligned} K_1(p) &= \frac{1}{1 - e^{-pT}}, \\ K_2(p) &= K_1(p)e^{-pT}. \end{aligned}$$

If the process of fluctuation of the quantity α is fairly slow (compared with the period T), then the discrete sequence of the values α_m can be replaced by the function $\alpha(t)$ whose spectrum does not contain frequencies greater than $1/T$.

In order to obtain an estimate of this function we assume

$$e^{-pT} \approx 1 - pT,$$

so that

$$K_1(p) \approx \frac{1}{pT}. \quad (3)$$

This means that the recirculator can be replaced by an integrator. Then

$$K_2(p) \approx \frac{1 - pT}{pT} = \frac{1}{pT} - 1, \quad (4)$$

applies, which corresponds to the voltage difference between the output and input of the integrator.

In practice, instead of the difference $\alpha_m \text{ otsch} - \alpha_{m-1}$, we can introduce in the circuit scheme Fig. 8.4 quantity which is proportional

to it, which correspondingly modifies A in this circuit. The quantity proportional to $(\alpha_m \text{ otsch} - \alpha_{m-1}^*)$ is obtained, for example, by means of a time discriminator in the form of a error signal voltage.

Thus, the scheme devised in Fig. 8.4 corresponds to the well-known selftracking distance circuit with single error signal integration.

The scheme of Fig. 8.4 records only the measured coordinate (distance) and does not record the rate of its change. If in contrast to the above assumptions the first increment has a finite mathematical expectation, the error on account of not knowing the rate of motion is transformed from a random to a systematic error. This error has been given the special designation dynamic speed error. It is not present in a circuit with two recirculators (integrators) which is the best for a motion model with independent second increments.

§8.5. OPTIMUM CONSECUTIVE PROCESSING OF THE OBSERVATION RESULTS FOR A MOTION WITH INDEPENDENT SECOND INCREMENTS

For the motion model with independent second increments there is a connection not only between the measured quantities α_m and α_{m-1} but also for their first increments δ_m and δ_{m-1} . Hence it is preferable to store data on α as well as on δ .

Assuming that in the result of the reading $(m-1)$ a postexperimental probability density $p_{m-1}(\alpha_{m-1}, \delta_{m-1})$ is obtained corresponding to a two-dimensional normal distributional law:

$$p_{m-1}(\alpha_{m-1}, \delta_{m-1}) = \frac{1}{2\pi \sqrt{D_{\alpha(m-1)} D_{\delta(m-1)} - K_{\alpha\delta(m-1)}^2}} \times \\ \times \exp \left[-\frac{D_{\delta(m-1)}(\alpha_{m-1} - \alpha_{m-1}^*)^2 + D_{\alpha(m-1)}(\delta_{m-1} - \delta_{m-1}^*)^2 - 2K_{\alpha\delta(m-1)}(\alpha_{m-1} - \alpha_{m-1}^*)(\delta_{m-1} - \delta_{m-1}^*)}{2(D_{\alpha(m-1)} D_{\delta(m-1)} - K_{\alpha\delta(m-1)}^2)} \right]. \quad (1)$$

Here $D_{\alpha(m-1)}$ and $D_{\delta(m-1)}$ are the scatter of the measured quantities α_{m-1} and δ_{m-1} after the $(m-1)$ th measurement; $K_{\alpha\delta(m-1)}$ is

the correlation element connecting these quantities; α_{m-1} and δ_{m-1} — are the mathematical expectations or, which is the same, the optimum estimates of these quantities.

Using the distribution (1) and taking into account the regularities of the motion and the result of the m th reading of α_m otsch, we can find the probability density $p_m(\alpha_m, \delta_m)$ in analogy to §8.2, where the distribution $p_{m-1}(\alpha_{m-1})$ had been found on the basis of the distribution $p_m(\alpha_m)$.

An intermediate stage is the prediction, i.e., the detection of the conditional probability density $p_{m-1}(\alpha_m, \delta_m)$ of the distribution of the predicted values α_m and δ_m by means of the data of the preceding $(m-1)$ readings.

We shall carry out the prediction in accordance with the relations

$$\alpha_m = \alpha_{m-1} + \delta_{m-1} + \gamma_m,$$

$$\delta_m = \delta_{m-1} + \gamma_m.$$

We take advantage of the wellknown expressions for the mathematical expectations, scatters and correlation moments of the connectivity of the sums of random quantities:

$$M\{u+v+w\} = M\{u\} + M\{v\} + M\{w\}, \quad (4)$$

$$D\{u+v+w\} = D\{u\} + D\{v\} + D\{w\} + 2K\{u, v\} + 2K\{u, w\} + 2K\{v, w\}, \quad (5)$$

$$K\{u+v+w, r+s\} = K\{u, r\} + K\{u, s\} + K\{v, r\} + K\{v, s\} + K\{w, r\} + K\{w, s\}. \quad (5)$$

In particular, using expression (4), we take the mathematical expectations from both parts of the Eqs. (2), (3).

We take into account that after the $(m-1)$ th reading the mathematical expectations of the quantities α_{m-1} and δ_{m-1} correspond to their estimates α_{m-1} and δ_{m-1} , those of α_m and δ_m by the estimates $\alpha_{m \text{ pr}}$ and $\delta_{m \text{ pr}}$, predicted on the basis of the previous reading,

and that the mathematical expectation of γ_m has been stipulated to be zero.

We then obtain

$$\alpha_{m \text{ up}} = \dot{\alpha}_{m-1} + \dot{\gamma}_{m-1}, \quad (7)$$

$$\delta_{m \text{ up}} = \dot{\gamma}_{m-1}. \quad (8)$$

Using (5) we find the scatter of both parts of Eqs. (2) and (3). Taking into account the independence of the increments γ_m from all preceding increments, and of course, from α_{m-1} and δ_{m-1} , we have

$$K\{\alpha_{m-1}, \gamma_m\} = K\{\delta_{m-1}, \gamma_m\} = 0.$$

The scatter of the predicted values of α_m and δ_m then will be

$$D_{\alpha m \text{ up}} = D_{\alpha(m-1)} + D_{\delta(m-1)} + D_{\gamma m} + 2K_{m-1}, \quad (9)$$

$$D_{\delta m \text{ up}} = D_{\delta(m-1)} + D_{\gamma m}. \quad (10)$$

Finally, using (6), we find the correlation moment of connectivity $K_{m \text{ up}} = K\{\alpha_{m \text{ up}}, \delta_{m \text{ up}}\}$. By virtue of the relations (2), (3), (6) and the independence of the second increments, we obtain

$$K_{m \text{ up}} = K_{m-1} + D_{\delta(m-1)} + D_{\gamma m}. \quad (11)$$

The quantities α_m and δ_m obviously have a normal distribution as the sum of normally distributed quantities.

Hence the five parameters [expressions (7)-(11)] found in analogy to (1) determine the without ambiguity the distribution law of α_m and δ_m after the prediction

$$p_{m-1}(\alpha_m, \delta_m) = \frac{1}{2\pi \sqrt{D_{\alpha m \text{ up}} D_{\delta m \text{ up}} - K_{m \text{ up}}^2}} \times \\ \times \exp \left[-\frac{D_{\delta m \text{ up}} (\alpha_m - \alpha_{m \text{ up}})^2 + D_{\alpha m \text{ up}} (\delta_m - \delta_{m \text{ up}})^2 -}{2(D_{\alpha m \text{ up}} D_{\delta m \text{ up}} - K_{m \text{ up}}^2)} - \right. \\ \left. - \frac{2K_{m \text{ up}} (\alpha_m - \alpha_{m \text{ up}}) (\delta_m - \delta_{m \text{ up}})}{D_{\alpha m \text{ up}} D_{\delta m \text{ up}} - K_{m \text{ up}}^2} \right]. \quad (12)$$

This law we shall consider as preexperimental with respect to the moment of the m th reading.

After the reading has been obtained one can find the postexperi-

mental distribution law of the same quantities

$$\begin{aligned} p_m(a_m, \delta_m) &= p_{m-1}(a_m, \delta_m | a_{m \text{ oTCY}}) = \\ &= K p_{m-1}(a_m, \delta_m) p(a_{m \text{ oTCY}} | a_m, \delta_m). \end{aligned} \quad (13)$$

If, as in [(1) §8.2], it is assumed that the measurement errors a_m are caused only by noise* and that the law of their distribution is normal with a mathematical expectation of zero (absence of systematic error), we obtain

$$\begin{aligned} p(a_{m \text{ oTCY}} | a_m, \delta_m) &= p(a_{m \text{ oTCY}} | a_m) = \\ &= \frac{1}{\sqrt{2\pi D_{m \text{ oTCY}}}} e^{-\frac{(a_m - a_{m \text{ oTCY}})^2}{2D_{m \text{ oTCY}}}}. \end{aligned} \quad (14)$$

Substituting (12) and (14) into (13) and using for $p_m(a_m, \delta_m)$ a notation analogous to (1) with the substitution of $(m-1)$ by m , we find after taking of the logarithms

$$\begin{aligned} \frac{D_{\delta m}(a_m - a_m^*)^2 + D_{a m}(\delta_m - \delta_m^*)^2 - 2K_m(a_m - a_m^*)(\delta_m - \delta_m^*)}{2(D_{a m}D_{\delta m} - K_m^2)} &= \\ = \frac{D_{\delta m \text{ np}}(a_m - a_{m \text{ np}})^2 + D_{a m \text{ np}}(\delta_m - \delta_{m \text{ np}})^2 -}{2(D_{a m \text{ np}}D_{\delta m \text{ np}} - K_{m \text{ np}}^2)} & \quad (15) \\ \frac{-2K_{m \text{ np}}(a_m - a_{m \text{ np}})(\delta_m - \delta_{m \text{ np}})}{K_{m \text{ np}}^2} + \frac{(a_m - a_{m \text{ oTCY}})^2}{2D_{m \text{ oTCY}}} + \text{const.} \end{aligned}$$

By consecutively comparing the coefficients at a_m^2 , δ_m^2 , $a_m\delta_m$, a_m and δ_m in the left and right part of Eq. (15), we obtain five equations, which connect the parameters of the postexperimental distribution with the parameters of the postexperimental distribution with the parameters of the preexperimental (predicted distribution and the distribution (14) of the reading errors:

$$\frac{D_{\delta m}}{D_m} = \frac{D_{\delta m \text{ np}}}{D_{m \text{ np}}} + \frac{1}{D_{m \text{ oTCY}}}, \quad (16)$$

$$\frac{D_{a m}}{D_m} = \frac{D_{a m \text{ np}}}{D_{m \text{ np}}}, \quad (17)$$

$$\frac{K_m}{D_m} = \frac{K_{m \text{ np}}}{D_{m \text{ np}}}, \quad (18)$$

$$\left. \begin{aligned} \frac{D_{\Delta m} \alpha_m^* - K_m \delta_m^*}{\Delta_m} &= \frac{D_{\Delta m \text{ np}} \alpha_{m \text{ np}} - K_{m \text{ np}} \delta_{m \text{ np}}}{\Delta_{m \text{ np}}} + \frac{\alpha_{m \text{ отсч}}}{D_{m \text{ отсч}}}, \\ \frac{K_m \alpha_m^* - D_{\Delta m} \delta_m^*}{\Delta_m} &= \frac{K_{m \text{ np}} \alpha_{m \text{ np}} - D_{\Delta m \text{ np}} \delta_{m \text{ np}}}{\Delta_{m \text{ np}}}. \end{aligned} \right\} \quad (19)$$

Here is $\Delta_m = D_{\Delta m} D_{\Delta m} - K_m^2$, $\Delta_{m \text{ np}} = D_{\Delta m \text{ np}} D_{\Delta m \text{ np}} - K_{m \text{ np}}^2$.

By multiplying the equations (16) and (17) and subtracting the squared equation (18), we find the relation for Δ_m

$$\frac{1}{\Delta_m} = \frac{1}{\Delta_{m \text{ np}}} \left(1 + \frac{D_{\Delta m \text{ np}}}{D_{m \text{ отсч}}} \right).$$

Using the value of Δ_m thus determined, we find from (16)-(19) the expressions for the parameters of the mth distribution of $D_{\Delta m}$, $D_{\Delta m}$, K_m and α_m^* , δ_m^* . If we introduce the coefficients

$$A_m = \frac{D_{\Delta m \text{ np}}}{D_{\Delta m \text{ np}} + D_{m \text{ отсч}}}, \quad B_m = \frac{K_{m \text{ np}}}{D_{\Delta m \text{ np}} + D_{m \text{ отсч}}},$$

the sought-for expressions assume the simpler form:

$$\begin{aligned} D_{\Delta m} &= A_m D_{m \text{ отсч}}, \\ D_{\Delta m} &= D_{\Delta m \text{ np}} - B_m K_{m \text{ np}}, \\ K_m &= B_m D_{m \text{ отсч}}, \\ \alpha_m^* &= \alpha_{m \text{ np}} + A_m (\alpha_{m \text{ отсч}} - \alpha_{m \text{ np}}), \\ \delta_m^* &= \delta_{m \text{ np}} + B_m (\alpha_{m \text{ отсч}} - \alpha_{m \text{ np}}). \end{aligned}$$

By substituting in the expressions thus obtained the parameters (7)-(11), which characterize the results of the prediction, we express the parameters of the mth distribution directly via the parameters of the (m - 1)th distribution of the mth reading:

$$A_m = \frac{D_{\Delta(m-1)} + D_{\Delta(m-1)} + 2K_{m-1} + D_{\gamma m}}{D_{\Delta(m-1)} + D_{\Delta(m-1)} + 2K_{m-1} + D_{\gamma m} + D_{m \text{ отсч}}}, \quad (20)$$

$$B_m = \frac{D_{\Delta(m-1)} + K_{m-1} + D_{\gamma m}}{D_{\Delta(m-1)} + D_{\Delta(m-1)} + 2K_{m-1} + D_{\gamma m} + D_{m \text{ отсч}}}, \quad (21)$$

$$D_{\Delta m} = A_m D_{m \text{ отсч}}, \quad (22)$$

$$D_{\Delta m} = D_{\Delta(m-1)} + D_{\gamma m} - B_m (K_{m-1} + D_{\Delta(m-1)} + D_{\gamma m}), \quad (23)$$

$$K_m = B_m D_{m \text{ otsch}}, \quad (24)$$

$$\alpha_m^* = \alpha_{m-1}^* + \delta_{m-1}^* + A_m (\alpha_{m \text{ otsch}} - \alpha_{m-1}^* - \delta_{m-1}^*), \quad (25)$$

$$\delta_m^* = \delta_{m-1}^* + B_m (\alpha_{m \text{ otsch}} - \alpha_{m-1}^* - \delta_{m-1}^*). \quad (26)$$

Using the above formulas (20)-(26) and introducing the results of the readings ($m = 1, \dots$), we can, as in the case considered in §8.2, find consecutively the parameters of the distributions of the measured quantities, thus determining the corresponding optimum estimates. Any subsequent estimate (25), (26) is composed of the estimate ($\alpha_{m-1}^* + \delta_{m-1}^*$ and δ_{m-1}^* , respectively) predicted on the basis of the preceding reading and the error signal ($\alpha_{m \text{ otsch}} - \alpha_{m-1}^* - \delta_{m-1}^*$), multiplied by the corresponding weight factor A_m or B_m . The error signal is calculated as before as the difference of the reading $\alpha_{m \text{ otsch}}$ and the predicted value of the measured quantity, which, in contrast to §8.2, is plotted by taking into account the estimate of the first increment δ_{m-1}^* (i.e., the speed estimate).

§8.6. UNSTEADY AND STEADY OPTIMUM CONSECUTIVE PROCESSING REGIME FOR A MOTION WITH INDEPENDENT AND STATIONARY SECOND INCREMENTS

In order to illustrate the relations of §8.5 and to trace the accumulation of information on distance and speed, let us first consider the simplest case, when $D_{1m} = D_1 = 0$. With periodic target sweep this corresponds to a target motion with a strictly constant, although unknown speed. For the sake of simplification we assume that the scatter of all readings is the same and equal to D_0 .

Let us trace out the consecutive processing of the readings for this case.

Assuming that up to the first reading information on α_1 and δ_1 is lacking, we assume $\alpha_1^* = \alpha_1 \text{ otsch}$ and $D_1 = D_0$. In view of the fact that one cannot give a speed estimate on the basis of the results of a single reading, we assume $D_{11} = \infty$, $K_1 = 0$. Substituting these values into

[(20)-(26) §8.5] and assuming $m = 2$, we find $A_2 = B_2 = 1$ i.e.,

$$D_{a2} = D_0, D_{b2} = 2D_0, K_2 = D_0,$$

$$\dot{a}_2 = a_{2 \text{ орчч}}, \dot{b}_2 = a_{2 \text{ орчч}} - a_{1 \text{ орчч}}.$$

Assuming that $m = 3$, we obtain $A_2 = 5/6$ and $B_3 = 1/2$, i.e.,

$$D_{a3} = \frac{5}{6} D_0, D_{b3} = \frac{1}{2} D_0, K_3 = \frac{1}{2} D_0,$$

$$\dot{a}_3 = \dot{a}_2 + \dot{b}_2 + \frac{5}{6} (a_{2 \text{ орчч}} - a_2 - \dot{b}_2),$$

$$\dot{b}_3 = \dot{b}_2 + \frac{1}{2} (a_{2 \text{ орчч}} - a_2 - \dot{b}_2)$$

or

$$\dot{a}_3 = -\frac{1}{6} a_{1 \text{ орчч}} + \frac{1}{3} a_{2 \text{ орчч}} + \frac{5}{6} a_{3 \text{ орчч}},$$

$$\dot{b}_3 = \frac{1}{2} (a_{2 \text{ орчч}} - a_{1 \text{ орчч}}).$$

For $m = 4$ we shall have $A_4 = \frac{7}{10}$, $B_4 = \frac{3}{10}$ i.e.,

$$D_{a4} = \frac{7}{10} D_0, D_{b4} = \frac{3}{10} D_0, K_4 = \frac{3}{10} D_0,$$

$$\dot{a}_4 = \dot{a}_3 + \dot{b}_3 + \frac{7}{10} (a_{4 \text{ орчч}} - a_3 - \dot{b}_3),$$

$$\dot{b}_4 = \dot{b}_3 + \frac{3}{10} (a_{4 \text{ орчч}} - a_3 - \dot{b}_3)$$

or

$$\dot{a}_4 = -\frac{2}{10} a_{1 \text{ орчч}} + \frac{1}{10} a_{2 \text{ орчч}} + \frac{4}{10} a_{3 \text{ орчч}} + \frac{7}{10} a_{4 \text{ орчч}},$$

$$\dot{b}_4 = -\frac{3}{10} a_{1 \text{ орчч}} - \frac{1}{10} a_{2 \text{ орчч}} + \frac{1}{10} a_{3 \text{ орчч}} + \frac{3}{10} a_{4 \text{ орчч}}.$$

It can be seen that in proportion to the inout of new readings, the scatters D_{am} and D_{bm} are reduced.

The scatter D_{bm} decreases particularly quickly, which is the case in reality only if the motion is completely regular ($D_y = 0$). The optimum coefficients $A_m = \frac{D_{am}}{D_{m \text{ орчч}}}$ and $B_m = \frac{K_m}{D_{m \text{ орчч}}}$, by means of which the new estimates are worked out, also vary from one measurement to the next in consequence of the improvements of the estimates.*

If the optimum measurements are carried out periodically, and if $D_{\text{гн}} = D_{\text{гн}} = \text{const}$ and $D_{\text{н.отч}} = D_{\text{н.отч}} = \text{const}$, the stable values are found

$$\left. \begin{aligned} D_{am} &= D_a, \\ D_{bm} &= D_b, \\ K_m &= K, \end{aligned} \right\} \quad (1)$$

$$\left. \begin{aligned} A_m &= A, \\ B_m &= B. \end{aligned} \right\} \quad (2)$$

$$\left. \begin{aligned} \dot{\alpha}_m &= \dot{\alpha}_{m-1} + \dot{\delta}_{m-1} + A(\alpha_{m \text{ отсч}} - \alpha_{m-1} - \dot{\delta}_{m-1}), \\ \dot{\delta}_m &= \dot{\delta}_{m-1} + B(\alpha_{m \text{ отсч}} - \alpha_{m-1} - \dot{\delta}_{m-1}). \end{aligned} \right\} \quad (3)$$

- 259 -

In this scheme the operations of algebraic summation are carried out by the adders 1, 2, 3. The first adder calculates the signal error on the basis of the result of the last reading α_m otsch and the preceding estimates α_{m-1}^* and δ_{m-1}^* . The calculated error signal is used for obtaining the estimates α_m^* and δ_m .

The estimate α_m^* is delivered by the second adder, whose input is supplied with the preceding estimates α_{m-1}^* and δ_{m-1}^* and the error signal, multiplied by the constant weight coefficient. The preceding estimate α_{m-1}^* is taken from the output of the delay line at the time T. The input of this line is connected with the output of the second adder. The estimate α_{m-1}^* is supplied to the first adder for the calculation of the error signal.

The third adder delivers the running estimate δ_m^* , and the preceding estimate δ_{m-1}^* , which is used in the first two adders is taken from the output of the delay line. For this purpose, the input of the third adder is supplied with the preceding estimate δ_{m-1}^* and the error signal from the first adder multiplied by the weight coefficient B.

This computer circuit scheme contains several closed circuits equipped with feedback, two of which represent recirculator circuits. The recirculators, as pointed out previously in §8.4, are analog integrators.

Finally, let us analyze the stationarity conditions (1), (2) and find the stable values D_α , D_δ , K, A and B as a function of D_0 and D_γ . Omitting in [(20)-(24) §8.5] the subscripts m and $(m-1)$, we obtain for the five desired quantities five equations, three of which are nonlinear. In order to facilitate the solution, we introduce the new variable

$$s = \frac{1}{D_0} (D_\alpha + D_\delta + 2K + D_\gamma). \quad (4)$$

The equations [(20)-(24) §8.5] can then be transformed thus:

$$A(s+1)=s, \quad (5)$$

$$B(s+1)D_0 = D_0 + K + D_1, \quad (6)$$

$$D_0 = AD_0, \quad (7)$$

$$B(D_0 + K + D_1) = D_1, \quad (8)$$

$$K = BD_0. \quad (9)$$

($D_0 + K + D_1$) and B in (6) and (8) we express by D_0 , D_1 and s :

$$D_0 + K + D_1 = \sqrt{D_0 D_1 (s+1)}, \quad (10)$$

$$B = \sqrt{\frac{D_1}{D_0(s+1)}}. \quad (11)$$

Then, by virtue of (9) and (11), we have

$$K = \frac{1}{s+1} \sqrt{D_0 D_1 (s+1)}. \quad (12)$$

Further, by virtue of (10) and (12), we have

$$D_1 = \frac{s}{s+1} \sqrt{D_0 D_1 (s+1)} - D_1. \quad (13)$$

Finally, from the relations (7) and (5) follows

$$D_0 = \frac{s}{s+1} D_0. \quad (14)$$

Thus, the three unknown quantities D_0 , D_1 and K are expressed by the new unknown s . Substituting the values (12)-(14) thus obtained in (4), we find the equation for s :

$$s - \frac{s}{s+1} = \frac{2+s}{1+s} \sqrt{\frac{D_1}{D_0} (1+s)}. \quad (15)$$

Squaring the two parts of Eq. (15), we transform the equations for s thus

$$f(s) = \frac{s^2}{(2+s)^2(1+s)} = \frac{D_1}{D_0}. \quad (16)$$

The function $f(s)$ is monotonous and Eq. (16) can easily be solved graphically. This enables us to find s for any relation $\frac{D_1}{D_0}$ and to calculate A , B , $\frac{D_0}{D_1}$, $\frac{D_1}{D_0}$ and $\frac{K}{D_0}$.

Let us stop to consider the case of small values of the relation

$\frac{D_1}{D_0}$, which is convenient for computation. At the same time this case enables us to follow the increase in the accuracy of the estimates and its limitation by means of the final value of D_γ . To a small relation

$\frac{D_1}{D_0}$ correspond small values of s , so that we can assume in (16) $(2+s) \approx 2$ and $(1+s) \approx 1$. Then we obtain from (16) $\frac{s^2}{4} \approx \frac{D_1}{D_0}$ or $s \approx \sqrt[4]{\frac{D_1}{D_0}}$. (This approximation can be used if $s \ll 1$).

The relations (12)-(14) then give:

$$A = \frac{D_a}{D_0} \approx \sqrt[4]{\frac{4D_1}{D_0}}, \quad (17)$$

$$B = \frac{K}{D_0} \approx \sqrt[4]{\frac{D_1}{D_0}}, \quad (18)$$

$$D_2 = \sqrt[4]{4D_1^2 D_0} \left(1 - \sqrt[4]{\frac{D_1}{4D_0}} \right) \approx \sqrt[4]{4D_1^3 D_0}. \quad (19)$$

Let us illustrate these relations by an example. Let $D_0 = 10^5 \text{ m}^2$, and $D_1 = 10^{-1} \text{ m}^2$. Then from the approximate relations (17)-(19) we obtain $s \approx 0.14$, $A \approx 0.14$, $B \approx 0.01$ and $D_2 \approx 140 \text{ m}^2$, i.e., the mean square measurement error in this case amounts to approximately 12 m at a mean square error of a single reading of about 30 m.

Thus, consecutive processing enables the measurement error to be greatly reduced as compared with the error of a single reading.

It should be pointed out that in the absence of constant accelerations this reduction is limited by the random accelerations of the secondary emission center of the target. The latter can be displaced not only in consequence of the nonuniformity of the target motion but also in consequence of the fluctuation effect.

The smaller D_γ , the greater is the possibility of increasing the measurement accuracy during the process of repeated processing. However, more time is then required for the establishment of the stationary regime. Conversely, at $D_1 \gg D_0$, when $s \approx 1$, the value $D_2 \approx D_0$, i.e., the measurement accuracy, are not increased and the stationary regime begins practically instantaneously.

This case corresponds to a very high degree of discreteness of the readings. when the information on the target arrives rarely. Hence it is evident that a reduction of the scatter is impossible if the information on the target arrives too infrequently.

It is readily apparent that the scheme of Fig. 8.5. with two recirculators (integrators) was developed in consequence of the assumption of a stationary second increment. The hypothesis of the stationary first increment, as we have shown earlier, leads to a scheme with a single integrator.

Schemes with consecutive processing can be designed not only when independent readings of the measured coordinate are carried out but also when a linear combination of a coordinate and its derivative is read off. As has been shown in §7.7, this case is typical for a signal which is frequency modulated in accordance with a linear law.

When consecutive measurements are carried out it is possible to compensate for the distance measurement error (at the moment when the sweep is carried out or at any other moment of time), connected with the lack of information on the radial speed, because the processing scheme contains information on distance as well as speed.

In the analysis in §8.5 we examined the case in which only the readings of only one measured coordinate α were introduced into the processing circuit. For the signals, discussed, for example, in §7.8 and 7.9, independent speed readings on the basis of the Doppler frequency are also possible.

If the accuracy of these readings is not too low, it is feasible to feed them into the processing circuit (Fig. 8.5) in combination with the generated speed error signal ($\delta_{m \text{ or } \dot{\alpha}} - \delta_{m-1}^*$). A case in which the single speed measurement is accurate but ambiguous, is then also possible (§7.8). If the processing circuit for the coordinate readings en-

ables this ambiguity to be eliminated, the modified circuit will deliver accurate and unequivocal speed values which results in a decrease in the error of the measurement of the coordinate α (distance).

Manu-
script
Page
No.

[Footnotes]

- 235 Let us point out, however, that most of these relations remain valid also for other cases of periodical as well as nonperiodical measurements.
- 250 Instead of this line, a nonlinear time delay circuit can be used.
- 255 In particular, we have in mind that the speed error of a single reading (§7.7) is absent, i.e., that the result of the reading depends only on α_m and not on δ_m .
- 258 Let us point out that the variation in the optimum values of the coefficients A_m and B_m takes place not only during the regime of estimate improvement but also during the reading dropout when the scatter of the individual readings becomes infinite.

Manu-
script
Page
No.

[Transliterated Symbols]

- 244 otch = otsch = otschet = reading
- 244 np = pr = prognozirovanny = predicted

APPENDIX .

Appendix 1

QUALITATIVE DETECTION INDICES WITH SQUARE SIGNAL SUMMATION

Let the voltage at the output of the square-law adder be

$$U = U_1^2 + U_2^2 + \dots + U_M^2, \quad (1)$$

where U_1, U_2, \dots, U_M are independent random quantities, distributed in accordance with the generalized law of Rayleigh

$$p(U_i) = U_i I_0(q_i, U_i) e^{-\frac{q_i^2 + U_i^2}{2}} \quad (U_i \geq 0), \quad (2)$$

The mean square noise voltage in the relation (2) has been assumed to be equal to unity. Let us now find the distribution law of the voltage U at the adder output. For this purpose we write first the distribution law for a random quantity $\eta_i = U_i^2$

$$p(\eta_i) = p(U_i) \frac{dU_i}{d\eta_i},$$

i.e.,

$$p(\eta_i) = \frac{1}{2} I_0(q_i, \sqrt{\eta_i}) e^{-\frac{q_i^2 + \eta_i}{2}}. \quad (3)$$

The characteristic of the distribution function (3) can be represented in the form

$$\Phi_i(s) = \int_{-\infty}^{\infty} e^{js\eta_i} p(\eta_i) d\eta_i. \quad (4)$$

By replacing the modified Bessel function with its integral representation [(9) §3.3] we obtain

$$\theta_i(s) = \frac{1}{4\pi} \int_0^{2\pi} d\beta \int_{-\infty}^{\infty} \exp \left[q_i \sqrt{\eta_i} \cos \beta - \frac{q_i^2 + \eta_i}{2} + js\eta_i \right] d\eta_i.$$

Changing over to the new integration variables $\sqrt{\eta_i} \cos \beta = x$, and

$\sqrt{\eta_i} \sin \beta = y$, we find

$$\begin{aligned} \theta_i(s) &= \frac{1}{\sqrt{2\pi}} \int_{-\infty}^{\infty} e^{-\frac{1-j2s}{2} \left(x - \frac{q_i}{1-j2s}\right)^2} dx \times \\ &\times \frac{1}{\sqrt{2\pi}} \int_{-\infty}^{\infty} e^{-\frac{1-j2s}{2} y^2} dy e^{-\frac{q_i^2}{2}} e^{\frac{q_i^2}{2(1-j2s)}} \end{aligned}$$

or

$$\theta_i(s) = e^{-\frac{q_i^2}{2} \frac{e^{\frac{q_i^2}{2(1-j2s)}}}{1-j2s}}. \quad (5)$$

The characteristic distribution function $p(U)$ is found as the product of the characteristic functions $\theta_i(s)$. Considering that the energy of all pulses is the same, we obtain

$$\theta_U(s) = \prod_{i=1}^M \theta_i(s) = e^{-A} \frac{e^{\frac{A}{1-j2s}}}{(1-j2s)^M}, \quad (6)$$

where $A = M \frac{q^2}{2}$, or

$$\theta_U(s) = e^{-A} \frac{d^{M-1}}{dA^{M-1}} \left(\frac{e^{\frac{A}{1-j2s}}}{1-j2s} \right). \quad (7)$$

The desired distribution of the quantity U then is

$$p(U) = \frac{1}{2\pi} \int_{-\infty}^{\infty} \theta_U(s) e^{-jUs} ds$$

or

$$p(U) = \frac{1}{2\pi} e^{-A} \frac{d^{M-1}}{dA^{M-1}} \int_{-\infty}^{\infty} \frac{e^{\frac{A}{1-j2s}}}{1-j2s} e^{-jUs} ds. \quad (8)$$

In order to find the value of the integral in relation (8) it is sufficient to make the assumption $M = 1$, i.e., $U = \eta_i$. The probability density $p(U) = p(\eta_i)$ can then be calculated by means of formula (3). Noting that at $M = 1$, the quantity $q_i = \sqrt{2A}$, we find

$$\frac{1}{2\pi} \int_{-\infty}^{\infty} \frac{e^{\frac{A}{1-j2s}}}{1-j2s} e^{-Us} ds = \frac{1}{2} I_0(\sqrt{2AU}) e^{-\frac{U}{2}} \quad (U \geq 0). \quad (9)$$

Because (9) is valid for any U and A , it can be substituted into (8). Then we obtain

$$p(U) = \frac{1}{2} e^{-\frac{A-U}{2}} \frac{d^{M-1}}{dA^{M-1}} I_0(\sqrt{2AU}) \quad (U \geq 0). \quad (10)$$

In the differentiation of the modified Bessel functions one can consecutively use the following relation:

$$\frac{d}{dx} I_n(x) = I_{n+1}(x) + \frac{n}{x} I_n(x) \quad (n=0, 1, 2, \dots).$$

Then we obtain finally

$$p(U) = p_{en}(U) = \frac{1}{2} \left(\frac{U}{2A} \right)^{\frac{M-1}{2}} e^{-\frac{A-U}{2}} I_{M-1}(\sqrt{2AU}), \quad (11)$$

where $A = M \frac{\sigma^2}{2}$.

Formula (11) describes the distribution at the adder output in presence of signal plus noise. The corresponding formula for the noise alone can be obtained if in (11) we go over to the limit at $A \rightarrow 0$. In order to discover the ambiguity thus obtained, we make use of the fact that

$$I_n(x) \approx \frac{\left(\frac{x}{2} \right)^n}{n!} \quad \text{for } x \rightarrow 0.$$

Then we obtain

$$p(U) = \frac{U^{M-1}}{2^M (M-1)!} e^{-\frac{U}{2}} \quad (U \geq 0). \quad (12)$$

From the relations (11) and (12) we can derive expressions for the correct detection and false alarm probabilities in the case of a rectangular incoherent and non-fluctuating pulse packet.

$$D = \frac{1}{2} \int_{U_{\text{report}}}^{\infty} \left(\frac{U}{2A} \right)^{\frac{M-1}{2}} e^{-\frac{A-U}{2}} I_{M-1}(\sqrt{2AU}) dU. \quad (13)$$

$$F = \frac{1}{2^M(M-1)!} \int_{U_{\text{porog}}}^{\infty} U^{M-1} e^{-\frac{U}{2}} dU. \quad (14)$$

where U_{porog} is the magnitude of the threshold, selected in accordance with the above-defined false alarm probability F .

The above found relation (12) makes it possible to estimate also the qualitative detection indices in presence of independent fluctuations of individual pulses in the packet. Because this case (see §3.6) is equivalent to a single multifrequency emission with independent fluctuations at different carrier frequencies, the qualitative indices can be estimated also for this type of signal. Square summation (1) is the optimum form of processing for any signal with independent fluctuations (see §4.9) at an arbitrary ratio of the mean pulse energies and the spectral noise density.

It is then logical to conclude that in presence as well as absence of a useful signal, the amplitudes U_i in formula (1) are distributed in accordance with the Rayleigh law. Hence the distribution (12) for the sum $U = \sum_{i=1}^M U_i^2$ can be used in both these cases. It is merely necessary to remember that the quantity $\frac{\sigma^2}{N_s}$ taken in (12) as equal to unity for the case of the absence of a useful signal, increases in its presence in accordance with the relation [(10) §6.3] $1 + \frac{q^2}{2} = 1 + \frac{\sigma^2}{N_s}$ times. Taking this into account, we obtain

$$p_{\text{sa}}(U) dU = p_{\text{a}} \left(\frac{U}{1 + \frac{\sigma^2}{N_s}} \right) d \left(\frac{U}{1 + \frac{\sigma^2}{N_s}} \right). \quad (15)$$

Thus, the probability D of correct detection of an M pulse packet or M frequency signal with independent fluctuations with optimum processing (part of which is the square summation) will be

$$D = \frac{1}{2^M(M-1)!} \int_{\frac{U_{\text{porog}}}{1 + \frac{\sigma^2}{N_s}}}^{\infty} \xi^{M-1} e^{-\frac{\xi}{2}} d\xi.$$

Integrating by parts, we find

$$D = e^{-\frac{U_{\text{porog}}}{2\left(1+\frac{\vartheta}{N_s}\right)}} \sum_{i=1}^M \frac{1}{(i-1)!} \left[\frac{U_{\text{porog}}}{2\left(1+\frac{\vartheta}{N_s}\right)} \right]^{i-1}. \quad (16)$$

The false alarm probability F can be found from the same expression (16) by substituting into it $\vartheta=0$.

For example, at $M = 2$ and $U_{\text{porog}} = 38$ (in units v_0^2) we have $F \approx 10^{-7}$. In order to secure a correct detection probability $D = 0.9$ we must have a ratio of the energy of a single pulse to the spectral noise density of $\frac{\vartheta}{N_s} \approx 35$ or the same ratio for the total energy of two pulses $\frac{\vartheta_t}{N_s} \approx 70$ (instead of the ratio $\frac{\vartheta_t}{N_s} \approx 150$ in single-frequency operation).

A slightly less accurate result is obtained if the detection of the packet or multifrequency signal is carried out without utilization of optimum square summation. Let, for example, the presence of a signal be assumed if even only one of M independently fluctuating pulses exceeds the threshold. If D_1 and F_1 are the probabilities of exceeding of this threshold by any of these pulses (in presence or absence of a useful signal, respectively), the probabilities of the threshold not being exceeded by a single pulse will be $(1 - D_1)^M$ and $(1 - F_1)^M$, and the probabilities of exceeding the threshold by even one pulse will be

$$D = 1 - (1 - D_1)^M$$

and

$$F = 1 - (1 - F_1)^M.$$

In particular, at $M = 2$ for $D = 0.9$ and $F = 10^{-7}$, we have $D_1 \approx 0.63$ and $F_1 \approx 0.5 \cdot 10^{-7}$, from which, using [(12) §6.3] we derive $\frac{\vartheta_t}{N_s} \approx 85$.

Compared with a single nonfluctuating signal, the fluctuation losses at $D = 0.9$ and $F = 10^{-7}$ amount to: for a single-frequency fluctuating signal (see Fig. 6.5) to about 8.5 db, for a two-frequency signal

to 5 db and 6 db, respectively, for the square and above-discussed form of non-optimum processing. For signal packets we must also take into account the incoherent integration losses (§6.4).

Appendix 2

QUALITATIVE INDICES OF THE OPTIMUM MEASUREMENT OF TWO PARAMETERS FOR A SIGNAL WITH RANDOM INITIAL PHASE

If two parameters α_1 and α_2 , for example, the lag time and the Doppler frequency, are measured simultaneously, the postexperimental probability density $p_y(a_1, a_2) = p_y(a)$ in Eq. [(3) §6.5] is replaced by $p_y(a_1, a_2)$ and the quantity Z will be $Z = Z(a_1, a_2)$. By carrying out the analysis for a fairly strong signal, we can use the wellknown mathematical relation [(10) §6.5]. Because the distribution peak $p_y(a_1, a_2)$ is then fairly narrow, we neglect the variation of the denominator [(10) §6.5] within the limits of the peak. In contrast to §6.5 we assume that the preexperimental probability density is not necessarily constant but has a normal distribution with scatters d_1, d_2 , the correlation moment k and the preexperimental mathematical expectations α_1 and α_2 . Considering that the signal energy is independent of the measured parameters, we obtain

$$p_y(a_1, a_2) = C \exp \left[\frac{2}{N_0} Z(a_1, a_2) - \frac{d_2(a_1 - \alpha_1)^2 + d_1(a_2 - \alpha_2)^2 - 2k(a_1 - \alpha_1)(a_2 - \alpha_2)}{2(d_1 d_2 - k^2)} \right]. \quad (1)$$

We use a Taylor expansion of the functions $Z(a_1, a_2)$ in the neighbourhood of the true values of the parameters α_{10} and α_{20} , which are unknown during the measurement, limiting the expansion to the second-order infinitesimal terms:

$$\begin{aligned} Z(\alpha_1, \alpha_2) = & Z(\alpha_{10}, \alpha_{20}) + Z'_{\alpha_1}(\alpha_1 - \alpha_{10}) + Z'_{\alpha_2}(\alpha_2 - \alpha_{20}) + \\ & + Z''_{\alpha_1 \alpha_1}(\alpha_1 - \alpha_{10})^2 + \frac{1}{2} Z''_{\alpha_1 \alpha_2}(\alpha_1 - \alpha_{10})(\alpha_2 - \alpha_{20}) + \frac{1}{2} Z''_{\alpha_2 \alpha_2}(\alpha_2 - \alpha_{20})^2. \end{aligned} \quad (2)$$

All derivatives here correspond to the point α_{10}, α_{20} .

The expression (1) is then transformed into the two-dimensional normal distribution law

$$p(\alpha_1, \alpha_2) = C \exp \left[-\frac{D_1(\alpha_1 - \alpha_1^*)^2 + D_2(\alpha_2 - \alpha_2^*)^2 - 2K(\alpha_1 - \alpha_1^*)(\alpha_2 - \alpha_2^*)}{2(D_1 D_2 - K^2)} \right]. \quad (3)$$

We put together consecutively the coefficients at α_1^2 , α_2^2 and $\alpha_1 \alpha_2$ in the expressions (1) and (3), using (2). Thus we obtain three equations, containing the unknown parameters D_1 , D_2 and K of the post-experimental distribution. Multiplying the first of these equations by the second and subtracting the third, we find the quantity $D_1 D_2 - K^2$ after we obtain:

$$D_1 = \frac{\Delta_2}{\Delta_1 \Delta_2 - \Delta_{1,2}^2}, \quad (4)$$

$$D_2 = \frac{\Delta_1}{\Delta_1 \Delta_2 - \Delta_{1,2}^2}, \quad (5)$$

$$K = \frac{\Delta_{1,2}}{\Delta_1 \Delta_2 - \Delta_{1,2}^2}, \quad (6)$$

where

$$\Delta_1 = -\frac{2}{N_0} Z''_{\alpha_1} + \frac{d_2}{d_1 d_2 - k^2}, \quad (7)$$

$$\Delta_2 = -\frac{2}{N_0} Z''_{\alpha_2} + \frac{d_1}{d_1 d_2 - k^2}, \quad (8)$$

$$\Delta_{1,2} = \frac{2}{N_0} Z''_{\alpha_1 \alpha_2} + \frac{k}{d_1 d_2 - k^2}. \quad (9)$$

If we compare in an analogous manner the coefficients at α_1 and α_2 in (1) and (3), we can find the corresponding expressions for α_1^* and α_2^* .

We use the relations thus found for determining the scatter of the measurement errors for the lag time and Doppler frequency. For this purpose it is sufficient to put $\alpha_1 = \tau$, $\alpha_2 = F$, $Z = \mathcal{E}_r(\tau, F)$, $\alpha_{10} = 0$ and

$\alpha_{20} = 0$ (see §7.1 and 7.2).

As an example, let us calculate $D_1 = D_1$ and $D_2 = D_F$ on condition that $d_1 = \infty$, $k = 0$, $d_1 = d_F$ and that the emitted signal is a frequency modulated pulse with the deviation $\Delta f \gg 1/\tau_n$, $\Delta f \gg d_F$ and with nondegenerate peak. In analogy with [(3) §7.7] we put in the neighbourhood of the peak, i.e., for $\tau \ll \tau_n$,

$$p(\tau, F) \approx \frac{\sin \pi(F\tau_n + \Delta f\tau)}{\pi(F\tau_n + \Delta f\tau)} \approx 1 - \frac{1}{6} [\pi(F\tau_n + \Delta f\tau)]^2. \quad (10)$$

Transforming (10), we obtain

$$p(\tau, F) = 1 - \frac{\pi^2 \Delta f^2 \tau_n^2}{3} \tau^2 - \frac{\pi^2 \tau_n^2}{6} F^2 - \frac{\pi^2 (\Delta f)^2}{6} \tau_n^2. \quad (11)$$

Regarding (11) as a Taylor expansion, we have

$$p''_{\tau} = \frac{\pi^2 (\Delta f)^2}{3}, \quad p''_F = \frac{\pi^2 \tau_n^2}{3}, \quad p''_{\tau F} = \frac{\pi^2 \Delta f \tau_n}{3}.$$

Then, carrying out the calculation in accordance with the formulas (7), (8) and (9), we obtain

$$\Delta_1 = q^2 \frac{\pi^2 (\Delta f)^2}{3}, \quad \Delta_2 = q^2 \frac{\pi^2 \tau_n^2}{3} + \frac{1}{d_F^2}, \quad \Delta_{1,2} = q^2 \frac{\pi^2 \Delta f \tau_n}{3},$$

where $q = \sqrt{\frac{2\pi}{H_0}}$. Hence, by virtue of (4) and (5)

$$D_1 = D_2 = \frac{3}{q^2 \pi^2 (\Delta f)^2} + d_F^2 \left(\frac{\tau_n}{\Delta f} \right)^2, \quad (12)$$

$$D_1 = D_F = d_F.$$

In this case the information on the speed as compared with the preexperimental, has not been improved because $d_1 = \infty$ in contrast to d_F . The smaller the product $d_F \tau_n^2$, and the greater Δf , the less is the scatter of the error in measuring the lag time D_1 .

Appendix 3

ELEMENTS OF RESOLUTION THEORY

Let us assume the oscillation $y(t)$, which may contain superposed signals and noise,

$$y(t) = A_1 x_1(t, \alpha_{11}, \alpha_{12}, \dots, \beta_{11}, \beta_{12}, \dots) + \\ + A_2 x_2(t, \alpha_{21}, \alpha_{22}, \dots, \beta_{21}, \beta_{22}, \dots) + n(t) \quad (1)$$

Here, A_1 and A_2 are discrete random parameters, which can assume values of 0 or 1; α_{1i} and α_{2i} are random measurable parameters; β_{1i} , β_{2i} are random nonmeasurable parameters. If the presence of signal 1 does not reduce the qualitative indices of detection or measurement of the parameters of signal 2 to such a degree that they become inaccessible, we say that the signal 2 is resolved out of signal 1, in the sense of detection or in the sense of measurement, respectively. However, if this is also true of signal 1 (in presence of signal 2) we can state that the two signals are reciprocally resolved.

In this connection let us consider the detection of signal 2 in presence of a nonrandom value $A_1 = 1$ on the assumption that both signals have independent Rayleigh amplitude coefficients, equally probable initial phases and do not contain any other measurable or nonmeasurable parameters. Then

$$y(t) = n(t) + x_1(t, \beta_1, B_1) + A_2 x_2(t, \beta_2, B_2) \quad (2)$$

applies, where A_2 (0 or 1) is a discrete quantity, which can be estimated after reception of $y(t)$. The solution 0 or 1 can be assumed (see §2.7) on the basis of the probability

$$I[y(t)] = \frac{p_{c_2 c_1 n}[y(t)]}{p_{c_1 n}[y(t)]}, \quad (3)$$

keeping in mind that the role of signal 1 consists in an increase in the active noise. The subscripts at the probability densities in (3) characterize the conditions for the presence of both signals and noise $n(t)$ or the signal $x_1(t, \beta_1, B_1)$ only and this noise. Because with the first of these conditions $A_2 = 1$,

$$p_{c_2 c_1 n}[y(t)] = \int_0^\infty dB \int_0^{2\pi} p_{c_1 n}[y(t) - x_2(t, \beta, B)] p(\beta, B) d\beta. \quad (4)$$

From (3) and (4) we can obtain

$$I[y(t)] = \int_0^\infty dB \int_0^{2\pi} I'_2[y(t)] \frac{I_1[y(t) - x_2(t, \beta, B)]}{I_1[y(t)]} p(\beta, B) d\beta. \quad (5)$$

Here $I_1[y(t)]$ is the probability relation, corresponding to the case of detection of the first signal $x_1(t, \beta_1, B_1)$ with the random amplitude B_1 and the initial phase β_1 against the background of the noise $n(t)$,

$$I_1[y(t)] = \frac{p_{c_1 n}[y(t)]}{p_n[y(t)]}, \quad (6)$$

$I_2[y(t) - x_2(t, \beta, B)]$ corresponds to a substitution of $y(t)$ by $y(t) - x_2(t, \beta, B)$ in the numerator and denominator of (6);

$I'_2[y(t)]$ is the probability relation corresponding to the detection of the second signal $x_2(t, \beta, B)$ with the fixed parameters β, B against the background of the noise $n(t)$,

$$I'_2[y(t)] = \frac{p_n[y(t) - x_2(t, \beta, B)]}{p_n[y(t)]}. \quad (7)$$

The expression $z^2 = |z|^2$ is found by means of the formula [(8) §3.4] If the quantity $I_1[y(t)]$ in this formula is expressed via the complex amplitudes [(3) §4.7], the substitution $|z|^2 = z z^*$ is carried out, and the product of the integrals thus obtained is represented in the form of a double integral, we obtain

$$I_1[y(t)] = \frac{N_0}{\vartheta_1 + N_0} \exp \left[-\frac{1}{4N_0(\vartheta_1 + N_0)} \times \right. \\ \left. \times \int_{-\infty}^{\infty} \int_{-\infty}^{\infty} Y(t) Y^*(s) X_1^*(t) X_1(s) dt ds \right]. \quad (8)$$

Then

$$\frac{I_1[y(t) - x_2(t, \beta, B)]}{I_1[y(t)]} = \exp \left\{ -\frac{1}{4N_0(\vartheta_1 + N_0)} \left[\int_{-\infty}^{\infty} \int_{-\infty}^{\infty} [Y(t) - \right. \right. \\ \left. \left. - BX_2(t) e^{i\beta}] [Y^*(s) - BX_2^*(s) e^{-i\beta}] X_1^*(t) X_1(s) dt ds - \right. \right. \\ \left. \left. - \int_{-\infty}^{\infty} \int_{-\infty}^{\infty} Y(t) Y^*(s) X_1^*(t) X_1(s) dt ds \right] \right\}.$$

It follows from the relations §3.1 that

$$I'_2 = \exp \left[-\frac{1}{N_0} \int x_2^2 dt + \frac{2}{N_0} \int y x_2 dt \right] = \\ = \exp \left\{ -\frac{1}{N_0} \left[\int (y - x_2)^2 dt - \int y^2 dt \right] \right\},$$

where

$$x_2 = x_2(t, \beta, B); \quad y = y(t) \quad \text{и} \quad I'_2 = I'_2[y(t)].$$

Changing over to the complex form of notation, we obtain

$$I'_2[y(t)] = \exp \left\{ -\frac{1}{2N_0} \left[\int_{-\infty}^{\infty} [Y(t) - BX_2(t) e^{i\beta}] [Y^*(t) - \right. \right. \\ \left. \left. - BX_2^*(t) e^{-i\beta}] dt - \int_{-\infty}^{\infty} Y(t) Y^*(t) dt \right] \right\}.$$

As a result, the relation (5) is transformed into

$$I = \frac{1}{\pi} \int_0^{\infty} dB \int_0^{2\pi} B e^{-B^2} e^{-\frac{B^2 \vartheta_{2K\beta}}{N_0}} e^{-\frac{2BZ_{2K\beta}}{N_0} \cos(2-\theta)} d\beta$$

or in analogy to [(8) §3.4]

$$I = \frac{N}{\vartheta_{2K\beta} + N_0} e^{-\frac{1}{N_0} \frac{Z_{2K\beta}^2}{\vartheta_{2K\beta} + N_0}}. \quad (9)$$

Here Z_{ekv} characterizes the optimum signal processing;

$$Z_{ekv} = \frac{1}{2} \left| \int_{-\infty}^{\infty} Y(t) R^*(t) dt \right|, \quad (10)$$

and

$$\mathcal{Q}_{ekv} = \frac{1}{2} \int_{-\infty}^{\infty} X_2(t) R_2^*(t) dt = \frac{1}{2} \int_{-\infty}^{\infty} R_2(t) X_2^*(t) dt, \quad (11)$$

where in turn

$$R(t) = X_2(t) - \frac{X_1(t)}{\mathcal{Q}_1 + N_0} - \frac{1}{2} \int_{-\infty}^{\infty} X_2(s) X_1^*(s) ds. \quad (12)$$

Thus, the optimum processing operation is carried out in accordance with formula (10), where the function $R(t)$ generally does not coincide with $X_2(t)$. The equality $R(t) = X_2(t)$ applies only in the case when the signals $X_1(t)$ and $X_2(t)$ are orthogonal, i.e., when the integral

$$\int_{-\infty}^{\infty} X_2(s) X_1^*(s) ds$$

vanishes. The ratio of the modulus of this integral to the square root of the products of the integrals of the squares of the moduli $X_1(t)$ and $X_2(t)$ is termed the correlation coefficient of these signals

$$\rho = \frac{\left| \int_{-\infty}^{\infty} X_2(s) X_1^*(s) ds \right|}{\sqrt{\int_{-\infty}^{\infty} |X_1(s)|^2 ds \int_{-\infty}^{\infty} |X_2(s)|^2 ds}}. \quad (13)$$

if the signals $X_1(t)$ and $X_2(t)$ differ only by the lag time and Doppler frequency, the definition (13) gives the relations of §7.2.

Having carried out the analysis of the qualitative detection indices during processing in accordance with the relation (10), we can show that the detection is qualitatively determined by the energy E_{2ekv} . In other words, only the part of the energy E_2 determined by the magnitude of the relation

$$\frac{\partial_{\text{max}}}{\partial_i} = 1 - \frac{\partial_i}{\partial_i + N_0} \quad (14)$$

is effectively utilized. The smaller rho, the greater is this proportion, i.e., the better are the signals resolved. At equal

$$q_{\text{max}} = \sqrt{2\partial_{\text{max}}/N_0}$$

it is possible to obtain equal probabilities D and F in absence as well as in presence of a signal $x_i(t, \beta_i, \beta_i)$, in which only the amplitude and the initial phase are random.

It is found that analogous concepts can be developed also for the spatial resolution which is carried out, for example, when the signals are received at a certain linear aperture $-l/2 < x < l/2$. Depending on the position of the emitters in space, a certain field distribution is created in the section l . Superposed on this field is the field of the thermal noise with the spectral density N_0 , which we shall consider as isotropic. Information on the presence of the emitter 2 in the presence of a fluctuating emitter 1 (and vice versa) can be obtained by analysis of the voltage of the field as a function of the two variables $Y(t, x)$. As the calculations analogous to those described above, show, this analysis consists in taking the integral

$$Z_{\text{max}} = \frac{1}{2} \left| \int_{-l/2}^{l/2} dx \int_{-\infty}^{\infty} Y(t, x) R^*(t, x) dt \right|. \quad (15)$$

Additional integration over x at the aperture l can be carried out in practice by means of a multielement antenna or an antenna with a single output with an equivalent directivity pattern. The minimum of the latter at optimum resolution of the source of the oscillations 2 should be directed at the source of the oscillations 1 [30].

Manu-
script
Page
No.

[Transliterated Symbols]

- 267 $\text{порог} = \text{porog} = \text{porog} = \text{threshold}$
- 268 $\mathcal{E} = E = \text{energiye} = \text{energy}$
- 276 $\text{экв} = \text{ekv} = \text{ekivalentnyy} = \text{equivalent}$

REFERENCES

1. Kotel'nikov, V. A., Teoriya potentsial'noy pomekhouystoychivosti [Theory of Potential Noise Stability], MEI [Moscow Power Engineering Institute] 1946; Gosenergoizdat [State Publishing House for Power Engineering], 1956..
2. Siforov, V. I., Radiopriyemnyye ustroystva [Radio Receiving Devices] Voenizdat [Publishing House for Military Science], 1954.
3. Bunimovich, V. I., Flyuktuatsionnyye protsessy v radiopriyemnykh ustroystvakh [Fluctuation Process in Radio Receiving Devices], Publishing House "Sovetskoye Radio" [Soviet Radio], 1951.
4. Woodward, F. M., Teoriya veroyatnostey i teoriya informatsii s primeneniymi v radiolokatsii [Probability Theory and Information Theory with Applications in Radar], Publishing House "Sovetskoye Radio", 1955.
5. Vaynshteyn, L. A. and Zubakov, V. D., Vydeleniye signalov na fone sluchaynykh pomekh [Isolation of Signals from the Noise Background]. Publishing House "Sovetskoye Radio", 1960.
6. Fal'kovich, S. Ye., Priyem radiolokatsionnykh signalov na fone flyuktuatsionnykh pomekh [Reception of Radar Signals Against the Background of Fluctuating Noise], Publishing House "Sovetskoye Radio", 1961.

7. Gutkin, I. S., Teoriya optimal'nykh metodov radiopriyema pri flyktuatsionnykh pomekhakh [Theory of the Optimum Methods of Radioreception in Presence of Fluctuating Noise]. Gosenergoizdat, 1961.
8. Middleton, D., Vvedeniye v statisticheskuyu teoriyu svyazi [Introduction to Statistical Communications Theory], Vol. 1 and 2. Publ. House "Sovetskoye Radio", 1961-62.
9. Basharinov, A. Ye., Fleyshman, B. S., Metody statisticheskogo posledovatel'nogo analiza i ikh prilozheniya [Methods of Statistical Consecutive Analysis and Their applications], Publ. House "Sovetskoye Radio", 1962.
10. Bakut, P. A., Bol'shakov, I. A., Gerasimov, B. M., Kuriksha, A. A., Repin, V. G., Tartakovskiy, G. P., and Shirokov, V. V., Voprosy statisticheskoy teorii radiolokatsii [Problems of the Statistical Theory of Radar], Vol. 1, Publ. House "Sovetskoye Radio", 1963.
11. Helstrom, K., Statisticheskaya teoriya obnaruzheniy signalov [Statistical Theory of Signal Detection], Izd-vo inostrannoy literatury [Publishing House for Foreign Literature], 1963.
12. Priyem signalov pri nalichii shuma [Signal Reception in Presence of Noise] Collection of translations ed. by L. S. Gutkin. Izd-vo inostrannoy literatury, 1960.
13. Priyem impul'snykh signalov v prisutstvii shumov [Reception of Pulse Signals in Presence of Noise] Collection of translations edited by A. Ye. Basharinov and M. S. Aleksandrov. Gosenergoizdat, 1960.
14. Shirman, Ya., D., Spetsob povysheniya raxreshayushchey sposobnosti radiolokatsionnykh stantsiy i ustroystvo dlya ego osushchestvleniya [Method of Increasing the Resolving Power

- of Radar Stations and Devices for its Realization]. Avotrskoye svidel'stvo [Author's Certificate] No. 146803 on the basis of the claim No. 461974/40 of the 25th July, 1956.
15. Siebert, W., Obshchiye zakonomernosti obnaruzheniya tseley pri pomoshchi radiolokatsii [General Regularities of Target Detection by Means of Radar], VRLT = Vestnik radiolokatsionnoy tekhniki [Herald of Radar Engineering] 1957, No. 4 (41).
 16. Kronert, R., Impulsverdichtung [Pulse Compression]. Nachrichtentechnik [Communications Engineering], 1957, No. 5.
 17. Huffman, D. A., Sintez lineynykh mnogotaktnykh kodiruyushchykh skhem [Synthesis of Linear Sequential Coding Circuits], In collection "Teoriya peredachi soobshcheniy" [Theory of Message Transmission]. Izd-vo inostrannoy literatury, 1957.
 18. Klass. Radiolokatsionnaya stantsiya s uvelichennoy dal'nost'yu deystviya, ispol'zuyishchaya metod raznosa chastot [Radar Station with Increased Range, Using the Frequency Separation Method]. VRLT, 1958, No. 3.
 19. Amiantov, I.N., Primeneniye teorii resheniy k zadacham obnaruzheniya signalov i vydeleniya signalov iz shumov [Application of the Solution Theory to the Problems of Signal Detection and Signal Separation from Noise] VVIA imeni N. Ye., Zhukovskogo [N. Ye., Zhukovskiy All-Union Institute of Aerohydrodynamics?] 1958.
 20. Lerner, R., Signals with Uniform Ambiguity Functions, I.R.E. Convention Record, 1958.
 21. Shirman, Ya., D., Teoriya obnaruzheniya poleznogo signala na fone gaussovykh shumov i proizvol'nogo chisla meshayushchikh signalov [Theory of Useful Signal Detection Against the Background of Gaussian Noise and An Arbitrary Number of Inter-

- fering Signals]. "Radiotekhnika i elektronika (Radio Engineering and Electronics), 1959, No. 12.
22. CHERNYAK- Yu. B. O nekotorykh sposobakh obrabotki flyuktuiruyushchikh signalov v d'rukhhkanal'nykh sistemakh [On Some Methods of Processing of Fluctuating Signals in Two-channel Systems]. "Radiotekhnika i Elektronika", 1959, No. 12.
23. Walter, Atkin, Bikel. Sravnitel'naya otsenka razlichnykh sposobov opredeleniya azimuta putem imitatsii signalov poiskovogo radiolokatora i tsifrovoy obrabotki dannykh [Comparative Evaluation of Different Methods of Aximuth Determination by Imitation of the Signals of a Search Radar and Digital Data Processing]. Radiotekhnika i elektronika za rubezhom [Radio Engineering and Electronics Abroad] 1959, No. 2.
24. Sragovich, V. G., O raschete kharakteristik obnaruzheniya pri kvadratichnom summirovanii signalov [On the Calculation of the Detection Characteristics with Square-Law Summing of Signals]. "radiotekhnika i elektronika", 1960, No. 4.
25. Meitzler, A. H., Ultrasonic Delay Lines Using Shear Modes in Strips. J. E. May, Wire-Type Dispersive Ultrasonic Delay Lines. T. R. Meeker., Dispersive Ultrasonic Delay Lines Using the First Longitudinal Mode in a Strip. IRE Transactions on Ultrasonics Engineering. June, 1960, Vol. UE-7, No. 2.
26. Markush. Statisticheskaya teoriya obnaruzheniya tseley impul'snoy radiolokatsionnoy stantsiy [Statistical Theory of Target Detection by a Pulse Radar Station]. "Zarubezhnaya radioelektronika [Foreign Radio Electronics], 1960, No. 10.
27. Cook. Povysheniye effektivnosti radiolokatsionnykh ustroystv za schet szhatiya impul'sa [Increase in the Efficiency of Radar Devices by Pulse Compression]. "Zarubezhnaya Radioelek-

- tronika', 1960, No. 9.
28. Lerner, R. A., Matched Filter Detection System vor Complicated Doppler Shifted Signals. IRE Trans. on Information Theory. June 1960, Vol. IT-6, No. 3.
 29. Bol'shakov I. A., Repin, V. G., Voprosy nelineynoy fil'tratsii [Problems of Nonlinear Filtering] "Avtomatika i telemekanika" [Automation and Remote Control], 1961, No. 4.
 30. Shirman, Ya., D., Statisticheskiy analiz optimal'nogo razresheniya [Statistical Analysis of Optimum Resolution]. "Radio-tehnika i elektronika", 1961, No. 8.
 31. Klauder, Price, Darlington, Elbersheim. Teoriya i raschet impul'snykh radiolokatsionnykh stantsii s chastotnoy modulyatsiei [Theory and Calculation of Pulse Radar Stations with Frequency Modulation], "Zarubezhnaya radioelektronika", 1961, No. 1.
 32. Burges., Budushcheye radiolokatsii [The Future of Radar]. "Zarubezhnaya radioelektronika", 1961, No. 12.
 33. Turin, Soglasovannyye fil'try [Matching Filters]. "Zarubezhnaya radioelektronika", 1961, No. 3.
 34. Levine, N. A., A new technique for increasing the flexibility of recursive least squares data smoothing. Bell System, Tech. 1961, 40, No. 3.
 35. Shapiro, I. I., Rashchet trayektoriy ballisticheskikh snaryadov po dannym radiolokatsionnykh nablyudeniya [Calculation of the Trajectory of Ballistic Missiles on the Basis of Radar Data]. IL, 1961.
 36. Velti., Chetvertichnyye kody dlya impul'snogo radiolokatora [Quaternary Codes for Pulse Radar]. "Zarubezhnaya radioelektronika". 1961, No. 4.

37. Tims., Korrektsiya bokovykh lopestkov v kanale dal'nosti radiolokatsionnoy stantsii so szhatiem impul'sov [Correction of the Lateral Lobes in the Range Channel of a Radar Station with Pulse Compression]. "Zarubezhnaya Radioelektronika", 1963, No. 5.
38. Muller, Goodwin., Shirokopolsnyy priemnik so szhatiem impul'sov dlya razvedki v santimetrovom diapazone voln [Wideband Receiver with Pulse Compression for Reconnaissance in the Centimeter Wavelength Range]. "Zarubezhnaya radioelektronika", 1963, No. 6.
39. Hall, Obobshchennoye uravneniye radiolokatsii dlya sopostavleniya kharakteristik RLS razlichnykh tipov [General Radar Equation for the Establishment of the Characteristics of Radar Stations of Different Types]. "Zarubezhnaya radioelektronika", 1963, No. 4.